UNIVERSITÀ DEGLI STUDI DI CATANIA

Facoltà di Scienze Matematiche, Fisiche e Naturali

Dipartimento di Scienze Geologiche

DOTTORATO DI RICERCA in

"Evoluzione geologica di orogeni di tipo mediterraneo"

XXIII CICLO

"Paleoseismological off- fault analyses in eastern Sicily: a contribute to the characterization of seismic sources"

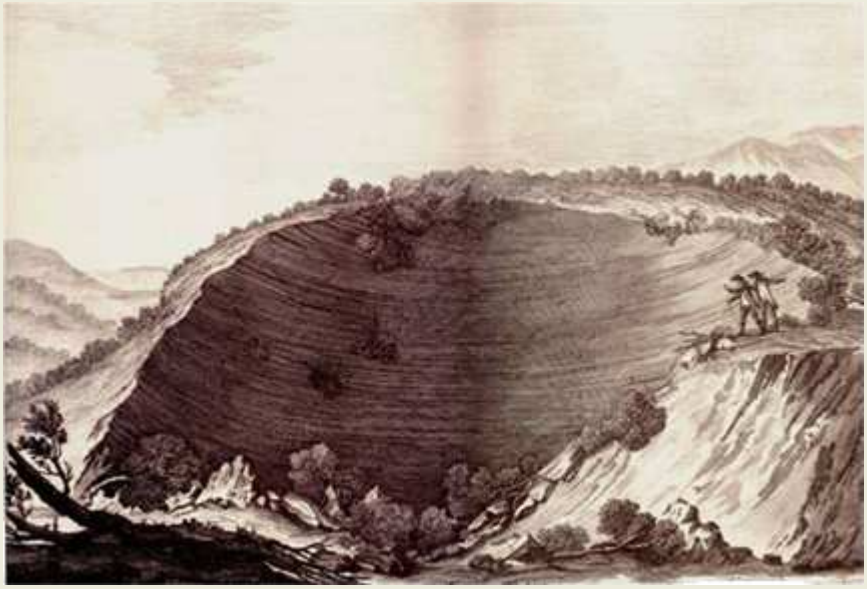

Tesi di dottorato di:
Claudia Pirrotta

Coordinatore: Prof. C. Monaco
Tutor: Prof.ssa M.S. Barbano

Anno Accademico 2009/10

PALEOSEISMOLOGICAL OFF- FAULT ANALYSES IN EASTERN SICILY: A CONTRIBUTE TO THE CHARACTERIZATION OF SEISMIC SOURCES

Riassunto…….…….....i

Abstact …….....i

Chapter 1

1- Geological and seismological features of Sicily……..…...1

1.1- Geological and structural setting of eastern Sicily……...……...2

1.2- Eastern Sicily historical earthquakes and related seismogenic sources ……..……7

Chapter 2

2- Earthquake Geology……...……..18

2.1- Primary effects…….....20

2. 2- Secondary effects ……...……..22

2.2.1- Landslides and rock-falls ……...…....23

2.2.2- Ground deformations ……...……...26

2.2.3- Liquefactions: soft sediment deformations …….…...30

2.2.4- Hydrological anomalies ……...……..34

2.2.5- Tsunami deposits ……..…… 35

Chapter 3

3- Paleoseismology ……..39

3.1- Paleoseismological investigations.…….……..……40

3.1.1- Historical data analysis ……..……...41

3.1.2- On-fault Paleoseismology …….……...….....43

3.1.3- Off-fault Paleoseismology ……...….....45

3.1.3.1- Near fault geomorphological investigation …….……..….....46

3.1.3.2- Stratigraphic record analysis …….. ……..…….…...47

3.2- Paleoseismological investigations in Italy: the state of the art…….……..……...49

Chapter 4

4- Historical databases of seismogeological effects in Sicily and empirical relationships between source parameters vs epicentral distances..……...….53
4.1-Historical records of seismogeological effects in Sicily: analysis and classification….53
4.1.1- A-class: landslides. ……....55
4.1.2- B-class: ground deformations…….....56
4.1.3- C-class: liquefactions…….....57
4.1.4- D-class: hydrological anomalies ……...…58
4.2- Databases of the seismogeological effects……..…...…59
4.3- Empirical relationships between magnitude/ intensity versus epicentral distance (Re)……61
4.4- Data analysis……..…61

Chapter 5

5. Study of the deformative structures ……..…72
5.1- Method……...…72
5.2- Minissale site……...…..74
5.2.1- Minissale trench study……...…….76
5.3- Agnone site. ……..……...…….80
5.3.1- Agnone trench study……..…….……82
5.4- Vendicari site……..……..…….……88
5.4.1- Analysis of the deformation structures ……..……..…….……..91
5.4.1.1- Brittle deformation analysis……..……...…93
5.4.1.1.1- Microscopic thin section analysis……..…..……..…...97
5.4.1.2- Soft sediment deformation structure analysis ……..…..……..98
5.4.2- Deformative phases reconstruction ……....……...…...101
5.5- Data analysis ……..…..……..…….……101
5.5.1- Minissale site ……..…..……..…….103
5.5.2- Agnone site……..…..……..…….....104
5.5.3- Vendicari site……..…..……..……..105
5.5.3.1- Brittle deformations……..…..……...105

Claudia Pirrotta

5.5.3.2- Soft deformations……..……..……...……...……107
5.5.3.3- Chronology of the deformative events……...……...…….109

Chapter 6

6- Study of tsunami deposits ……..……110
6.1- Analysis of sandy deposits ……..111
6.1.1- Method ……....……111
6.1.2- Study sites ……...…….112
6.1.2.1- The Augusta Bay……..….112
6.1.2.1.1- On shore study ……...……113
6.1.2.1.2- Off shore study……..…..….116
6.1.2.2- Pantano Morghella……..…..…..121
6.2- Study of boulders …….....123
6.2.1- Method …….…....123
6.2.2- Study sites…….127
6.2.2.1- Capo Campolato site…….…….127
6.2.2.2- Vendicari site…….....131
6.2.2.3- S. Lorenzo site…….…….133
6.3- Data Analysis…….…….….134
6.3.1- Study of sandy deposits……...…….….135
6.3.2- Boulder study…..……...……..…....…….135

Chapter 7

7- Discussions and conclusions……..137

Appendix A……....141
Appendix B ……..……..……170
Appendix C……...…….179

References……..…….....182
Acknowledgements……..…….....211

Riassunto

La ricerca effettuata consiste in uno studio paleosismologico off-fault**,** ovvero nell' analisi e datazione di effetti sismogeologici innescati in Sicilia dai terremoti storici e paleo terremoti della Sicilia e della Calabria meridionale. La scelta del tipo di effetto studiato è dettata dalle problematiche sismogeologiche di questa regione. Infatti in Sicilia sono avvenuti eventi tra i più disastrosi della storia sismica Italiana, ma la reale definizione e collocazione delle sorgenti sismogenetiche è un argomento tutt'oggi aperto e fortemente dibattuto, poiché questi eventi sono avvenuti in epoca pre- strumentale e non hanno lasciato evidenze geologiche di fagliazione superficiale. Al contrario, questi terremoti hanno innescato numerosi effetti sismogeologici nell'area epicentrale, ben descritti dalle fonti storiche. Pertanto, considerando anche il suo ricco e antico patrimonio storico, la Sicilia rappresenta un ottimo laboratorio dove testare diverse metodologie di studio paleosismologico off fault.

Gli scopi della ricerca svolta sono molteplici ed in particolare consistono da un lato nella possibilità di fornire nuovi e utili dati per meglio comprendere la sismicità della Sicilia, dall'altro lato di testare studi innovativi in una regione dove questo tipo di indagine è stata scarsamente applicata.

La ricerca effettuata segue due principali linee. In una prima fase è stata analizzata la sismicità regionale della Sicilia ed è stata effettuata la raccolta e l'analisi delle fonti storiche originali e del patrimonio documentario esistente, successivamente è stato realizzato uno studio di campagna al fine di trovare ed analizzare direttamente in sito le strutture sismogeologiche.

I dati storici raccolti, che consistono in descrizioni di effetti sismogeologici, quali frane, liquefazioni, deformazioni del terreno e anomalie idrogeologiche, sono stati criticamente analizzati e classificati. A questo scopo è stata effettuata la caratterizzazione litologica e geomorfologica dei siti mediante l'utilizzo di carte geologiche e l'analisi aerofotogrammetria, al fine della corretta assegnazione al fenomeno descritto del corrispondente effetto sul terreno. Questi dati sono stati utilizzati per realizzare database georeferenziati, mappe riportanti la distribuzione degli effetti sismoindotti e mappe di

suscettibilità del territorio al loro verificarsi, mediante l'utilizzo di software GIS. Inoltre, i dati sono stati utilizzati per l'estrapolazione di relazioni empiriche tra i parametri di sorgente (Maw, Mas e Io) e le distanze epicentrali del sito (Re) per ogni effetto sismogeologico, mediante il metodo dell' upper bound-curve che indica la soglia massima di innesco dell'effetto.

Questa prima fase di ricerca ha messo in luce che la Sicilia è una regione altamente suscettibile allo sviluppo degli effetti sismogeologici. In particolare frane e deformazioni del terreno rappresentano gli effetti più frequenti, che si verificano per i più bassi valori di energia e sono maggiormente concentrati nel fianco orientale del Monte Etna, che risulta caratterizzato sia da fatturazione cosismica che asismica, e nel settore settentrionale della cintura Orogenica (Catena Appenninico Maghrebide e Catena Kabilo Calabride), caratterizzato da complesse formazioni strutturali in stato di persistente instabilità. Liquefazioni e anomalie idrologiche sono risultate meno frequenti, si generano per più alte soglie di energia, ed i settori maggiormente suscettibili sono la valle del Belice e la Piana di Catania, caratterizzate da depositi olocenici, non consolidati e generalmente saturi d'acqua. Inoltre, l'utilizzo delle upper- bound curves ha messo in luce possibili errori nella definizione dei parametri focali di alcuni terremoti ottenuti dal campo macrosismico. Per esempio il terremoto del 5 Marzo 1823 della Sicilia settentrionale, che è stato localizzato nei cataloghi vicino Cefalù, potrebbe essere localizzato a mare e avere una magnitudo maggiore di quella stimata. Infine possibili effetti di amplificazioni di sito e di eccezionale risposta di sito sono stati messi in luce nei grafici delle upper bound curves, da punti ricadenti a distanza superiore da quella prevista, come dimostrato dagli effetti osservati a Messina durante il terremoto del 1783 (M= 4.20) e a Calatafimi (Trapani) durante l'evento del 1693.

I risultati ottenuti durante la prima fase di studio sono stati anche utilizzati come punto di partenza per indirizzare l'analisi in sito delle strutture deformative sismoindotte. Infatti questa ricerca è stata focalizzata in settori, lungo la costa orientale della Sicilia, dove le fonti storiche descrivono il verificarsi di effetti sismogeologici e che, grazie alla definizione delle upper-bound curves, risultano suscettibili al loro sviluppo. In particolare sono state

ricercate strutture da liquefazione e depositi di tsunami poiché, per le loro caratteristiche, questi effetti risultano logisticamente più facili da trovare ed analizzare.

Lo studio in sito delle strutture sismoindotte consiste in una fase preliminare focalizzata alla definizione dei settori dove le deformazioni potrebbero essersi sviluppate durante passati eventi, mediante l'analisi di foto aeree e di immagini satellitari, e di una successiva fase di rilevamento geologico e geomorfologico delle aree selezionate. Quando possibile, la sequenza stratigrafica locale è stata studiata mediante sondaggi effettuati con carotiere a mano e sono stati prelevati campioni di terreno per ulteriori analisi sedimentologiche. Questi dati sono stati usati per la ricostruzione paleoambientale del sito, cui è seguita l'analisi delle strutture deformative individuate. La datazione di queste ultime, con il metodo del radiocarbonio, ha inoltre permesso di realizzare correlazioni con alcuni dei terremoti storici e con paleo-eventi.

Lo studio in sito è stato effettuato in tre aree della Sicilia orientale: Minissale (fianco orientale del Monte Etna), Agnone (Piana di Catania) e Vendicari (Sicilia sud orientale). Nei primi due siti le strutture deformative (*lateral spreading, dikes, faults, drag folds, recumbent folds, sheet slumps, warped top levels* e *boudinage*) sono state individuate su due pareti artificiali che sono state analizzate mediante il metodo della divisione in quadranti. A seguito di un'attenta analisi queste strutture sono risultate riconducibili a due distinti eventi sismici e la loro datazione, combinata con le upper bound curves, ha permesso di ricollegarle ai terremoti del 1169 e del 1693 per il sito di Minissale, ed a quelli del 1542 e del 1693 per il sito di Agnone.

A Vendicari sono state individuate strutture deformative che hanno coinvolto depositi di età compresa tra il Pliocene ed il Quaternario. Queste strutture consistono sia in *soft sediment deformations (autoclastic breccias, diapyr-like injections* e *thyxotropic wedges*), probabilmente legate a effetti di liquefazione, che in fratture, generalmente aperte e riempite da sedimenti (*sedimentary dykes*). Le fratture sono state studiate mediante un'analisi sistematica, mesostrutturale e mediante l'analisi al microscopio del materiale di riempimento, per mettere in luce possibili relazioni con il campo di stress tettonico regionale. A seguito di questa analisi e grazie alla ricostruzione paleoambientale del sito, le strutture deformative sono state ricondotte ad almeno quattro eventi sismici, con magnitudo

maggiore di 5 e intensità superiore a IX, che sono i valori soglia per cui queste deformazioni possono innescarsi in un sito. L'assenza di materiale databile non ha permesso di ottenere informazioni circa il momento in cui queste deformazioni sono avvenute. Comunque, i rapporti tra le strutture de formative hanno permesso di ipotizzare che i primi due eventi sono avvenuti dopo il Pliocene e prima del Tirreniano, mentre gli ultimi due sarebbero successivi al Tirreniano. Dal momento che gli ultimi due terremoti sembrano aver causato lo sviluppo di *neptunyan dykes*, ancora in buono stato di conservazione nonostante l'alto grado di erosione carsica che caratterizza l'area, questi sembrerebbero essere di recente età.

Lo studio delle tsunamiti, rappresentate sia da depositi sabbiosi che da accumuli di megaclasti, è stato intrapreso a terra e a mare, lungo le costa della Sicilia sud- orientale. Questa ricerca ha richiesto la combinazione di diverse indagini quali analisi geologiche, geomorfologiche, paleontologiche, petrografiche, morfoscopiche e magnetiche. Una campagna di indagine geofisica a mare, mediante sismica chirp, è stata inoltre effettuata in uno dei siti studiati (Augusta Bay, Sicilia sud-orientale), al fine di mettere in luce possibili depositi di tsunami nella sequenza sedimentaria. Infine, equazioni idrodinamiche, relative all'attenuazione dell'altezza di onde sulla costa, insieme ad analisi statistiche, hanno permesso di determinare gli eventi estremi responsabili del trasporto e della deposizione di massi a Capo Campolao, Vendicari e San Lorenzo (Sicilia sud-orientale).

Il sito di Augusta ha registrato tre probabili eventi a terra. Le datazioni con il radiocarbonio hanno permesso di ricondurre l'ultimo evento allo tsunami del 365 AD, mentre gli altri due risultano più vecchi e pertanto non riconducibili ad eventi storici. A seguito di una campagna di indagine geofisica e dell'analisi dei profili sismici chirp ottenuti, è stato effettuato un sondaggio a mare nel porto di Augusta. In questo sono stati trovati 11 possibili livelli di tsunamiti in una sequenza sedimentaria di circa 4500 anni. Le datazioni hanno rivelato che gli ultimi quattro livelli potrebbero essere collegati ad alcuni eventi storici della Sicilia orientale come il 1169, il 1693 ed il 1908 e ad altri eventi provenienti dal Mediterraneo orientale come quello di Santorini (circa 3600 BP) e di Creta (365 AD).

A Pantano Morghella (Sicilia sud orientale) tre livelli di sabbia dello spessore di circa 10 cm, sono stati trovati intorno a 30 cm, 1 m e 4 m di profondità all'interno di una sequenza sedimentaria prettamente lagunare. Le analisi sedimentologiche, micro paleontologiche e l'uso di raggi X, hanno permesso di ricondurre il livello trovato a 1m di profondità ad un deposito di tsunami. Le datazioni con il metodo del radiocarbonio consentono di ipotizzare che questo evento sia relativo allo tsunami del 365 AD (terremoto di Creta). Ulteriori indagini sugli altri due livelli sono in corso per mettere in luce la loro possibile tsunamigenica origine e la loro eventuale età.

Accumuli di massi sono stati ritrovati in tre aree della Sicilia orientale (Capo Campolato, Vendicari and San Lorenzo) e sono stati studiati con lo scopo di distinguere il tipo di onda che li ha depositati lungo la fascia costiera, se tsunami o onda di tempesta. L'analisi effettuata ha permesso di dimostrare che le forti tempeste che avvengono nel Mediterraneo, producono onde in grado di trasportare sulla costa massi anche di grandi dimensioni e fino a notevole distanza. Tuttavia, alcuni massi che si trovano ad eccezionale distanza dalla costa, necessitano di un'onda più energetica, con un periodo più lungo delle onde di tempesta, per essere trasportati nella loro posizione. Quest'onda potrebbe essere uno tsunami o un'onda relativa ad una tempesta straordinaria mai registrata nel Mediterraneo in tempi strumentali. Le datazioni effettuate su due massi che si trovano ad una distanza maggiore dell'ambito delle tempeste, hanno messo in luce che almeno due eventi estremi sono avvenuti e questi possono essere ricondotti ad alcuni degli tsunami storici della Sicilia orientale (1169, 1542, 1693 e 1908).

La ricerca effettuata ha permesso di trovare evidenze di terremoti e tsunami sia storici che paleo- eventi, direttamente in sito, offrendo la possibilità di implementare e migliorare le tecniche paleosismologiche off- fault e di arricchire la casistica di questo tipo di effetti sismogeologici. Questo lavoro ha particolare rilevanza dal momento che la paleosismologia off- fault rappresenta una disciplina nuova della geologia dei terremoti inoltre poco testata in Sicilia orientale.

I risultati ottenuti confermano la potenzialità e l'utilità delle tecniche di studio paleosismologico off-fault e, se integrati con ulteriori dati forniti da futuri studi, possono contribuire alla definizione della sismicità della Sicilia.

Abstract

In this thesis a paleoseismological off-fault research, consisting in the analysis and dating of seismogeological effects triggered by both historical and paleo- earthquakes (seismites), was performed.

Off-fault paleoseismology results particularly useful in areas, like Sicily, where the seismogenic sources are scantly defined and so they can't be directly investigated by on-fault researches. Indeed, even if this study does not provide precise and direct information on the seismogenic fault and the earthquake parameters (magnitude, intensity, fault length and elapsed time), however, it can supply useful information on the epicentral distance of the site where the effects developed, the earthquake magnitude threshold and the intensity reached at the site. Moreover, the finding of structures dated before the historical records can be useful to extend the seismic catalogues back in time.

Sicily was affected by strong earthquakes among the most disastrous of the seismic Italian history, with intensity Io up to XI (MCS) and equivalent moment magnitude Mw up to 7 (CPTI04, Working Group 2004). The northeastern sector was destroyed by the 1908 Messina Strait earthquake and also suffered for seismic events located in southern Calabria, such as the 1783 seismic sequence. The southeastern sector was hit by the 1169 and the January 11th 1693 earthquakes and by other minor, however damaging, events such as the 1542 one. Western Sicily suffered a destructive seismic sequence started on January 13th 1968. Nevertheless, the seismogenic sources of these earthquakes are not well constrained because they occurred in pre-instrumental time and without clear evidence of surface faulting. Recently, different seismogenic source models have been proposed on the basis of geological and geomorphological evidences, historical and instrumental seismicity data and macroseismic intensity analyses, but the debate is still opened.

However, these strong earthquakes triggered several geological effects described by the historical accounts, such as landslides, liquefactions, ground deformations and fracturing, hydrological anomalies and tsunamis characterized by waves that damaged the cities along the eastern coast of Sicily.

Then, given its critic seismicity and its millenary historical memory, Sicily is an optimal laboratory to test different paleoseimological off fault methods.

This work was undertaken with the main aim on a side of providing new and useful data to better define the eastern Sicily seismicity, on the other side to test original multidisciplinary approaches in a region where this kind of investigations are scarce. Indeed, off-fault paleoseismology is a young and yet few tested discipline of Earthquake Geology. For this reason there is not a unique technique of investigation, instead methods need severe testing and systematization and every study case requires a specific approach related to the site conditions and to the seismite typology.

The performed research follows two different main lines: first the examination of the regional seismicity and of the historical accounts has been performed; then a multi-theme research was carried out in field to investigate directly the seismites.

The Italian historical bibliography reporting seismogeological effects in Sicily (original sources and previous seismic catalogues) has been analyzed. Descriptions of effects such as landslides, ground deformations, liquefactions, hydrological anomalies have been collected in a georeferenziated database embodying all the information about the causative event, as well. Interactive maps of effects distribution have been realized by the use of Gis software. These data have been also used to define empirical relationships between earthquake parameters (intensity and magnitude) and epicentral distance of the sites where the effects occurred. Then, upper bound-curves, at regional scale, have been realized.

This step of the research highlighted that Sicily is a region highly prone to the seismogeological effect development, especially as it regards landslides and ground deformations, mainly clustered in the eastern flank of Mt. Etna and in the northern sector of the region characterized by critical geological and structural setting. Whereas, liquefactions and hydrological anomalies occurred more numerous in areas with specific geological and hydrological features (Belice Valley and Catania Plain). Upper bound-curve graphs also showed that seismic parameters of some events could be misinterpreted, such as the magnitude of the 1823 earthquake (M = 5.87) that could be underestimated, while the new value proposed in the literature (M = 6.7) seems to be more plausible. The same analysis

indicated the happening of possible site amplifications and/or exceptional site response during some events as showed by effects occurred at unexpected long epicentral distance at Messina during the 1783 earthquake and at Calatafimi (Trapani) for the 1693 event.

Off-fault paleoseimological field study was focused to the finding and examination of liquefaction- induced deformations and tsunami deposits, because their investigation in field results easier than other effects. Indeed, liquefaction structures and tsunamiites remain in the sedimentary sequence as marker of seismicity and tsunami inundations; they have well defined features and take place in areas with specific characteristics, easily recognizable after geological and geomorphological surveys. On the contrary, for instance, hydrological anomalies are transitory phenomena and seismic landslides are not well differentiable from no seismic ones.

Hence, after a critical examination of the historical data indicating the localities where these effects occurred during past earthquakes, fluvial and coastal areas of eastern Sicily have been chosen. A further selection was performed using satellite imagines and aerial photos and by geological and geomorphological field surveys, aimed to define the most prone areas. In three sites (Minissale, Agnone and Vendicari) field study allowed to investigate deformational patterns linked to liquefaction mechanism. In other sites (Augusta, Pantano Morghella, Capo Campolato, Vendicari and San Lorenzo) probable tsunami deposits, both sand and boulder accumulations, were found.

As it regards the examination of deformational pattern, the detailed investigation of their features and a paleo-environmental reconstruction have been performed to exclude other possible causative mechanisms different from the seismic one. In general, the method for distinguishing subsequent events is based on stratigraphic criteria and cross-cutting relationships. When possible radiocarbon dating has been carried out, on charcoals and bulks, to constrain the age of the structures and to associate them with historical or paleo-earthquakes.

At Minissale (eastern flank of Mt. Etna, central eastern Sicily) and Agnone (Catania Plain, central eastern Sicily) liquefaction structures have been detected on two artificial trench walls. In these sites a preliminary hand-auger coring campaign was also performed

to characterize the stratigraphic sequence and to qualitatively evaluate the terrain liquefaction susceptibility. Then, the deformational patterns, consisting of lateral spreading, dikes, faults, drag folds, recumbent folds, sheet slumps, warped top levels and boudinage, have been studied by the square division method. Terrain samples have been collected for sedimentological and micro-paleontological investigations. Paleo-environmental reconstruction allowed to exclude other causative mechanisms and to associate these deformations to seismic shaking. Radiocarbon dating, combined with the upper bound curves, allowed to associate the seismites detected at Minissale site with the 1169 and 1693 earthquakes and those of the Agnone site with the 1542 and 1693 earthquakes.

At Vendicari (southeastern Sicily) a singular association of structures, affecting terrains since Pliocene up to Quaternary age, has been detected. Besides soft sediment deformations (autoclastic breccias, diapyr-like injections and thyxotropic wedges), probably linked to liquefaction mechanisms, brittle deformations, consisting of fractures generally opened and filled by sediments (sedimentary dykes) have been found. Fractures have been examined by a mesostructural investigation and the detailed observation under the microscope of filling material thin sections, as well, to highlight possible relationships with the regional stress field. After a critical analysis of the forms and the paleo-environmental reconstruction, seismic shaking was proposed as the most probable cause of the deformation development. Fractures could be also linked to the regional tectonics characterized by an almost NW-SE trending σ_1. The overall investigation of seismites at Vendicari highlighted at least four triggering seismic events, whose age is not precisely constrained given the lack of datable material. However, their finding mark that these events had magnitude greater than 5.0 and intensity greater than IX, that are the threshold values for which this pattern can trigger in the epicentral area.

The tsunamiite study was undertaken both searching anomalous sandy deposits and examining boulder accumulations along the southeastern coast of Sicily, inland and off-shore. This research required a multi-theme approach combining geological, geomorphological, paleontological, X-ray, petro-chemical, morphoscopic and magnetic examinations. Geophysical applications, analysing sonar chirp profiles, were a precious

instrument to find deposits off-shore. In some cases wave transport equations were used jointly with statistical analysis in order to determine the extreme events– geological or meteorological– responsible for the deposition.

At Augusta and Pantano Morghella (southeastern Sicily) anomalous sandy layers, whose analysis highlighted a tsunamigenic origin, were found into a fine sedimentary sequence. Augusta site probably recorded tree events inland but, given their old interval age, no correlation can be made with the historical record. Only the more recent level could be tentatively related to the 365 AD Crete tsunami. Eleven anomalous layers have been also found off-shore thanks to the geophysical investigation of sonar chirp profiles. The age of some of these layers well matches with some disastrous tsunamis that hit eastern Sicily in historical time (such as the 1169, the 1693 and the 1908 events) and with that coming from Eastern Mediterranean such as the 365 AD Crete tsunami and the event of Santorini (about 3600 BP). At Pantano Morghella three anomalous levels were found. Deep investigations on one of the layers highlighted that it can be ascribed to a tsunami and in particular to the 365 AD Crete one. Further investigations and dating are in progress to understand the tsunamigenic origin and to constrain the age of the further two levels.

Boulder accumulations at Capo Campolato, Vendicari and San Lorenzo, were studied with the aim to distinguish if they were deposited by storm waves or tsunamis. This analysis showed that strong storms occurring in the Ionian Sea are capable to emplace large boulders on the coast but up to a given distance from the shoreline. Indeed, boulders very far from the shore seem to require more energetic waves, with periods longer than that of known storms, to be deposited. These waves could be extraordinary unknown storm waves or tsunamis. Dating on some very far boulders highlighted the occurrence of at least two different probable tsunami inundations. The first event could correspond to the 1169, the 1542 or the 1693 tsunami, the second inundation can be ascribed to the 1693 or the 1908 tsunami.

The following research allowed to find evidences of both historical and paleo-earthquakes and tsunamis in field. Results confirm the potentiality and usefulness of the

paleoseismological off- fault methods and their integration with further information, provided by ulterior studies, should help to better define the seismicity of Sicily.

This thesis is divided in seven chapters. First a general definition of the geologic and tectonic setting of Sicily and of the seismic source models, proposed for the strongest earthquakes, are exposed (Chapter 1). Then, a brief treatise on paleoseismology and the investigation methods is provided (Chapters 2 and 3). Performed researches are discussed separately for each different approach, exposing methods and results in the Chapters 4, 5 and 6. Finally, in the Chapter 7 a summary and a discussion on the main matters of this thesis, the applicability and usefulness of this kind of researches are exposed, arguing on how they can contribute to the improving of the knowledge of the eastern Sicily seismicity.

1. GEOLOGICAL AND SEISMOLOGICAL FEATURES OF SICILY

Sicily lies in a sector of the Central Mediterranean region, whose tectonics and seismicity are the product of a complex geodynamics determined by the interaction of several crustal components (Ben-Avraham and Grasso, 1991; Lentini et al., 1996; Lentini et al., 2006). The present day geological setting of this region developed in consequence of an almost N-S convergence process between the Africa and the Eurasia plates that lead to the crustal collision, active since 65 Ma (Dercourt et al., 1986; Dewey et al., 1989; Patacca et al., 1990).

The geodynamic frame encloses the following structural domains: the foreland, the orogenic, and the hinterland domains (Ben Avraham et al., 1990; Lentini et al., 1996; Finetti et al., 1996). The foreland domain is represented by the Apulian and Pelagian Blocks, characterized by continental crust and by the Ionian Basin (Fig. 1.1), whose old oceanic crust has been partially consumed under the orogenic arc. The orogenic domain is composed of three superimposed tectonic belts: the External Thrust System that is the lowermost tectonic element, on which the Apenninic-Maghrebian chain overrode, and finally the Calabride chain lying at the top (Fig. 1.2). Finally, the hinterland domain is represented by the Tyrrhenian Basin, whose abyssal plane is made of new oceanic crust (Fig.1.1) (Ben Avraham et al., 1990; Lentini et al., 1996; Finetti et al., 1996).

Lentini et al. (2002) recognized two tectonic phases responsible of the orogenic domain building, characterized by compressive deformation tied to a thin-skinned tectonic context and that lead to the formation of two tectonic wedges. The first orogenic phase caused the development of the more ancient accretionary wedge, the origin of the Liguride- Sicilide nappes (late Oligocene–early Miocene), due to the subduction of the Tethyan Ionian oceanic crust and to the collision between the European margin and the “Maghrebian” continental crust, originally located between the Tethys and the Ionian oceanic crusts. The second orogenic phase occurred from middle Miocene times with the opening of the present-day back-arc Tyrrhenian basin and, at the end of Pliocene, the consumption of part of the Paleo-Ionian oceanic crust and the collision of the “Maghrebian” continental crust with the Africa and Adria ones (Finetti et al., 2005a).

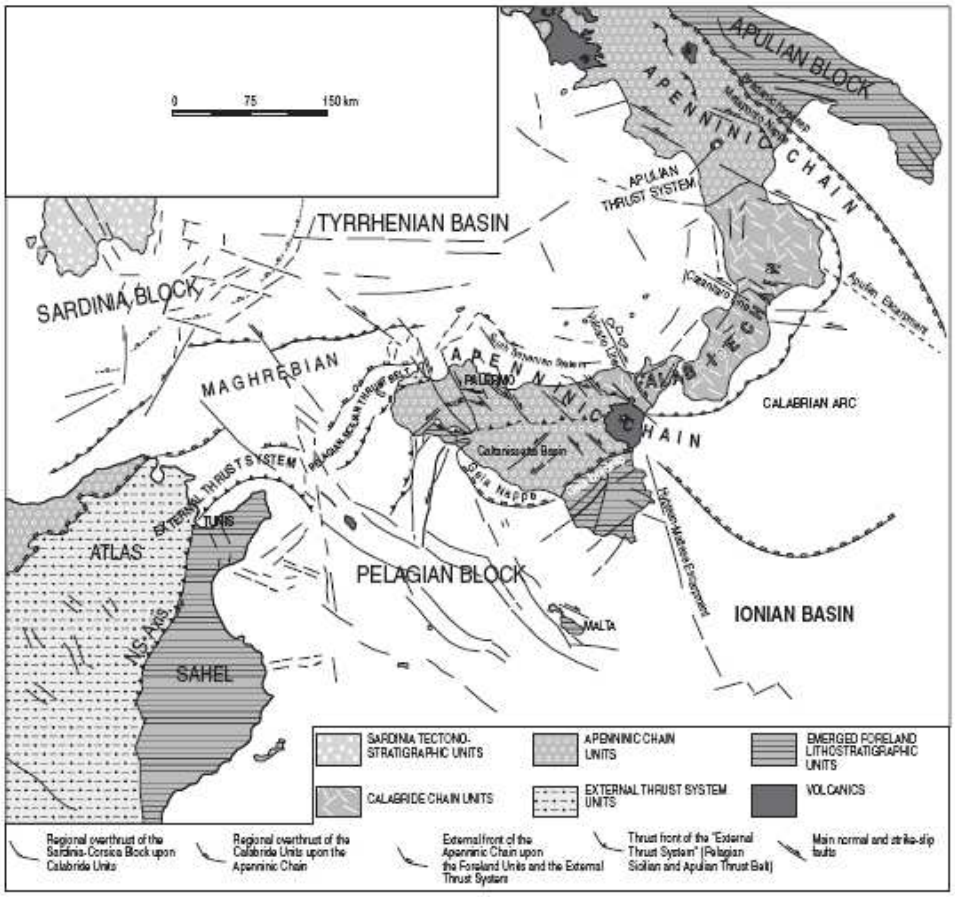

Fig: 1.1: Regional distribution of the structural domains in the central Mediterranean (after Lentini et al., 1996).

1.1 Geological and structural setting of eastern Sicily

In the eastern sector of Sicily, the foreland domain includes the currently undeformed continental areas of the Pelagian Block and, more at east, the Ionian basin. The Pelagian Block, that represents an east-west segment of the Africa continental margin (Dewey et al., 1989), has been separated since the late Paleozoic from the Apulian block (of the Eurasia) by the oceanic crust of the Ionian Basin. This Block is characterized by a 25–35 km–thick continental crust (Cassinis, 1979; Scarascia et al., 2000) that underlies a 6–7 km–thick

Mesozoic–Cenozoic shallow-water to basinal carbonatic sedimentary succession, with repeated intercalations of volcanites (Fig. 1.3). The Pelagian Block is separated to the east from the Ionian Basin by a north-south-trending tectonic discontinuity, the Hyblean-Maltese escarpment that partially affected the original margin of the Block and was responsible for the progressive collapse of its eastern margin facing the Ionian basin (Carbone et al., 1982a; Grasso and Lentini, 1982). The Hyblean- Maltese system, characterized by prevalently normal faults, was active during the Pliocene and the Quaternary (Scandone et al., 1981; Fabbri et al., 1982; Casero et al., 1984) and it also involved the eastern slope of Mount Etna volcano and seems to plays an important role in the seismotectonic evolution of the area (Carbone et al., 1982; Monaco et al., 2005). The Pelagian Block is divided into an uplifted element, the Hyblean plateau (Fig. 1.3) and a sector flexured north-westward below the tectonic units of the orogenic domain. The two sectors are separated by a system of northeast-southwest-oriented normal faults that delimit the Gela foredeep, which is fully occupied by the allochthonous units of the front of the chain, the Gela nappe (Bianchi et al., 1987; Grasso et al., 1990). The Hyblean plateau has been characterized by intermittent volcanic activity from the Triassic up to the early Pleistocene. The late Pliocene activity was marked by a drastic compositional change from mafic alkaline to tholeiitic and by the eruption of large volumes of lava.

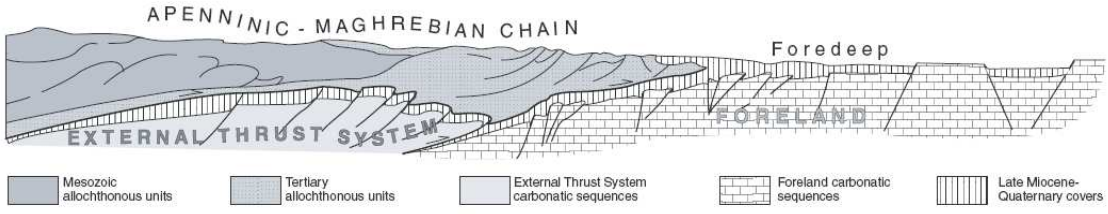

Figure: 1.2: Southwest-northeast-oriented schematic cross section of the southern Apennines showing the structural domains of the Apenninic-Maghrebian orogen (after Lentini et al., 1996).

This activity occurred when the north-western sector of the Hyblean foreland collapsed and the normal fault system developed, originating the foredeep (Behncke, 2001). The

younger volcanic units of the northern margin of the Hyblean foreland indicate a shift of the volcanic activity toward the Etna area.

The peculiarity of the orogenic belt mainly lies in a general duplex geometry, where the roof thrust system, some thousand meters thick, is composed of the allochthonous units of the Apenninic- Maghrebian chain, while the floor thrust is represented by the External Thrust System (Fig. 1.2). This latter has been generated by the detachment of the more or less rooted carbonate, representing the internal sedimentary covers of the flexured sector of the continental foreland. In Sicily it formed at the expense of the Africa plate covers and is represented by the Pelagian-Sicilian thrust belt, exposed in western Sicily (Pelagian-Sicilian thrust belt) where it consists of shallow-water (Triassic–Liassic) and pelagic carbonates (Middle Jurassic to early Oligocene) and of continental shelf to slope syntectonic terrigenous deposits (late Oligocene to early Tortonian). In the eastern sector of Sicily it is buried below the unrooted nappes of the Apenninic-Maghrebian chain and has been detected at high depth only in seismic lines.

The Sicilian Apenninic-Maghrebian chain widely overthrust the Pelagian-Sicilian thrust belt and in some cases tectonically overlies the margin of the foreland with the Gela nappe. This chain, forming an imbricated thrust system, originated in the late Oligocene, first at the expense of the sedimentary sequences that floored the oceanic crust of Tethys, the Alpine Tethys basinal sequences (Sicilide Units). Successively, since the middle Miocene, it formed through tectonic denudation of continental crust sectors due to the orogenic transport of the allochthonous carbonatic covers (the Panormide-Apenninic carbonate platforms) onto the Ionian basinal successions (the Ionides), interpreted as the original deposits of branches of the Paleo-Ionian basin (Lentini et al., 2002; Finetti et al., 1996).

The Calabride chain is constituted by the European margin delamination products and partially from those of the Austroalpine belt (Fig.1.3).

Sicily confines at north with the hinterland domain represented by the Tyrrhenian Basin, a triangular-shaped deep basin with a maximum depth of more than 3600 m, characterised by an oceanic crust. It developed since Neogene times by means of extensional processes affecting the Apenninic-Maghrebian orogenic system. From a morphotectonic point of view, the Tyrrhenian sector located between the abyssal plain and

the coastline of Sicily, Calabria and of the southern Apennine, corresponds to a paleoforearc basin developed since the late Miocene above the back-stop of the chain and the accretionary wedge (the Calabrian arc) (Guarnieri, 2005; Lentini et al., 2006).

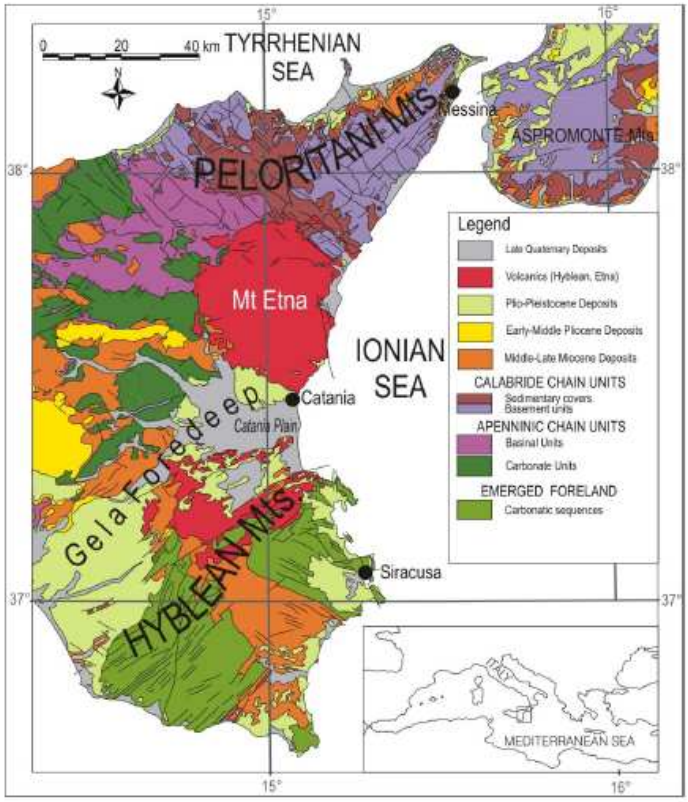

Fig. 1.3: Geological map of Eastern Sicily (after Lentini et al, 1996).

Present day geological setting of eastern Sicily is linked to the migration of the Apenninic-Maghrebian Chain front toward the Hyblean Plateaux, the collision between the orogenic back-stop and the Africa continental crust, the retreat of the Ionian subduction hinge (Malinverno and Ryan, 1986; Patacca and Scandone, 1989), and the roll-back of the African and Adriatic plates (Doglioni et al., 1994; Guarnieri et al., 2002). The collision continental, that results diachronous from west to east, began in late Tortonian times and has given rise to a transpressive tectonics with dextral movements (Ben Avraham et al.,

1990). In northern Sicily and its off shore, transpressive and transtensive tectonics is accommodate by a complex structural systems acting at different crustal levels (Finetti et al., 1996; Del Ben and Guarnieri, 2000). The superficial expression of the present collisional stage is the northwest-southeast right transcurrent fault system, named South Tyrrhenian System (Finetti et al., 1996). These structures caused differential shortening in the collisional margin, accompanied by the southeast-ward migration of the orogenetic front of the Calabrian Arc toward the Ionian basin (Lentini at al., 1996).

The retreat of the Ionian subduction hinge and the roll-back of the African and Adriatic crusts caused, in the sector containing the forearc basin, the collapse and the development, from the late Pliocene onward, of the present peri-Tyrrhenian margin (Guarnieri, 2005). Since late Pliocene– early Pleistocene times, an early southeast-ward migration of the subduction hinge has been accompanied by the development of NW-SE -trending tear faults and northeast-southwest-trending extensional systems. During middle–late Pleistocene times new NNW-SSE -trending tear faults (the Volcano and Catanzaro lines) (Fig. 1.1) and N70°E-trending collapse systems developed probably as a consequence of a second SSE-ward retreat of the subduction hinge that led to the structural reorganization of a new back-stop and a corresponding collapse behind it.

The remains of a Paleo-Ionian slab, probably deactivated, are detected by north-south-oriented offshore seismic lines close to the Palermo coastline; moving progressively toward eastern Sicily, the same old slab is recognizable in onshore seismic lines (Lentini et al., 2006). To the east of the Vulcano line, in north-eastern Sicily and southern Calabria, where the foreland is represented not by a continental crust but by the Ionian oceanic crust, the seismic imaging shows the subducted upper Ionian slab and highlights that no collisional setting occurs here. Deep seismicity of the Tyrrhenian Sea also confirm the presence of a north-westward subduction slab (Giardini and Velonà, 1991), while the absence of earthquakes up to 200 km below northern Calabria implies the presence of Tyrrhenian asthenosphere and the detachment of the oceanic lithosphere deeper than 200 km (Lentini et al., 2006).

On the basis of geological observations and seismological data, the Siculo-Calabrian Rift Zone (Monaco and Tortorici, 2000) has been proposed as an alternative model of the

most recent evolution phase of eastern Sicily and southern Calabria. According to this model an incipient Rift Zone affects this area and it manifests by a normal fault belt that runs from the Crati Valley (southern Calabria) to the Hyblean Plateau (south-eastern Sicily) for a length of about 370 km. The rift process developed since about 500 kyr, following the end of the subduction of Ionian lithosphere beneath the Calabrian arc (Wortel and Spackman, 1993; Westaway, 1993), in response to the large scale motion (Ward, 1994) characterizing the two blocks dissected by the rift zone.

The faults border the main Plio- Pleistocene basins of the region (Crati basin, Mesima-Gioia Tauro basin, Messina Strait) and they also control the eastern Sicily coastline, bordering wedge-shaped extensional basins in the Ionian offshore (Scandone et al., 1981; Casero et al., 1984; Monaco et al., 1995; Hirn et al., 1997; Bianca et al., 1999). On shore, the faults deform Upper Pleistocene-Holocene sediments and exhibit steep linear escarpments and typical geomorphologial features such as triangular and/or trapezoidal facets. This tectonics also seems to have reactivated pre-existing structures, as the northernmost portion of the Malta Escarpment Fault System as shown by the distribution of the crustal seismicity. Most of the events that have occurred in this area are located in the hanging walls of the main Quaternary normal faults thus suggesting a strong relationship between seismic activity and the growth of extensional structures (Monaco and Tortorici, 2000). Furthermore, these faults are considered to be responsible for the middle Pleistocene-Holocene volcanism of the eastern sector of the Aeolian archipelago (Stromboli, Salina, Lipari and Vulcano) and of the Mt. Etna (Mazzuoli et al., 1995; Tortorici et al., 1995; Monaco et al., 1995, 1997).

1.2 Eastern Sicily historical earthquakes and related seismogenic sources

Eastern Sicily falls on an almost continuous seismogenic belt capable of producing M ~ 7 earthquakes and that extends from the Calabrian Arc through the Messina Straits, as far as south-eastern Sicily (Fig. 1.4). According to the Italian earthquake catalogue (CPTI04 Working Group, 2004) some of the last millennium's most destructive earthquakes (Io > X

MCS) are located along the southernmost part of the Calabro–Peloritan Arc (1783, 1894 and 1908 earthquakes) and in south-eastern Sicily (1169, 1542 and 1693 earthquakes) (Fig. 1.4).

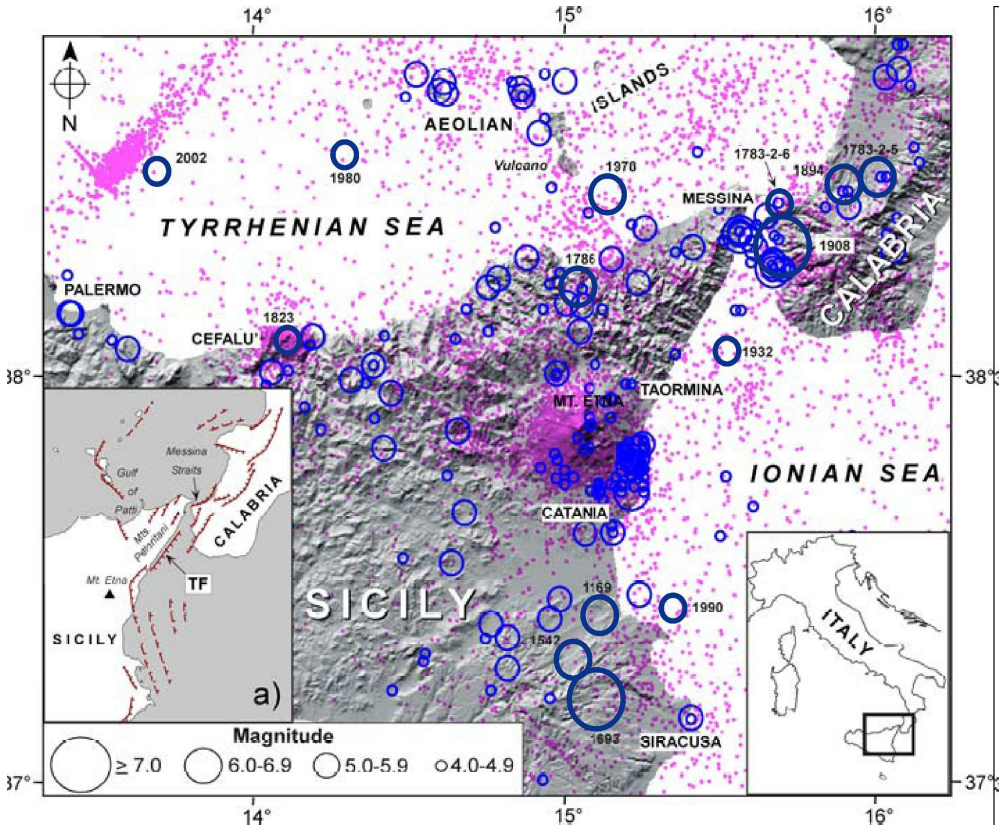

Fig. 1.4: Southern Tyrrhenian Sea and eastern Sicily epicentral map showing the location of historical earthquakes, blue circles (data from CPTI Working Group 2004) and the instrumental seismicity (2.2 ≤ ML≤ 4.0) from 1983 to 2002, full dots (data from Castello et al. 2005) (after Azzaro et al., 2007, modified).

Sources parameters for most of these events were assessed on the basis of historical macroseismic data and some Authors tried to realize source models combining macroseismic data with geological and geomorphological evidences (Fig. 1.5, 1.6) (Monaco et al., 1997; Bianca et al, 1999; Sirovich and Pettenati, 1999; Azzaro and Barbano, 2000). However, there are not yet enough elements to accurately define the seismogenic sources of eastern Sicily and there is still an open debate about their real

location. This uncertainty is mainly due to the fact that the majority of the earthquakes occurred before the seismic instruments development and without clear and unquestionable surface faulting evidences.

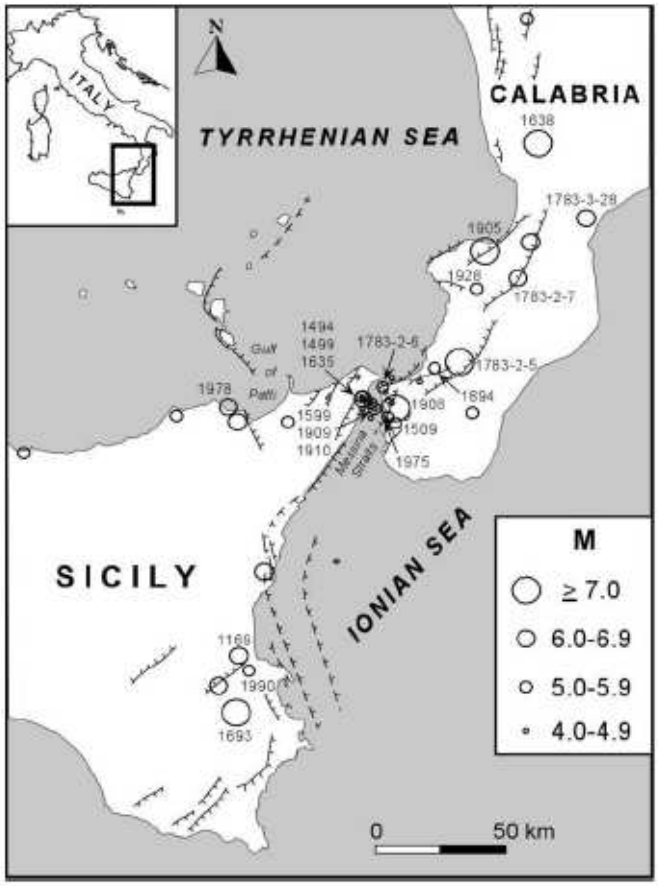

Fig. 1.5: Relationship between Quaternary faults and earthquakes (M ≥ 4); epicentres from CPTI04 (Working Group, 2004) (modified from Monaco and Tortorici, 2000).

Meletti (2008), reviewing existing models available for Italy and Europe countries, recently presented a new seismogenic model, termed ZS9, based on historical earthquakes data, instrumental seismicity, active fault models and seismotectonic evidence from recent earthquakes (Fig. 1.7). In this model Sicily encloses five seismic source zones (Fig. 1.7a).

The DISS database 2009 (Working Group, 2009) brought together a large amount of published and original data along with geographic, seismological, geological and tectonic

information defines the seismogenic sources, having a potential for a M $\geq$ 5.5, for the whole Italian country and for Sicily (Fig. 1.7).

North-eastern Sicily was hit by the strong December 28th 1908 earthquake (Mw = 7.2, Boschi et al., 2004) that was one of the most disastrous event never occurred in the Italian history. It caused the complete disruption of the Messina and Reggio Calabria cities and widespread damage in several localities of Sicily and southern Calabria. Moreover 40 feet (12 m) high tsunami struck nearby coasts causing even more devastation (Baratta, 1909).

Models proposed for this event generally locate the source in the Messina Strait (Fig. 1.5, 1.6 and M1 and M2 in Fig. 1.7 b). Proposed faults are all normal one, but they differentiate for the strike and dipping (Fig. 1.6). However, the most accepted model is that of a crustal blind E-dipping, low-angle, normal fault, with a minor strike-slip component (Pino et al. 2000). Bottari et al. (1986), on the basis of macroseismic data, considered a northeast-southwest striking fault with west dipping directions. On the basis of levelling data inversion Capuano et al. (1988), Boschi et al. (1989) and De Natale and Pingue (1991) performed source models involving east-dipping faults characterized by low dipping angles (30-40°), differing mainly for the strike direction and fault dimensions. Valensise and Pantosti (1992) hypothesize a source dipping mainly toward east that would be responsible of the 125-ka marine terrace deformation and uplift on both the side of the Messina Strait. On the basis of geological and morphological data Monaco and Tortorici (2000) consider a north-south to northeast-southwest striking fault with west-northwest dipping directions as responsible of this event (fig. 1.5). A further model proposed by Jacques et al. (2001) considers a southwest dipping normal fault (M1 in Fig. 1.7b).

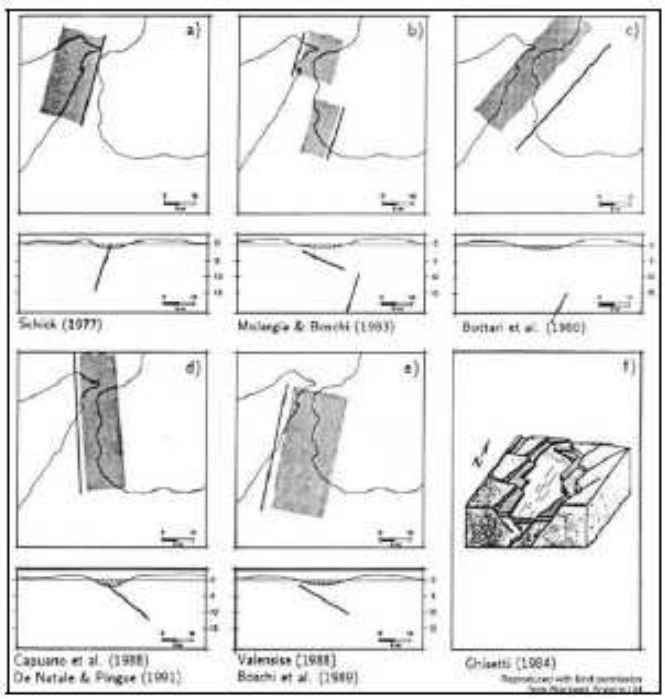

Fig. 1.6: Source models proposed for the 1908 earthquake (after Pantosti and Valensise, 1992).

The 1783 Calabrian seismic sequence ($5.9 \leq Mw \leq 6.9$) caused very strong earthquakes occurred in a short span time (February-March) and it was able to damage several places of north-eastern Sicily. The second event of this sequence, occurred on February 6 th, caused a big landslide-induced tsunami. A possible source proposed for this earthquake is the Scilla fault (SF in Fig. 1.7b) (Jacques et al., 2001). A further strong Calabrian event causing damage in Sicily was the 1894 earthquake (Mw = 6.0).

Meletti (2008) included the earthquakes of southern Calabria and northeastern Sicily into the 929 zone, characterized by a seismically active set of approximately NNE-SSW trending extensional faults (Tortorici et al., 1995, Monaco and Tortorici, 2000, Monaco et al., 1997) (Fig. 1.7b). This zone involves the Crati, Savuto areas, the Mesima basins and the Messina Straits.

Moreover, the faults of southern Calabria and northeastern Sicily have also been associated with the DISS09 (Working Group, 2009) source zone named ITCS069-Southern

Calabria (A in Fig. 1.7a) enclosing the source of the February 6th 1783 and 1908 earthquakes (SF and M1 respectively, in Fig. 1.7b).

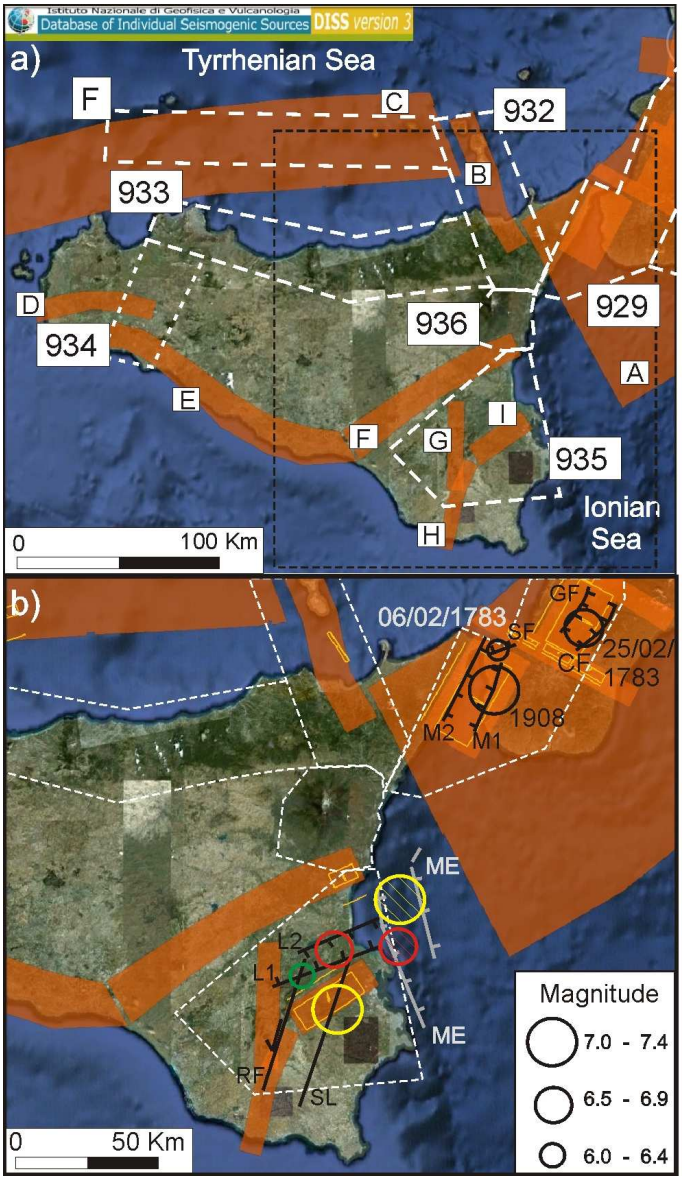

Fig. 1.7: a) Google Earth Map and some seismogenic sources proposed in literature: white dashed lines delimitate the seismogenic zones by Meletti el al. (2008); orange areas are seismogenic zones by DISS09 (Working Group, 2009); rectangle is the location of figure b; b) seimogenic source models compared with epicentre location of some of the strongest historical earthquakes, marked by circles: unfilled circles from the CPTI4 catalogue (Working Group, 2004) and filled circles from the NT4.1 catalogue (Camassi and Stucchi, 1997). Possible source proposed for the February 6th 1783 earthquake is the SF = Scilla fault (Jacques et al., 2001); for the December 28th 1908 earthquake the M1 = Straits of Messina fault (Jacques et al., 2001) and M2 = Straits of Messina fault (DISS Working Group, 2009 and references therein). For south-eastern Sicily red circles indicate two different source models for the February 4th 1169 event, yellow circles indicate that proposed for the January 11th 1693 event; green circle indicates the location of the January 9th 1693 event. Possible seismogenic faults proposed for the January 11th 1693 earthquake are: L1-L2 faults associated with the Scordia-Lentini graben (D'Addezio and Valensise, 1991); SL = Scicli Line (Sirovich and Pettenati, 1999); ME = Malta Escarpment (Azzaro and Barbano, 2000; Jacques et al., 2001); RF = Ragusa fault (DISS Working Group, 2009).

The north-eastern sector of Sicily, between Messina and Cefalù, suffered some comparatively minor earthquakes such as that of the 1786 (Mw = 6.0), the 1823 (Mw = 5.8) and the 1978 Patti Gulf earthquake (Mw=6.1) (Fig. 1.4). Some of these events was considered in the 932 source zone of Meletti (2008) (Fig. 1.7a), enclosing the transfer faults that accompany the slab retreat beneath the Calabrian Arc plus the faults responsible for the segmentation of the E–W Cefalù basin and Patti Gulf. Some of these faults are also enclosed into the ITCS042- Patti Eolie zone of the DISS09 (B in Fig. 1.7a).

Zone 933 (Fig. 1.7a) partially overlaps with the Mt. Kumeta–Alcantara fault system, a large and presumably active corridor that extends between Mt. Etna and Palermo. This relatively low-seismicity zone, originally proposed by Ghisetti and Vezzani (1984), is characterised by extensional and strike-slip kinematics, but its geometry is not very well defined from the point of view of active tectonics. This zone collects a number of historical earthquakes, e.g. the September 1st 1726 (Mw 5.6), the March 5th 1823 (Mw 5.9) and the January 15th 1940 (Mw 5.3).

The southernmost sector of the Tyrrhenian sea is characterized by a seismogenic belt named F zone by Meletti (2008) and ITSA014 Southern Tyrrhenian according to the DISS09 (C in Fig. 1.7a). This zone, that also comprises part of the western Aeolian seismicity, includes some events of the instrumental era such as the September 6th 2002 earthquake (Mw 5.9), that caused minor damage to Palermo (Azzaro et al., 2003), and other relatively large events (Pondrelli et al., 2004; Vannucci et al., 2004).

Moreover, this zone could include some significant historical earthquakes whose sources are currently located inland, in the Zone 933, but with high uncertainty. Indeed location of these events is based on the modelling of intensity pattern (Gasperini et al., 1999), but unfortunately the computer code used for this reconstruction has a known tendency to place on the coastline earthquakes that occurred offshore. As showed by the case of the 2002 earthquake, the lack of intensity points offshore causes the shift onshore of the epicentre (Azzaro et al., 2004). Even if there aren't strong enough historical evidence to relocate offshore the strongest earthquakes occurred in this area in the past centuries, several Authors considers that these events may be ascribed to offshore seismic sources as strongly supported by the distribution of the instrumental seismicity of the last two decades,

that defines a cluster of earthquakes along an E-W trending strip, developing north of the Sicilian coast (Azzaro et al., 2004).

The March 5th 1823 earthquake (Mw 5.9) heavily afflicted Palermo and it also damaged sites further east in a large area along the Tyrrhenian coast (Imax = 8–9 MCS) and was felt almost throughout the whole of Sicily (Boschi et al., 1995). The macroseismic epicentre of this event proves to be inland near Cefalù and was hardly related to the activation of inland structures on the basis of the elongation and asymmetry of its intensity pattern. Recently the hypothesis that the epicentre of this event could be located off shore on the Tyrrhenian Sea and that its parameters could have been underestimated was advanced (Azzaro et al., 2004; Meletti, 2008). According to Meletti (2008) if this earthquake occurred in zone F, its magnitude would has been underestimated and should hence be reassessed. For instance on the basis of scaling relationships derived for the 2002 earthquake (observed Mw 5.9; intensity-based Mw 5.1) the 1823 earthquake would have magnitude reaching 6.7.

In western Sicily the almost W-E seismogenic zone of DISS09 named ITSA021 Marsala Belice (D in Fig. 1.7a) partially corresponds with the about NNE-SSW-trending, 934 zone, by Meletti (2008) (Fig. 1.7a). In this zone only one destructive sequence occurred: the Belice seismic period that started on January 13th 1968 (Mw 6.1). However different seismotectonic hypotheses have been performed on the basis of geological investigations (Michetti et al., 1995; Monaco et al., 1996). Some Authors consider that this seismogenic area represents a portion of foreland affected by large strike-slip faults and that the source of these events is part of a “flower” structure belonging to this system. Another hypothesis considers the source as a S-verging blind thrust having an E–W direction (Valensise and Pantosti, 2001). However, no conclusive evidence on the location and geometry of the causative source has been given.

The southernmost belt of Sicily encloses the ITSA006 Castelvetrano-Gela seismogenic area (DISS09, Workink Group, 2009) (E in Fig. 1.7) linked to the Apenninic Maghrebian orogenic belt advancing.

The sector along the Ionian coast between the Messina Straits and the Mount Etna, represents an area of lacking of relevant seismic activity evidence in historical times. In this area, analysing some young geomorphologic elements, such as Holocene marine notches

and raised terraces, some Authors observe evidence of abrupt vertical movements and propose them as consequence of repeated coseismic displacements due to the motion of seismogenic faults belonging to the Siculo Calabro Rift Zone (Stewart et al., 1997; De Guidi et al., 2003). These faults would be responsible of three events in the past 5 ka, the strongest of which (M ~ 7) was dated at about 3.2 ka (De Guidi et al., 2003). However, the seismicity of this sector was recently revaluated. Indeed, the location of March 28 th 1780 event, originally established near Messina, was reconsidered by Azzaro et al. (2007) after a systematic analysis of the 18th century journalistic sources (gazettes). According to the new model this event was considered as the main shock of a seismic sequence located on the Ionian coast of north-eastern Sicily. Therefore, different epicentral parameters and a higher macroseismic magnitude (Io = VII–VIII MCS, Mw = 5.6) were considered for this event.

More at south, the Etna region represents one of the most active volcanic areas worldwide, characterized by moderate (2,9< M< 4.8) shallow (H < 5 km) earthquakes (Fig. 1.4) producing macroseismic intensities reaching even the IX-X grade (MSK) an occurring with short recurrence time (tens of years) (Azzaro, 1999). According to Meletti et al. (2008) the source zone surrounding Mt. Etna volcano (936 in Fig. 1.7) includes seismogenic features completely different from the rest of Sicily linked to the volcanic activity. Recent studies have been devoted to the clarification of the relationships between tectonics and shallow sesmicity in this area (Lo Giudice and Rasà, 1992; Gresta et al., 1997; Monaco et al., 1997) but at the present these relationships are not well defined. However, the earthquake occurred on February 20th 1818 in this area has been considered a tectonic event, that could be related to a segment of the Maghrebide thrust system as already hypothesized by Lavecchia et al. (2007).

In south-eastern Sicily, nearly 60% of the accumulated strain has been released by only few large earthquakes during the last millennium, the February 4th 1169 (Mw = 6.6, Working Group CPTI, 2004), the January 9th 1693 (M= 6.2) and the January 11th 1693 (M= 7.4, Io up to XI MCS, Working Group CPTI04, 2004) earthquakes.

The large 1169 earthquake (Fig. 1.4; 1.5; 1.7b) was one of the strongest events, it is among the better described by the historical reports and hit with high intensity south-

eastern Sicily causing large damage. This strong earthquake was also followed by a disastrous tsunami.

The January 11th 1693 earthquake and its large January 9th 1693 foreshock (Fig. 1.4; 1.5; 1.7b) belong to a long seismic period that destroyed several localities of Eastern Sicily. Numerous descriptions of damage and ruins are reported by the historical sources for these events that were felt in the whole Sicilian country and also caused a damaging tsunami.

The December 10th 1542 earthquake (Mw = 6.6) (Working Group CPTI, 2004) was less strong but however damaging and was also followed by a strong tsunami. It represents the main shock of a seismic period that started in the last day of November and lasted 40-days (Chronaca Siciliana, 16th century). Damage related to this event, run from the Ionian coast up to Caltagirone in the central part of Sicily.

Given the lack of surface faulting evidence, the sources of the previously described earthquakes have been approximately located in the southern sector of eastern Sicily and tentatively associated to some active faults observed by geological- structural and geomorphologic approaches or modelled by processing levelling data and macroseismic data analyses (Fig. 1.5 and 1.7b).

The 935 zone proposed by Meletti et al. (2008) (Fig. 1.7a), enclosing the Hyblean Plateau area and whose eastern boundary coincides with the Malta Escarpment, hosts some destructive events of south-eastern Sicily such as the previously described January 9th 1693 and January 11th 1693.

The DISS09 associated the 1169, 1693 and 1818 events to the ITCS029 Gela –Catania Seismogenic source (F in Fig. 1.7a), located along the NE-SW trending outermost front of the Maghrebian thrust belt and running along the inner margin of the Gela- Catania foredeep. Moreover, the January 11th 1693 quake is also associated to the ITIS036 source named Monte Lauro (I in Fig. 1.7). However, according to DISS09 the Hyblean Plateaux is characterized by other seismic areas that could enclose the important events occurred in southeastern Sicily, such as the ITCS035 Ragusa-Palagonia (G in Fig. 1.7a), encompassing the northern portion of the Scicli Fault Zone, that is the most prominent structural element of the Plateaux, and the ITCS017 Scicli Giarratana (H in fig. 1.7) encompassing the central and southern portion of the Scicli Fault Zone.

Several authors proposed source models for the January 11th 1693 earthquake, associated both with inland active faults and with the off-shore fault system of the Malta Escarpment. On the basis of geologic, geomorphic or macroseismic intensity analysis D'Addezio and Valensise (1991) consider an on-land normal fault within the Scordia-Lentini graben as the seismogenic fault (L1 and L2 in Fig. 1.7b). Valensise and Pantosti (2001) suggested that this earthquake was caused by a splay of the NNE-SSW Scicli–Ragusa fault system (SR in Fig. 1.7b). This hypothesis had already been put forward by Sirovich and Pettenati (1999) that associate this event to a blind strike slip fault, parallel to the Scicli line (SL in Fig. 1.7b) and was also backed by the work by Barbano and Rigano (2001). Current seismic activity of the inner Hyblean Plateau is also supported by large-scale tectonic reconstructions (Bousquet and Lanzafame, 2004) and seismological data (Musumeci et al., 2005), while the left-lateral reactivation of the southern portion of the Scicli–Ragusa fault is the object of ongoing field investigations (Catalano et al., 2006). A further recent interpretation considers the likelihood of two main shocks during the January 11th 1693 associated to two different compressive seismogenetic sources at south and at north of the Catania Plain. The southernmost one is the NNE-SSW trending, left-lateral strike-slip fault running through the Hyblean region, partially coinciding with the Mt. Lauro Fault (ITIS074 according to the DISS08; Basili et al., 2008); the northernmost proposed source is the Gravina di Catania Fault (ITIS106 according to the DISS08; Basili et al., 2008), a northeast southwest trending, low-angle thrust recognised at the front of the Maghrebian Thrust Belt. This thrust probably represents the superficial expression of a major seismogenic source located on the north of the Catania Plain (Sleiko and Valensise, 2007).

The off-shore models for the 1693 earthquake are based on tectonic and seismic prospecting data analysis and suggest the rupture of a segment of the Hyblean-Malta escarpment (ME in Fig. 1.7b) (Azzaro and Barbano, 2000; Jacques et al., 2001) or of a locked subduction zone fault, part of the Ionian slab, more at south-east (Gutsher et al., 2006).

2. EARTHQUAKE GEOLOGY

"Enormous landslides fall on farms; entire towns come down for soil downfall; scary sea waves take away builds, people and everything that they meet along the way; large potholes opened getting down carts, farmers and animals; glows lighted up the nocturnal sky transforming the night to day, the water became red in colour and the air became unhealthy" (Bonito, 1691; Mongitore, 1743; Longo, 1908; Baratta, 1909). All these phenomena are described, since old time, by witnesses during strong earthquakes worldwide and they frightened people also fomenting beliefs and superstitions. Today these effects are better known and carefully studied by the scientific community also because they can represent the first cause of damage during the earthquakes.

Indeed, strong earthquakes, generally with M>5, are capable to produce effects on the geology and geomorphology, like ground fracturing and opening, dislocation and tilting, landslides, tsunamis and effects on the rivers and aquifers. Many of these geologic structures can rest recorded as fossil marker of seismicity, testifying the occurrence of past earthquakes. These fossils are generally defined by the international scientific community *seismites* (Seilacher, 1969; Vittori et al., 1991) and are investigated by means of Paleoseismological studies.

Since Paleoseismology is a young discipline of Earthquake Geology, more than a classification has been given by the literature for the seismites. However, an absolute distinction in classes is not always easy also because the seismites often occur contemporary and the relationships with the seismogenic source can be not clear. Nevertheless, a division in category is necessary because the paleoseismological approaches change on the basis of the seismite typology.

Vittori et al. (1991) define as seismites any geologic effects produced by earthquakes.

Michetti (1991; 1994) distinguish three main classes of coseismic effects, *class-A* includes those induced by the shaking; *class-B* those produced by the tectonic deformation at regional scale (uplift, subsidence, tilting); *class-C* those due to surface faulting (ground fracturing and dislocation) (Tab. I).

Effects induced by an earthquake can be "*primary effects*" that are a direct consequence at surface of the deformation at the main-shock depth on the seismogenic

fault, and "*secondary effects"* that are indirectly linked to the fault activity, because they are not trigger by the fault movement but by the seismic shaking and the seismic wave propagation in the sediments. Both the effects can have consequences on the geomorphology and the stratigraphy (Tab. I) (McCalpin and Nelson, 1996).

Tab. I Hierarchical classification of seismogeological effects according to McCalpin and Nelson (1996) modified and simplified; letters at the apex refer to the Michetti's (1991) classification.

	On fault	**Off fault**
Primary	**Geomorphic effects** Fault scarp[C] Fissures[C] Fold[B] Moletracks[B] Pressure ridges[B] **Stratigraphic effects** Faulted strata[C] Folded (tilted) strata[B] Colluvial wedge Fissure fills[A/C]	**Geomorphic effects** Tilted surfaces[B] Uplifted shorelines[B] Drowned shorelines[B] **Stratigraphic effects** Tsunami deposits
Secondary	**Geomorphic effects** Sand blows (liquefaction) [A] Landslides[A] **Stratigraphic effects** Sand dykes[A] Rapidly deposited lake or estuarine sediment	**Geomorphic effects** Sand blows (liquefaction)[A] Landslides[A] Fissures[A] **Stratigraphic effects** Sand dykes[A] Turbidites[A]

Seismites can also be divided in those developing on the fault (*on-fault seismites*) and those developing at some distance from it widespread in the epicentral area (*off-fault seismites*) (Tab.I).

Another distinction can be performed on the basis of the time when the effects develop. Primary effects can be defined "*short term primary effects"* because they occur contemporary to earthquake happening; these effects can be surface faulting, including permanent displacement (uplift and subsidence). Secondary effects can be *"short term"* effects if they occur suddenly and like contemporary or short time after the quake occurrence. These effects include liquefaction, landslides, tsunamis and floods. Secondary effects, linked to the tectonic processes for which the earthquake occurred and that develop slowly during the time, are defined "*long term secondary effects*". These include deformation developing at regional scale, linked to subsidence or uplift of

landmasses and regional change in groundwater levels, or modification of the fluvial network (Keller and Pinter, 1996).

2.1 Primary effects

Fault movement during the earthquakes can produce geomorphologic modifications in proximity of the fault itself or far from it. Scarp development, fissures, fold occur as *on-fault* geomorphologic structures. Vertical deformation, including both uplift or subsidence and ground surface tilting can occur no many far from the fault as *off-fault* geomorphic effects. The slip along the fault can also perturb the equilibrium of geomorphologic elements and produce anomaly of the geological processes causing their acceleration or modification in the tentative to restore equilibrium. Fluvial network, fluvial or marine terraces or lakes are particularly prone to these modifications (Tab. I). Indeed, river systems are the most sensitive elements capable of quick adjusting both over periods of decades and of centuries (Keller and Pinter, 1996).

Fault movement and dislocation cause on the stratigraphic sequence effects like faulted, folded or tilted strata; fissure fills; colluvial wedges due to the acceleration of erosional/depositional processes in effort to restore equilibrium (*on-fault* stratigraphic structures). Moreover, off shore fault displacement can produce a tsunami that can left a particular deposit in the stratigraphic sequence named *tsunamiite* (*off-fault* stratigraphic structures) (Tab. I).

Surface fault rupture is the manifestation of the displacement where the fault slip extends up to the ground surface. In the international literature the term “surface faulting”, or “earthquake fault”, corresponds to the whole of tectonic dislocation (scarps, fractures, downwarping and upwarping) that generally form on the ground surface as a consequence of strong crustal earthquakes (Fig. 2.1) (Michetti, 1994). However earthquake surface faulting not necessary corresponds to the seismogenic fault but it can be simply a physical consequence of movement on primary source. The common classification of earthquake faulting includes its relevance in term of seismic activity. A fault having a significant potential for relative displacement at or near the ground surface during future earthquakes is defined a *capable fault* (Michetti, 1994;

IAEA 1991, 2002). This fault can also be an *active fault* if it moved during the past 10ky and if it is capable to move with potentially damage effects in a span of time of social interesting. Moreover, a capable and active fault can also be a *seismogenic fault* if it has produced at least an earthquake in historical time and in a span of time of social interest, detectable on instrumental bases or of macroseismic data (analysing the historical data on damage and on the effects at the surface which allow to define the macroseismic epicentral area). However, capable and active faults can be *non seismogenic* if they are only physically linked to the seismogenic one and moves during an earthquake with it, but their fault plane doesn't embody the quake focus.

Surface faulting is the most relevant among primary earthquake effects, because the detection and successive study of the seismogenic source, and/or other faults physically linked to it, allow obtaining information on the seismic history of that source useful to know future earthquake occurrence (*paleoseimological on-fault study*, see chapter 3).

Generally, fault rupture reaches the surface only during moderate- to large-magnitude earthquakes with a hypocentre depth of less than 15-20 km and magnitudes greater than 6.5 (Bonilla and Buchanan, 1970). Surface faulting length may range from a fraction of an inch to 80 km (in some cases over 200 km) (Fig. 2.1) and offsets up to several meters (about 4-7 m) (Fig. 2.2) in a narrow zone along the main fault trace, depending on the earthquake magnitude, steepness of the fault plane, type of movement and so on. These same factors, as well as the nature of the geologic materials, also influence how wide the zone of surface rupture is likely to be (Pantosti and Yeats, 1993).

Fig. 2.1: Surface faulting of the 1915 Pleasant Valley Earthquake, Nevada (M= 7.5) (http://www.usgs.gov/).

Fig: 2.2: Fault scarp of the Irpinia 1980 earthquake (from Pantosti et al, 1993).

In particular areas, such as volcanic zones (e.g. Mt. Etna) surface faulting occurs for low magnitude threshold, even less than 4, due to local unusual tectonic conditions (Buchanan-Banks, 1987; Rasà et al, 1996; Smith et al., 1996). These areas are also characterized by very shallow seismic sources ($h < 2$ km) and low stress-drops.

Not all moderate-to large-magnitude earthquakes produce fault slip at the ground surface. In some cases, the fault displacement may occur entirely at depth, with little or no apparent permanent surface deformation (e.g., 1989 Loma Prieta, California earthquake of Mw 7.0) or with more subdued or diffuse surface warping and fracturing (as the 1994 Northridge, California earthquake of Mw 6.7). However, these earthquakes can produce at the surface other effects on geology and geomorphology (see also Paragraph 2.2).

2. 2 Secondary effects

Seismic wave propagation in the sediment and shaking at the ground surface can cause instability of slopes and basins and excess in pore water pressure of the

sediments, triggering for example turbiditic flows, landslides, liquefactions and fractures, finally hydrological modifications. These effects develop in the mesoseismic area, more numerous and evident near the epicentre, in proximity of the seismogenic fault, becoming scarce and feeble away from it: *on-fault* and *off-fault* secondary effects. The development and entity of these seismites depend on the seismic parameters, such as earthquake magnitude (they are generally triggered for a threshold of magnitude M=5), intensity, depth, duration and frequency of shaking and direction of slip and on the topographic and lithological site conditions.

Secondary effects can represent the primary hazard to the build and environment associated with earthquakes, causing more damage than the seismic shock itself.

Given that these effects develop quickly in the sediments that are exposed to the erosion and other geologic processes, they are generally prone to be easily cancelled. However seismites can rest preserved in the sedimentary sequence, when they occur under the ground surface or they are quickly buried by successive sedimentation.

Among secondary effects the most frequent and spectacular are sediment liquefactions, ground fissuring and landslides. They generally occur suddenly during the earthquake but some of them, e.g. landslides, can occur a brief period after the seismic wave passage.

Landslides, liquefactions, ground deformation, hydrological anomalies and tsunamiites are the topic of this thesis because they triggered during the strongest earthquakes of eastern Sicily, as reported by the historical accounts. These effects can also occur for mechanisms not linked to the earthquake but to processes internal of the sedimentation environment or to other no seismic external ones. Then, they can be defined “seismites” after a critical analysis aimed to exclude all the other possible causative mechanisms.

2.2.1. Landslides and rock-falls

Landslides are among the most important and dangerous seismically-induced phenomena, causing severe damage and great loss of life (Fig. 2.3). The 1970 earthquake in Peru caused more than 70000 fatalities, about 20000 persons were killed

by a landslide; the Loma Prieta 1989 earthquake caused extensive landslides damaging towns, roads and other structures.

Landsliding occurs due to the propagation of the seismic wave and ground shaking which cause intra-particle vibration and loss of soil strength and inertia forces. Moreover, shaking-caused dilation of soil materials should allow rapid infiltration of water making the slope more prone to slide. Landslides can also be due to earthquakes as a consequence of the sediment liquefaction.

Seismically induced landslides can develop in stable slope as neo-activation slides or they can be the reactivation of pre-existing landslides. The morphology and internal processes which occur into a seismically-induced landslide are the same of a no-seismic one, so it can be classified according to the standard classification adopted in the literature (Varnes, 1978; Cruden and Varnes, 1996).

Landslide occurrence can also produce other effects e.g. modification of the fluvial network with lake development (Adams, 1981; Perrin and Hancox, 1992). In coastal area the fall of big sediment masses into the sea can produce devastating tsunamis. For example, during the February 6th 1783 southern Calabria earthquake numerous landslides occurred (Fig. 2.4) (Sarconi, 1784; Baratta, 1910; Cotecchia et al., 1986), also causing modification of river courses and weir lakes (Torcia, 1783; Minasi, 1783). Moreover a destructive tsunami was probably produced by a large volume of rock fell in the Messina Strait (Billi et al., 2010) recently associated to the Mt. Paci landslide (Reggio Calabria) (Mazzanti, 2008).

Several factors are predisposing causes for slope sliding. Geological factors are weak or sensitive materials; sheared, jointed, or fissured and weathered materials; adversely oriented discontinuity (bedding, schistosity, fault, unconformity and so forth); contrast in permeability and/or stiffness of materials. Other causes can be linked to tectonic or volcanic uplift, glacial rebound and subterranean erosion. Moreover, the human activity in terms of slope excavation activity, loading of slope or of its crest, drawdown (of reservoirs) and deforestation, can be a very significant predisposing cause.

Fig. 2.3: Landslide triggered by the Soloman Islands (M=8.0) earthquake April 2, 2007 (http://www.usgs.gov/).

Among the triggering causes the most important is slope saturation by water due to intense rainfall, snowmelt, changes in ground-water levels, and water level changes along coastlines. Landslides due to volcanic activity are also some of the most devastating types. Volcanic lava may melt snow at a rapid rate, causing a deluge of rock, soil, ash, and water that accelerates rapidly on the steep slopes of volcanoes, devastating anything in its path. These volcanic debris flows (also known as lahars) reach great distances. However their development is restrict close to the volcano.

In areas that, like Sicily, are characterized by high seismicity, overuse of its mountainous and hill lands and extreme climatic phenomena (alternating intense rainfall and snowmelt to drought periods), earthquake induced landslides are not easily distinguishable from no seismic one. In these countries, beside a careful geological analysis, the unique criteria to asses a seismic origin to the landslides is the use of the historical data, reporting their occurrence during the earthquakes (Fig. 2.4). Indeed, Nicoletti (2005) associated 15 landslides, observed in south-eastern Sicily, to some of the historical earthquakes occurred (the 1169, 1542 and 1693 events) on the basis of the coeval sources and papers available in the literature.

Fig. 2.4: Landslide triggered by the 1783 earthquake at Oppido (Calabria, Italy) (after Sarconi, 1784).

2.2.2 Ground deformations

Earthquake induced shaking can trigger deformation of the ground surface, producing anastomosing open fissures (Fig. 2.5), ground settlement and change of the topographic level. They can also form as a consequence of adjustment of the underground due to both the fault movement and the terrain movement and compaction caused by the seismic shaking. Moreover, these effects can be the superficial expression of an incipient landslide or of underground liquefaction phenomena. Indeed, fractures can develop in a cemented unliquefiable level that, lying on a liquefied one, cracks forming clods that float and move laterally especially under a gravitative gradient (Fig. 2.6). This mechanism is named *lateral spreading* (Obermeier, 1996).

Montenat et al. (1991, 2008) consider opened fractures filled by sediments, named *sedimentary dykes*, as the product of the deformative adjustment near the fault during the earthquake (Fig. 2.7); these cracks can also be roughly parallel to the main trend of an incipient normal faulting. Among these dykes, *Injection dykes* are generated by intrusion of material derived from some underlying source and emplaced upwards under abnormal pressure, so resulting from a combination of fluidisation phenomena and hydrofracturing (or hydraulic "jacking"); on the contrary *Neptunian dykes* can form by

both introduction of material under pressure and simple filling of pre-existing fractures by an heterogeneous deposit deriving from above and from the marine environment (Montenat et al., 1991).

However, fracturing can occur for not seismic causes due both to internal processes of the sedimentary environment, such as gravitational genetic component, thermal gradient, pore overpressure, and diagenesis and to external ones however linked to tectonic stress field (Caputo, 2005). Indeed, in a general definition, fractures are mechanical discontinuities produced in a rocky body that, starting from initial equilibrium conditions, have been brought to critical conditions by a stress field, acting at different scale. Thus, fractures form to permit minor adjustments, when rock changes in location, orientation, size, shape in response to burial or compaction, heating and expansion, uplift, cooling and contraction.

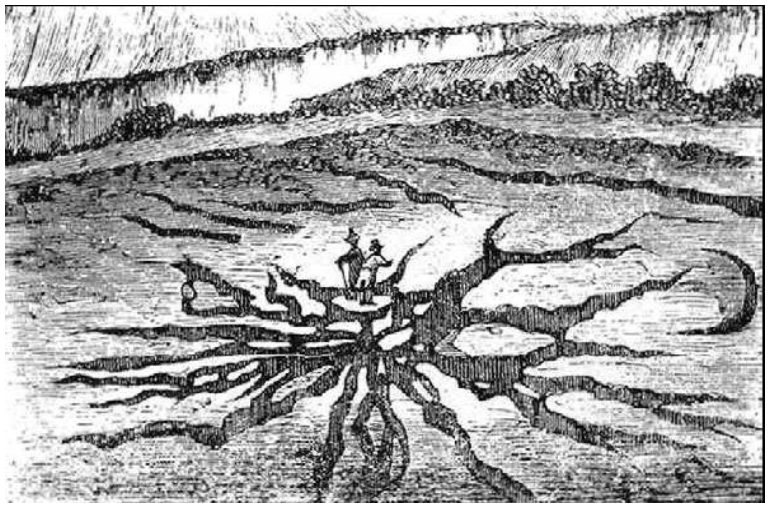

Fig 2.5: Anastomizing ground fracturing triggered by the 1783 in Calabria earthquake (after Torcia, 1784).

Every causative mechanism is restrict to a specific environmental context and depends on the sediment characteristics (e.g. thickness, weight, density, porosity and lithology) and on their setting (e.g. depth of burial, vicinity to morphological scarps). For instance, gravitational genetic component occurs for burial under thick deposits capable to generated high confining pressure, so it increases with the density and the weight of the overburden sediment and with the depth of burial (e.g. Timoshenko and

Goodier, 1951). Thermal stresses are in general of limited magnitude and significantly occur at high depth, except in geological settings associated to volcanic activity (magmatic intrusions or lava flow) (Caputo et al., 2005 and reference therein). Fluid overpressure is due to rapid compaction without a complete leakage of marine sediments and also depends on the burial depth, density of fluids, depth of the water table, porosity and permeability; for example it is facilitated by alternating of permeable and impermeable layers (Wangen, 2001). Rocky diagenesis can induce volumetric variations either positive (i.e. expansion) or negative (i.e. contraction) and other chemical and physical processes capable to produce fracturing. Opened fissures can also be due to gravitative mechanisms, such as sliding associated with stretching, relaxation of scarps and so on (Montenat e al., 2008). Finally, sedimentary dykes can form, in the marine pelagic environment, for deposition of material into fissures on the sea bottom or as a result of overloading causing sand injection in unconsolidated marls (Beaudoin and Friès, 1982; Beaudoin et al., 1983).

Seismic fractures and sedimentary dykes do not differ in shape and characteristics from aseismic ones in absence of the general context (Demoulin, 1996). Only fractures due to tectonic stress field show specific features. Indeed, these cracks, generally opened and without visible dislocation (joints), are usually planar parallel, evenly oriented and spaced and show regular geometry and kinematic indicators. They can be grouped in one or more precise systems whose orientation reflects the stress field (*systematic joints*) (Hodgson, 1961; Hanckock, 1985). On the contrary, fractures not linked to the tectonic stress filed are irregular in form, spacing and orientation and cannot be readily grouped into specific sets.

Therefore, possible relationships between fractures and tectonic regional stress field can be highlighted by mesostructural and systematic analyses. Whereas, to recognize seismic shacking as the most plausible cause of fracturing, a paleoenvironmental reconstruction and sedimentary analysis, jointly with the detailed study of the fracture features is necessary.

Fig 2.6: Ground fracturing of the 1989 Loma Prieta California Earthquake (M=7.1) (http://www.usgs.gov/).

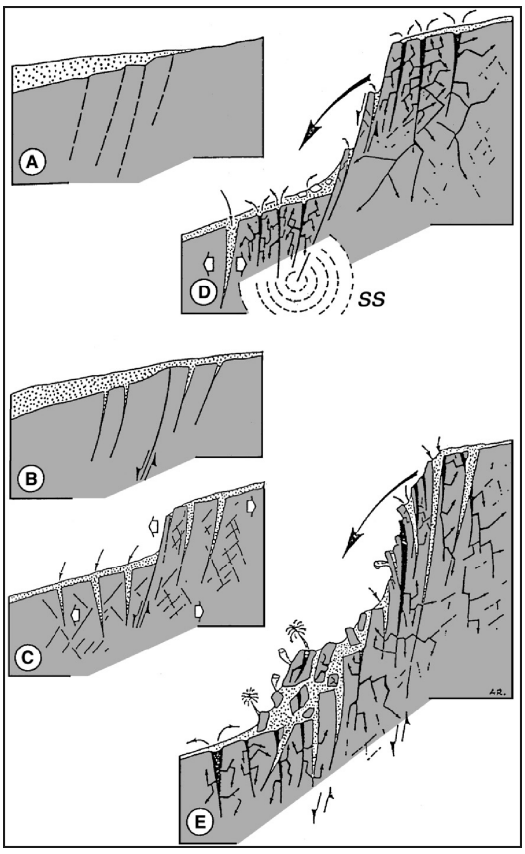

Fig. 2.7: Schematic illustration of sedimentary dykes related to active faults. A to C, formation of *Neptunian dykes*; D and E, formation and evolution of *Injection dykes* in relation to earthquake occurrence (after Montenat et al., 1991).

2.2.3 Liquefactions: soft sediment deformations

A soft sediment deformation occurs in unconsolidated deposits that are subject to a strong hydraulic pressure causing liquefaction and fluidization mechanisms. Liquefaction is the in situ disruption of the grain packing, with consequent obliteration of primary sedimentary structures and lateral variations in thickness, due to the increase in pore-fluid pressures that reduce, up to zero, the shear strength between grains. Fluidization is due to instantaneous segregation of the liquid from the solid sedimentary phase and sudden expulsion and/or injection of the fluidized phase (water and smaller grains and mud). Fluidization can be also due to large injection of an external fluid upward, through the sediment, and the consequent involvement of the sediment that achieves a liquid-like condition, until the immersed weight of the grains is balanced by the total fluid drag (Allen, 1982; Owen, 1987).

These structures can be produced by several mechanisms occurring in the sedimentary basin both linked to internal processes that to external ones, such as tsunamis and earthquake shaking.

Deposition of denser sediments on less dense causes gravitationally unstable density gradients and unequal loading producing bedforms foundering of the first sediment into the second. Load-type deformations are characterized by pseudonodules and convoluted zones between undisturbed cross-lamination layers (Moretti et al., 2001; Owen and Moretti, 2008).

In oceanic context the passing of wave train can produce cyclic shear stresses below the ocean bottom causing the progressive build up of the pore pressure in the sediments that, if large enough, can produce liquefaction (Dalrymple, 1979; Nataraja and Gill 1983). Similarly transient and impulsive stresses induced by breaking waves are important deformational agents in proximal environments (see Dalrymple 1979, and references therein). Typical structures due to wave activity consist in isolated casts and slump bodies, sharply peaked anticlinal structures, bedforms such as hummocky, cross-stratifications and symmetrical mega-ripples, generated on the upper side of the deposit (Brenchley, 1985; Cheel and Leckie, 1993; Molina et al., 1998).

According to Alfaro et al. (2002) storm waves can produce liquidization and liquefaction as a consequence of three mainly processes: (i) cyclic stresses caused by

pressure differences between crests and troughs of successive wave trains inducing the increase of interstitial pressure and subsequent liquefaction and/or fluidization in seabed sediments (Allen 1982; Owen 1987); (ii) direct impact of breaking waves on the sediments (Dalrymple 1979, 1980; Allen 1982; Owen, 1987); (iii) remobilization and rapid deposition of offshore sand into a muddy sediment that can so liquefy (Molina et al. 1997). Typical structures due to these processes are generally associated with tempestites and they show symmetrical morphology such as: (i) wave-ripple and climbing-ripple cross lamination; (ii) lenticular bedding; (iii) thin and tabular layers with planar lamination; (iv) load casts, ball-and-pillows and pipes.

Lateral shear stress and gravitative flow, induced by the downslope component, can produce soft sediment deformation structures like slumping and turbiditic levels.

Less frequently soft sediment deformations can be due to cryoturbation ("ice wedges" produced by melting ice) occurring in periglacial, especially glacio-lacustrine, environment, and to bioturbations (Van der Meulen, 1990). The resulting structures, characterized by infilling of sediment from above, are very similar to earthquake-induced ones, but differently from these, they show limited extension, size and frequency.

Tsunami action can produce large erosion in shallow marine environments and deposition in transitional environments (Shiki et al. 2000). Tsunami run-up and drawdown can cause liquefaction failure of fine sand in the coastal area near to the shoreline as a consequence of high excess pore pressure generation and the effective overburden pressure reduction during the drawdown (Yin L. Young et al., 2009).

Earthquake shaking and shear wave propagation can trigger liquefaction and fluidization of sediment and violent expulsion of water. Indeed the wave passage can augment the neutral pressure of the pore water, before it can flow away. Another mechanism of triggering is due to the compaction of the sediment consequently to the shacking that reduce the interstitial volume favouring the water pressure increase.

Several structures can develop for seismically induced liquefaction like pseudonodules, silts, mixed layers, disturbed varved lamination and loop bedding (Ambraseys and Sarma, 1969; Seilacher, 1969; Sims, 1973; Moretti 2000; Rodriguez et al., 2000). According to Obermeier (1996), that discussed several study cases in widely separated and different geological settings, the structures typical of seismic liquefaction

have a morphology that is consistent with a very sudden application of a large hydraulic force. These structures consists in dykes, sand boils and sand volcanoes, craters, clay clasts and lateral spreading (Fig. 2.8 and 2.9).

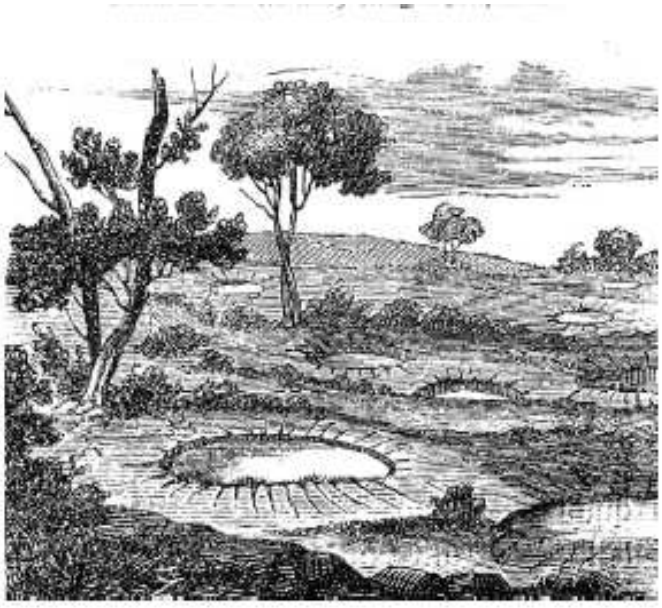

Fig 2.8: Field of sand volcanoes and craters due to the 1783 earthquake (Calabria) (after Torcia, 1784).

Fig 2.9: Lateral spreading (due to sediment liquefaction) caused by the 22 April 1991 Costa Rica Earthquake (http://www.usgs.gov/).

Montenat et al. (2008) recognize like typical seismically induced liquefaction structures: autoclastic breccias, thixotropic wedges, hydroplastic faulting, diapir-like injections and dishes.

Autoclastic breccias, associated to seismic events (Montenat et al., 2008), result from the brecciation of more indurated beds (in many cases early lithified carbonates), alternating with liquefied layers subject to thixotropic mechanism (the property of a body to transform in liquid state under the application of a specific mechanic stress, and to become a solid body again when the stress stops). The liquefaction and fluidization of the thixotropic levels cause the disruption of the indurated ones that rest like polygonal fragments of variable size (cm to dm). These fragments almost remain in connection and are intruded by the fluidised material. The brecciation occurs without any evidence of slope, erosion or desiccation.

Thixotropic wedges form within the sediment but relatively close to the surface, in fine sandy to pebbly deposits. Bedding follows the wedge pattern generally characterized by V-shape becoming from initially horizontal, in the external sides, to vertically arranged in the central part of the wedge. Several beds may also fit into one other.

Fig 2.10: Liquefaction damage on building produced by the Niigata earthquake of June 16, 1964 (M= 7.5) (http://www.usgs.gov/).

Diapir-like injections are plastic intrusions due to liquefaction associated to upward water escape. They show variable size and their development generally cause the cutting of the above intruded levels.

Other liquefaction structures are described by Galadini et al. (1995) that recognized and analyzed these kinds of structures in the Fucino Plain (central Italy) and associated

them to the 1915 Marsica earthquake. The Authors distinguish two different types of deformational processes: the intrusion of liquefied material in the overlying sediments through fractures; brittle deformation of the more competent sediments overlying the liquefied level.

Seismically induced liquefaction structures differ from not seismic ones for environmental contest, shape and features; therefore a detailed analysis of these diagnostic elements is necessary to highlight the most plausible triggering mechanism. Generally this analysis is performed through the excavation of explorative trenches because the liquefaction mechanism occurs underground and the developed structures not always reach the ground surface. However, in these cases their occurrence can be revealed by other associated phenomena such as ground fissures with water or fluids emission, surface deformation, differential compaction, local swelling or collapse, differential settlement of building also capable to cause great damage (e.g., Kuribayashi and Tatsuoka, 1975; Galli, 2000) (Fig. 2.10).

2.2.4 Hydrological anomalies

Earthquakes can produce a high variety of hydrological anomalies such as (i) variation in the flood of springs, rivers and aquifers; (ii) variations of the water level in wells; (iii) variation of the chemical/physical parameters e.g. changes in the underground water temperature and rising of the water salinity; (iv) appearing or disappearing of springs and lakes.

Fault displacement can influence the aquifers causing flood control or change in porosities (Kuo-Chin Hsu et al., 2005). The Loma Prieta earthquake (October 17th, 1989, M 7.1) caused not significant structure damage or surface feature development, but in the Waddel Valley (California), it caused transient increase in discharge of Waddell Creek River and nearby springs, followed by an exponential recession (Briggs, 1992). Also surface ground movement, due to fault activity and landslides triggered by earthquakes can cause lake development. The August 17th 1959 Yellowstone earthquake (M=7.4) (Montana, USA) triggered a big landslide that killed 28 people and make a natural dam that filled the canyon with water, so creating the Hebgen Lake. Other

seismically induced effects can indirectly cause hydrological anomalies. For instance, sand liquefaction can make torpid the water of springs, rivers and aquifers. Moreover, deep ground fractures can cause coming up of gases also producing change in the chemical composition of the water and its heating.

These effects can also occur as pre-seismic ones. One of the best examples is the Haicheng earthquake in 1975, for which a lot of hydrological anomalies occurred before the earthquake and the city was then evacuated (Molnar et al., 1976). In the last decades these effects were used as precursor signals of earthquakes jointly to other instrumental monitoring methods (Savaresky and Rikitake, 1972; Scholtz et al., 1973; Rikitake, 1974, 1975; Whitehead et al., 1985; Chengmin, 1985; Mogi, 1987; Kissin and Grinevsky, 1990; Igarashi et al., 1992 Asteriadis and Livieratos, 2003). In Italy, a possible correlation between earthquakes and piezometric anomalies has been recognised (Albarello et al., 1991; Albarello and Martinelli, 1994; Onorati and Tranfaglia, 1994; Onorati et al., 1994; Pece et al., 1999; Esposito et al., 1998, 1999).

However, hydrological effects occur suddenly and contemporary with the earthquake and stop when it end; so they generally don't rest as geological record observable many time after the quake occurrence.

2.2.5 Tsunami deposits

A tsunami is a water wave train triggered by a disturbance effect occurring in the water environment (sea and large lakes). The highest and energetic tsunamis are generally associated to strong tectonic earthquakes, with magnitude bigger than 6.5 (Bryant, 2001), causing sea floor sudden deformation and vertical displacement of the overlying sea water. Similarly, fall of big mass of terrains, that can also be triggered by large earthquakes, collapse of volcanic edifices or violent submarine volcanic eruption can uplift and move a large volume of water from its equilibrium position. Consequently a sequence of waves (tsunami) propagates into the sea with a period proportional to the uplift (Okal et al., 1991). Generally a tsunami is characterized by long period on the order of the hour and wave lengths in excess of 100 km. Because the rate at which a wave loses its energy is inversely related to its wave length, tsunamis not

only propagate at high speeds, but can also travel great, transoceanic distances with limited energy losses. So, this kind of wave violently reaches the coast and is capable to inundate hundreds of meters inland (Fig. 2.11).

Therefore, a tsunami has great erosional and depositional potential, both off-shore and inland. Waves can erode sandy beach and tearing away trees and vegetation and are capable to detach large boulders from rocky coast or move them from the near shore landward. This material can be deposited further inland or into the sea, for backwash effect, and is commonly named *tsunamiite* (Yamazaki et al., 1989; Shiki and Yamazaki, 1996).

This kind of deposit can rest into the sedimentary sequence as record of past tsunamis (Fig. 2.12). It is generally made of sand, eroded from the shoreline zone and deposited on vegetated surfaces, characterized by reworked matherial (Dawson et al., 1996; Jaffe and Gelfenbaum, 2007). A tsunamite can be represented by a single sheetlike layer of sand or by chaotic sediment layers containing abundant stratigraphic evidence for sediment reworking and re- deposition. Tsunamiites can be also made of boulder accumulations along the coast. Indeed, tsunamis are capable to move and emplace rocky fragments up to several tens of tons in weight. These boulders appear as isolated mega-clasts (e.g. up to 1500 t in French Polynesia and in the Bahamas: Kelletat et al., 2004) or fields of scattered boulders up to hundreds of meters inland on coastal platforms (e.g., Noormets et al., 2002; Mastronuzzi and Sansò, 2004; Whelan and Kelletat, 2005; Scheffers and Scheffers, 2006; Paris et al., 2009), cliff-top boulders, boulder ridges and ramparts (e.g. De Lange et al., 2006).

However, material eroded from marine/beach environment (sand and rocky fragment) can be moved and deposited inland by strong storm waves, too.

Sedimentary differences between tsunami and storm wave boulders are nil, therefore there is not still a definitive criteria advanced to distinguish them (e.g. Noormets et al., 2004; Imamura et al., 2008; Dawson et al., 2008; Goto et al., 2009b).

Fig. 2.11: Waves from the Indian Ocean tsunami of 2004 swirl back out to sea after inundating the land in the top photo. Lower photo shows same area prior to the tsunami (http://www.usgs.gov/).

On the contrary some general criteria have been proved to distinguish between storm and tsunami sandy deposits recorded into the sedimentary sequence (see for instance Morton et al., 2007). Indeed, according to Barbano et al. (2009) tsunamiites commonly exhibit some specific characteristics:

i) evidence of rapid deposition, such as gradation or massive structure can be locally patchy and not diffused over the entire inundated surface (Clague and Bobrowsky, 1994);

ii) the layers are found beyond storm-wave influence; the area where storm-wave influence is nil is characterized by changes in vegetation from beach grasses to less tolerant plants, by the presence of (sand-poor) peat and by long distance from the shoreline that, in the Mediterranean, where storms are substantially no many powerful, rarely exceed some tens of meters;

iii) the layers are similar to local beach sand, generally comprising well-sorted and well-rounded particles and may include fragments of plants (Pinegina and Bourgeois, 2001);

iv) layers are sheet-like, with typical thicknesses of a few millimetres to a few centimetres, generally thinning away from the shoreline (Pinegina and Bourgeois, 2001); the sediments occurring immediately below the sand layer exhibit evidence of wave erosion; sometimes plant leaves rooted in the underlying peat extend upward through the sand or are matted down at the base of the sand indicating burial by flooding.

v) contained biogenic component mainly made of macro- and microfauna of marine environment. Macrofauna can be made by fish remains and shell debris. Microfauna include a wide range of species such as diatoms and benthic foraminifera typical of the deep water (e.g. Dawson et al., 1996). One of the major characteristics of diatoms and foraminifera found in tsunami deposits is the presence of a majority of broken individuals due to the turbulent water transport (Dawson and Shi, 2000).

vi) frequency of the tsunamiites into the sedimentary sequence minor than that of storm deposits.

Fig. 2.12: Example of tsunami sandy deposit into a muddy sequence. (http://www.usgs.gov/)

3. PALEOSEISMOLOGY

Paleoseismology is the study of large earthquakes of the past by the analysis of their traces (seismites) using geologic and geomorphologic methodologies.

The basic principle of paleosesimology is that to understand when and where the next earthquake will occur in a region and its parameters, it is necessary to know when and where earthquakes, linked to the same seismogenic source, occurred in the past and their parameters. Indeed, a seismogenic fault moves periodically producing earthquakes with about regular intervals (elapsed time, recurrence interval). Three cases can be distinguished:

a) a seismogenic fault moves with little time intervals (hundreds of years), and it surely is well detected by seismic instrument. In this case it is possible to hypothesize when and where next earthquake will occur and with which parameters.

b) a fault moves with large recurrence time but however well covered by the historic memory (e.g. interval time in the order of less than a millennium). In this case the seismogenic fault and its parameters could not to be known at instrumental level, but historical descriptions of earthquake damage, allow to assess local intensity values and so to reconstruct the macroseismic field, whose modeling allows obtaining the fault parameters.

c) a fault moves with recurrence time longer than the time span covered by the historical memory. In this case it is not possible to establish the seismogenic source and to know source parameters or where and when next quakes will occur.

In the latter two cases (b and c) paleoseismology is a powerful instrument to investigate past earthquakes and to better define the occurrence of the future ones. Indeed, the recognition and dating of seismites (see chapter 2) is equivalent to the recognition and dating of individual earthquakes.

In the 1970, the earthquake geologists of California discovered that the average recurrence interval between large earthquakes was much longer than the period of historic settlement. This provided the impulse for the development of paleoseismological studies, with the aim to extend the historical record of seismicity back in time until prehistoric period. More than three decades ago, paleoseismological studies started in the high seismic regions of Western United States and New Zealand,

characterized by a brief historical memory covering a span of time of just two or three centuries. Successively paleoseismology diffused in Japan, region with high seismicity and a millenary civilization. However, the term *Paleoseismology* was introduced for the first time by Wallace in the 1981.

Italy hosts millenary civilizations and has one of the most complete and historically extensive seismic catalogues in the World. Nevertheless, the historical memory is however too brief and incomplete to describe the seismicity of this region. Indeed in the catalogues probably lack many M≥6.5 events that repeat in large span of time bigger than that covered by the historical sources. For instance, areas such as the Fucino Plain and the Belice Valley, which were considered non-seismic ones, have been destroyed by two strong earthquakes in the 1915 and 1968 respectively. Paleoseismological studies in Italy allowed to better define the seismic frame of several regions (e.g., Bosi, 1975; Valensise and Pantosti, 1992; Pantosti et al., 1993; Galli and Bosi, 2003; De Martini et al., 2003).

Paleoseismological studies permit to estimate the main parameters that characterize a seismogenic fault: extend of the rupture and distribution of the slip during the individual event, time elapsed since the last event, recurrence interval and slip rates. They also provide information on the behavior of the seismogenic fault useful to understand the seismogenic processes in different tectonic environment (Pantosti and Yeats, 1993 and reference therein). Moreover, the analyses of the seismogeological data are a useful tool for the seismic risk mitigation and the seismic hazard assessment of a given region, which are important aspects also for earthquake engineering applications.

3.1 Paleoseismological investigations

Given their great relevance, paleoseismological study cases are quickly growing worldwide. However, since paleoseismology is a new field of scientific investigation and every study case needs a different specific approach, there are not well defined paleoseimological investigation methodologies. Indeed, an earthquake occurs with different characteristics and can trigger different geological effects and superficial

expressions (see also chapter 2), consequently for each seismogeological effect a different strategy of research corresponds following several lines of investigation.

On the basis of the seismically-induced effect classification it is possible to define two major paleoseismological study typologies: *on-fault paleosismological investigation* and *off-fault paleosismological investigation*. The first type analyses the *on-fault effects,* both primary and secondary (e.g. fault scarp and liquefaction structures), directly on the fault plane. Whereas *off-fault paleosismological investigation* regards the effects developing relatively far from the fault (*off- fault* effects). These are both primary, such as geomorphological modifications and tsunamiites, and secondary, for example deformations of the sedimentary sequence (ground fracturing and liquefaction-induced soft sediment deformations, see chapter 2 for descriptions).

An alternative study method of past earthquake consists in the analysis of the historical record describing seismogeological effect occurrence. This examination is also useful for the choose of the site where to undertake future paleoseismological field study (see also chapter 5). Indeed, a site where the seismogeological effects developed in historical time is prone to their development during future events with similar characteristics and it can have also recorded paleo-events.

3.1.1 Historical data analysis

In regions where disastrous earthquakes occurred without clear evidence of surface faulting and their ancestors are not well known, historical data represent a powerful tool for the evaluation of the seismicity and for the seismic hazard assessment (Galadini et al., 2001).

However, several difficulties are linked to the historical data use, since their abundance and distribution depend on the urbanization in the territory, which cause a gap of data in few populated areas, and on the witness sensibility. Moreover, according to Guidoboni and Mariotti (1999), the lack of data for some Italian towns with well known and long history could be due to their state of degradation, to the numerous and different domination and to the damaging catastrophes such as earthquakes. This is particularly true for Sicily that has been also dominated by numerous populations from

Greeks, to Romans to Spanish. Another problem linked to the use of historical data is due to the language of the time, characterized by terms and grammatical constructions lost in common one. This latter aspect sometimes made difficult the correspondence between the described phenomenon and the real effect triggered in field.

Historical data collection represents also the starting point for further analyses, such as the drawing of maps of susceptibility of a given region to the seismogeological effect development or the extrapolation of empirical relationships between source parameters (intensity and magnitude) and epicentral distance of the sites where the effects developed. Indeed, a given seismogeological effect occurs in a site, also in dependence of its characteristic and setting, for a given minimum threshold of reached energy. Since in the macroseismic area energy attenuates with the distance from the epicenter, obviously these effects became less numerous with the augment of the latter. At excessive distance, ground motion is too weak to induce seismogeological effects. Observations worldwide confirm that a relationship exists between source parameters and epicentral distance. Therefore, empirically obtained relationships, provide the threshold of the effect occurrence in a site in terms of epicentral distance and source parameters. They are obtained drawing graphically the upper bound curves that delimit the area prone to the effect development from that no prone, where the effect occurrence is not expected. These relationships are useful tools both in geotechnical applications, for the hazard assessment at the regional scale, and in seismic application, i.e. for the evaluation of the minimum energy of an earthquake capable to induce effects on the environment, for the reconstruction of the macroseismic zone and the revaluation of probable wrongly estimated source parameters.

Several studies have been carried out to acquire empirical relationships between earthquake source parameters and maximum epicentral or fault distance of sites in which seismogeological effects occurred, both at regional scale that worldwide. In Japan Kuribayashi and Tatsuoka (1975) obtained the correlation between maximum epicentral distance of liquefied sites and associated magnitude for strong earthquakes. In USA Youd (1977) and Youd and Perkins (1978) related earthquake magnitude and epicentral distance of sites where liquefaction occurred. Ambraseys (1988; 1991) considering both epicentral and fault distance computed the relationships between moment magnitude and epicentral distance for 137 liquefaction events, scattered around

the world, including earthquakes in areas of lower attenuation and differentiating between shallow and intermediate-depth earthquakes. Papadopoulos and Lefkopoulos (1993) obtained a bounding equation revisiting the worldwide curves proposed by Ambraseys (1991), adding their Greek data and other liquefaction observations in several places of the world. Moreover, Troften (1997) evaluated intensity and magnitude of paleoevents that occurred in southern Sweden.

Keefer (1984) analyzed the distribution of landslides for several earthquakes occurred worldwide and found the empirical relationships between Magnitude *vs* distance from the seismogenic fault.

Some authors founded relationships among magnitude, precursor time and distance from epicentre for hydrological anomalies effects reported in various parts of the World (Kissin and Grinevsky, 1990; Esposito et al., 2001).

In this work historical data analysis and successive elaborations have been performed and described in the chapter 4.

3.1.2 On-fault paleoseismology

The method to study a seismogenic fault consists in trench excavations, specifically oriented respect to the fault itself. In case of a dip-slip fault one or more parallel trenches, perpendicularly oriented respect to the fault trace, had to be realized; in case of a strike slip fault a double set of trenches, parallel and perpendicular to the fault, are necessary (Fig. 3.1) (Pantosti and Yeats, 1993).

A trench site has to be selected from place where young (Holocene) sediments recording past fault displacement coincide with the active fault trace. Moreover the site had to have no too sedimentation, because the Holocene sediment of specific interest could be at excessive depth, nor erosion because they could have been erased. After cleaning, flagging and gridding, logging is performed by three different techniques: standard hand-drawing, scale 1:20, theodolite measurements of flagged points and rectified photograph mosaics coupled with hand-drawings (Fig. 3.2) (Pantosti and Yeats, 1993).

In general, recognition of individual paleoearthquakes is mostly based on the study of: i) buried scarp-derived colluvial wedges, and/or debris-filled fissures; ii) abrupt increases in the offset of stratigraphic units, or specific markers across the fault; iii) upward termination of faults and cracks at the base or within a stratigraphic unit; and iv) thickening of a stratigraphic unit across the fault, or deposition of a newly formed (Galli et al., 2008).

The dating of the deformed terrains and of the terrains lying above or below the deformed ones, by a variety of techniques, including radiocarbon analysis and soil profile development, allows obtaining information about the recurrence time of the fault activity. Fault investigations by trenching are critical to paleoseismic analysis also because they allow to directly observe deformations, displacements and secondary fractures (splays). These data with the information on length, geometry and cinematic allow to obtain a clear frame of the seismogenic source useful for estimation of slip per event and slip rate, recurrence time, elapsed time, magnitude and other parameters (Wells and Coppersmith, 1994).

Fig. 3.1: Example of *on- fault* paleoseismological investigation. Parallel and like-grid trench sets (after Pantosti and Yeats, 1993).

However, on-fault study has some critic aspects. Indeed, typically fault zones are wider and more complex of the fault trace in map view, or within stopovers, and their

surface expression might be distributed over a significant fault width across strike. Moreover, fault trace can also include second-order surface ruptures, such as antithetic, en-echelon, and release faults. Finally, earthquake rupture may not occupy exactly the same trace every time. For these reasons trenching on fault segment could not capture all the recent surface faulting events which occurred along that segment.

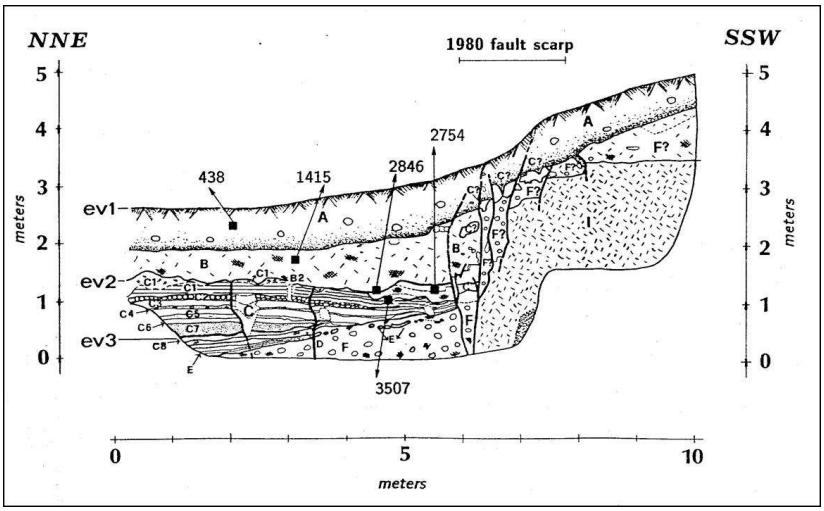

Fig. 3.2: reconstruction of the trench performed on the Irpinia fault responsible of the 1980 earthquake (from Pantosti and Valensise, 1990)

3.1.3 Off-fault paleoseismology

Off-fault Paleoseismology is particularly useful when the seismogenic fault is not known and consequently it cannot be directly studied, because the earthquake did not produce surface faulting (blind or hidden fault) or it occurred off-shore or its evidence have been cleaned by erosion.

A high variety of *off-fault* seismogeological structures can be analysed. At regional scale geomorphological studies allow to investigate several geomorphologic seismically induced structures: uplifted paleo-shorelines (e.g. notches and beach-rocks), uplifted and deformed fluvial and marine terraces, modified stream networks. While, deformations and other effects recorded into the sedimentary sequence, such as

liquefaction-induced soft sediment deformations, fractures and tsunamiites, are studied at site scale by more detailed geological and stratigraphic approaches.

3.1.3.1 Near fault geomorphological investigation

Coseismic deformation, on the fault plane at depth, affects a wide region of the surface and can produce a distinct imprint on the geomorphology. The amount of deformation at different sites is strictly dependent on the structure itself (geometry, cinematic, slip distribution) (Pantosti and Yeats, 1993). The most common geomorphological effects are the anomalies of the fluvial network such as fluvial catchments, offset and deflected streams, rejuvenation of stream profiles, dammed basins, shutter ridges, offset or deflected terraces. Landform modification and geomorphological effects can occur even if the fault is blind or hidden, since movement at depth can create disequilibrium at the surface.

Studies of landform modifications require a geomorphological and geological approach. They have been undertaken worldwide also with the aim to highlight the presence of active faults that can be seismogenic ones. Moreover, the evaluation of the landform modification induced by earthquakes can provide information on the individual or cumulate long-term deformation along the fault. McGill and Sied (1991) evaluated the deformation along the San Andreas fault, during the 1857 earthquake, analysing the offset-streams at Little Rock (South California) whose dislocation have been estimated about 3 m. Sieh (1981) and Sieh and Jahns (1984) estimated the long-term slip-rate of the same fault, from 30 to 40 mm/yr, analysing the older and younger offset-channels at Wallace Creek (165 miles from Los Angeles).

Coastal elements, e.g. paleo-coastlines, are important markers for the estimation of absolute sea level elevation changes (Lajoie, 1986). Since sea level modification can also occur as immediate uplift or subsidence linked to earthquakes their study can be useful for paleoseismological purposes (Adams, 1992, Atwater and Moore, 1992).

3.1.3.2 Stratigraphic record analysis

Seismites recorded in the sediments and distributed in the epicentral area can be both primary effects such as tsnunamiites and secondary such as liquefaction-induced soft sediment deformations, fractures and so on.

Even if the analysis of these effects does not provide precise and direct information on the seismogenic fault and the causative earthquake parameters (magnitude, intensity, fault length and elapsed time), it provides some other important data such as the epicentral distance of the site where the effects developed and the magnitude and intensity threshold reached at the site. Moreover, the finding of structures dating before historical records, can be useful to extend the seismic catalogues back in time.

Not all the *off- fault* seismogeological effects can be easily studied. For example, the analyses in field of landslides and hydrological anomalies presents some difficulties since the first effect can't be differentiate from the not seismic one and the second is generally transitory and there are not irrefutable elements resting as marker of seismicity. Therefore, earthquake-induced landslides could be tentatively studied by the collections of historical data and the analysis of their distribution in map. Hydrological anomalies are generally analyzed suddenly after the quake by instruments monitoring the water table and measuring chemical composition and temperature.

On the contrary liquefaction-induced soft sediment deformations, ground deformations (e.g. fractures) and tsunamiites generally rest well recorded in the sediments and they are the topics of the most of the paleoseismological researches.

Field study of liquefaction phenomena has been used worldwide to obtain information on the location of possible future liquefaction effects and also on earthquake recurrence time; these studies may thus contribute to the seismic hazard assessment and risk scenario of an area (Russ, 1982; Talwani and Cox, 1985; Saucier, 1989; Amick et al., 1990). A good example is represented by the Western United States case, characterized by low seismicity. In this region, where the historical accounts are very limited in the time and no surface rupture is documented, two strong earthquakes occurred: the New Madrid 1811 (Missouri) and the 1866 Charleston quakes (South Carolina). For these events the most significant triggered effect was represented by liquefaction phenomena. Consequently, the most efficient methodology to reconstruct

the seismic history of this region was the study of the paleo-liquefaction evidences in the Holocene fluvial and marine deposits (Talwani and Cox, 1985).

Tsunamiite studies were carried out worldwide along coastal areas of seismically active continental margins from Japan to Cascadia (northern California to southern British Columbia), New Zealand, Russian Far East, Alaska, Chile and Peru. Study cases were also performed in Indonesia, Philippines, Papua New Guinea, Hawaii and in Mediterranean. Finally the effects of the famous Sumatra December 26th 2004 tsunami were investigated in detail (e.g., Abe et al., 1993; Sato et al., 1995; Shi et al., 1995; Bourgeois et al., 2001; Bourgeois et al., 2006; Gelfenbaum and Jaffe, 2003; Jaffe et al., 2002).

Effects such as liquefactions, ground deformations (fractures) and tsunamiites, can be studied in section on trench, similarly to the *on- fault* paleoseismological investigation method (Fig. 3.3). Alternatively, fractures and liquefactions reaching the ground surface can be detected by aerial-photos analysis and reported in map view, describing shape, dimension and frequency. Sandy tsunamiites can be also analysed by core campaigns, whereas tsunamiites consisting in large boulder accumulation had to be studied by a field work aimed to observe all the characteristics of the megaclasts such as shape, orientation, distance from the coastline and so on.

Since these effects rest in the sedimentary sequence and they can be easily analyzed directly, they have been chosen as topic for the field study representing the second phase of this thesis. the adopted *off-fault* paleoseismological methods and results are illustrated in the chapters 5 and 6.

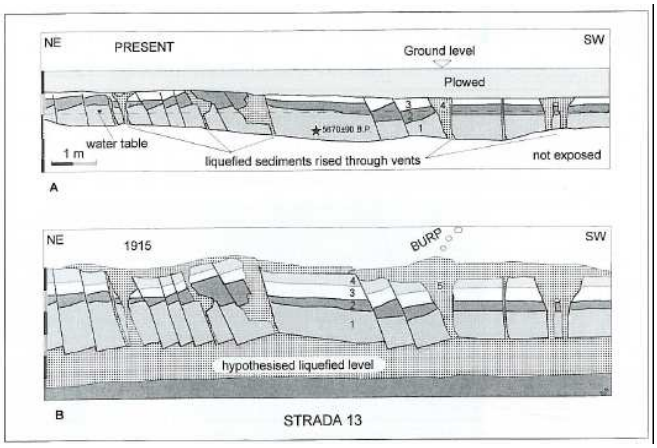

Fig. 3.3: Schematic section of a trench view showing liquefaction structures (from Galadini et al., 1995).

3.2 Paleoseismological investigations in Italy: the state of the art

Until three decades ago in Italy the earthquake hazard evaluation was based exclusively on the historical record, given that this country has one of the most complete and extensive seismic catalogues in the World, from Bonito (1691) to the catalogue CFTI04 (Working Group, 2004), and no attention has been devoted to the geological evidence of past earthquakes.

The first approach to the paleoseismological study in Italy occurred at the end of the 1980, with the recognition of recent surface faulting in the Apennines (e.g., Bosi, 1975). The first pioneering paleoseismological excavation occurred in 1987, on behalf of the former Italian Committee for Nuclear Energy (CNEN, at the time ENEA), in a small intermountain basin of central Italy (Giraudi, 1987; 1989).

Paleoseismology became a scientifically accepted practice in Italy only in the 1990, when the Irpinia fault, responsible of the disastrous 1980 earthquake (Mw=6.9), was investigated by trench excavations (Pantosti et al., 1993). Since this moment several peloseismological trench studies have been realized in Italy, for a total of more than hundred trenches, excavated across dozens of faults from the Alps to Sicily (Galli et al., 2008 and references herein).

These studies allowed to geologists and engineers to have a more clear vision of the seismic setting of several seismogenic areas of the Italian country. Recently, Galli et al. (2008) realized a catalogue of 56 paleoearthquakes (PCI), occurred mainly in the past 6 kyrs, which integrates the historical/instrumental seismic catalogue and extends it beyond the recurrence time of the seismogenic faults (2000±1000 yr).

The first recognition in Italy of earthquake induced liquefactions was thanks to Sauret and Bosquè (1984) which describe several effects of soil deformation linking them to the 1908 Messina Strait earthquake. Galadini et al. (1995), also thanks to the contemporary witness reports, founded and analyzed liquefaction structures in the Fucino Plain (central Italy) associated to the 1915 Marsica earthquake (Fig.3.3). Moretti (2000) observed soft-sediment deformation structures in aeolian sediments of middle-late Pleistocene, at Torre San Gennaro (Brindisi—southern Italy) probably linked to paleo-earthquake of the Apulian foreland. Galli and Bosi (2003) found evidence of liquefaction in one of their four trenches opened in the Sila massif (Calabria, southern

Italy) linked to the 1638 Calabria earthquake. De Martini et al. (2003) recognized evidence of liquefaction structures possibly related to the 1627 seismic event, along the Northern Gargano coast.

Tsunamiite study recently growth in central-southern Italy where several core campaigns were performed with the aim to found and date past tsunamis. The first work describing tsunami deposits in Italy began no more than 10 years ago. It focused on the Gargano coast (Adriatic sea side) and highlighted deposits possibly related to the 1627 tsunami and previous ones occurring with a time interval of about 1700 years (De Martini et al., 2003). In the same area, washover fans along the Lesina coastal barrier were interpreted as an effect of tsunami waves (Gianfreda et al., 2001). In north-eastern Sicily evidences of past earthquake tsunamis were found at Capo Peloro in an archaeological excavation and they were associated to the February 6th 1783 earthquake and to a more ancient event dated 17 A.D. (Barbano et al, 2007; Pantosti et al., 2008a; Pantosti et al., 2009b). Southward evidences of tsunamiites were found in several sites, form Anguillara (northeastern flank of Etna Mount) up to Morghella (South-eastern Sicily), associate to historical earthquakes and paleo-events dated up to 4000 yr ago (Barbano et al., 2009; De Martini et al., 2010) and in the offshore of Augusta (Smedile et al., 2010). These finding allowed to extend back in time the tsunami catalogue in this region and to observe that over the last 2000 years, at least 11 tsunamis have affected the 250 km long Ionian coast of Sicily (De Martini et al., 2010).

Boulders up to 80 t in weight, scattered along the Ionian coast of Apulia (Southern Italy), were supposed to be related to tsunamis between the 15th and 18th centuries (Mastronuzzi and Sansò, 2000, 2004; Mastronuzzi et al., 2007). Recently, Scicchitano et al. (2007) interpreted anomalous boulder deposits along the coastal area of south-eastern Sicily, between Augusta and Siracusa, as having been deposited by historical tsunamis. Barbano et al. (2010a) and Barbano et al. (2010b) analyzed boulder accumulations in three areas (Capo Campolato, Vendicari and San Lorenzo) along the Ionian coast of Sicily. Combining field observations with hydrodynamic equations jointly with statistical analysis, the Authors distinguished the boulders deposited by storm waves from that probably deposited by tsunamis.

Studies of other co-seismic secondary effects have been also performed. Valensise and Pantosti (1992) considered the uplift of 125kyr-old marine terraces of the Messina

Strait (north-eastern Sicily and southern Calabria) as the result of repeated earthquakes with a recurrence time of about 700–1500 years, whose last episode was the 1908 Messina Strait earthquake (M= 7.1). De Guidi et al. (2003) analysing the coastal morphology of the Taormina area (north-eastern Sicily) hypothesized the occurrence of at least three seismic events during the Holocene time. Similarly, Ferranti et al. (2007) on the basis of geomorphological analysis consider the Scilla fault, a 30 km normal fault on the Calabrian side of the Messina Strait, as capable of generating earthquakes with a maximum moment magnitude of 6–6.5, similar to the February 6th 1783 earthquake.

Guarnieri and Pirrotta (2009) thanks to a multidisciplinary study, including geological- structural, geomorphological and morphometric approaches, highlighted the presence of active faults in the northern portion of the Sicilian sector of the Messina Strait, where the disastrous 1908 earthquake occurred.

Recently historical data were collected to realize datasets and to extract empirical relationships between source parameters and epicentral distance of the site where the effects occurred. As result of a modern, strongly focused, historical seismological research, the Italian literature offers a number of inventories reporting accounts of seismo-geological effects. Berardi et al. (1991) reported 158 liquefaction events occurred during 31 quakes. ISMES (1991) compiled catalogues of historical liquefaction cases within the Italian territory, also selected from ENEL Seismic Catalogue (1975). Galli and Velonà (1991) compiled a catalogue of earthquakes with high liquefaction potential. Galli and Meloni (1993), updating the previous works, assembled a catalogue for the whole Italian country, including 307 liquefactions occurred during 63 earthquakes; this was subsequently improved by Galli et al. (1999) which analyzed all the events occurred in Italy since AD 1117. Galli and Ferreli (1995) using a probabilistic approach developed a catalogue of earthquakes that may have induced liquefaction, from year 1000 to 1982 AD, and correlated the distance of liquefied soils with the earthquake epicentral intensity. Galli (2000) compiled a catalogue which is a completely reviewed and updated version of previous compilations. Prestinzini and Romeo (2000) assembled a catalogue of ground failures induced by strong earthquake in Italy (Intensity equal or greater VIII MCS). A complete documentation about secondary effects occurred during the main Italian historical earthquakes is also included in the Catalogue of strong Italian earthquakes from 461

B.C. to 1997 A.D. (CFTI04, Working Group 2004). Combining a seismic probabilistic approach with geological data, a map of liquefaction-prone areas was published for the Italian country (ISMES 1991); moreover, liquefaction-prone area maps have been draw for Italy (Galli and Meloni, 1993) and, at local scale, for the Catania town (Azzaro, 1999) by the use of the available datasets.

Galli and Ferreli (1995) correlated the distance of site where liquefaction occurred, during the events that hit Italy from year 1000 to 1982 A.D., and the earthquake epicentral intensity. Recently, the magnitude upper bound method was applied by Galli (2000) to historical liquefactions induced by 61 earthquakes occurred in Italy from 1117 A.D. to 1990 A.D. The Author related epicentral intensity I_o (MCS), magnitude M_s and equivalent moment magnitude M_e, reported in the previous version of the Italian parametric catalogue CPTI99 (Working Group, 1999), to the epicentral distance Re; finally, magnitude *Ms* to the epicentral distance Re considering only the instrumentally observed values for the period 1900 A.D.-1990 A.D. Prestininzi and Romeo (2000) found for the whole Italian territory maximum epicentral distance at which ground failures occur as a function of epicentral intensity, dividing the ground effects in: topographic changes, liquefactions, landslides and fractures. Pirrotta et al. (2007) updated previously compiled liquefaction datasets and used historical data to define relationships at regional scale, between intensity/magnitude values and epicentral distance, for central- eastern Sicily.

4. HISTORICAL DATABASES OF SEISMOGEOLOGICAL EFFECTS IN SICILY AND EMPIRICAL RELATIONSHIPS BETWEEN SOURCE PARAMETERS *VS* EPICENTRAL DISTANCES

Since Italy hosts a millenary civilization and consequently has a wide historical memory it offers the opportunity to collect useful information on past earthquakes.

Historical data collection and successive elaborations (maps of areas prone to the seismogeological effect development and empirical relationships between source parameters and epicentral distance of the sites where the effects occurred) represent an useful tool also for the evaluation of the minimum energy of an earthquake capable to induce effects on the environment, for the reconstruction of the macroseismic zone and the revaluation of probable wrongly estimated source parameters.

4.1 Historical records of seismogeological effects in Sicily: analysis and classification

The Italian historical bibliography has been analyzed to collect information on seismogeological effects such as landslides, liquefactions, ground deformations and hydrological anomalies, triggered in Sicily by the strong earthquakes with sources both in Sicily and in southern Calabria. Tsunami effects have been discarded because their occurrence and distribution is restrict to the coastal areas.

This analysis has been performed through the revision of historical accounts, retrieved from the aforementioned catalogues and through an original research of historical primary sources and the analysis of the technical/scientific bibliography.

The CFTI97 (Boschi et al., 1997) and the updated version CFTI00 (Boschi et al., 2000), reporting description of effects produced by earthquakes from 461 BC to 1990 AD, have been the most useful instruments for the data collection. The CEDIT catalogue (Romeo and Delfino, 1997), reporting soil displacements due to strong earthquakes (Io >8, MCS) occurred in Italy during the last millennium, has also been analyzed.

Some descriptions of seismogeological effects triggered by earthquakes occurred during the last century and not reported into the previous datasets have been obtained from the scientific bibliography. These are linked to the following events: the 1993 south Tyrrhenian Sea (I=7.0), the 1999 Patti (I=6.0), the 2001 Madonie (I=4.5) finally the 2002 Palermo (I=6.0) earthquakes. For instance Azzaro et al. (2004) described hydrological anomalies at Termini Imerese and slope instability at Cerda, for the 2002 Palermo earthquake. Finally, numerous descriptions have been retrieved by original historical sources, never reported in the previous datasets, such as Lo Giudice (1909) that described effects occurred near Messina during the December 28th 1908 earthquake.

Given the difficulties linked to the use of the historical data, especially as it regards the interpretation of the language not more used, the lithological and geomorphological characterization of the sites have been realized for a better understanding of the phenomenon described by the witnesses. This has been possible through the use of geomorphological and geological maps (at scale 1:100.000 and 1:50.000) available in literature and aerial photo analyses.

For the Mt. Etna a more detailed and critical analysis has been realized, because it shows very different structures associated to a variety of processes mainly linked to the volcanic activity (e.g. Smith et al., 1996). Indeed, this area is generally subjected to both aseismic surface ruptures and creeping (Rasà et al., 1996; Gresta et al., 1997; Azzaro, 1999), probably due to dyke-induced rifting and sliding (Borgia et al., 1992; Lo Giudice and Rasa, 1992; Montalto et al., 1996; McGuire et al., 1997), and coseismic faulting. For instance Azzaro (1999) considered some ground ruptures, observed in the eastern flank of the Mount, as consequence of coseismic reactivations of minor shear planes connected with the seismogenic fault associated to the earthquakes occurred in this area since 1818. Moreover, Mt. Etna is subjected to phenomena of secondary volcanism characterized by continuous emissions of water and CO_2, leading to the typical mud volcanoes (Chiodini et al., 1996).

For these reasons, after a critical selection, some of the seismogeological effects described by the historical sources for this area were discarded from the data collection, especially as it regards ground deformations and liquefactions. For instance, liquefactions reported by Longo (1818) for the 20 February 1818 event in the Salinelle

site (South Etna) were not ascribed to real seismically induced effects (Azzaro, 2000).

After data collection, the seismogeological effects have been classified as reported in Tables II, III, IV and V. Each class refers to a specific effect: A-class landslides; B-class ground deformations; C-class liquefactions, D-class hydrological anomalies. Since some descriptions report more than one effect occurring contemporary in the same site during the earthquake (e.g. ground fracturing and liquefaction or ground fracturing and landslide), these simultaneous effects have been insert in subclasses named with a mixed wording. For example to describe the development of new springs (D-type) with bituminous and sulfur material emission (C-type) the D-C wording was used.

4.1.1 A-class: landslides

In this category not only the descriptions of landslides *s.s.* have been considered but also those effects on the ground surface, such as fracturing, settlement and down-warping that, occurring in hill and/or mountain context, could be linked to sliding or could be the first expression of an incipient landslide (Table II).

Since seismically induced landslides do not differ from the no seismic ones in terms of morphology and triggering internal processes (see also chapter 2 for descriptions) they could be classified according to the categories defined by Varnes (1978). Unfortunately, the use of the Varnes's (1978) classification was not possible in this work because, given the scarce technical unknown of the time about the slide movements, rarely landslides have been described by the witness distinguishing their cinematic and characteristics.

In this classification landslides that caused important geomorphological modifications have been included, e.g. landslides causing deviation of the fluvial network and lake development (mixed wording A-D and A-D1 in Table II), for the high impact that they had on the environment.

Table II. Landslide classification.

A Landslide		
A1 Superficial slide	A-B Ground fracturing in hill/mountain area	A-D Landslide causing impediment and/or modification of the river flow
A2 Rock-fall		A-D1 Landslide causing lake development

4.1.2 B-class: ground deformations

Ground deformation generally consists in fractures and ground settlement (Table III). However, since the distinction between ground deformation *s.s.* and that linked to other seismogeological effects, such as landslides or liquefaction, is not always easy, this phenomenon is generally considered an hybrid one and it was often included into the other classifications with a mixed wording (Tables II and IV). In general, if ground deformations occurred in a mountain context, characterized by more or less high slope, they could be linked to slide mechanism (Table II). If the same effect occurred in a flat area with incoherent, saturated, liquefiable terrains they could be the manifestation of liquefaction mechanisms (Table IV). Whereas, if the site where ground deformations occurred does not show peculiar conditions (critical slope, liquefiable sediments) these deformations can be considered as ground deformation *s.s.* (Table III).

Table III. Ground deformation classification.

B Ground deformations
B1 Ground fracturing
B2 Ground settlement
B3 Ground fracturing and settlement

4.1.3 C-class: liquefactions

Liquefactions generally occur underground and the triggered structures not always reach the ground surface. However, these effects can be revealed by other associated phenomena. In fact ground surface deformation, volumetric and differential compaction, local swelling and collapse, down-warping/up-warping, differential settlement of building, and finally fracturing with violent expulsion of hot and sulphur water, can be expression at surface of underground liquefaction (e.g., Kuribayashi and Tatsuoka, 1975; Galli, 2000). For this reason, besides to liquefaction *s.s.*, whose structures develop at the surface (i.e. sand boils, dikes and mud volcanoes, C1 subclass in Table IV), other hybrid effects directly connected to the liquefaction mechanism at depth have also been reported and named with mixed wording (C-B1, C-A, B-C, B1-C, B2-C in Table IV).

Soil deformation phenomena such as ground fissuring, collapse and surface settlements, occurring in recent alluvial depositional areas, flat enough to suggest a liquefaction-induced origin have been considered in according to the Galli's (2000) classification as well. Example of these effects are those described by Bottone (1718) for the Catania Plain during the 1693 earthquake: "la terra si aprì in modo spropositato … Da questa fenditura fuoriuscì una polla di acqua calda: si osservò che ciò era avvenuto in molti luoghi della pianura" (The ground surface excessively opened… The crack ejected hot water: this phenomenon was observed in several places of the plain). Using the same criteria, exhalation of gases and fluids occurred together with sediment liquefaction, as described for the 1908, 1894 and 1783 earthquakes by Lo Giudice (1909) and Baratta (1910), have been also considered in this class.

The C-A subclass refers to a typology of liquefaction mechanism named *lateral spreading* that causes the lateral movement of the terrains, with a vertical component of movement under a light slope (see also chapter 2 for descriptions). Finally, B-C subclass refers to liquefactions accompanied with large ground fracturing.

Table IV. Classification of liquefaction and associated phenomena.

<table>
<tr><td colspan="3">C
liquefaction</td></tr>
<tr><td rowspan="4">C1
Liquefactions: sand boils, sand hills, dikes and sand/mud volcano</td><td rowspan="4">C-A
Ground fracturing with lateral spreading</td><td>C-B1
Liquefaction and ground fracturing</td></tr>
<tr><td>B-C
Ground deformation with liquefied material emission</td></tr>
<tr><td>B1-C
Ground fracturing with liquefied material emission and gases exhalation</td></tr>
<tr><td>B2-C
Ground fracturing and settlement with hot water, bituminous material and/or fluids emission and/or gases exhalation</td></tr>
</table>

4.1.4 D-class: hydrological anomalies

Earthquake effects on springs, rivers and aquifers are reported in Table V. Spring apparition and/or disappearance, lake development (both temporary that enduring) and finally stream flow deviation and modification have been considered. This classification comprises also variation of the chemical/physical parameters including salt water intrusions in the aquifers. Hydrological effects associated to liquefaction (Tab. V) have been included into the D-C subclass.

Table V. Hydrological anomalies classification.

<table>
<tr><td colspan="6">D
Hydrological anomalies</td></tr>
<tr><td>D-1.1
Torpid water, alteration of the water chemistry, temperature, colour and taste.</td><td>D-2.1
Change of the fluvial course and fluvial overflow</td><td>D-3.1
New springs and/or river development</td><td>D-4.1
Lake development</td><td>D-5
River flow change</td><td>D-C
Development of spring with sulphur, hot and bituminous water</td></tr>
<tr><td>D-1.2
Infiltration of salt water.</td><td>D-2.2
Change of the spring location</td><td>D-3.2
Springs and/or river disappearing</td><td>D-4.2
Lake disappearing</td><td></td><td></td></tr>
</table>

4.2 Databases of the seismogeological effects

New and updated datasets of seismically-induced effects have been compiled for landslides, liquefactions, ground deformations and hydrological anomalies by the use of the historical data.

Appendix A report the descriptions from historical accounts used in this work. Data are divided for each seismogeological effect.

Tables in Appendix B report the causative earthquake signed by a number (N), the year, month and day of occurrence, the epicentral area, the reference sources (Rt), the latitude and longitude of the epicentre (Lat/Long) and the earthquake parameters (I_o: epicentral intensity; M_{aw}: magnitude moment equivalent; M_{as}: superficial wave magnitude). Then, tables report the localities where the seismogeological effects have been observed, their latitude and longitude (Lat (s)/Long (s)), the intensity reached at the site (Is –MCS; "n.p." wording indicates not available data; NR no existing data); the epicentral distance of the site (Re - km), the observed phenomenon (on the basis of the previous classifications reported in tables from II to V), finally the historical sources. Grey squares in Appendix B indicate the M_L (local magnitude), available for few events occurred in instrumental time.

Parametric data have been obtained from the CPTI04 (Working group CPTI04, 2004); the sources of macroseismic observations are the catalogues CFTI00 (Boschi et al., 2000), DOM (Monachesi and Stucchi, 1997), POS85 (Postpishl, 1985), and finally Azzaro et al. (2004) indicated as Azz**. New data with respect to previous databases and catalogues are indicated by asterisk.

The epicentral distance has been measured for each site thanks to Free Web Software Gis (Google Earth).

The localities where the effects occurred have been insert into a Gis platform, by the use of specific software such as ArcGis3.2 and Map Info Professional 7.0. The software allowed to realize automatically maps of distribution of seismogeological effects, which are geographic-interactive datasets containing all the information about the effect and the causative earthquake, finally maps showing the areas of major frequency of

seismogeological effect occurrence for Sicily (Fig. 4.1a and 4.1b).

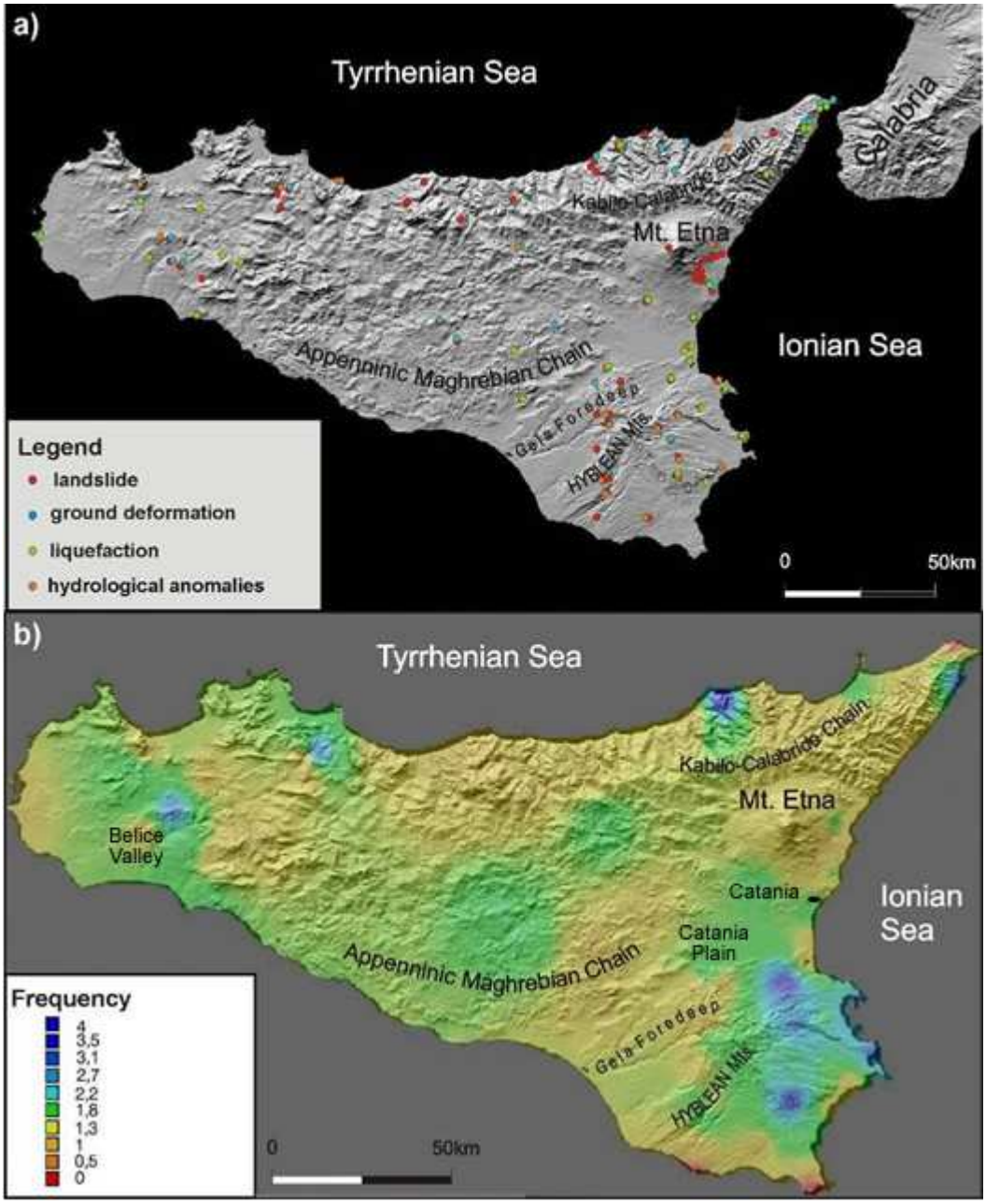

Fig. 4.1: (a) Map of seismogeological effects distribution and (b) map of frequency of the seismogeological effect occurrence, obtained by the use of Gis Software (ArcGis3.2 and MapInfo Professional 7.0).

4.3 Empirical relationships between magnitude/intensity versus epicentral distance (Re)

The regional datasets of the seismogeological effects, realized in this work (Appendix B), have been used to find local relationships between earthquake source parameters, *Maw*, *Ms* and *Io* (CPTI04; Working Group, 2004) and the epicentral distance of the sites where the effects developed (*Re*).

These relationships are obtained graphically by the plotting of data in a Cartesian graph reporting the specific source parameter, on the y-axis, and the epicentral distance, on the x-axis. The point cluster delimitates the area of occurrence of the seismically-induced effect. The best-fit of the most external points (a logarithmic function) gives the upper bound-curve. This curve delimits the prone area and separates it from the area where the effect is not expected (Fig. 4.2-I and 4.2-II). The equations corresponding to the obtained curves are reported in Appendix C.

4.4 Data analysis

30 historical earthquakes, occurred in Sicily and southern Calabria, from the 1169 up to 2002 A.D. with $4 \leq M_{aw} \leq 7.5$ and $5 \leq I_o \leq 11$ (CPTI04; Working Group, 2004), triggered seismogeological effects in Sicily. The historical datasets, herein compiled, account for an amount of 212 cases of seismogeological effects: 79 cases of landslides in 61 sites, triggered by 21 earthquakes; 55 of ground deformations occurred in 36 sites, during 14 earthquakes; 45 cases of liquefactions in 28 sites for 15 earthquakes; finally 33 hydrological anomalies occurred at 26 sites, triggered by 14 earthquakes.

Table VI summarises the frequency of occurrence of seismically induced environmental phenomena for magnitude classes. 48% of observed effects are induced by earthquakes with $M_{aw} \geq 6.5$; while 33% are related to M_{aw} ranging from 5.5 to 6.5 and only 19% for $M_{aw} < 5.5$.

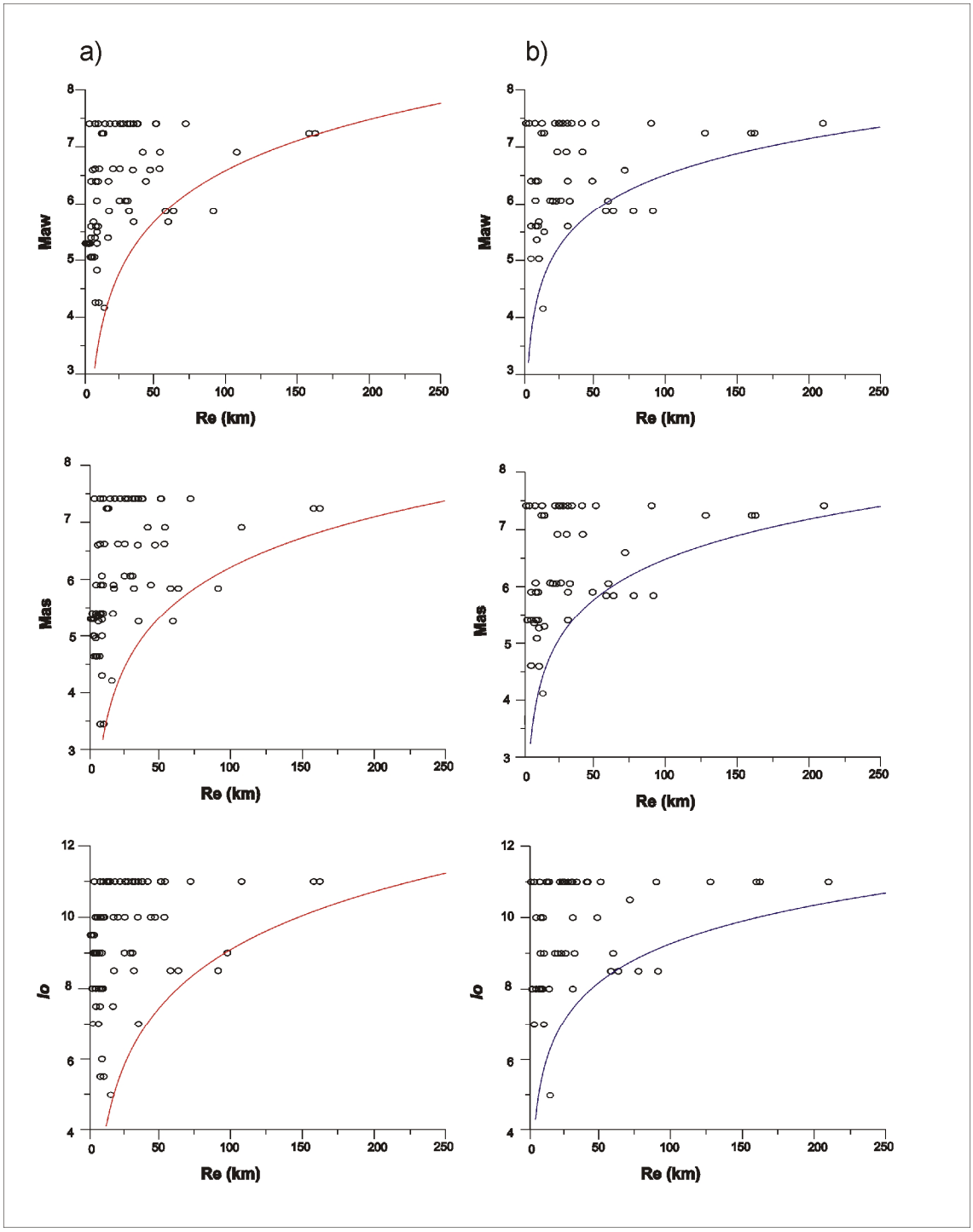

Fig. 4.2-I: Upper bound curve graphs of seismogeological effects: (a) landslides and (b) ground deformations. Curves are obtained empirically on the basis of earthquake effect distribution, in terms of epicentral distances and *Maw*, *Mas* and *Io* values. Points falling down the curves correspond to anomalous sites where the effect developed in spite of the source parameters and the distance from epicentre.

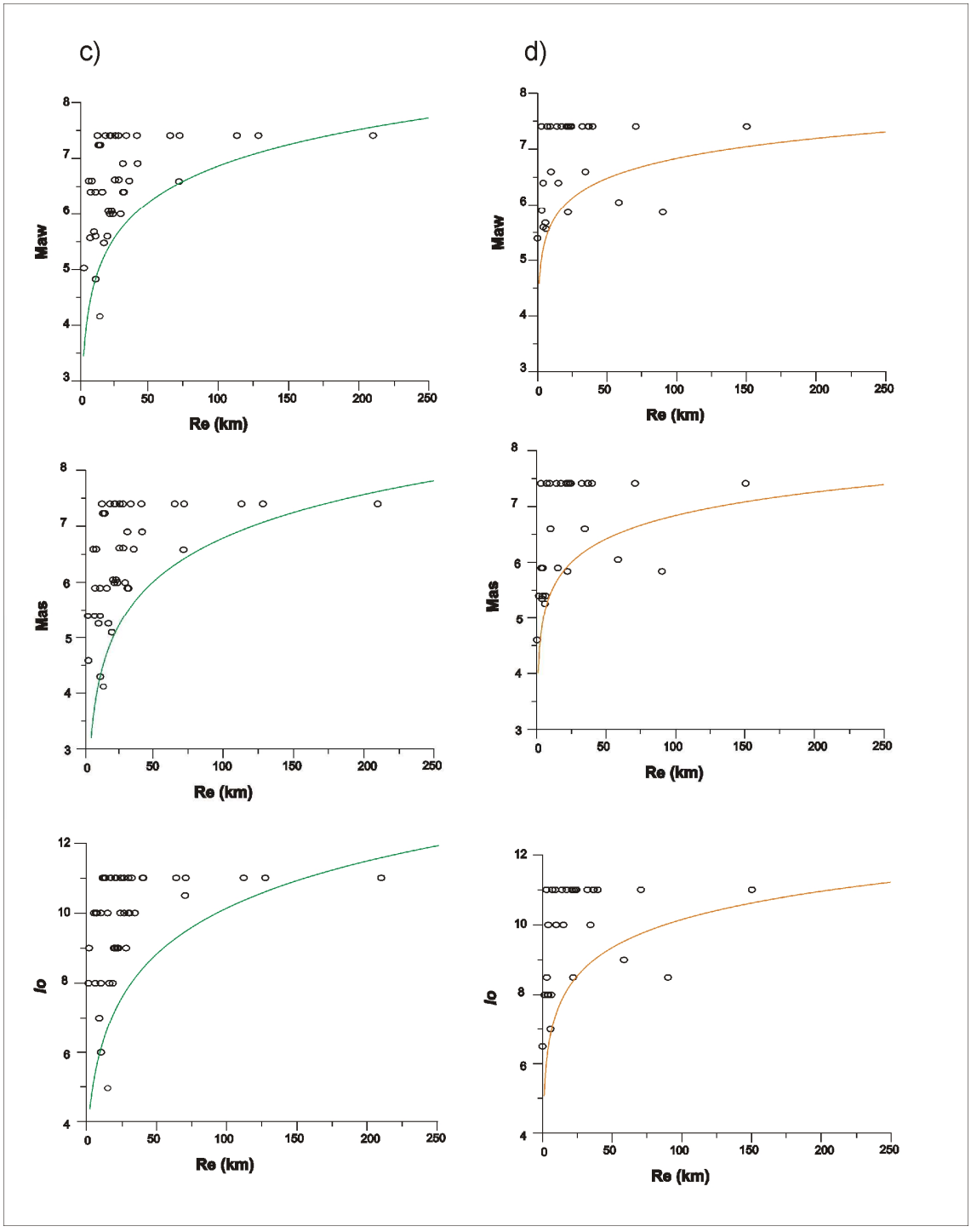

Fig. 4.2-II: Upper bound curve graphs of seismogeological effects: (c) liquefactions and (d) hydrological anomalies.

Among the 212 effects, the most frequents are represented by the landslides (38%) and by the ground deformations (26%). These effects occur for the lowermost threshold of magnitude (M_{aw} = 4.2) and energy (I_o = 5) and for longer epicentral distances than the other effects (Re= 161,78 and Re= 210 respectively).

Table VI. Number of cases of seismically induced effect occurrence for *Maw* interval.

M_{aw} interval	**Nr. of landslides**	**Nr. of ground-deformation**	**Nr. of liquefactions**	**Nr. of hydrological anomalies**
7.0-7.49	24	21	16	16
6.5-6.99	11	4	8	2
6.0-6.49	9	13	12	3
5.5-5.99	15	9	3	6
5.0-5.49	17	7	4	5
4.5-4.99	1	0	1	0
4.0-4.49	3	1	1	0

21% and 15% are respectively represented by liquefactions and hydrological anomalies, the latter occurring for the highest threshold of magnitude and energy ($M_{aw}\approx$ 5 and I_o > 6) and at minor distance (maximum Re= 150).

Figure 4.3 shows that landslides occur for lower thresholds of sources parameters and distance than the other effects, followed by ground deformations, liquefactions and finally hydrological anomalies. However, for epicentral distance exceeding 80-120 Km landslides need higher values of M_{aw} and I_o to occur than ground deformations (Fig. 4.3, M_{aw} *vs* Re and I_o *vs* Re graphs). Similarly, at distance exceeding 90-100 km, hydrological anomalies need minor energy than liquefactions to occur. This can be due to the fact that liquefactions occur for complex and concomitant site conditions; so the earthquake shacking can not be enough at long distance. On the contrary hydrological anomaly occurrence is more regular despite the increase of distance, because according to Romeo and Delfino (1997), the aquifer are particularly sensible to the changes of stress due to the seismic shaking.

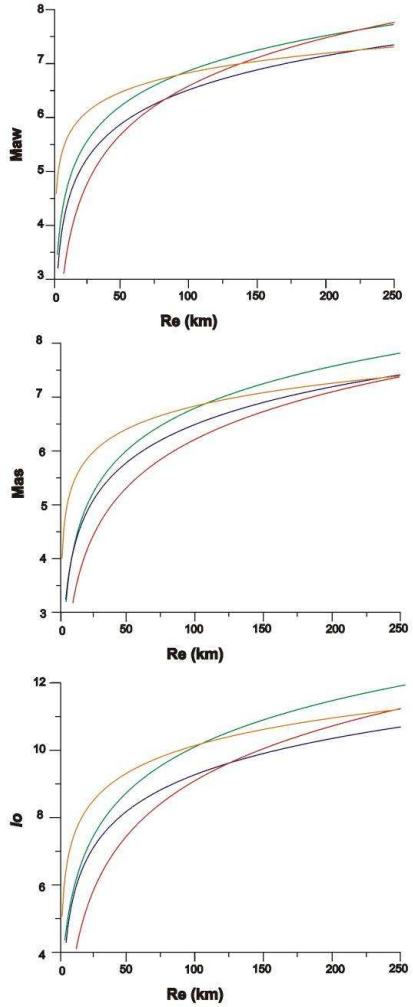

Fig. 4.3: Comparison between M_{aw}, M_{as}, I_o *vs* Re upper bound curves for the collected seismo-geological effects; red line, landslides; blue line: ground deformations; green line, liquefactions; orange line: hydrological anomalies.

Comparing the liquefaction upper-bound curves obtained by this analysis (curve 1 M_{aw}, curve 2, M_{as}, and curve 3, $I_{0,}$ in Fig. 4.4) and those obtained by several authors worldwide a good correspondence can be observed, in particular as it regards the curves obtained by Galli (2000): curve 8 (M_e, equivalent magnitude) (Fig. 4.4a) and curve 4 in I_o vs. R_e graph (Fig. 4.4b). Mismatching is found for M_s vs. R_e curve (9) proposed by Galli (2000) and for the curves proposed by other authors (5, 6 and 7 in Fig. 4.4a). These differences can be explained with the use of unlike source parameters.

As it regards landslides, the empirical relationships proposed in this work are in good agreement with that proposed by Keefer (1984), as showed in Table VII reporting a comparison between the epicentral distance values for magnitude intervals, obtained

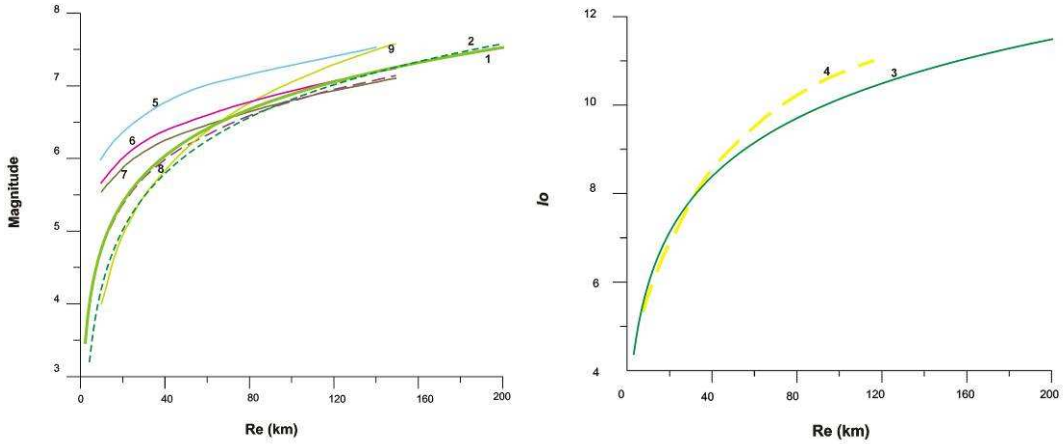

Fig. 4.4: (a) Comparison among different upper bound curves from literature and those proposed in this study: continuous green line (1) and dashed dark green line (2) are related to M_{aw} and M_{as} relationships obtained in this work, respectively; light blue line (5) is related to M values from Kuribayashi and Tatsuoka (1975); pink line (6) to M_w from Ambraseys (1991); brown line (7) to M_s from Papadopulos and Lefkopulos (1993); dashed purple line (8) to M_e (equivalent magnitude) and continuous light green line (9) to M_s from Galli (2000). (b) Comparison between the upper bound curves concerning epicentral intensity I_o provided by Galli (2000), dashed yellow line (4), and that proposed in this paper, continuous green line (3).

Table VII. Comparison between the epicentral distance intervals obtained in this work (3rd column) and those from Keefer (1984) (2nd column), for Magnitude intervals (1st column).

M	Re (km) from Keefer (1984)	Re (km)
> 7.0	≥200	≥150
6.1-7.0	100-200	75-150
5.1- 6.0	35-100	37-75

from Keefer (1984) and from this work.

In the upper bound graphs, some anomalous points, falling out from the area prone to the seismogeological effect development (Fig. 4.2-I, 4.2-II and 4.5), could indicate mislocation and/or wrong magnitude estimate of historical seismic events or cases of site amplifications and/or exceptional site response. As it regards landslides the points that are below the upper bound curve represent the Ogliastro and Naso sites for the 1823

earthquake (M = 5.87) (Fig. 4.6) and Ispica for the 1990 earthquake (M = 5.68). Ground deformation upper bound curve reveals some anomalous sites such as Ogliastro, Naso, Librizzi and Caltanissetta for the 1823 earthquake (M = 5.87) (Fig. 4.6) and Messina site for the 1783 (M = 4.20). Upper bound curve of liquefaction effect highlights two anomalous points: Messina for the 1783 (M = 4.20) and Calatafimi for the 1693 earthquake (M = 7.41). Hydrological anomalies upper bound curve reveals that other two sites are anomalous considering their distance and the parameters of the causative quakes: Barcellona P.G. for the 1894 Calabria event (M = 6.5) and Ogliastro for the 1823 (M = 5.87) (Fig. 4.6).

This analysis reveals that the 1823 earthquake produced seismogeological effects at unpredicted distance from the epicentre (Fig. 4.6). Recently the location of the epicentre of this event, and consequently its parameters, have been revaluated. Indeed, according to Azzaro et al. (2004) and Meletti (2008) this earthquake, located near Cefalù (northern coast of Sicily) on the basis of intensity pattern modelling (Gasperini et al., 1999), really should be located off-shore. According to this new hypothesis, a bigger 6.7 magnitude was estimated for this event (Meletti, 2008). In figure 4.5 red points represent the site where the 1823 earthquake triggered effects, blue points and dark gray curves represent the new points and upper bound curves reconstructed with the revaluated magnitude value (M= 6.7; from Meletti, 2008). These curves show a similar trend respect to the previous ones, only slightly more increasing with the epicentral distance, especially in the case of ground deformations. New points are not anomalous, instead they lie in the area prone to the effect triggering, considering both the old and the new upper bound curves.

Other points representing occasional anomalies could be due to exceptional site effects. E.g. at Messina, ground deformations and liquefactions occurred at anomalous distance during the 1783 Milazzo event. This site resulted highly prone the these phenomena as revealed by their frequent trigger during the strongest historical earthquakes occurred at very distance, too.

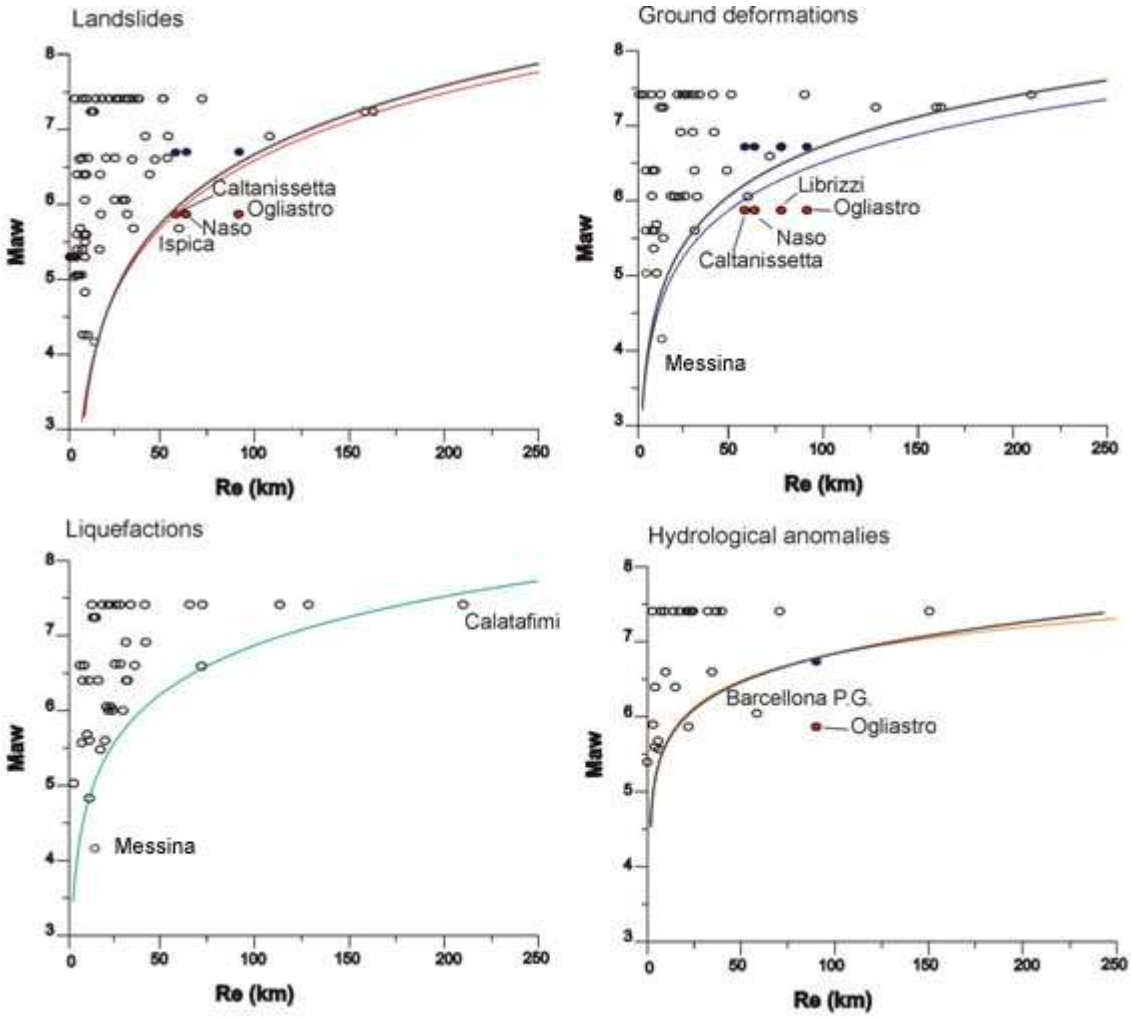

Fig 4.5: Upper bound curve graphs relating Maw *vs* epicentral distance; the anomalous points falling down the curves in the no prone area represent sites where the effects occurred at unpredicted, exceptional distance. Red points indicate the sites where effects occurred during the 1823 earthquake for magnitude 5.87 (Working Group, 2004), blue points indicate the previous sites considering the new magnitude value proposed for this event (M=6.7), dark grey lines represent the new calculated curves. Liquefactions are not reported for this earthquake.

Similarly at Calatafimi (TP), liquefactions and ground deformations, occurred during the 1693 earthquake at 210 Km away from the epicentre, could be due to the critical geological and geomorphological setting of the site. Indeed, here the terrigenous and fluvio-deltaic terrains, belonging to the Terravecchia formation, and the calcareous deposits, of the Baucina one (from Tortonian up to Messinian age), crop out on mountain whose slopes are characterized by complex landslides and superficial deformations.

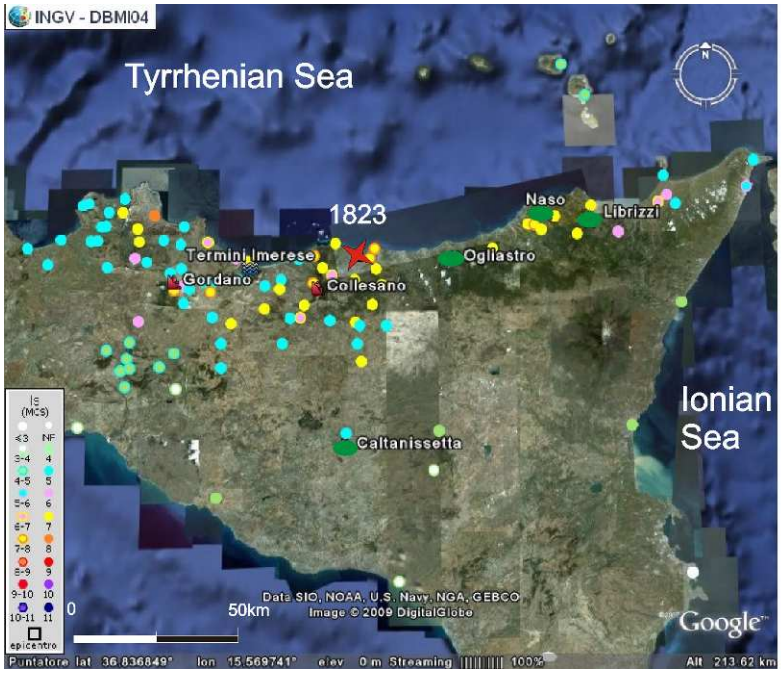

Fig 4.6: Map of intensity distribution for the 1823 earthquake. Red star shows the epicentre location obtained on the basis of intensity pattern modelling; green ellipses are the site where seismogeological effects occurred at unexpected distance on the basis of the upper bound curve analysis.

The use of the upper bound curves and of the empirical relationships regarding the seismically induced landslides, allowed to clarify some subject that have been already tackled by the scientific community. Nicoletti (2005), besides some landslides described by the historical accounts as seismically induced (see also Appendix A), recognized other 15 landslides, in the western sector of the Hyblean Mountains (eastern Sicily) (Fig. 4.7), and considered them of seismic origin because other causes (climatic or lithological) are not possible in his opinion. Moreover, the Author hypothesized a paleo-seismic origin for these landslides, because historical earthquakes would have not enough energy and occurred at excessive distance to be capable to trigger them. The use of the upper bound curves and of the empirical relationships highlight that all the considered landslides could be linked to the 1169, 1542 and January 11th 1693 earthquakes; moreover for five of them that lie easternmost, the 1990 earthquake could be the trigger event, too.

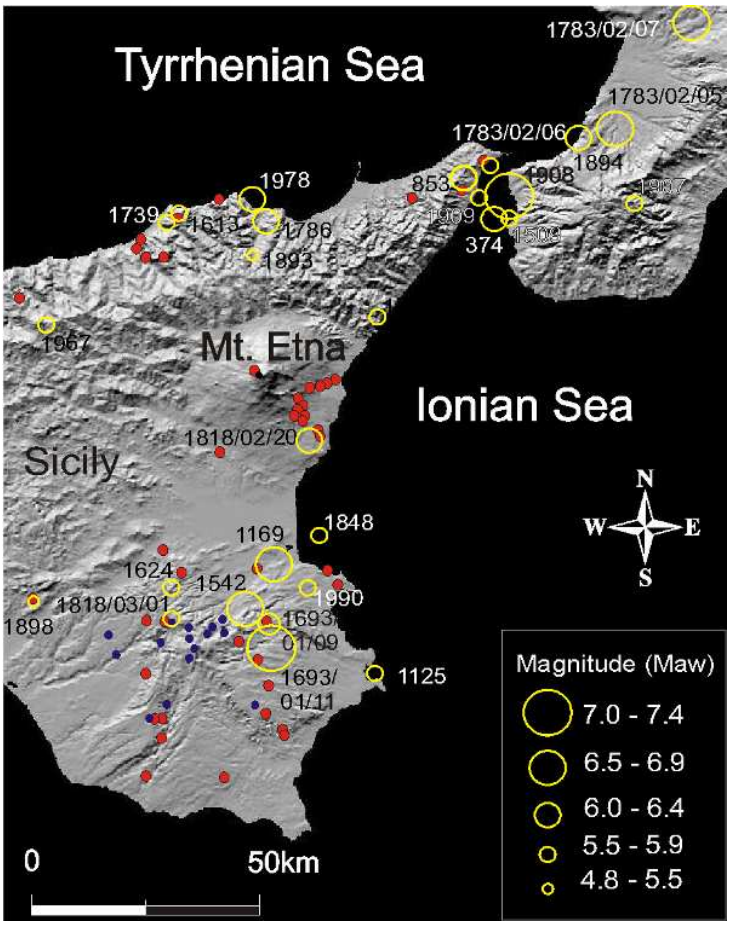

Fig. 4.7: DEM of eastern Sicily showing epicentres of historical events, seismically induced landslides retrieved from the historical accounts (red points) and that observed by Nicoletti (2005) and associated to paleo-events (blue points). These latter landslides lie close to some of the strongest historical sources of south-eastern Sicily, such as that of the 1169, 1542 and January 11th1693 events, also characterized by magnitude enough to trigger them.

Map of distribution of seismogeological effects (Fig. 4.1a) highlights the high susceptibility of the Sicilian country to the earthquake-landslide occurrence, probably due to its geological and structural setting. Moreover, landslides are more frequent in the eastern flank of Mount Etna and in the northern sector of Sicily. Indeed, according to Rasà et al. (1996), the eastern flank of the volcano is a mobile sector that is slowly sliding southeastward under the control of major faults such as the Pernicana fault and the Trecastagni-Mascalucia fault. Whereas, the instability of the northern sector of Sicily could be due, besides to the geomorphological setting of the steep mountain

slopes, to the lithological nature and to the structural setting of the outcropping terrains: Flysh and alloctonous complexes (e.g. the Argille Varicolori) often in persistent instability conditions. Similar distribution is observed for the ground deformations.

Liquefactions are more frequent in south-eastern Sicily, in the Gela foredeep and in the large alluvial plain, south of Catania city (Catania Plain) (Fig. 4.1). The alluvial region of the Catania plain, characterized by the Simeto river, results quite susceptible to the occurrence of liquefaction phenomena not only during strong quakes (Ms = 7.0) but also during moderate shaking (Ms = 6.2). In western Sicily the most prone area is the Belice Valley (Fig. 4.1). These remarks confirm that liquefactions occur in specific geological environment showing favourable setting, such as alluvial plain and depositional basin characterized by young (Holocene), loose, saturated by water, prevalently sandy and silty deposits and flat landform.

Hydrological anomalies are prevalently located in areas characterized by thermal activity (north-eastern Sicily) and in presence of large hydrographical network (Catania Plain, Hyblean sector) (Fig. 4.1).

The map of Figure 4.1b is based on historical data and it is possible the lack of effects due to the incompleteness of the catalogues. However, given that a site, where a specific seismogeological effect occurred in the past, is prone to its development for future events with the same or bigger energy, this map can be considered a valid basis for evaluation of susceptibility to the seismogeological effect trigger. Unexpectedly the map shows that the area mainly prone to the development of these effects is the Hyblean Plateaux (foreland domain), where the outcropping terrains are more stable and less distressed. This could be due in part to the fact that the majority of the strongest historical events are clustered in this sector. However critical geological conditions and site amplification effects cannot be excluded as cause of the high susceptibility of this sector to the seismogeological effect occurrence.

5. STUDY OF THE DEFORMATIVE STRUCTURES

5.1 Method

Field study of seismogeological effects allowed to analyze directly deformative structures triggered by earthquakes, with the main aim to improve the study cases and the methods of paleoseismological analysis. Moreover, finding of seismites dated before the historical time can be useful to extend the seismic catalogue further.

This work is focused to find and investigate both fragile and soft sediment deformations, because they are easier to be found. Indeed, these effects rest as markers of seismicity in the sedimentary sequence and the area where they develop has specific characteristics.

Since a site where seismogeological effects occurred is prone to their development during future earthquakes, with similar parameters, and it could have recorded paleo-events too, the study sites were chosen among those for which accounts report seismogeological effects during historical earthquakes.

The areas prone to liquefaction mechanism are characterized by generally flat landform and loose, saturated, Holocene deposits (see chapter 2). Therefore, sites have been further chosen after geological and geomorphological analyses, by using geological maps available in literature and aerial photos, at the scale 1:10.000. After detailed field surveys, some sites in alluvial plains, along the eastern coast of Sicily, were selected. In some cases the reconstruction of coastline change during time, by the use of historical maps, has been realized. During field survey, pre-existing natural or artificial walls (fluvial channel walls, quarry, building excavations), possibly capable to highlight deformative structures, were sought to realize paleoseismological exploratory trenches, given the high price of the excavations.

When possible, coring campaign, using hand auger equipment, has been carried out in the chosen area with the aim to obtain a preliminary stratigraphical reconstruction directly in the field and successively for elaboration with specific software. Coring was always accompanied by GPS surveys for the exact positioning.

On the trench walls, after cleaning, flagging and gridding, by nails and strings, logging was performed. The stratigraphic units were marked by color buntings to facilitate the analysis. Then rectified digital photograph mosaics, coupled with hand-drawings, allowed to study the trench walls and to reconstruct the stratigraphic sequences and the deformational structure shape by graphical software (CorelDraw and Photoshop).

Samples for laboratory analysis and for radiocarbon dating were collected from the stratigraphic sequence. Sedimentological and paleontological analyses have been performed by the Dott.ssa Alessandra Smedile (INGV-Roma) for the paleoenvironmental reconstruction. Radiocarbon dating was performed on charcoals, organic sediment and bulks, generally selected from the deformed layers and/or from that above or below them, which post date and pre date, respectively, the deformative event. The dating has been realized through accelerator mass spectrometry (AMS) at the Poznan Radiocarbon Laboratory (Poznańskie Laboratorium Radiowęglowe, Poland; c.fourteen@radiocarbon.pl). Measured ages were dendrochronologically corrected in calibrated dates, reflecting the real ages, according to dendrocalibration curves of Calibration data set intcal04.14c (Reimer et al., 2004) and Radiocarbon Calibration Program CALIB14 REV5.0.2 (Stuiver and Reimer, 2005) freely available on the Web.

Given the high deformation degree that generally characterize the pattern assemblage and in absence of datable material the method for distinguishing subsequent deformational events is based on stratigraphic criteria, cross-cutting relationships, and deformational mechanism analysis.

Deformative structures, possibly due to seismic events, where found in three sites of eastern Sicily (Fig 5.1). At Minissale (eastern flank of Mt. Etna) and Agnone (Catania Plain) liquefaction-induced soft sediment deformation structures were found (Guarnieri et al., 2009); at Vendicari (South-eastern Sicily) soft deformations were also observed jointly to fragile structures (fractures) (Pirrotta and Barbano, submitted).

Since soft-sediment deformation structures and fractures can be triggered by more than a mechanism, both of internal origin with respect to the sedimentary environment and of external origin, due to the occurrence of extraordinary events (tsunamis and earthquake

shaking), a detailed paleoenvironmental reconstruction and the analysis of the deformational structures were performed with the aim to highlight the most plausible causative mechanisms.

Fig. 5.1: Google Earth image of eastern Sicily and location of the study sites.

5.2 Minissale site

Minissale is located between the north-eastern flank of the Mt. Etna and the Ionian shoreline (Fig. 5.1 and 5.2a), characterized by recent uplift probably due to thrusting at depth (Di Stefano and Branca, 2002). This highly urbanized area is characterized by

Holocene beach deposits, littoral dunes, and fluvial terraces of the Minissale River. This river, that rises from the north-eastern flank of the Mt. Etna, cuts in its upper part volcanites and Neogene siliciclastic deposits, whereas in its final part it crosses the Late Pleistocene fluvio-marine deposits of Serra S. Biagio and the Early-Middle Pleistocene calcarenites of the foredeep (Lanzafame et al., 1999; Di Stefano and Branca, 2002).

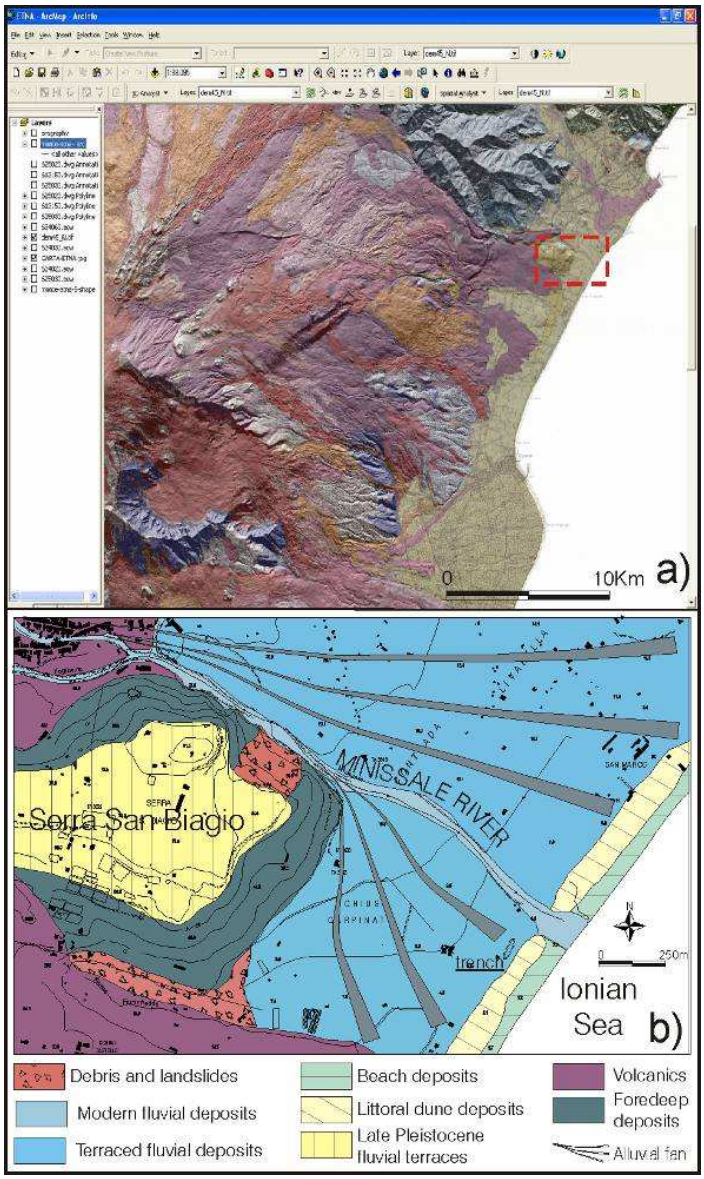

Fig. 5.2: (a) Arc Gis map of the eastern flank of Mt. Etna; (b) Geological sketch map of the Minissale site (modified from Guarnieri et al., 2009).

The river is characterized by a remarkable slope which abruptly decreases in the outfall with a gently dipping Holocene alluvial fan that extends for about 2 km until the coastline where a system of littoral dunes develops. The surface of the sea-ward gently dipping fluvial terrace extends from the slope of Serra S. Biagio hills, about 20 m a.s.l, up to the littoral dunes, 4 m a.s.l. (Fig. 5.2b).

Only one hand core, reaching a depth of 2.45 m, has been realized in the site, in fact it is not favourable to the hand coring activity due to the presence of coarse sediments at shallow depth. In any case the unique core highlighted the presence of a stratigraphy favourable to liquefaction, with a highly permeable sandy sequence alternate with silty layers and only a gravely one; this sequence is capped by an 80 cm thick soil level.

5.2.1 Minissale trench study

The Minissale explorative trench is located at about 180 m of distance from the coastline (Fig. 5.2b). It has been realized exploiting an artificial ditch, about 80 m long, 20 m large, 3 m deep and partially submerged by water, used as water reservoir for agricultural purposes. The artificial excavation cuts through the sedimentary sequence of the Minissale River alluvial terrace.

The trench wall is about 4 m long and 1.50 m deep. It was cleaned out, smoothed, made as much vertical as possible and then logged using a reference string grid and coloured buntings (Fig. 5.3b and 5.4). On the trench the exposed stratigraphic sequence together with deformational structures were studied in detail. In all ten samples have been collected for sedimentological and micropaleontological analyses and two samples for radiocarbon dating (FTM5 and FTM7 in Table VIII).

The sedimentary sequence consists of very coarse gravels and sands, alternated with silt and sands, passing upward to thinner layers capped by the pedogenic one (Fig. 5.3a).

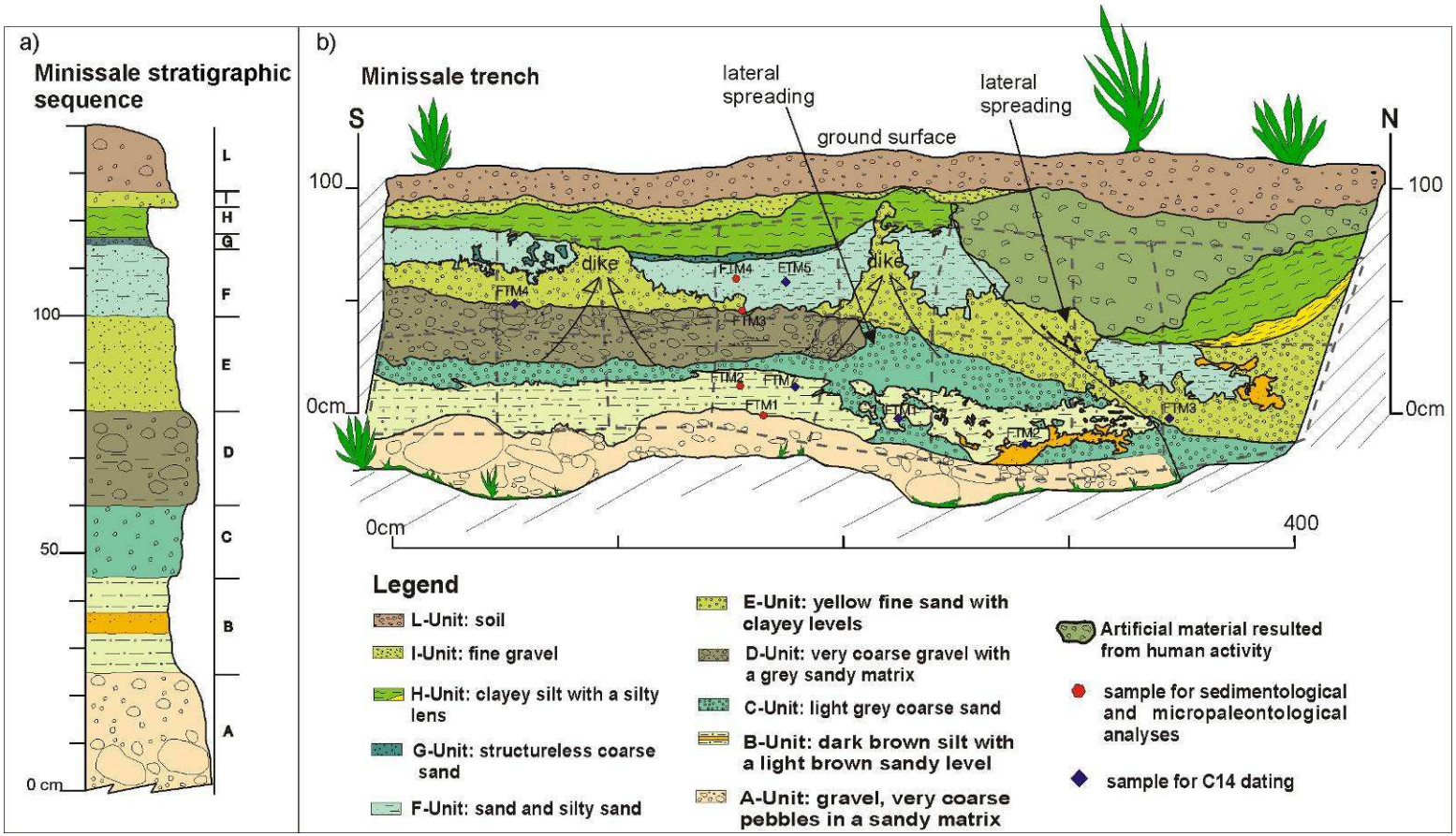

Fig 5.3: (a) Stratigraphic log of the fluvial terrace outcropping in the Minissale exposure: gravel, very coarse pebbles in a sandy matrix (A- Unit); dark brown silt with a light brown sandy level (B- Unit); light grey coarse sand (C- Unit); very coarse gravel with a grey sandy matrix (D- Unit); yellow fine sand with clayey levels (E- Unit); sand and silty sand (F- Unit); coarse sand (G- Unit); clayey silt with a silty lens (H- Unit); fine gravel (I-Unit); Soil (L- Unit); (b) Line drawing of the Minissale exposure. The arrows represent the flow direction of the liquefied sand. The polygons indicate the samples for micro-paleontological analysis and for 14C dating (modified from Guarnieri et al., 2009).

Table VIII: Measured and calibrated ages, according to Calib REV5.0.2 by Stuiver and Reimer (2005), of the samples collected in the excavation walls (after Guarnieri et al., 2009).

Sample	Type	Measured age years BP	2 σ calibrated age years	(Probability distribution)	UNIT
FTM5	Charcoal	185 ± 30 BP	AD 1650 - 1694 AD 1726 - 1813 AD 1838 - 1842 AD 1853 - 1867 AD 1918 - 1952	(0.220) (0.566) (0.003) (0.014) (0.196)	F
FTM7	Bulk	1120 ± 30 BP	AD 784 - 787 AD 824 - 842 AD 862 - 994	(0.003) (0.017) (0.980)	B
CAM12	Bulk	410 ± 30 BP	AD 1431 - 1521 AD 1578 - 1581 AD 1591- 1620	(0.877) (0.002) (0.120)	B
CAM15	Bulk	165 ± 30 BP	AD 1662 - 1700 AD 1703 - 1706 AD 1720 - 1819 AD 1833 - 1881 AD 1915 - 1953	(0.177) (0.003) (0.519) (0.106) (0.195)	E
CAM16	Bulk	350 ± 30 BP	AD 1458 -1531 AD 1537 -1635	(0.432) (0.568)	E

Starting from the bottom it is possible to observe the following layers: gravel with very coarse pebbles in a sandy matrix (A-Unit); dark brown silt with a light brown sandy level (B-Unit); light grey coarse sand (C-Unit); very coarse gravel with a grey sandy matrix (D-Unit); yellow fine sand with clayey levels (E-Unit); sand and silty sand (F-Unit); very coarse sand (G-Unit); clayey silt with a silty centimetric lens on the basis (H-Unit); fine gravel (I-Unit) and soil (L-Unit).

The most prominent observed deformational structures consist in the interruption of A and B-Units and the crack and opening of F and H-Units and consequent lateral movement and down-throwing in the northern part of the section. This feature is observed jointly with a general deformation of the beds that form *boudinage*-like structures and *autoclastic breccias*. The observed deformation is interpreted as lateral spreading given the evidence of a strong hydraulic pressure application and the absence of elements indicating a tectonic control (Fig. 5.3b). In the central and southern part of the section, the yellow fine sand (E-Unit) is vented and creates two dikes: the central dyke (Fig. 5.4a) cuts the layers up to the middle part of H-Unit, whereas the southernmost dyke is less defined and seems to intrude

the F-Unit. Below the dykes the pebbles of D-Unit are clustered and iso-oriented. Moreover, in the northern sector, the breakage of B-Unit, with stretched beds (Fig. 5.4b) and cracks overfilled by sands also associated with the interruption of the coarse gravel layer (D-Unit), may suggest the presence of an older lateral spreading sealed by the sands of E-Unit (Fig. 5.3b).

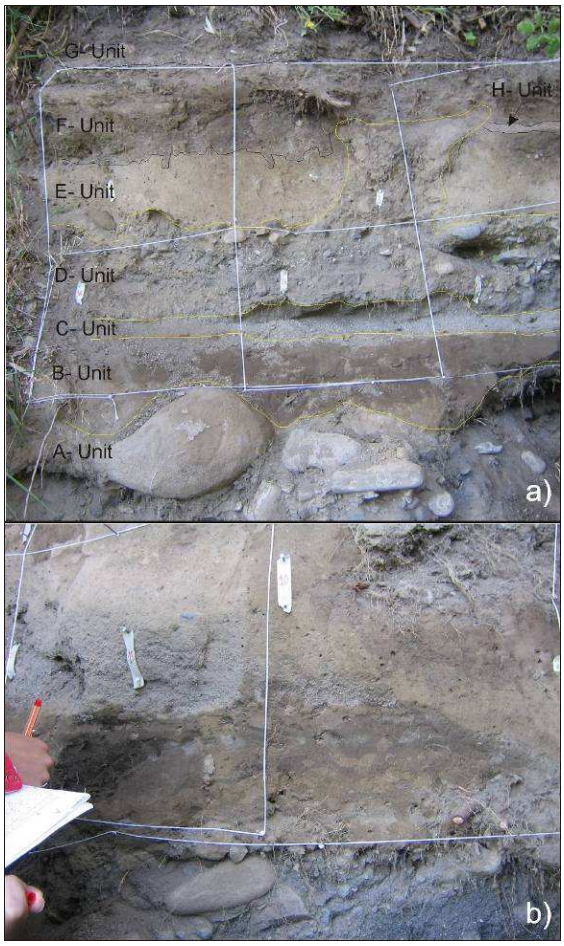

Fig 5.4: Deformational structures on the Minissale trench wall: (a) liquefaction associated dike; (b) deformed beds (*boudinage*-like structures and *autoclastic breccias*).

At Minissale site deformational feature morphology is consistent with sudden application of a large specifically-oriented hydraulic force of short duration, so, these structures have been interpreted as liquefaction induced sediment deformations (Guarnieri et al., 2009).

In summary, there is evidence for two liquefaction events highlighted by two different deformational styles. The most recent event is represented by the dikes and the uppermost lateral spreading, in this case the sequence is clearly driven by an upward hydraulic force and the lateral spreading, with downward component of movement, is due to the voiding of the liquefied levels (E Unit) going upward. Whereas the previous event was clearly driven by a downward mainly gravitative force as testified by the interruption of levels from A up to D-Units, the boudinage of B- Unit and the filling of C-Unit sands mixed to the deformed levels indicating the oldest lateral spreading.

To get an age control on the recognized liquefaction events, two samples collected at different depths have been dated (Table VIII). Sample FTM5, a piece of charcoal from F-Unit yielded a dendrochronologically corrected 2 sigma age of 1650–1950 AD, whereas a bulk sample (FTM7), from B-Unit, gave a 2 sigma age of 825– 995 AD.

Given that the first event involved the levels up to D- Unit, it is predated by the FTM7 age and pos- dated by FTM5 one, thus this event should be younger than 825 AD and older than 1650-1950 AD; whereas the second event that occurred after F-Unit deposition and involved all the outcropping units is predated by the FTM5 age and so it should be younger than AD 1650-1950.

5.3 Agnone site

Agnone site is located in the Catania Plain, behind a thick littoral dune facing the Ionian Sea (Longhitano and Colella, 2007) (Fig. 5.1 and 5.5). This plain is an approximately 770 km^2 large upper Pliocene–Quaternary, fault-controlled, alluvial depression, representing one of the most important hydrogeological units in eastern Sicily and extending west-east

south of the Mt. Etna. The hills bordering are constituted by clayey marine deposits of Pleistocene age (Lentini et al., 1991) to the south, lavas and pyroclastic deposits from Etna volcano, to the north, and quartz-sandstones of the Numidian flysch, to the west (Lentini et al., 1991).

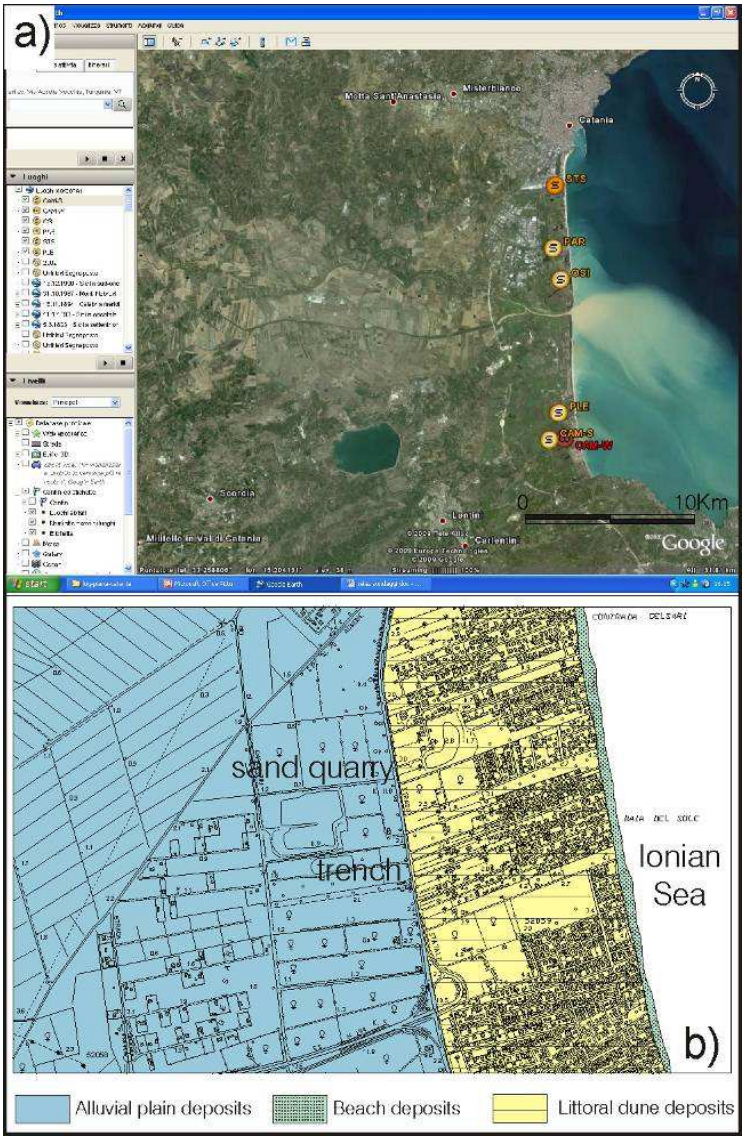

Fig. 5.5: (a) Google Earth of easternmost sector of the Catania Plain with the location of the hand cores; (b) Geological map of the Agnone site.

Thanks to AGIP oil wells, realized in the 1954 and 1956, the sedimentary sequence was observed. A 500 m thick Pleistocene blue-grey clayey deposit was detected; its top deepen from few meters up to about 80 m, and it results covered by permeable fluvial deposits, of about 45–76 m of thickness also characterized by volcanic products. The uppermost sequence consists in very shallow, low permeability, clayey and clayey–sandy deposits (recent flood deposits) overlying permeable gravels and sandy-gravels layers (ancient flood deposits) (Ferrara, 1979; 1999). This sequence hosts paleochannels and a multilayer aquifer also suffering salinization. On the plain the water-table is located at about 1–2 m b.s.l. (Capaccioni et al., 2005). Holocene alluvial infill is linked to the actual stream network composed by the Simeto, Dittaino and Gornalunga rivers.

According to Nunziata et al. (1999) the uppermost depositional sequence is highly susceptible to liquefaction for earthquake of magnitude in the range 7–7.5.

5.3.1 Agnone trench study

A total of 15 head cores, reaching a maximum depth of 3.50 m, have been realized in the Catania Plain. These allowed to characterize the stratigraphic sequence and qualitatively define the liquefaction susceptibility of the deposits. The cores have been realized in 5 sites from north to south: STS, South Tiro a Segno site; PAR, Paradiso degli Aranci site; OSI, Oasi del Simeto site; PLE, Pantano Lentini site; CAM, Cava Agnone Marina site (Fig. 5.5a and 5.6). Laboratory analyses confirm the fluvial nature of the stratigraphic sequence composed mainly of loose sand alternated and covered by clayey occasionally silty layers (Fig. 5.6). The sequence qualitatively shows a high liquefaction susceptibility also considering the superficial position of the water table in the plain.

The Agnone trench is located at about 1 km of distance from the coastline (Fig. 5.5b), in a 450 m long and 250 m large quarry, almost completely overfilled by water, used for the excavation of Holocene sand. The trench wall was realized exploiting a 10 m long and 1.50 m deep section of the eastern portion of the quarry (Fig. 5.7).

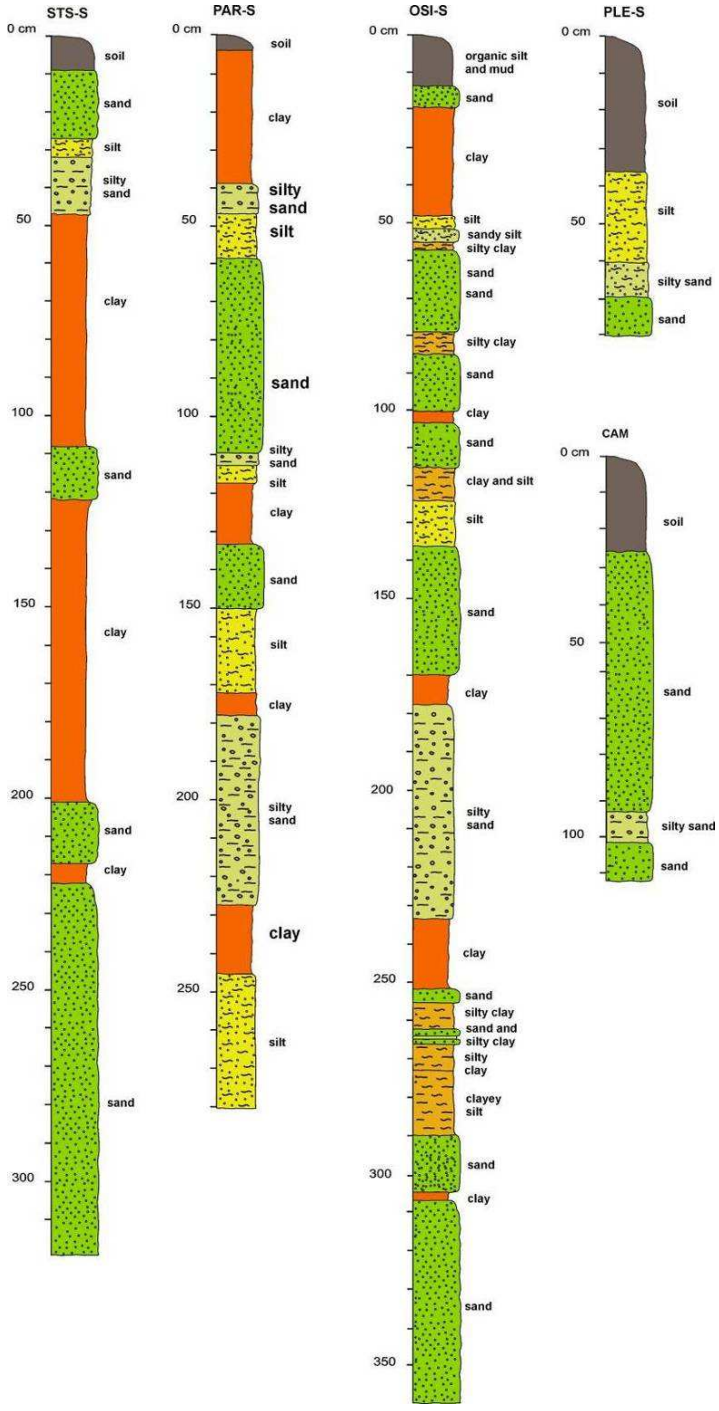

Fig. 5.6: Representative logs of the sedimentary sequence in the Catania Plain. Letters refer to: STS-S, South Tiro a Segno site; PAR-S, Paradiso degli Aranci site; OSI-S, Oasi del Simeto site; PLE-S, Pantano Lentini site; CAM, Cava Agnone Marina site.

The local stratigraphic sequence together with sedimentary and deformational structures have been studied in detail, 11 samples have been collected for sedimentological and macro/micropaleontological analysis and 6 for radiocarbon dating.

The sequence is prevalently composed by sand with clayey lenses and silt, passing upward to a pedogenic level and laminated clay (Fig. 5.7a). This sequence has been divided into 5 levels from A to E- Units. Given the high deformation degree of the outcropping layers, their thickness has been only deduced and approximate. The lowest layer consists of light brown structureless sand with a yellow sandy level on the basis (A-Unit). On this a dark brown silty-sandy layer crops out on the southern sector of the trench (B-Unit). Rising in the section a layer of grey sand with grey clayey lenses (C-Unit) crops out. On this a 50 cm thick layer constituted by yellow and brown sands alternated with brown silt and grey clayey lenses (D-Unit) lies. At the top of the sequence a level of dark structureless sand which heteropically evolve to grey clay (E-Unit) crops out.

Macro- and micro-paleontological analyses (foraminifera and ostracods) suggest an alluvial origin for all the units cropping out in the trench wall. Only for C-Unit benthic foraminifera (Ammonia sp., Asterigerinata planorbis, Florilus boueanum and miliolids) and ostracodes (Aurila sp., Cyprideis torosa and Palmoconcha turbida) indicate a provenance from a close marginal marine environment.

Important deformational events affected the studied exposure (Fig. 5.7b). A-Unit is sharply downthrown in the southern part of the section where the top of yellow sand is lowered of about 50 cm. The vertical boundary between A and B- Units has been interpreted as a structure due to lateral spreading with vertical component of movement, since there are not evidence of a tectonic deformational style (such as kinematic indicators) but rather of a high hydraulic force, testified by deformed bands and squeezed sand, too (Fig. 5.8a).

The most prominent deformational structure is a 100 cm high and 50 cm large sand dike in the central sector (Fig. 5.8b). This dike, developed by the pumping of the light brown sand (A-Unit), cuts through the sequence intruding up to E- Unit (Fig. 5.8c).

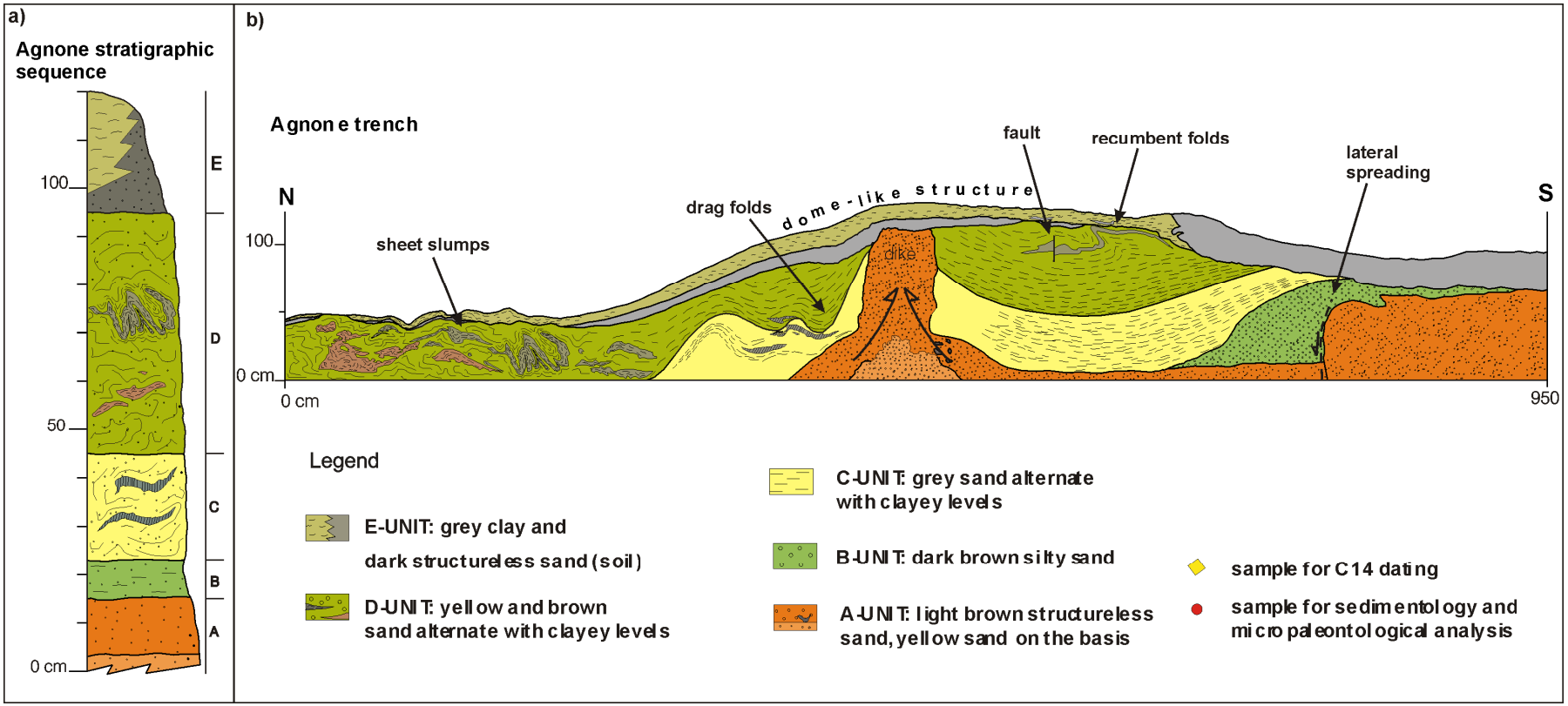

Fig 5.7: (a) Line drawing of the Agnone exposure. The arrows represent the flow direction of the liquefied sand. The polygons indicate the samples for micro-paleontological analysis and for 14C dating; (b) Stratigraphic log of the alluvial sequence outcropping in the Agnone sand quarry: light brown structureless sand, yellow sand on the basis (A Unit); dark brown silty sand (B Unit); grey sand alternatives with grey clayey lenses (C Unit); yellow and brown sand alternatives with grey clayey lenses (D Unit); grey clay and dark structureless sand, soil (E Unit); (modified from Guarnieri et al., 2009).

The C, D and E-Units appear strongly deformed, probably as a consequence of the dike intrusion. The alternated sandy and clayey layers of C-Unit show the presence of drag-folds (Fig. 5.8d). D-Unit appears intensely deformed by boudinage, recumbent folds (Fig. 5.8e), and sheet-slumps (Fig. 5.8f). In the upper part of the section a small fault with an about vertical plane and 7 cm offset, cross-cuts a recumbent fold of D- Unit (Fig. 5.8g). Finally, the dome-like morphology of the top level (E- Unit) has been interpreted as result of the up-warping mechanism caused by the dike intrusion.

Analysis of deformational structures shows that these developed under a large specifically- oriented hydraulic force of short duration, for this reason they were interpreted like liquefaction induced sediment deformations (Guarnieri et al., 2009).

Summarizing, observations provide evidence for two events of liquefaction at this site. The oldest one is the event that produced lateral spreading in the southern part of the section involving the A and B-Units and creating the accommodation space for the deposition of the fluvial sequence (from C to E- Units). Then, the most recent event involved the whole sedimentary sequence and it is represented by the dike intrusion and by the boudinage, sheet slumps, folds, fault and the dome-like setting of the originally planar E-Unit.

To provide chronological constraints to the occurrence of the two liquefaction events, three samples of bulk organic sediments has been collected, because no charcoal was found in any unit. CAM15, collected into E-Unit, yielded a dendrochronologically corrected 2 sigma age of 1660–1950 AD; CAM12 and CAM16, collected into B and E-Units respectively, gave a similar age of 1430–1620 AD and 1460–1635 AD (Table VIII). Since CAM16 was collected in the youngest part of the sequence its age was expected to be close to that of CAM15. As a consequence this dating was considered wrong, or as alternative explanation, this charcoal could be an older element that came at the top of the sequence for reworking, probably human, activity. In any case the CAM16 dating was rejected and that of CAM15 was consider as the oldest possible age of E-Unit.

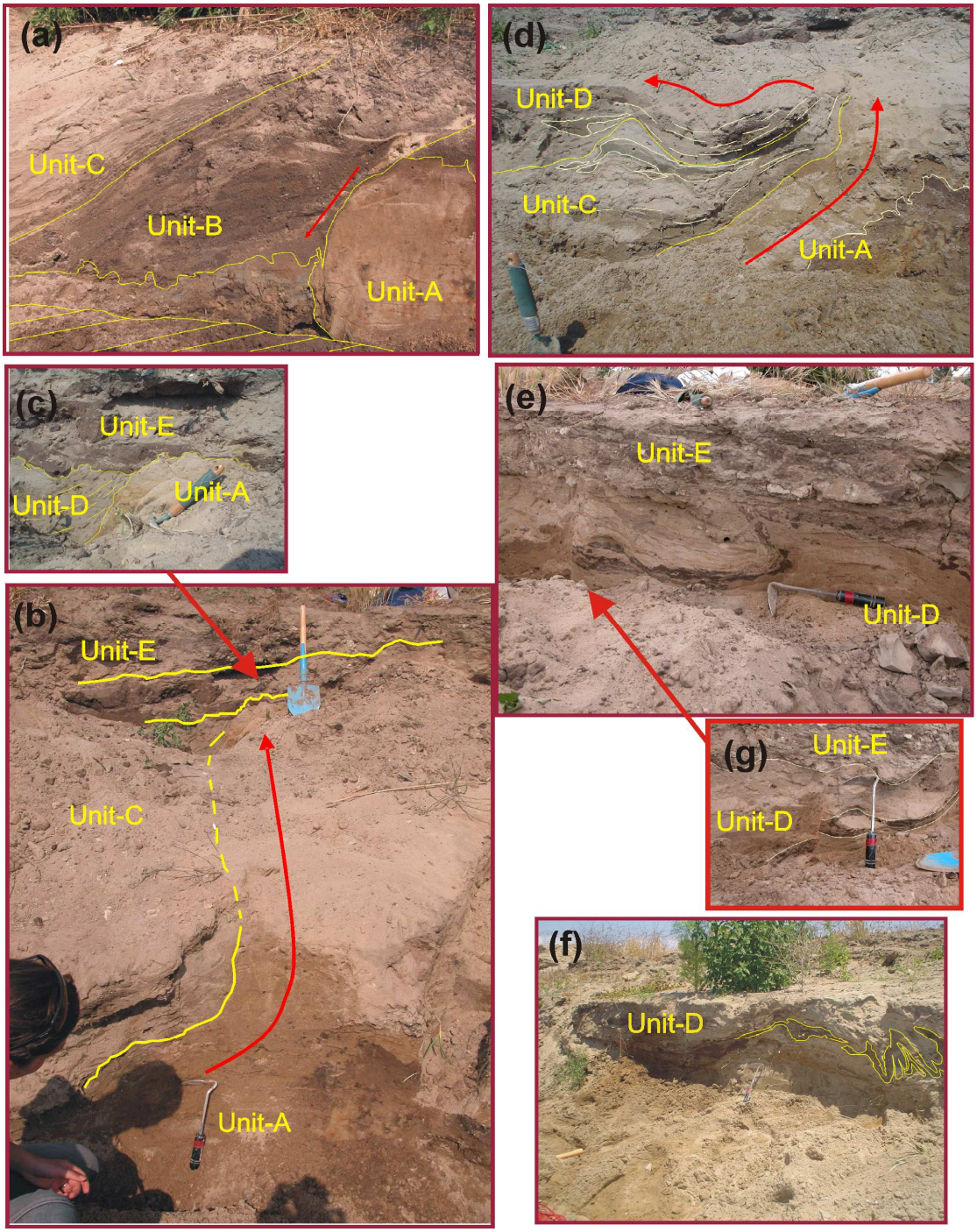

Fig 5.8: Agnone trench photos: (a) Lateral spreading involving the A and B-Units; (b) Dike of A-Unit sand that intrudes the E-Unit, the detail is in picture (c); (d) Dike and associated drag folds in the C- and D- Units; (e) recumbent fold in D-Unit offset for 7 cm by a little fault, the detail is in picture (g); (f) Slumping in the D-Unit, in the northern sector of the trench.

Since B-Unit was involved in the oldest deformational event it probably occurred after the interval age 1430-1620 AD. Whereas, the age of the uppermost level (E-Unit) involved in the last deformational event allows to conclude that it occurred after 1660-1950 AD.

5.4 Vendicari site

The study area is located in the northern part of the Vendicari Nature Reserve (Fig. 5.9a and 5.9b), characterized by a gently sloping rocky coast (4–8° of average slope) that occasionally rises to form low cliffs (Fig. 5.9d and 5.9c). Northernmost, the rocky coast isolates from the sea a lagoon system (Pantano Piccolo and Pantano Grande), whereas a sandy bar extends up to about 3 km south of Torre Vendicari bordering the Pantano Roveto (Fig. 5.9a).

The sedimentary sequence is composed of terrains from Pliocene to Quaternary age. The lower level consists of the Trubi Formation, made of white marls of Pliocene age (A-Unit in Fig. 5.10a) (Lentini et al., 1996). It shows rhythmic bedding, indicating an alternation of relatively carbonate-poor and carbonate-rich beds, probably originating from climatic and environmental conditions (De Visser et al., 1989). This Unit belongs to the carbonatic cycle of Pliocene age and testifies the restoring of deep water and open sea after the evaporitic episode of Messinian age. Above the A-Unit, yellow massive sandstones, of Pliocene age, crop out (B-Unit in Fig. 5.10a and 5.10b) showing the typical characteristic of beach deposit cemented in a littoral environment. On the B-Unit a probable fluvial deposit, roughly 50 cm thick (C-Unit in Fig. 5.10a and 5.10b) crops out; this is a red conglomerate constituted by cm-metric rounded pebbles in a red sandy matrix.

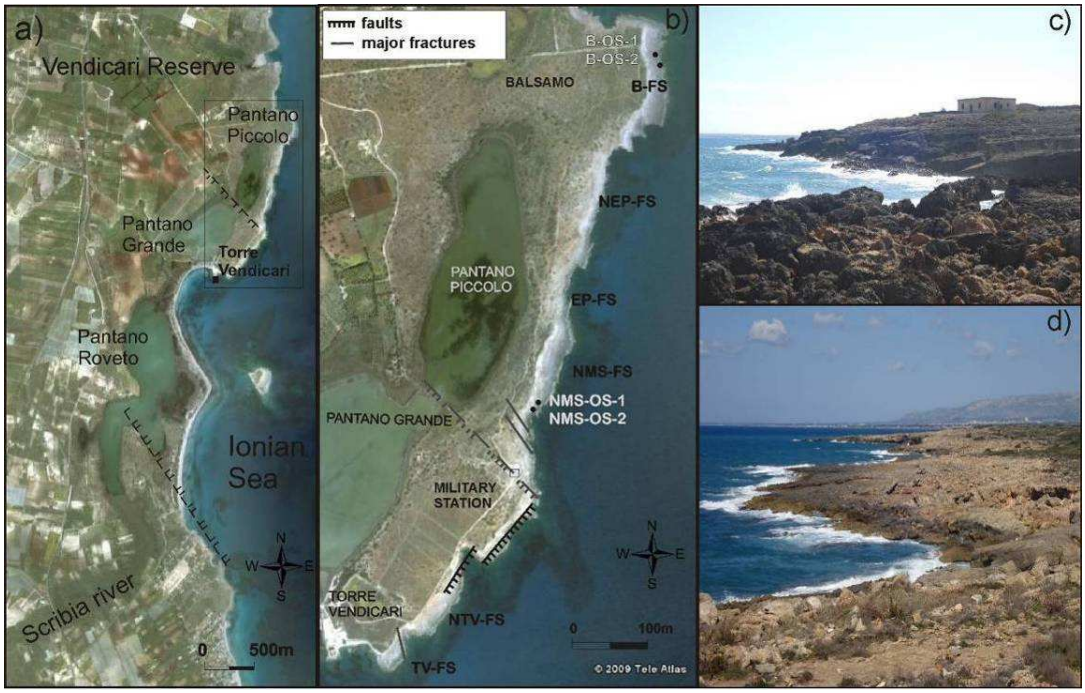

Fig. 5.9: (a) Google Earth map of the Vendicari Nature Reserve, rectangle is the location of the study area; (b) Study site with the structural features: faults and major fractures. Initials indicate the study stations for the mesostructural and systematic analyses performed at the field scale, FS (Torre Vendicari, TV-FS; North Torre Vendicari, NTV-FS; North Military Station, NMS-FS; East and Northeast of Pantano Piccolo, EP-FS and NEP-FS and Balsamo, B-FS) and at the outcrop scale, OS (North Military station, NMS-OS-1 and NMS-OS-2 and Balsamo Site, B-OS-1 and B-OS-2). (c) photo of the rocky coast uplifted by faults, north of the old Military station; (d) photo of the coast with low angle slope, south of the Military station.

Locally, especially in the northern sector (Balsamo area in Fig. 5.9b), it passes through lateral heteropy to a bioclastic red sand, rich in ultra-cm-metric shells, that could represent a paleo-beach. At the top of the sequence a white to yellowish organic calcaranitic and calciruditic deposit lies (D-Unit in Fig. 5.10a and 5.10b). This Unit shows cross and parallel lamination and frequent lenses form pelitic and conglomeratic intercalations of littoral and lagoonal facies (Amore et al., 1994); it lies unconformable on the oldest Pliocene cycles and locally passes to littoral aeolian faces of paleodunes. According to Ruggieri (1959) and Lentini et al. (1996) the D-Unit is a probable Tyrrhenian platform: “panchina”.

All the area is affected by an intense karstification process that accelerates the erosion of the rocky coast.

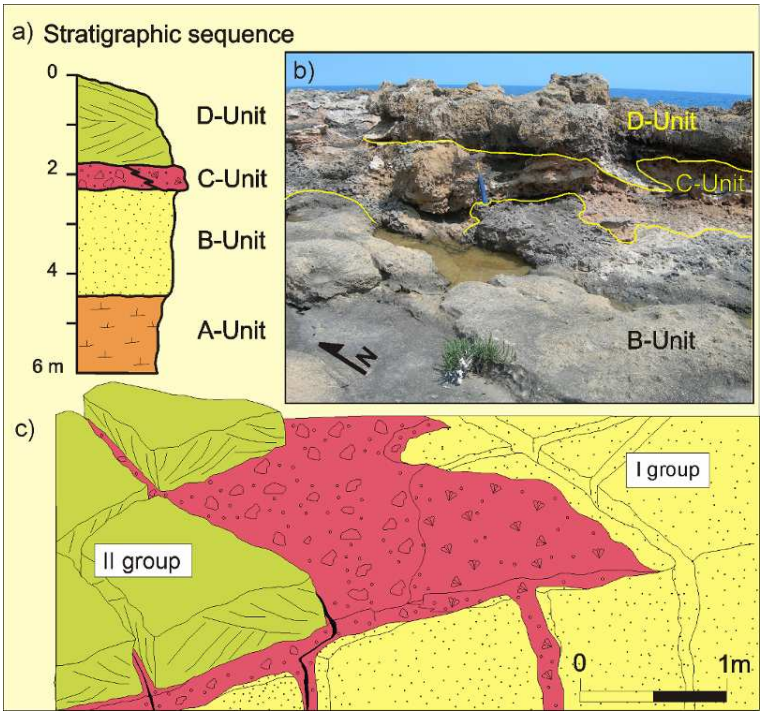

Fig. 5.10: (a) Reconstruction of the stratigraphic sequence cropping out at Vendicari Reserve. A-Unit is the marls of the Trubi Fm (Pliocene); B-Unit represents the sandstones of Pliocene age; C-Unit is the red conglomerate and sand interpreted as a paleosoil passing to a paleo-beach and D-Unit are calcarenite of Pleistocene age; (b) photo of the stratigraphic sequence showing the B- C- and D-Units; (c) scheme of the stratigraphic sequence and relationships between the I and II fracture groups.

Ponds of Hellenistic Age (about 323 BC to 30 BC), dug in the rock for fishing, lie roughly at present sea level, indicating that in this area the uplift was of the same order of the sea level rise over the last two thousand years (Ferranti et al., 2006).

Two major almost NW-SE normal faults (Fig. 5.9a) dislocate the whole previously described sedimentary sequence, at the Military station cut is assessed of about 6 m. South of the station, only the marls (A-Unit) and the sandstones (B-Unit) crop out and these are dislocated south-eastward by two NE-SW en-echelon normal faults (Fig. 5.9b). The faults outcropping near the Military Station (the northernmost NW-SE and the two NE-SW) probably caused the rising of the rocky coast, creating a 10 m high cliff (Fig. 5.9c), whereas

southward and northward the coast is characterized by a gently sloping platform bordered seaward by a little scarp, also continuing off-shore (Fig. 5.9d).

The aerial photo analysis also highlights morphological scarps, lowland and uplifted sectors in proximity of the faults, confirming that these have a role in the local coast uplift, the closure of the Pantano Piccolo from the sea and its separation from the Pantano Grande. Furthermore, the recent activity of the southernmost NW-SE fault progressively caused the leftward deflection of the Scribia River (Fig. 5.9a).

North of the Military station and near Torre Vendicari three NW-SE trending large fractures have been observed (Fig. 5.9b). They affect the Pliocene sandstones, are opened up to 1 m, reach about 40 m of length and are filled by the red conglomerate of the C- Unit, their walls have no kinematic indicators (Fig. 5.11a). These fractures continue in the long and narrow inlets, characterizing the coast, therefore they seem to have played a role in the geomorphological evolution of the area.

Besides these major fractures a thick crack network, affecting the rocky coast, has been observed and analysed together with the soft sediment deformations.

5.4.1 Analysis of the deformation structures

In the sedimentary sequence of Vendicari structures related to two different deformational styles, brittle and soft, have been observed. The brittle deformative pattern is represented by a dense network of steeply dipping fractures generally opened and filled by sediments made of carbonatic and clastic material. Soft sediment deformations are represented by autoclastic breccias, diapyr-like injections and thixotropic wedges, affecting the soft sediments of the A- Unit and the cemented ones of the B-Unit when they were not yet well-diagenized.

With the aim of defining the deformation mechanisms occurring in the area deformational structures were studied in detail, considering every possible triggering cause.

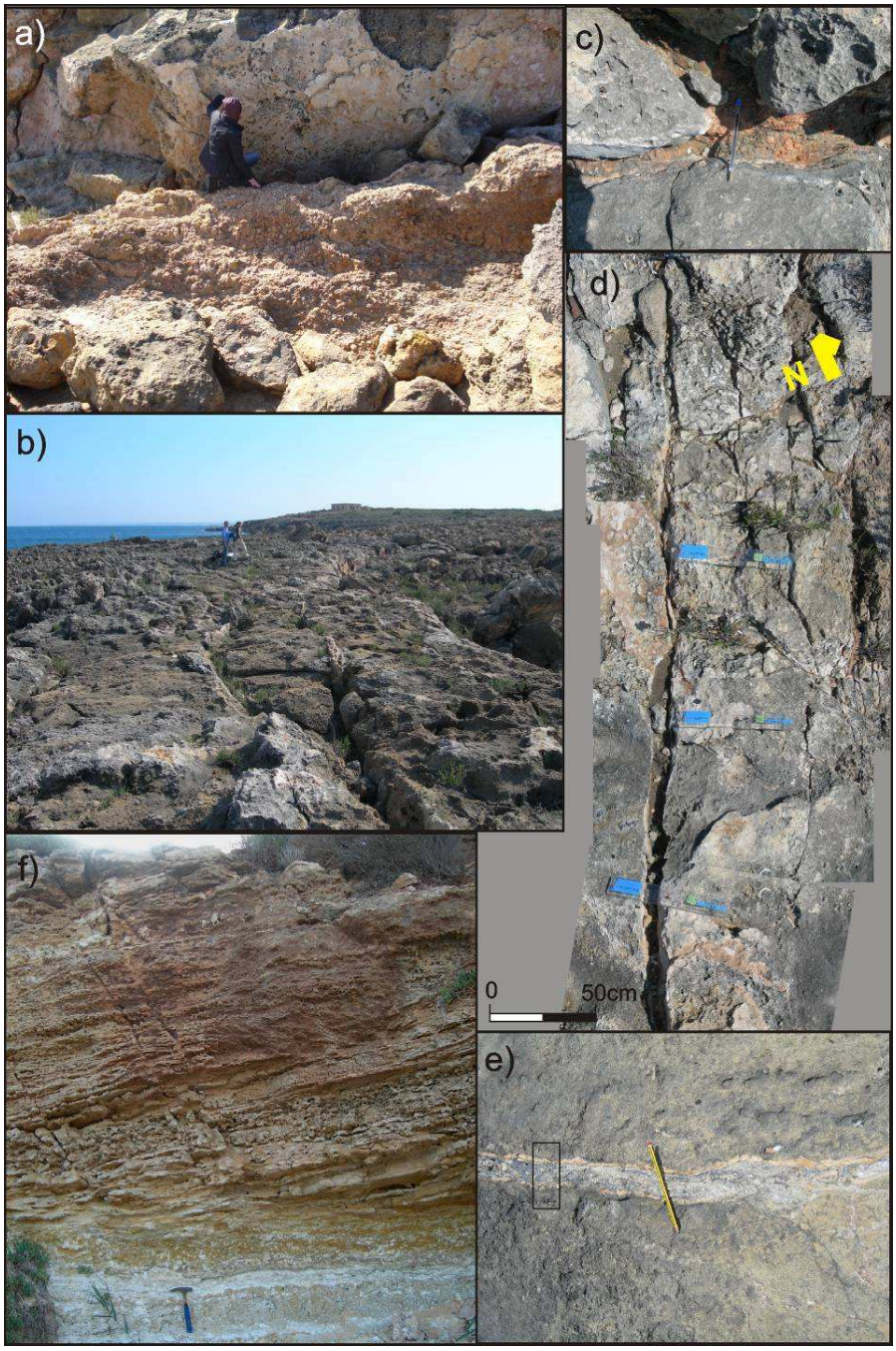

Fig. 5.11: (a). Extensional major fractures on the Pliocene sandstones filled by the red conglomerate, north of the old Military station; (b) fractures belonging to the I group; (c) detail of a fracture of the I group filled by the C-Unit; (d) fractures belonging to the II group; (e) detail of a fracture of the second group filled by carbonatic white material; (f) section view of the I group fractures.

Unfortunately, no datable elements have been observed in the sedimentary sequence to better constrain the age of the deformations and therefore the method for distinguishing event chronology is based only on the stratigraphic criteria, cross-cutting relationships, and deformational mechanism analysis.

5.4.1.1 Brittle deformation analysis

Fractures have been analysed performing a systematic study, following Hancock's (1985) and Dunne and Hancock's (1994) method, a mesostructural analysis (stereographic projections and rose diagrams) and then the analysis of the microscopic characteristic of the filling material, to highlight possible relationship between fractures and the tectonic regional stress field. Furthermore, fractures were classified in relation to lithological and morphological elements.

The systematic study consists in evaluating the fracture parameters and their mutual relationships (trend, architectural style, dihedral angle) in order to define the different typology (*pure extensional joints*, *hybrid joints* or *shear fractures*) (e.g. Hancock, 1985; Pollard and Aydin, 1988) and the causative stress field.

At Vendicari, the fracture analysis was made in six study stations from Torre Vendicari up to the Balsamo site, for a total area of about 1 km^2 (Fig. 5.9b). The stations have been investigated both at field scale (Field Scale study stations, FS) and at outcrop scale, using a digital photo device (Outcrop Scale study stations, OS). In all, 296 fractures have been detected and classified evaluating for each discontinuity the following features: (1) terrain where they develop; (2) length (m) and spacing (cm); (3) width and opening (cm); (4) filling material; (5) possible kinematic indicators; (6) dihedral angle (2θ); (7) geometry and architectural style (Pollard and Aydin, 1988); (8) dip direction and angle of dip.

Fractures have been distinguished in two groups on the basis of their characteristics and of the age of the affected deposits. The oldest and most developed group (I group) involves the Pliocene sandstones (B-Unit) (Fig. 5.10c and Fig. 5.11b) and is characterized by up to

40 m long fractures, with openings that sometimes reach several decimetres and a filling material constituted by the red conglomerate lying on the sandstones (C-Unit) (Fig. 5.11c). The second younger and less developed group (II group) affects the Pleistocene calcarenite (D-Unit) (Fig. 5.10c) and shows shorter and narrower fractures (Fig. 5.11d) sometimes filled by a white fine material (Fig. 5.11e).

Neither the first nor the second fracture group show kinematic indicators on the walls, moreover these cracks mainly involved the cemented B- C- and D-Units and they disappear in the less brittle marls of Trubi Fm, as observed at south of the Military station, where I group fractures stop in the A-Unit (Fig. 5.11f).

In this analysis, particular importance is given to the dihedral angle (2θ) and to the architectural style that are the most significant parameters to distinguish the fracture typology. *Pure extensional joints* are characterized by $2\theta = 0°$- $10°$ and architectural style tracing Y, K, I, T and H- shapes (Pollard and Aydin, 1988); *hybrid joints* by $10° < 2\theta < 50°$ and *shear fractures* by $2\theta > 50°$; the last two fracture types depict V, Y, X and A-shapes. Dihedral angle 2θ of Vendicari fractures generally varies between 5° and 90° with three peaks. The main peak, representing 20% of fracture- enclosed angle, is between 50° and 60°; the second and the third peaks, representing respectively 16% and 14% of the total, have value intervals 70°-80° and 0°-10° (Fig. 5.12a). Moreover, about 53% of the fractures show the typical architectural style of *pure extensional joints*, while 47% are typical of *hybrid joint* and *shear fractures* style (Fig. 5.12b). Fractures also show an irregular spacing from few cm to several metres.

Fracture plane directions have been plotted in stereonets (equal area projection, lower hemisphere) and rose diagrams (Fig. 5.13) to better classify them and define the stress field responsible for their development. The stereonet of all fractures shows a marked dispersion of the plane direction (Fig. 5.13a), so the data have been divided according to the fracture group (I or II group), the lithology where they develop (B-Unit- or D-Unit) and the study station where they were collected (Fig. 5.13b and Fig. 5.13c). However, separated stereonet data are still scattered. In the rose diagram of figure 5.13a, data have been divided on the basis of direction intervals of 10 degree.

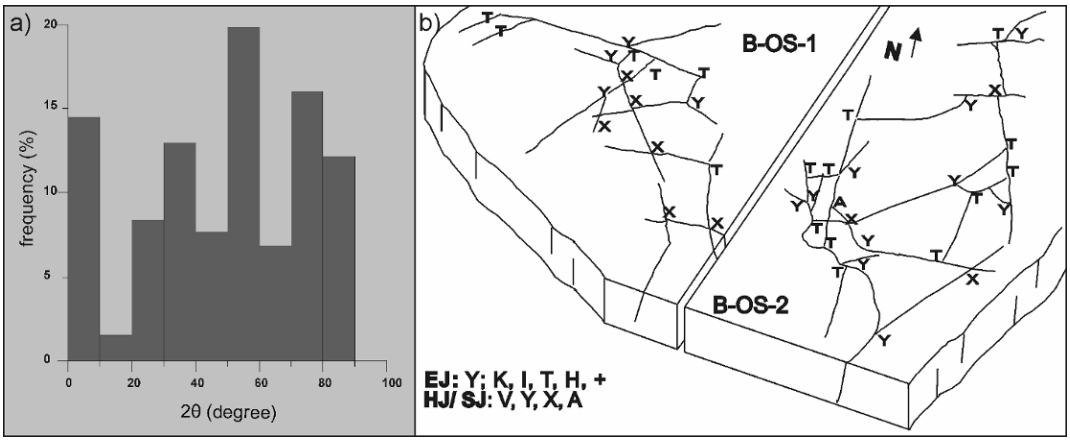

Fig. 5.12: (a) Dihedral angle 2θ *vs* frequency histogram, angles vary between 5° and 90°, but three joint-enclosed angle peaks are between 50° and 60°, 70° and 80°, 0° and 10°; (b) Sketch of the two outcrop scale scan areas at Balsamo site: B-OS-1 and B-OS-2. Letters indicate the shape created by two fractures when they join. Y, K, I, T and H shapes are typical of pure extensional joints; on the contrary V, Y, X and A shapes are indicative of shear component and of hybrid fractures or shear joints.

Statistical analysis shows that 60% of fractures have average frequency $f < 6\%$, these are also scattered in different directions; whereas 40% of fractures have frequency $f > 6\%$ and direction range from N0 to N50, with a frequency peak ($f = 12\%$) at N10-20.

Since at Vendicari, the coast is characterized by more or less developed off-shore scarps and at the Military station it rises creating a moderately high but steep cliff, the variation of the coastline in the different scan areas has been measured, to highlight possible geomorphological influence on the fracture formation. Data were plotted in a stereographic projection (Fig. 5.13d) showing that coastline directions, ranging between N5 and N50, well match with the directions of fractures with major frequency (40% with frequency $f > 6\%$ and direction range from N0 to N50) and especially with the frequency peak ($f = 12\%$) at N10-20.

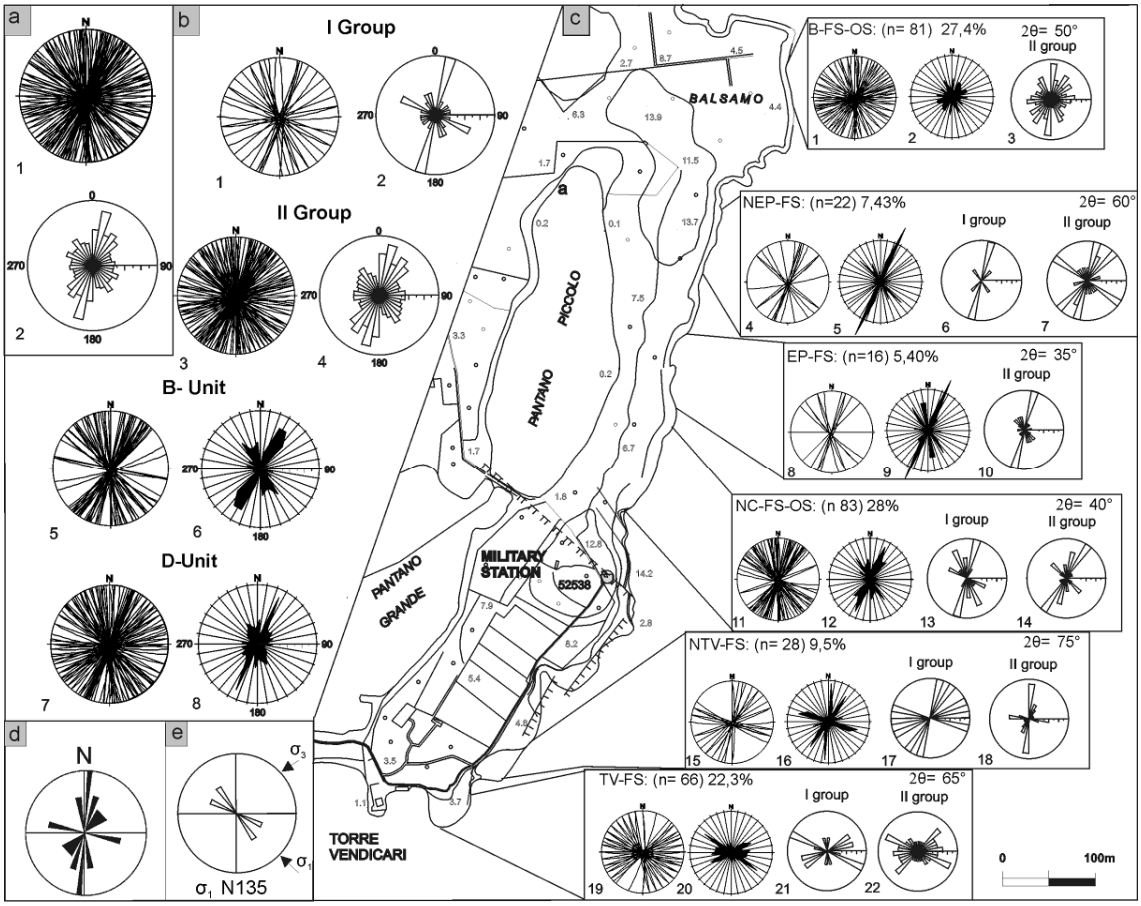

Fig. 5.13: Stereoplots (equal area projection, lower hemisphere) and rose diagrams referring to: (a) all the fractures detected at Vendicari site; (b) fracture divided on the basis of the group (I or II) to which they belong and according to the terrain age within they develop; (c) fractures divided on the basis of the scan area where they were detected. For each section (a, b, and c) the first stereonet (1a; 1, 3, 5 and 7b; and 1, 4, 8, 11, 15 and 19c) is the stereographic projection of all the fracture plane directions; the second stereonet (2a; 2, 4, 6 and 8b; 2, 5, 9, 12, 16 and 20c) is the rose diagram of the whole dataset. In section (c) the 6, 13, 17 and 21 stereonets are rose diagrams of I group fractures; the 3, 7, 10, 14, 18 and 22 stereonets are rose diagrams of II group; moreover, from left to right the study station name, the number of fractures, the percentage with respect to the total number and the average 2θ are reported; (d) rose diagram of the coastline direction; (e) stress field reconstruction.

5.4.1.1.1 Microscopic thin section analysis

To observe possible relationships between stress field and fracture development, analysis under the microscope has been performed on thin sections of samples collected from the second fracture group filling material and cut perpendicularly to the fracture walls (Fig. 5.11e and Fig. 5.14a). This examination reveals that the filling is made up of an assemblage of material deriving from the rocky fracture walls, the eroded platform and the marine environment.

The presence of shells (mostly lamellibranches and bryozoans) and planktonic and benthonic shallow water foraminifera (families of Globigerinidae, Elphidiidae and Bulimindae), indicate a transport from the sea, probably due to wave flooding and/or to the spray on the platform. Everything is cemented by prevalently calcitic minerals, linked to dissolution processes of the carbonatic rock with massive and granular texture (Fig. 5.14b).

No kinematic indicators were detected by the microscopic analysis and elements are unbroken and no aligned or reoriented.

The overall characteristics and the composition of the filling material reveal that it developed in pre-existing and propagating cracks, possibly enhanced by dilation from pre-depositional surface movements or weathering.

Therefore, these filled fractures can be classified as Sedimentary dykes and in particular as *Neptunian dykes* sensu Montenat et al. (2008). These are subaerially-exposed carbonate sediments that generally lithify very quickly after their deposition, for near surface meteoric or intertidal-supratidal marine diagenesis (Tucker, 2001) and are subject to dissolution in place with intense karstification (Dravis, 1996). Although at Vendicari the rocky platform is highly karstified, the sedimentary dykes are well preserved and not yet eroded and hence of recent formation.

The microscopic section analysis shows evidence of at least two repeated opening/filling and mineralisation/cementation events. Indeed, there are two different filling sediments in the II group fractures and two wall-parallel boundaries testify to two crack episodes. An earlier boundary remains between the Pleistocene calcarenite and the older and coarser

filling sediment, indicating a first crack episode. Another boundary remains between the older sedimentary filling and the younger and finer one, testifying to a second crack episode and subsequent filling (Fig. 5.14a).

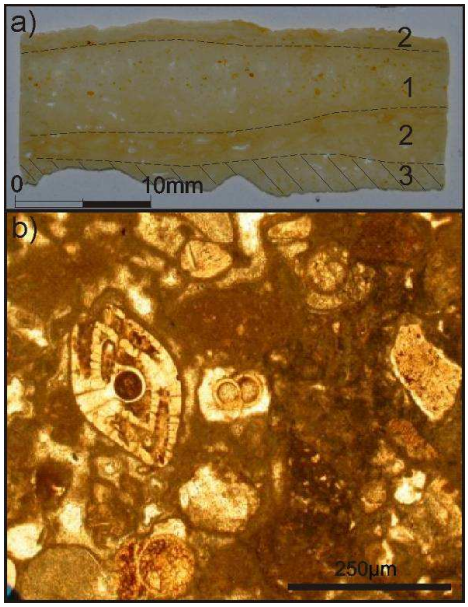

Fig. 5.14: (a) Thin section of the II group fracture filling material. Dashed area 3 is the Pleistocene calcarenite crack wall (I deformation event in the II fracture group), 2 is the earlier-formed dyke sediment (II deformation event in the II fracture group), 1 is the younger filling material; (b) microscopic photo of the section V1, enlargement 5X, showing planktonic foraminifera and lithic fragments in a massive texture made of calcite minerals.

5.4.1.2 Soft sediment deformation structure analysis

The soft sediment deformations affect the most ductile marls of the Trubi Fm. (A-Unit) and the sandstones (B-Unit) probably before their complete lithification. These structures consist of autoclastic breccias, diapyr-like injections and thixotropic wedges (Fig. 5.15 and Fig. 5.16).

In the inlet south of the old Military station, the Trubi Fm. (A-Unit) and the Pliocene sandstones (B-Unit) crop out on a roughly 3 m high scarp, related to the en echelon NE-SW normal fault activity (Fig. 5.15a). The white marls of the Trubi Fm. (A-Unit), generally showing a proper massive aspect, depict the typical layering and texture of "autoclastic breccias", being composed by almost horizontal thin levels of finer material wrapping *breccias* lenses of coarser material (Fig. 5.15b). This texture reveals fluidization of the sediment, also affected by a thixotropic mechanism, caused by the application of a horizontal shear stress and strong hydraulic pressure.

On the same scarp, these deposits also create *thixotropic wedges* that reach about 1 m of thickness and show a typical V-shape passing from a horizontal to a sub- vertical setting (Fig. 5.15c and d). The marls of the A-Unit show the breccias aspect while the calcarenites of the B-Unit are characterized by centimetric stratification, typical of these structures, that follows the V-shape of the wedge. The deformation degree decreases upward.

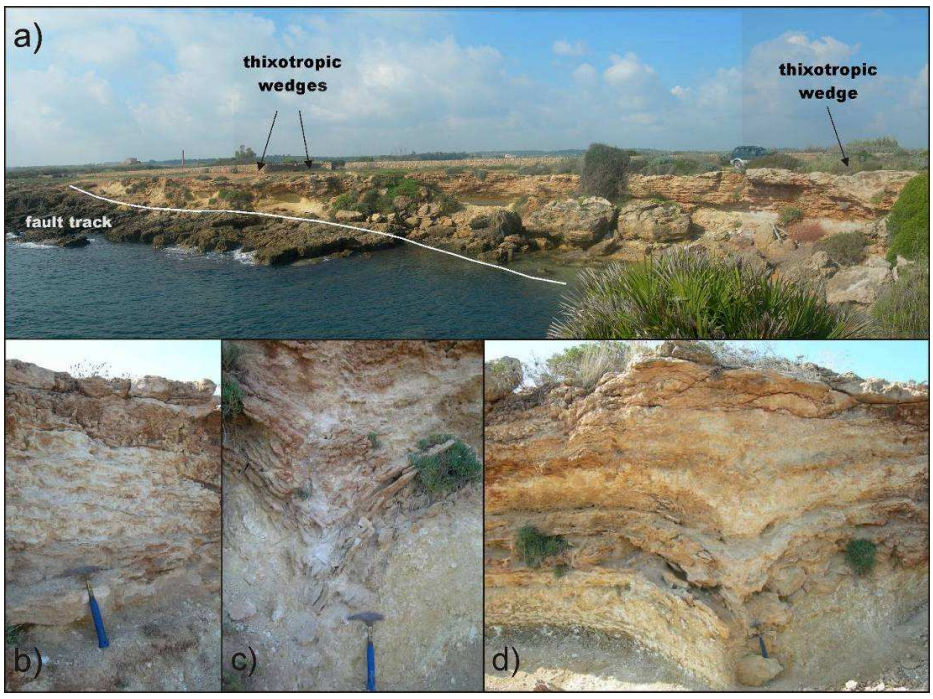

Fig. 5.15: (a) View of the NE-SW fault scarp to the south of the Military station. On the highly eroded fault scarp three thixotropic wedges outcrop; (b) levels of autoclastic breccias into the A-Unit; (c) and (d) details of the thixotropic wedges.

Northward, two *diapyr-like injections* made of the marls of the Trubi Fm. intrude the sandstones (B-Unit) and reach about 2 m of length (Fig. 5.16a). Again the intruding marls (A-Unit) show the breccias aspect (B-Unit). These injections show oblique setting and their upper part becomes thinner and stops in the uppermost layer (Fig. 5.16b and 5.16c).

These soft sediment deformation structures show characteristics typical of liquefaction/fluidization processes such as the absence of primary sedimentary structures, cancelled by the deformation, the presence of fluid-escape morphologies and the evidence of a sudden and high hydraulic force application.

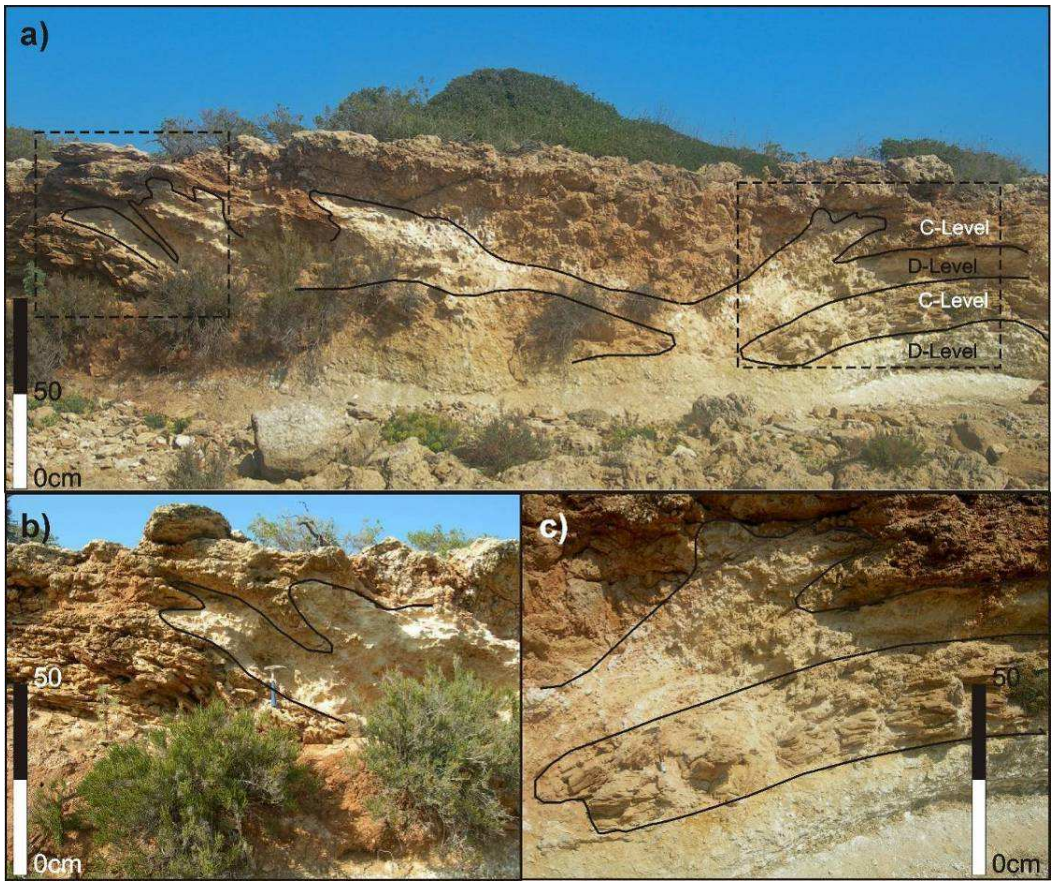

Fig. 5.16: Soft sediment deformation: (a) view of the two main diapir-like injections, rectangles are location of photos b and c; (b) and (c) details of the left and right injections.

5.4.2 Deformative phases reconstruction

Analysis of the seismo-induced deformation at Vendicari highlights that since the Pliocene age at least four seismic events occurred. The first involved the marls of the Trubi Fm. (A-Unit) and the Pliocene sandstones (B-Unit) not yet diagenized, causing the autoclastic breccias texture and the thixotropic wedges and diapyr-like injection development (Fig. 5.17a). The second event caused the brittle deformation of the now diagenized sandstones and the development of the I group fractures (Fig. 5.17b), organized in a swarm-pattern bursting out in all directions and in part oriented parallel to the coastline under a gravitative mechanism. Successively, these fractures were in part filled by the red sand (C-Unit) lying on the sandstones. The third event affected the Pleistocene calcarenite (D-Unit) with the II group fracture development (Fig. 5.17c), both randomly oriented and parallel to the coastline, successively filled by a first coarser sediment coming from above and from the marine environment, mixed with carbonatic re-crystallisation material. A further, fourth event is testified by the second finer filling sediment (Fig. 5.17d). Deformational structures are close to the normal faults affecting the whole stratigraphic sequence (Fig. 5.17d).

5.5 Data analysis

The analysis of the deformational structures in field shows evidence for the occurrence of repeated deformation events. These caused liquefaction-induced soft sediment deformations, pointed out by the morphology consistent with the sudden application of large specifically-directed hydraulic forces of short duration, and also fragile deformations with the development of thick crack networks.

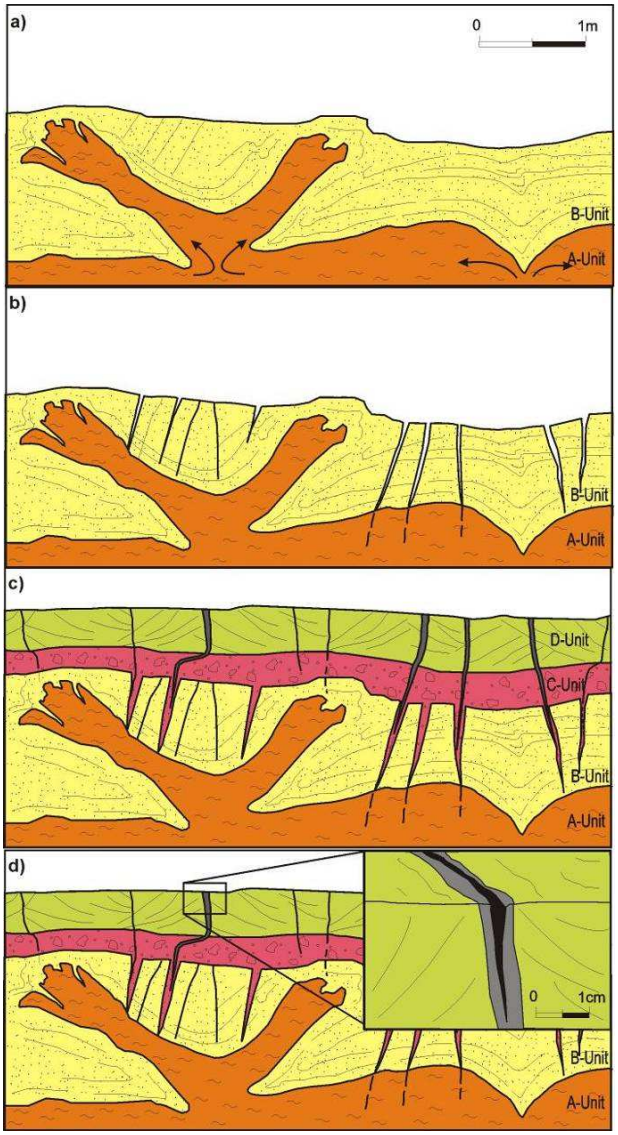

Fig. 5.17: Schematic illustration showing the proposed deformational feature genesis: (a) soft sediment deformations affecting the Pliocene marls (A-Unit) and the sandstones (B-Unit) when they were not yet diagenized; (b) first brittle deformation episode involving the now diagenized sandstones, fractures were successively filled by the red conglomerate deposit; (c) second brittle deformation episode involving the Pleistocene calcarenites, fractures are filled by a white deposit made of an assemblage of rocky fragment and marine elements in a calcitic matrix; (d) last brittle episode involving the previously described filling deposit, fractures are filled by a finer sediment. Arrows schematically indicate the extensional inferred stress, whose direction also partially matches with the tectonic stress field.

5.5.1 Minissale site

At Minissale site the performed study highlighted the occurrence of one, possibly two liquefaction events: the oldest deformation would be testified by the breakage of B-Unit with stretched beds and cracks overfilled by sands and by possible lateral spreading affecting up to D-Unit; the most recent one is clearly recorded by the dikes and lateral spreading involving the sediments up to H-Unit (Fig. 5.3b). The hypothesis that two different events occurred is supported by the deformational style of the involved levels, for which it is quite difficult to attribute the deformation affecting B-Unit and the dikes intruding up to H-Unit to the same event. Indeed, since the lateral spreading is linked to a sinking mechanism and the dike intrusion is driven by an upward venting, the overlapping of the dike upon the first lateral spreading suggests that the two events should not be coeval.

At Minissale, the depositional sequence has a fluvial nature, so liquefaction episodes occurred in a continental environment. For this reason all the possible causative mechanisms relate to the marine or coastal environment (see chapter 2) can be excluded. Consequently the unique possible triggering cause of liquefaction induced soft sediment deformations is seismic shacking.

At least two earthquakes should be responsible of the liquefactions. According to the radiocarbon ages measured at this site (FTM7 and FTM5, Table VIII), the oldest deformational event is expected to be younger than 825–995 AD and thus it is tentatively associated to the 1169 earthquake, whereas the younger event occurred after the interval 1650– 1950 AD and it can be produced by one of the three large earthquakes occurred during this interval in the area: 1693, 1818, and 1908. Considering the Magnitude vs. Epicentral distance relationships (chapter 4) the best candidates are the 1818 and the 1693 earthquakes since the epicentral distance for this site are 24 km and 76 km respectively.

5.5.2 Agnone site

Agnone site contains evidence for two distinct liquefaction events: the first caused lateral spreading with subsidence of the northern part of the section (Fig 5.8a); moreover, the most recent event induced the sand dike venting (Fig. 5.8b), with the intrusion of the low permeability cap (Fig. 5.8c), the dome-like structure of the top level, drag and recumbent folds (Figs. 5.8d, 5.8e) and sheet slumps (Fig. 5.8f). The recognition of the two individual events at this site is supported by the stratigraphic relationships and deformational styles. In fact C and D-Units show a discordant setting respect to B-Unit. They probably deposited in a basin developed for the lateral spreading mechanism (first event) and then the whole sequence was covered by the youngest E- Unit, deposited on a planar surface sealing off the previous deposits. Moreover, first deformational style is characterized by downward gravitative driven force (lateral spreading with vertical component of movement), whereas the second one is characterized by prevalently upward driven hydraulic force (dyke and consequent folding).

Similarly to Minissale site, also at Agnone site deposits are of fluvial environment, so liquefaction occurred in a continental contest and consequently the most probable deformational cause is earthquake shacking (see chapter 2). Considering the radiocarbon dating it is possible to tentatively associate the oldest event to the 1542 earthquake and the youngest one to the 1693 earthquake, also considering that they are the nearest and strongest events for which historical sources report liquefaction in the Agnone area. Indeed the epicentral distance for this site is 14 km from the epicentre of the 1542 earthquake and 20 km from that of the 1693 one.

5.5.3 Vendicari site

5.5.3.1 Brittle deformations

Field observations on fractures reveal the absence of kinematic indicators and offset elements that could indicate oblique dislocation with respect to the fracture planes.

Fractures are opened and filled by heterogenic material, characterized by the presence of marine elements, deposited from above into already opened fractures: C-Unit fills the I group fractures and a fine white deposit fills the II group. Microscopic analysis also confirms the absence of kinematic evidence, deformations and preferential orientations of the elements at the microscopic scale, too.

The systematic and mesostructural analysis highlights that on the whole fractures are irregular in shape, spacing and orientation. Variations of the 2θ dihedral angle and therefore of the fracture style could be justified by lithologic change of the layers where they develop, that could also be responsible for their curviplanar morphology. Indeed, extensional fractures, perpendicular to coarse grain size layers can become hybrid and shear fractures, where the grain size is finer (Dunne and Hancok, 1994). Still, terrains outcropping at Vendicari generally show a homogeneous stratigraphy, only the Pleistocene calcarenite (D-Unit) occasionally shows important granulometric changes. So, lithological diversities can be discard as cause of the wide variability in fracture style.

The stereonet and rose diagram representations of the overall data and data divided for area, lithology and belonging group, also confirm that the fractures do not follow well-defined trends, reflecting a clear stress field, but rather the 60% of them have frequency < 6%, and show an evident dispersion of the plane direction (Figs. 13a, 5.13b and 5.13c). Coastal landform, characterized by more or less developed scarps, seems to have concurred in the rock fracturing, probably inducing gravitative-driven mechanisms, as testified by the matching between scarp and crack directions.

The absence of kinematic indicators, both at the macroscopic and microscopic scale, the statistical analysis of the dihedral angle and the high variability in style and orientation,

indicate that fractures cannot be classified into a distinctive typology (pure extensional joints, hybrid joints or shear fractures), that could also reveal the tectonic stress field action. So, tectonic origin is discarded as the main or exclusive cause of fracture development. This is also supported by the evidence that these cracks mainly affected the cemented B- C- and D-Units and disappear in the less fragile A-Unit (marls of Trubi Fm.) (Fig. 5.11f), while if a tectonic stress was the cause of their development, all the units would be involved in the brittle deformation.

Paleo-environmental reconstruction highlights that B and D-Units are littoral-beach deposits and fracture filling material (C-Unit and the white fine sediment), deposited after opening, is of continental environment. So fractures developed in a probably littoral or emerged setting and there is not evidence of significant burial from thick deposits on the Units involved in the deformation. Therefore, internal fracturing causative mechanisms, such as cracking due to overloading for fast deposition and compaction without a complete leakage of the sediments and injection into not well consolidated deposits due to negative density gradient, can be excluded because these effects generally take place at higher depth of burial and are typical of the pelagic environment. Moreover the latter effects generally occur when more dense sediments bury less dense ones (Timoshenko and Goodier, 1951; Beaudoin et al., 1983; Wangen, 2001). Also thermal stress effects and volumetric variations during rock diagenesis (e.g. expansion or contraction) can be discard because they occur at high depth or in context linked to volcanism (e.g. magmatic intrusions and volcanic rock diagenesis) (Caputo et al., 2005 and reference therein) that are absent in the study area.

On the contrary seismic shock can be considered as possible causative mechanism since it can trigger anastomosing ground open fissures in on- shore setting, at low depth of burying (Montenat et al., 2008). These seismic fractures generally develop close to the fault to permit deformative adjustment and, given their superficiality, are generally opened and filled by sediments coming from above (sedimentary dykes) (Montenat et al., 1991, 2008).

Moreover, fracture formation seems to be due to lateral spreading too (Obermeier, 1996) that, under the moderate topographic gradient of the rocky coast, caused gravitative-driven

stretching, as testified by the matching between directions of fractures with major frequency (f > 6%) and coastline ones (Fig. 5.13).

Nevertheless, cleaning the dataset from the fractures due to the chaotic brittle deformation (testified by data with f < 6% and high dispersion of plane directions), and from that due to gravitative effect (testified by fractures with f > 6% and direction between N0 and N50), at least two sets of conjugate fractures, N120 and N150 trending, remain (Fig. 5.13e). These could reveal an about N135 trending σ1 that is compatible with the regional stress field of the Hyblean Plateau, characterized by a N145 direction (Adam et al., 2000; Musumeci et al., 2005). Then, tectonic stress should be superimposed to the brittle deformation due to seismic shaking.

Described seismites are usually found in rocks located close to active fault zones (Vachard et al., 1987; Bouillin and Naak, 1989; Bouillin and Bellomo, 1990; Montenat et al., 1991). Thus, they are evidence of recent tectonic movement in south-eastern Sicily, jointly with the active faults observed in the area (Fig. 5.9a. 5.9b and 5.11).

5.5.3.2 Soft deformations

Soft sediment deformations observed in the study area (autoclastic breccias, thixotropic wedges, diapir-like injections) reveal the liquefaction of thixotropic layers and the sudden application of a strong hydraulic pressure.

These deformations occurred after A and B-Units deposition when, as shown by the stratigraphic and paleoenvironmental analyses, there was a transition from deep sea to littoral-coastal environment. Thus, it is possible to exclude that these structures are due to marine environmental processes such as the action of sea waves and paleo-currents. Moreover, these marine processes and also the breaking or storm wave action, affect only the upper part of the sedimentary levels, whereas at Vendicari deformation involves the whole sequence. Finally, there aren't typical sedimentary structures due to marine effects.

Overloading unstable density gradient effect can be excluded as a possible cause of the liquefaction and/or fluidization mechanism, as well. Indeed, the unique lithological and density differences, enough to produce such an effect, is between the units A-Unit, consisting of marls, and B-Unit, made of sands, whereas the soft sediment deformation affects the entire internal stratification of each unit. Furthermore, typical structures due to this mechanism are absent.

Lateral shear stress induced by the down-slope component of the sedimentation basin can be excluded because there is no evidence either of a steep slope or a possible gradient. Moreover, the typical structures indicating lateral stresses, e.g slumping and turbiditic levels are lacking.

Cryoturbation occurrence ("ice wedges" produced by melting ice) is restrict to the periglacial, especially glaciolacustrine, environment and so it appears rather improbable. Bioturbation effects (Van der Meulen, 1990) can be discard because they occur at different cent-metric scale and involve a less wide zone.

No diagnostic structures due to tsunami occurrence have been observed. Moreover, recent studies performed in SE Sicily, where evidence of tsunami inundations have been detected both on- shore and off- shore, did not find liquefaction structures linked to these tsunami deposits (De Martini et al., 2010; Smedile et al., 2010).

Excluding all possible known "internal" trigger mechanisms, it is most probable that the liquefaction effects observed at Vendicari were induced by an "external" agent. Since these soft sediment deformations show typical shape and characteristics of liquefaction and fluidization structures studied worldwide and associated to earthquake shaking (Obermeier, 1996; Montenat et al., 2008), they can reasonably be interpreted as seismically induced.

Moreover, the limited lateral extent (no more than 50 m) of these structures, which are completely absent in the stratigraphic sections located southernmost and northernmost, can be considered a key factor for their association to seismic shaking (Sims, 1975).

5.5.3.3 Chronology of the deformative events

We cannot associate the seimites observed at Vendicari to particular seismic events in absence of dating of deformed sedimentary layers. The age of the Units only indicate that the two oldest events occurred after the Pliocene age and before the Tyrrhenian age, recorded by D-Unit that represents the youngest approximate datable element. The two more recent events occurred after Pleistocene age. Even if it is very probable that these last two events are older than the historical earthquakes, however they should be quite recent. Indeed, they caused the sedimentary dikes development, whose diagenesis and erosion should be extremely rapid (Dravis, 1996; Tucker, 2001), whereas at Vendicari they are not yet eroded although the recent strong karstification.

The seismite association testifies the occurrence of seismic events with magnitude greater than 5 and intensity greater than IX, that are the thresholds for which this association of seismo-geological structures may develop in a site (Ambraseys, 1991; Valera et al., 1994). However, parameter source values are related to the epicentral distance of the site where liquefactions develop (Kuribayashi and Tatsuoka, 1975; Youd, 1977) (see also Chapter 4 for discussion). According to Pirrotta et al. (2007), that realized upper bound curves of source parameters vs. epicentral distance of site where liquefactions developed during historical earthquakes of eastern Sicily, the earthquakes that could be responsible for the deformations at Vendicari occurred at a distance less than 20 km or at a longer distance but with magnitude bigger than the threshold parameter.

6. STUDY OF TSUNAMI DEPOSITS

A multi-disciplinary study focused on the recognition and dating of historical and paleotsunami deposits in eastern Sicily has been performed in order to provide new information on the extent and frequency of tsunami inundations.

In this work both anomalous sandy deposits and boulder accumulations were analysed. Since eastern Sicily is exposed to both earthquake induced tsunamis, also caused by far sources of Egean zone (e.g. the 365 Creta or the Santorini tsunamis), that to extraordinary strong hurricanes of Mediterranean Sea (Mediterranean Cyclones), the first step of the research was to understand if deposits were emplaced by storm waves or tsunamis. Geological evidence for tsunami sandy deposits were found in the Augusta Bay, both inland and off-shore, and at Morghella site (A and B in Fig. 6.1). Boulder accumulations were analyzed in three sites: Vendicari, Capo Campolato and S Lorenzo (C and D in Fig 6.1).

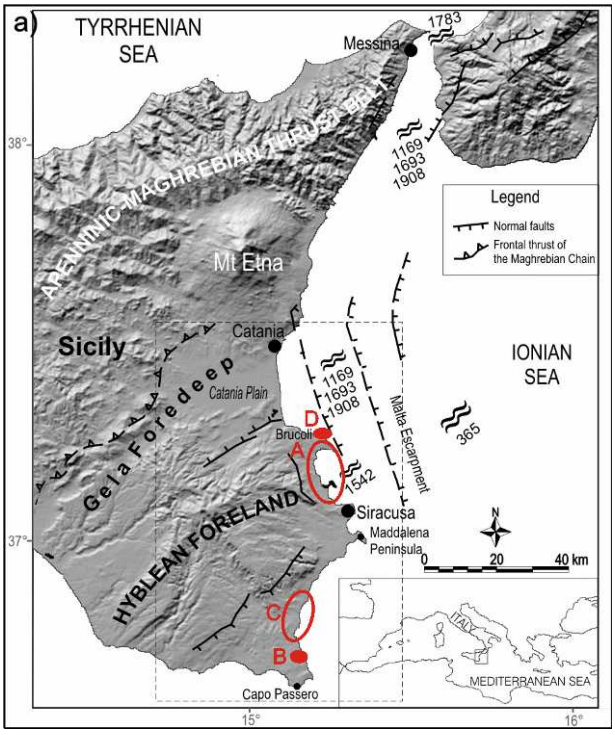

Fig. 6.1: Map of eastern Sicily with general data on historical tsunamis. Letters refer to the study areas: A Augusta Bay (investigated both on- shore and off- shore); B Pantano Morghella; C Vendicari and S. Lorenzo; D Capo Campolato.

6.1. Analysis of sandy deposits

6.1.1 Method

The investigated areas were chosen starting from a detailed analysis of historical accounts and the previously compiled databases storing information on the effects of known tsunamis (Geradi et al., 2008). Then areas, that can have been likely invaded by tsunamis in the past, have been investigated through a geomorphologic and geologic study, by the analysis of satellite images, aerial photographs and field surveys and also taking into account past centuries' coastline changes.

Coastal marsh/lagoon areas have been considered because they are suitable for deposition and preservation of tsunami deposits. Indeed, from a morphologic point of view they are coastal depositional traps also characterized by low-energy environment, continuous deposition, low erosion and accumulation of organic matter. Moreover, these areas have restricted condition for easy recognizing and identifying of tsunami deposits. Indeed, given that tsunamiites are deposited from the sea by high energetic events they have sedimentological and micropaleontological features different from that of the quite lagoonal sedimentation environment (see chapter 3 for description), generally characterized by marsh and muddy deposits.

In the selected areas coring field surveys using both hand auger equipment and a vibracoring (with a gasoline-powered percussion hammer) were performed for preliminary stratigraphical and sedimentological observations directly in the field, together with photographs of the core deposits, and sampling for environmental and dating analyses. Where the stratigraphic sequence showed evidence of anomalous levels, undisturbed samples (within specific PVC tubes), 100 cm long and 5 cm in diameter, down to 5-7 m total maximum depth, were collected. Coring was always accompanied by GPS surveys for the exact positioning with respect to the present shoreline.

In laboratory, undisturbed cores were opened to perform accurate sedimentological descriptions and subsequent sample collection for further investigations. On some samples paleontological and micropaleontological analyses were performed using optic microscopic, after a procedure of washing by sieves of 63

μms and drying in oven. Some other samples were examined by a FE-SEM equipped, with EDS, for observations on grain shape and size. On specifically selected cores, collected in PVC tubes, magnetic and X-ray analyses were made, with the aim to observe possible susceptibility variations and small-scale sedimentary structures (e.g., sharp contacts, convoluted layers, etc.).

Thanks to these analyses paleoenvironment reconstruction of the site and observation of features that can be diagnostic of high energetic marine waves, possible tsunamis, were performed.

Radiocarbon dating was made by the use of accelerator mass spectrometry (AMS) (Poznan Radiocarbon Laboratory) on charcoals, organic sediment and shells selected from the layers just above and below the possible tsunamiite and from this latter. Measured ages were dendrochronologically corrected according to Calib REV5.0.2 (Stuiver and Reimer, 2005). Alternative dating method consisting in tephra characterization was also performed in some sites. Dating allowed to constrain the age of the deposits anomalous respect to the sedimentary sequence. However, since the scarcity of datable material some tsunamiites are roughly constrained in age using average sedimentation rates. Dating also allowed to made correlation between the probably tsunamiites and the historical events or to provide an age range of occurrence for the other paleo-events.

Further dating methods such as the OSL (Optically Stimulated Luminescence) are in progress on some samples.

6.1.2 Study sites

6.1.2.1 The Augusta Bay

The Augusta Bay is located along the south-eastern coast of the Hyblean Plateaux. This area is natural gulf, about 15 km wide and with a 25 km-long shoreline, probably created under tectonic control that also caused the development of high and low morphological sectors. Indeed, some salt marshes, that are environments particularly favourable for the deposition and preservation of the tsunami deposits, developed in the

low-land sectors. The Augusta Bay was investigated both on- shore in collaboration with the INGV (Istituto di Geofisica e Vulcanologia, section of Rome; working group: De Martini P.M., Smedile A., Pantosti D. and Pinzi S.) and off- shore by a marine geophysics campaign also in collaboration with the ISMAR (Istituto di Scienze Marine, section of Bologna; working group: Gasperini L. and Polonia A.).

6.1.2.1.1 On shore study

On shore the Augusta site is characterized by a gently seaward dipping surface.

Outcropping stratigraphy consists in coarse sands, calcarenites and limestone as old as Late Cretaceous (Lentini et al., 1986) and alluvial and fluvial sediments of Holocene and Late Pleistocene age.

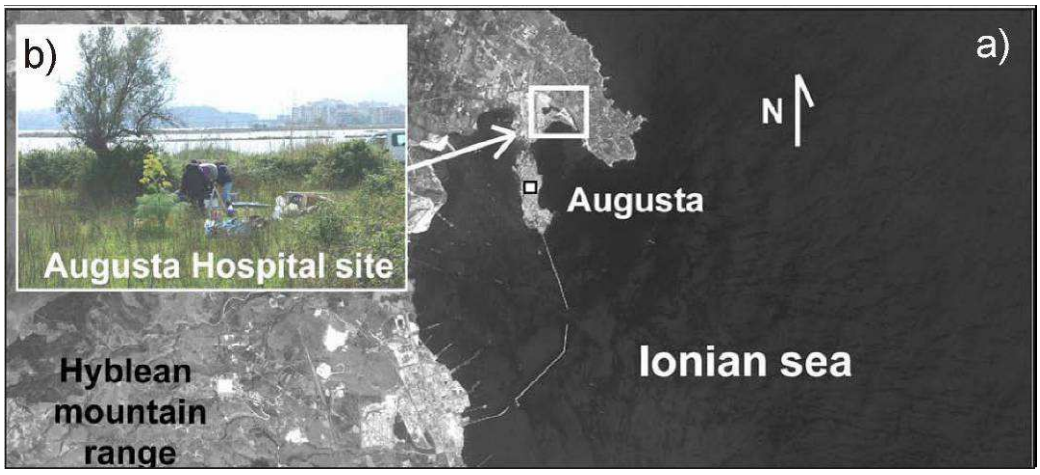

Fig. 6.2: (a) Map of the Augusta Bay area; (b) picture of the investigated site (from De Martini et al., 2010).

Coring campaign was undertaken in the NE sector of the bay in a small inlet near the Augusta Hospital. This area is characterized by a gently, south-eastward dipping, alluvial surface (1 to 5 m a.s.l.) bounding a salt marsh (0.3 km^2) separated from the sea by a sandy bar. Here 6 cores down to a maximum depth of 4.3 m and at a maximum distance of 460 m from the shoreline were dug.

The site stratigraphy, can be related to an alluvial environment, characterized by low-energy silty clay, clayey silt and silt deposits. Into some cores two “anomalous”

layers coarser than sediments lying above and below, were found: OSA-T1 at about 160-170 cm of depth, characterized by gravel with angular calcarenites clasts, and OSA-T2, at a depth of about 185-195 cm, characterized by bioclastite (Fig. 6.3). These two levels are about 10 cm thick and show a massive structure, sharp erosional lower contact and fining upward. Moreover they have significant shell detritus content and planktonic and rare marine benthic foraminifera. For their characteristics these layers represent high energy deposits of clear marine origin, probably tsunamiites, within a brackish lagoonal environment.

Therefore, two high energetic inundation events occurred in the area, AU-01 and AU-02 responsible of the deposition of OSA-T1 and OSA-T2 respectively. Moreover, the analyses reveals that a sudden modification of the local morphological conditions, from alluvial to marine environment, occurred at about 1.0 m depth. This change was interpreted like the occurrence of another event (the AU-00) possibly related to an earthquake/tsunami, that probably caused shoreline modification and change of the depositional environment from alluvial to marine, or the disruption of the sand bar that protected the area.

Radiocarbon dating, summarized in Table IX, suggest that the abrupt environmental change (event AU-00) at about 1.0 m depth occurred during the interval time 650–770 AD; event AU-01 is constrained in the age range of 900 BC–120 AD; finally, the age of event AU-02 can be constrained in the interval 975–800 BC. Given the interval age of found events no correlation can be made with the historical record. However the last event AU-00 could be tentatively related to the 365 AD Crete tsunami, considering that it occurred before the environmental change and so before the interval age 650-770 AD. However an dating uncertainty interval had to be considered.

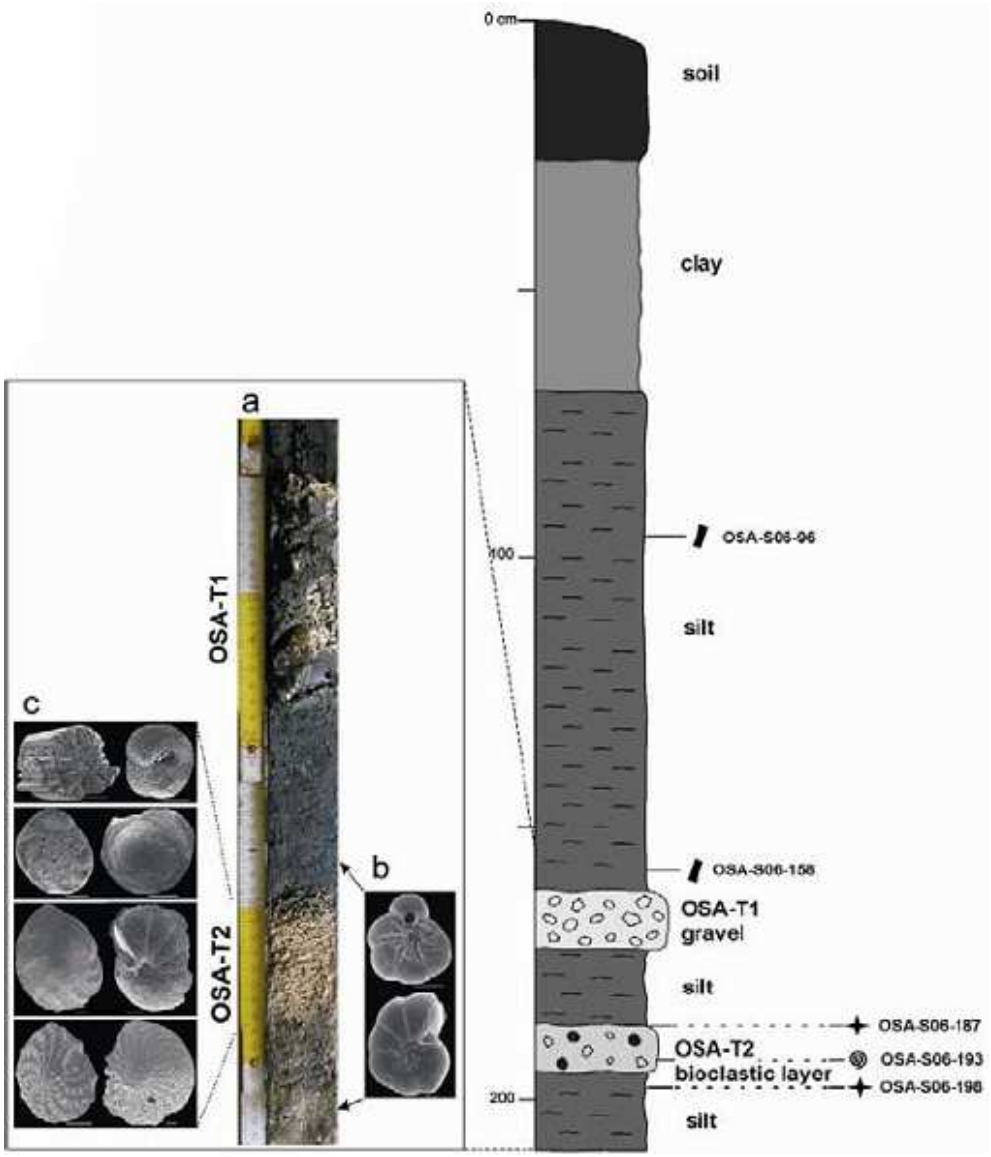

Fig. 6.3: Schematic and representative log of the stratigraphy at Augusta site. OSA-T1 and OSA-T2 are the anomalous layers interpreted as tsunamiites. Small black rectangles, stars and the snail indicate depth of the dated charcoals, organic sediments and shell specimens, respectively (see Table IX); b) SEM pictures (the scale bar represents 100 μm) of the benthic foraminifera assemblage typical of the lagoonal environment detected above and below the bioclastic layer OSA-T2; c) SEM pictures (the scale bar represents 100 μm) of marine elements observed within the bioclastic layer (from De Martini et al., 2010).

Table IX: Information on samples collected for radiocarbon dating (from De Martini et al., 2010)

Sample name / depth cm	Type	Measured age BP	δ13C	Calibrated age 2σ
OSA-S6–96	Charcoal	1320±30	−17.9	650–770 AD
OSA-S6–159	Peat	1960±30	−27.5	40 BC–120 AD
OSA-S6-187	Peat	2685±30	−22.8	900–800 BC
OSA-S6-193	Bivalve	3310±30	−1.1	1265–825 BC
OSA-S6-198	Peat	2745±30	−16.5	975–820 BC

6.1.2.1.2 Off shore study

In the off shore of the Augusta Bay a geophysics campaign of chirp-sonar seismic reflection, covering the 150 km^2 of the bay, was performed with the aim to investigate the local morphobatimetry and to find evidence of anomalous layers off-shore, too (Fig. 6.4a).

Chirp Seismic allows to investigate whit high resolution at low depth, so it is commonly used in the scientific research for the study of the structures and geometry of the actual and recent sedimentary bodies. The sub-bottom profilers constitute a group of mono-channel seismic sources, that has a single receiver (hydrophone) and generate an acoustic impulse signal (mono-frequency). The acoustic source which has a “compress impulse” is named LFM (Linear Frequency Modulation) or “Chirp”. This source produce an impulse characterized by two frequency bands (2-7 kHz and 10-20 kHz) whit long duration (1-100 ms) and by linear phase variations. Whit this characteristic the resolution isn’t direct function of the length of the impulse transmission, but of the wide of the frequency band of the FM signal, so both the penetration and the resolution improve.

The analysis of the close-spaced chirp profiles revealed that off shore the Augusta Bay shows a rather flat morphobathymetry with a narrow shelf characterized by few steep slope (values from 2% to 4%) extending up to about 5 km from the shoreline. A maximum depth of 100-120 m is reached at the shelf-break, behind it the bathymetry becomes deepest and characterized by high steep slope.

The sedimentary sequence was investigated by the use of apposite software, SEISPRO3.2, capable to elaborate the chirp- sonar seismic profiles and to extract the reflectivity values of the sediments for which a different granulometry correspond. The chirp imagines highlighted the presence of an uppermost, nearly transparent, homogeneous sedimentary sequence that, for its reflectivity values can be related to fine mud-dominated sediments. This sequence, likely deposited during the Holocene, shows variable thickness and lies unconformably over the acoustic bedrock (Fig. 6.4b). This latter should be made of Miocene to Pleistocene terrains, extensively outcropping onshore (Smedile et al., submitted to Marine Geology). Within the fine sequence a coarser level, at about 3m of depth, was pointed out by high reflectivity values. This prominent reflector can be widely correlated over the entire area and beside it other less prominent reflectors are also visible (Fig. 6.4b). The acoustic signal reveal the absence of geometrical unconformities and of features possibly related to erosional/re-depositional processes caused by currents or gravitative failures. Rather, the sedimentary sequence appears undisturbed.

In the northern sector of the investigated area, a 6.7 m-long sediment gravity core (MS-06) was collected on board of the CNR R/V *Urania*, at about 2 km off the coastline, in 72 m of water depth (Fig. 6.4a). The location of the core was chosen, after the chirp profile investigation, with the purpose to collect the high reflectivity levels.

Investigations of the core confirmed that sedimentary sequence is made by mud-dominated deposits and that the high reflectivity level, at about 3m of depth, is an ash one related the basaltic Plinian eruption occurred at Etna Mt in 122 BC (Fig. 6.5). Less marked, but however evident, signatures of the seismic imagines represent coarser levels with anomalous micropaleontologic content respect to the sedimentary sequence. Indeed, microplaeontological analysis has shown up 11 intervals with particular abundance of epiphytic foraminifera (species growing in vegetated substrates like the *Posidonia oceanica*) that seem to be displaced because they generally live at lower water depth. Moreover, a general grain size change and sandy inputs were observed in correspondence to the anomalous levels.

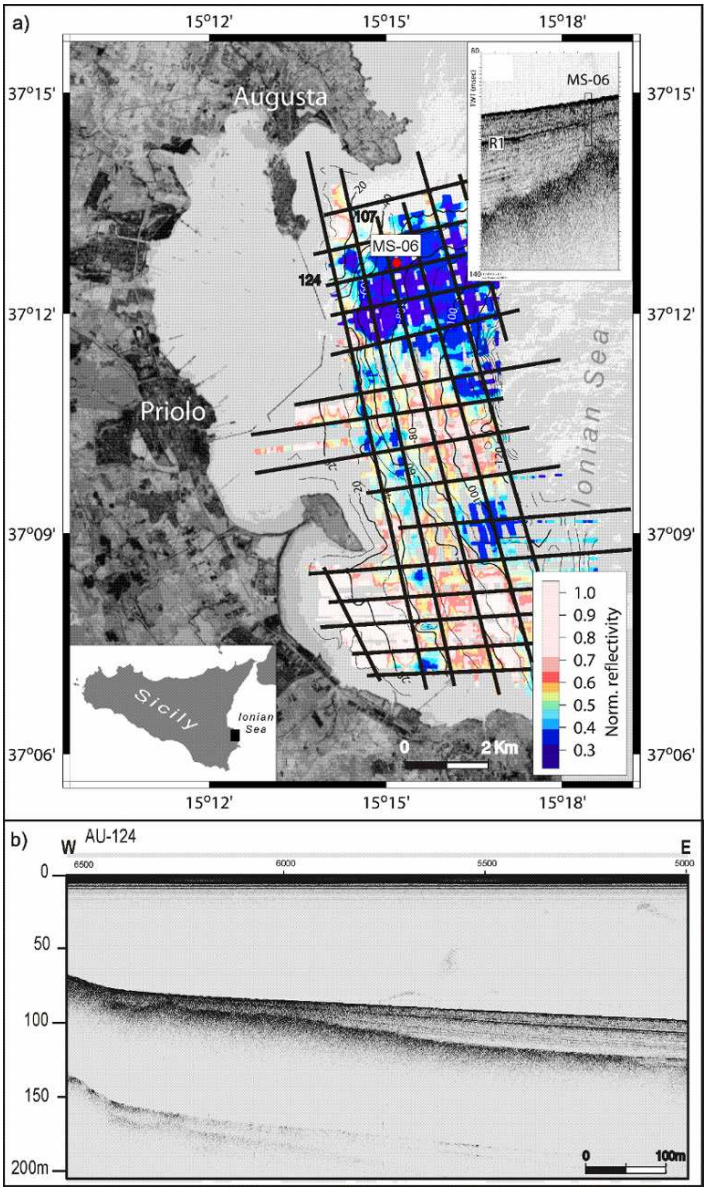

Fig. 6.4: (a) map of the Augusta bay with distribution of the sonar chirp geophysics grid and location of the MS-06 core (red point), colors refer to the reflectivity values; (b) chirp profile image (AU-124), the fine Holocene sedimentary sequence is represented by the transparent sediment (low reflectivity corresponds to low grain size) lying on the acoustic bedrock. Within the sedimentary sequence the coarser levels are pointed out by the prominent reflector (high reflectivity corresponds to higher grain size) (from Smedile et al., submitted to Marine Geology).

Therefore these levels were ascribed to high energy exceptional events able to disperse an extra amount of infralittoral epiphytic species toward deeper areas. Radiocarbon dating on samples collected from the core, reveal that the 6.7 m long sedimentary sequence recorded about 4500yr (Tab. X).

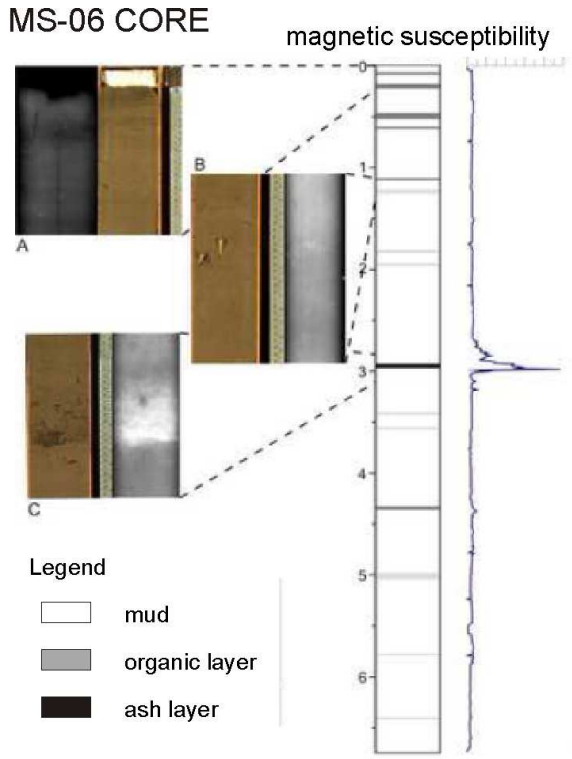

Fig. 6.5: MS-06 core log with magnetic susceptibility, (a and b) pictures of the anomalous layers and (c) of the ash related to the 122 BC eruption (from Smedile et al, submitted to Marine Geology).

All possible mechanisms capable to produce dislocation of epiphytic foraminifera species at more depth in a sedimentary basin, including earthquake shaking or tsunamis, have been considered and a critical analysis aimed to highlight the most probable was undertaken.

Turbidity currents are discarded because they cause erosion, important changes in the sedimentary sequence and convolute structures not observed in MS-06 core.

The hypothesis that storms can be the causative mechanisms appears unlikely. Indeed, a meteorological data analysis (ERA-40: a re-analysis of global atmosphere and surface conditions from September 1957 through August 2002 – by Spirito, 2006) reveals that both ordinary storms and also "exceptional storms" occur with high frequency consequently for the interval time recorded by the core MS-06 we would expect a bigger number of anomalous levels than the observed ones.

Table X. Measured and calibrated ages of the core samples. First column indicates the core number and depth (cm) where it was collected (from Smedile et al, submitted to Marine Geology).

Sample code	Sample type	Measured Age BP	1 or 2 σ	Cal age min	Cal age max
MS-06- 49	Marine shell	1495±30	1 2	AD 960 AD 885	AD 1125 AD 1200
MS-06- 84	Marine shell	1655±35	1 2	AD 785 AD 715	AD 950 AD 1015
MS-06- 127	Marine shell	1820±30	1 2	AD 640 AD 570	AD 775 AD 855
MS-06- 179	Marine mollusk	1960±30	1 2	AD 495 AD 420	AD 650 AD 690
MS-06- 278	Marine shell	2330±30	1 2	AD 70 BC 20	AD 235 AD 325
MS-06- 306	Foraminifera	3305±35	1 2	BC 1125 BC 1240	BC 920 BC 845
MS-06- 357	Marine shell	2680±35	1 2	BC 360 BC 435	BC 195 BC 80
MS-06- 467	Marine shell	2925±35	1 2	BC 720 BC 755	BC 505 BC 400
MS-06- 563	Marine shell	3270±35	1 2	BC 1085 BC 1185	BC 890 BC 810
MS-06- 6.63	Marine shell	4245±35	1 2	BC 2340 BC 2440	BC 2125 BC 2030

Earthquake shaking cannot be the cause because into the core, 3 anomalous events in the last 1000 yr were found, but during the same period the historical seismic catalogues contain only two strong earthquakes with local sources, the 1693 and 1169 events. Moreover, in saturated and no diagenized soft sediments earthquake shacking generally triggers deformation structures, due to liquefaction and fluidization processes (see chapter 2), that are not observed into the seismic image of chirp profiles.

Tsunamis backwash effects have enough energy to rework the onshore deposits, emplaced during inundation, and to transport them in the sea again. Thus, tsunamis seem to be the most probable causative mechanism.

One further evidence of relationships between levels and tsunamis is pointed out by the coincidence between the ages: four of the eleven layers are into an interval time including the date of three of major tsunamis that hit eastern Sicily, that are the 1169, 1693, and 1908 events and that of a more ancient event that could be the 365 A.D. Crete or the Santorini (about 3600 B.P.) tsunami.

6.1.2.2 Pantano Morghella

Pantano Morghella is a pond, 1.3 km long and 0.8 km wide, that was partially used as salt-pans in the recent past. This pound is surrounded by ancient deposits from Upper Cretaceous (lavas and volcanoclastic calciruditi, calcarenites and marls) up to Pliocene age and it is eastward bordered by a beach and by 3 m-high partially cemented fossil dunes of probable Pleistocene age. This dunes separate the Pantano from the sea to which it is connected only through a little channel.

When the pond is not filled by water (from August up to October) it represents a flat lowland and it can be investigated by coring campaigns. In all 33 hand and engine exploratory cores were performed, down to a maximum depth of about 6 m, along an transects running perpendicular from the coast up to 1.2 km inland (Fig. 6.6a).

The fine stratigraphic sequence mainly composed by clay and silty clay and representing a low-energetic deposition is interrupted, in almost all the cores of the central part of the pond, by a yellow bioclastic sandy deposit (MORT02) (Fig. 6.6b and c), from 3 to 10 cm thick, detected from about 1 m to 1.50 m of depth. Moreover in some cores other two sandy layers were found, at 4 m and at about 30 cm of depth, the latter was dug in an old salt-pan.

The yellow bioclastic sandy level (MORT02) was analyzed in depth. It shows different lithic and microfauna composition with respect to the sediments above and below. Indeed, it is mainly made of well-rounded yellowish carbonatic clasts and contains several reworked foraminifera (planktonic and benthonic) and macro fossils fragments (corals, sea urchins, bryozoa and molluscs), consistent with a marine assemblage, and only few lagoonal specimens. Moreover, it shows a composition close to the local beach sand. X-ray imaging performed on a PVC core, shows that the sandy layer is characterized by a fining upward grain size and a sharp, possibly erosional, basal contact (Fig. 6.6c).

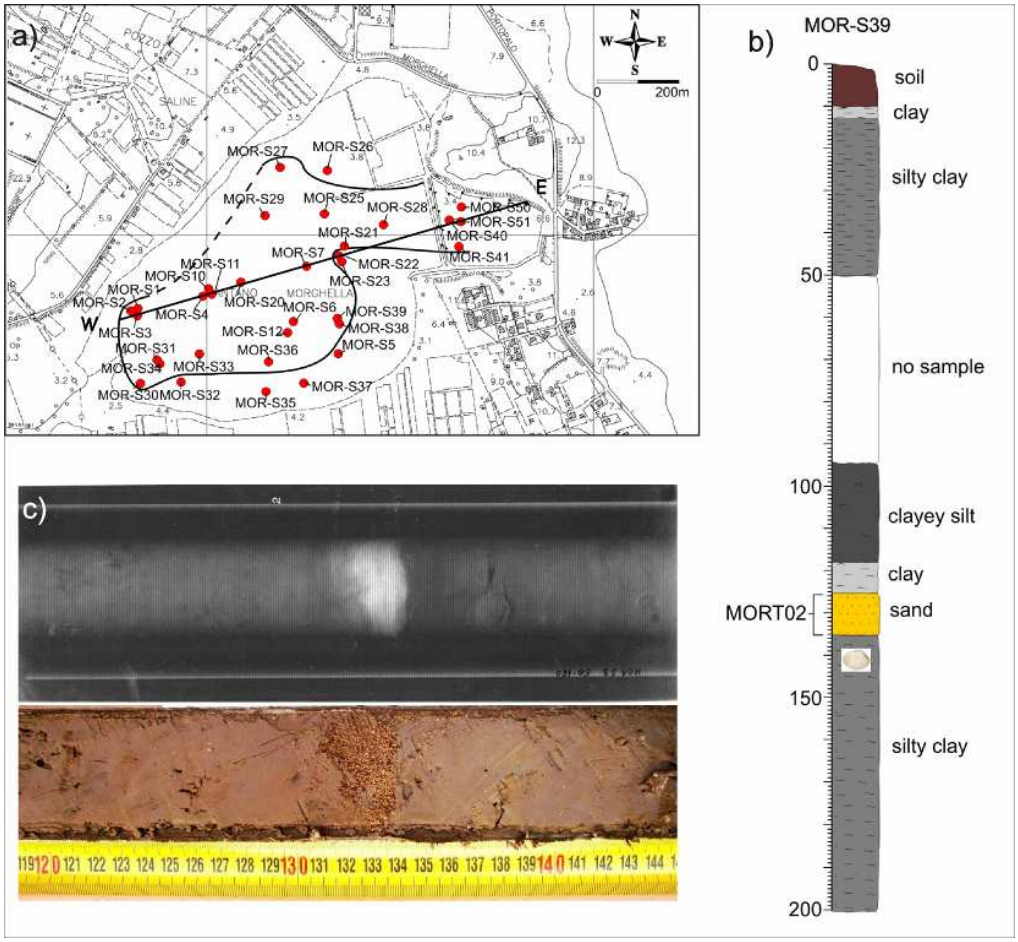

Fig. 6.6: (a) Map of Pantano Morghella site and location of the cores; (b) representative log of the sedimentary sequence with the anomalous sandy layer (MORT02); (c) pictures of the core and X-ray where the sandy layer is showed and its sharp basal contact and the fining upward grain size are pointed in evidence.

This deposit covers the Pantano surface in the central part almost continuously on gentle topography and extends for about 1200 meters away from the shoreline with a landward thickness decreasing. For its characteristics this out of sequence layer was interpreted as a tsunami deposit.

To constrain the age of the tsunami inundations 4 samples were collected for radiocarbon analyses just above, within and below the anomalous layer. The radiocarbon dating are close in time, confirming that sand deposition was a very sudden, highly energetic, event occurred in the interval time 270-650 AD Therefore this layer can be ascribed to deposition during the tsunami of the 365 Crete earthquake.

The analysis of the distribution of the deposit into the Pantano allowed to reconstruct a minimum inundation of about 1.2 km and run-up of about 3 m.

Further investigations are in progress for the other two sandy layers (at 4 m and 30 cm of depth) however, from a preliminary analysis, they seem to have the same characteristics of the first one. Dating by OSL (Optically Stimulated Luminescence) is in progress to better constrain the age of MORT02 and of the other two anomalous levels.

Table XI. Measured and calibrated ages of the core samples. First column indicates the core number and depth where it was collected.

Sample	Description	δ13C (‰)	Radiocarbon age (BP)	ΔR	Calibrated age	2 σ
MOR-S12-69	*Cerastoderma glaucum*	-6.2 ±0.4	1989 ± 45	124± 60	AD 235- 545	1.000
MOR-S12-85	*Cerastoderma glaucum*	-5.4 ± 0.3	1988 ± 40	124± 60	AD 270 - 585	1.000
MOR-S12-97	*Cerastoderma glaucum*	-3.8 ± 0.5	1927 ± 50	124± 60	AD 395- 685	1.000
MOR-S12-312	*Cerastoderma glaucum*	-2.5 ± 0.3	4081 ± 40	124± 60	BC 2285 - 1870	1.000
MOR-S39-142	*Cerastoderma glaucum*	- 9.3 ± 0.5	2096 ± 50	124± 60	AD 110-310	1.000
MOR-S39-415	*Cerastoderma glaucum*	- 9.1 ± 0.2	4746 ± 50	124± 60	BC 3335- 2950	1.000
MOR-S51-66	*Cerastoderma glaucum*	- 3.7 ± 0.5	582 ± 45	124± 60	AD 1685-1955	1.000
MOR-S51-284	*Cerastoderma glaucum*	- 14.0 ± 0.5	3207 ± 40	124± 60	BC 1400-1130	1.000

6.2 Study of boulders

From Capo Campolato southward, eastern Sicily is characterized by a rocky coastal belt that shows flat landscape, weakly incised by a poorly developed hydrographic network, which in some sectors rises to form high cliffs. Boulders deposited on the rocky shore platform were analyzed in three areas: Capo Campolato, Vendicari and San Lorenzo (fig. 6.1 and 6.7).

6.2.1 Method

Since the sedimentological and morphological characteristics of boulders are the same in case of storm waves or tsunamis, the method to distinguish their origin followed several approaches summarized below:

a) analysis of the storm-wave regime of the Ionian coast of Sicily. Anemometric and ondametric data were recorded by the nearest meteo-marine Catania station belonging to the RON — Rete Ondametrica Nazionale (=Italian Sea Wave Network, www.idro- mare.it) and elaborated applying the transposition method (Seymour, 1977; Vincent, 1984) to obtain the wave heights, at the sites, for the known storms occurred. Given that these values are in deep water, in order to obtain the breaking wave height Hb at the shoreline, the transposed data have been processed according to Sunamura and Horikawa (1974). So, knowing the wave height (Ho) and period (To) in deep water and the offshore slope, it is possible to calculate the wave height at the breaking point (Hb) (Tab. XII);

b) morphological analysis of the shore measuring both on-shore and off shore slope, morphology and length of the coast and roughness;

c) GPS field surveys of the boulders, at different times, before and after winter storms: the first survey during September 2006, the second one during October 2008-February 2009 and the last one in January-March 2010. The aim of this survey was to obtain the position of each boulder with respect to the shoreline and to measure possible boulder displacement due to winter storms.

d) mapping of the boulders and detailed measuring of their setting, sizes (axis length, A-axis > B-axis > C-axis), volume, shape, longest axes orientation and distance from the shoreline. Moreover, possible presence of erosion/encrustation markers, pre-transport position and arrangement (if single block or packed) were observed. Laboratory analyses on samples collected from some boulders allowed to asses an average density of 2.3 g/cm^3;

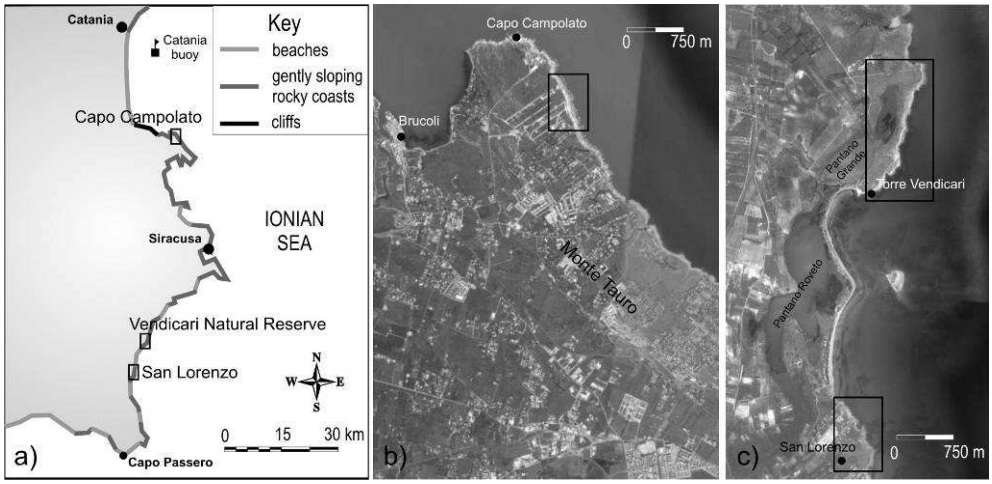

Fig. 6.7: (a) South-eastern Sicily map with the coast typologies; (b) location of Capo Campolato site and of Vendicari and S. Lorenzo sites (c) (from Barbano et al., in press in the BGTA).

e) hydrodynamic equations application. First, the hydrodynamic calculations of Nott (2003) were applied. However the Nott's approach only considers the wave height (both storm and tsunami) necessary to start the boulder movement but it does not consider the emplacement distance of the blocks that is related to the wave velocity and flooding inland. This latter parameter is influenced by the wave height at the breaking and by the wave length and period, which represent the most significant differences between storm wave and tsunami. For instance, tsunami wave lengths are in the order of kilometres, while storm wave lengths in the order of 100 m. So, tsunamis are capable to reach very long penetration distances.

Therefore, to distinguish the kind of wave, its length and period must be considered into the hydrodynamic elaborations and these parameters are taken into account in the equations proposed by Cox and Machemehl (1986) and Noormets et al. (2004). According to these models the decay in height of a wave overtopping the shore (due to the breaking, causing kinematic instability and consequent dissipation of energy) is proportional to the distance X from the shoreline and inversely proportional to wave period T. The elaborated formula (1) allowed to draw height attenuation curves for the strongest storm waves and historical tsunamis (1693 and 1908 events) occurred in the study areas and to obtain the maximum water flooding along the coast (2) considering that it occurs when the wave height Hi becomes nil.

$$H_i = [\sqrt{(R-E)} - (5X_i/T\sqrt{g})]^2 \qquad (1)$$

$$X_{max} = [(T\sqrt{g})\sqrt{(R-E)}] \cos\alpha/5 \quad (2)$$

Where H_i and X_i are the wave height and distance from the shoreline at a specific point i on the coast; R is the run-up, E the coast elevation at the breaking point; g is the gravity acceleration; X_{max} is the maximum inland flooding ($X_i = X_{max}/\cos\alpha$); cos α corresponds to the mean slope of the coast.

Starting from Noormet's (2004) force balancing formulas, equations indicating the wave heights of storm (H_{sf}) and tsunami (H_{tf}) at the moment that the blocks were deposited in their inland position have been evaluated for both entrained in the flow transport mechanism (3 and 4) and for sliding on the platform one (5 and 6):

$$H_{sf} = (2(\rho s-\rho w/\rho w)\, bc)/C_D c + C_L b \quad (3)$$

$$H_{tf} = (0.5(\rho s-\rho w/\rho w)\, bc)/ C_D c + C_L b \quad (4)$$

$$H_{sf} = (2\mu\rho s\, abc)/ (C_D\, \rho w\, ac) \quad (5)$$

$$H_{tf} = (0.5\mu\rho s\, abc)/ (C_D\, \rho w\, ac) \quad (6)$$

Where ρw is the density of water at 1.02 g/ml; ρs is the density of rock; a is the A-axis, b the B-axis and c the C-axis of boulder; C_D is drag coefficient=1.95; C_L lift coefficient=0.178; μ is the coefficient of friction=0.7.

Then, wave height values for each boulder were compared with the attenuation curves to evaluate if storms or tsunamis were able to emplace a given boulder in its final position. Indeed boulders that are beyond the curves obtained for storm waves need a more energetic wave to be emplaced, that could be a tsunami.

f) statistical analysis of boulders distribution. Generally, since wave energy decreases with the distance from the coast, an exponential landward decreasing of boulder size is ideally expected, both for tsunamis and storms. When this frame is not respected a backwash effect can be hypothesized and it occurs significantly only for tsunamis having major energy than storm waves;

g) samples of marine biogenic encrustations were collected for age determination, from the heaviest boulders at distances greater than the storm inundation limit. The calibration of radiocarbon dating was carried out using the program Calib 6.0 (Stuiver

and Reimer, 1993; Stuiver et al., 2005) for the marine environment with about 400 years reservoir age.

Table XII. Storm events with maximum wave height (H_0) and peak period (T_0) in deep water recorded by Catania buoy, used for Capo Campolato and transposed for Vendicari and San Lorenzo site (H_T and T_T) (from Barbano et al., in press in the BGTA).

Date	Wave data from Catania buoy				Wave data in Capo Campolato site		Wave transposed data			Wave data in Vendicari site		Wave data in San Lorenzo site	
	Direction (N)	H_0	T_0	L_0 (m)	CWH_b (m)	CX_{max} (m)	H_T	T_T	L_0 (m)	VWH_b (m)	VX_{max} (m)	SWH_b (m)	SX_{max} (m)
31/03/1991	70°	5.1	9.1	129.3	7.0	14.5	5.6	9.7	147.6	6.5	14	5.8	13.2
26/12/1992	94°	5.8	11.1	192.4	8.5	18.8	6.1	11.4	204.8	7.5	18	6.7	16.7
28/02/1996	104°	6.2	11.1	192.4	8.9	19.2	6.4	11.4	201.6	7.8	18	6.9	16.8
17/03/2003	162°	3.8	13.3	276.3	6.8	23.7	5.1	16.1	404.4	7.7	25	6.9	23.8
04/10/2004	40°	4.1	28.6	1277.7	10.6	57.6	4.5	31.4	1546.1	9.9	58	8.9	52.8
05/01/2005	129°	3.0	28.6	1277.7	8.4	49.8	3.3	30.5	1454.1	7.8	48	6.9	43.3
12/01/2005	119°	3.3	28.6	1277.7	9.1	50.5	3.6	29.7	1383.5	8.1	48	7.2	45

The average sea bottom slope was measured from −20 m depth to the shoreline, from the nautical maps (Istituto Idrografico della Marina, 1999); the slope values are: 5° at Capo Campolato, 2° at Vendicari and 1.2° at San Lorenzo. The estimated wave length in deep water ($L_0=gT^2/2\pi$; Sarpkaya and Isaacson, 1981) and the wave height at breaking point at Capo Campolato (CWH_b), Vendicari (VWH_b) and San Lorenzo (SWH_b) are determined with the Sunamura and Horikawa (1974) equation ($Hb/H0=(\tan\beta)^{0.2}(H0/L0)^{-0.25}$). CX_{max} = Capo Campolato; VX_{max} = Vendicari and SX_{max} = San Lorenzo are the maximum water flooding of the strongest storm waves in the study areas, obtained using the equations of Cox and Machemel (1986) and Noormets et al. (2004) (After Barbano et al., in press in BGTA).

6.2.2 Study sites

6.2.2.1 Capo Campolato site

At Capo Campolato the coast reaches a maximum wideness of about 80m, a maximum height of about 8-10m a.p.s.l. and an average slope of 10° (Fig. 6.8a).

In all 63 calciruditic boulders have been observed and studied in detail. These megaclasts are generally very large, with and average volume of about 5.0 m^3 and a maximum weight of 71 t and very far from the coastline (maximum distance about

80m). These megaclasts are characterized by no biogenic encrustations (e.g. vermetids, serpulids or algae) neither erosive littoral feature (e.g. pools and potholes). They appear intensely eroded and old in age and are scattered randomly along the wave cut platform (Fig. 6.8b, 6.8c and 6.8d).

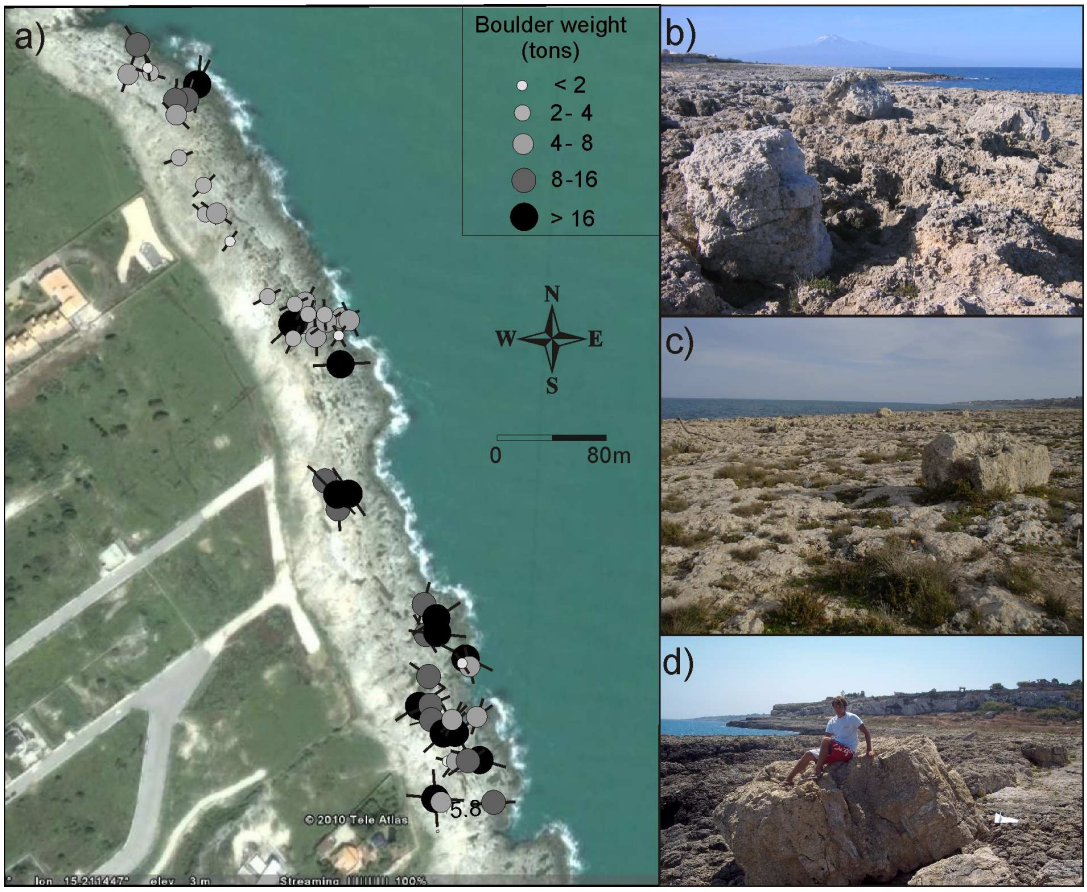

Fig. 6.8: (a) Google Earth map of Capo Campolato site showing boulder distribution, their weight and the orientation of the longest axis; (b), (c) and (d) pictures of boulders (from Barbano et al., in press, BGTA).

GPS survey allowed to observe that at Capo Campolato boulders were not moved by the strong storms recently occurred. Comparing the minimum heights of the waves capable to emplace the blocks in their inland position with the attenuation curves of the strongest storm waves occurred at the site, it is possible to observe that many boulders are beyond the storm wave transport limit (Fig. 6.9a and 6.9b), so they could have been deposited by stronger unknown storm waves or more probably by tsunamis that having a longer period attenuate further inland. Indeed all boulders are below the attenuation

curves of the considered historical tsunamis (the 1693, considering both minimum and medium run up and the 1908) as observed in figure 6.10a and 6.10b. Boulder distribution in relationships with their weight allowed to observe three different fining landward trends, which could be due to three different waves (Fig. 6.11a).

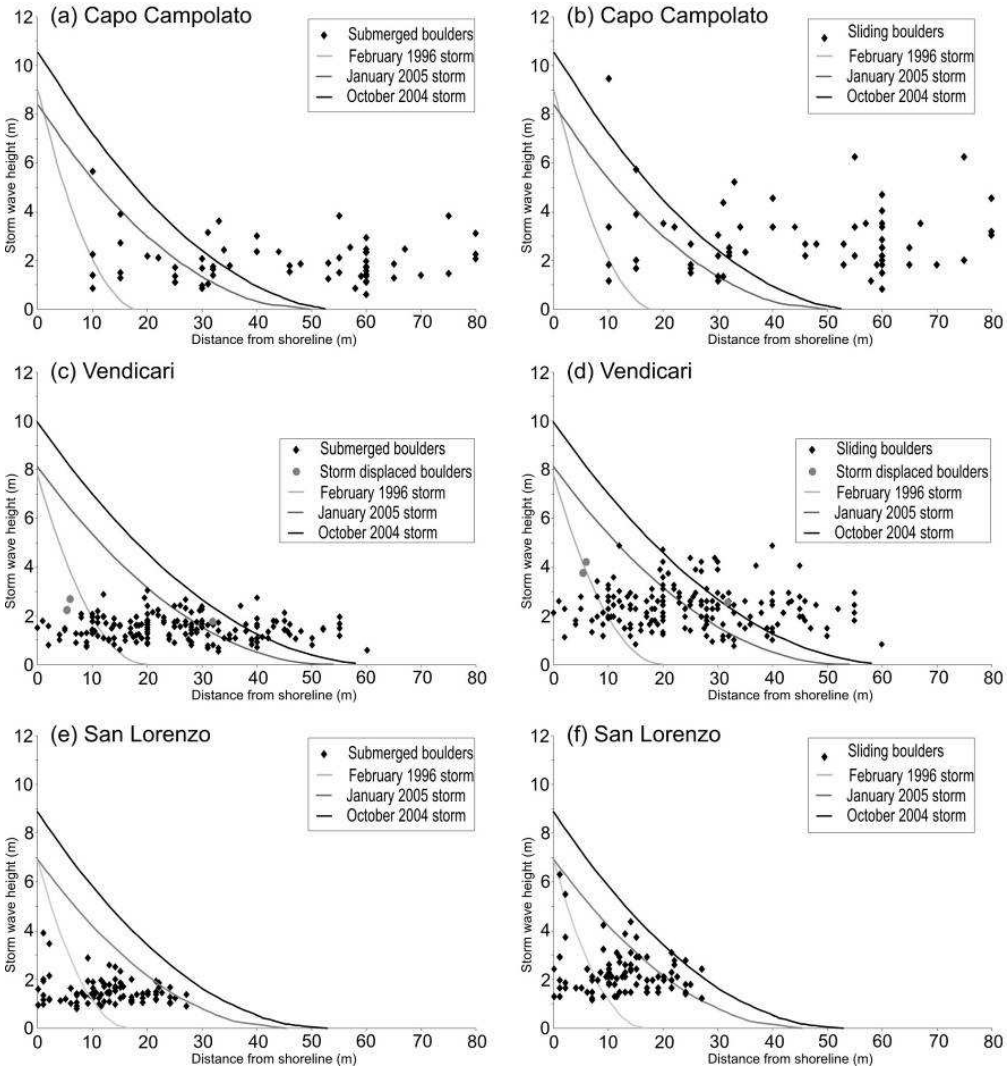

Fig. 6.9: Flooding landward curves of the strongest storm waves for the sites: (a) and (b) Capo Campolato; (c) and (d) Vendicari; (e) and (f) San Lorenzo. Black diamonds are the values of the storm wave heights capable to deposit boulder in its inland position, considering two different transport mechanisms: the flow transport mechanism (graphs on the left) and the sliding transport mechanism (graphs on the right) by Noormets et al. (2004). Gray dots are boulders emplaced by the 2009 winter storm waves at Vendicari (from Barbano et al., in press, BGTA).

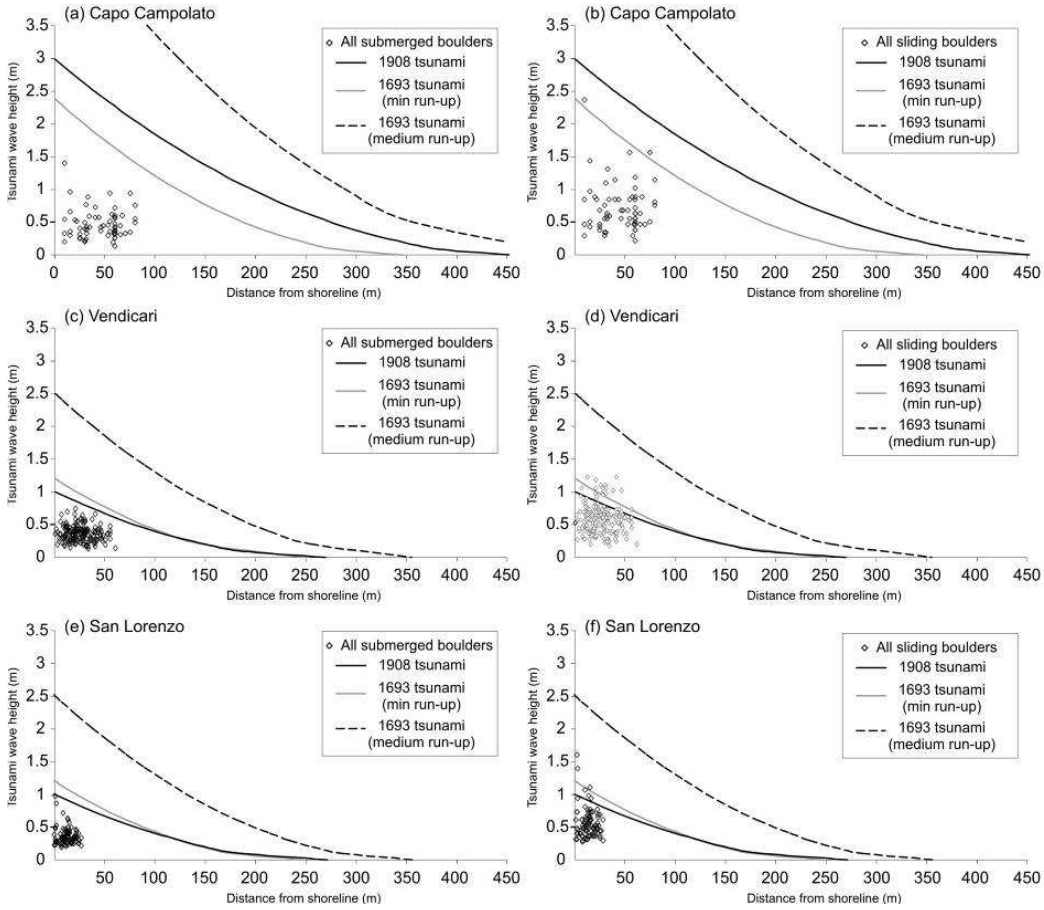

Fig. 6.10: Flooding landward limit of three probable tsunami waves (1908 tsunami, run-up R = 1 m and period T = 8 min; 1693 tsunami, Rmin = 1.2 m, Rmed = 2.5 m and T = 7 min) compared with the tsunami wave heights (Ht) at the moment that boulders were emplaced in their inland position, computed by applying the flow transport mechanism (left graphs) and the sliding transport mechanism (right graphs) (a) and (b) Capo Campolato; (c) and (d) Vendicari; (e) and (f) San Lorenzo. (from Barbano et al., in press in the BGTA).

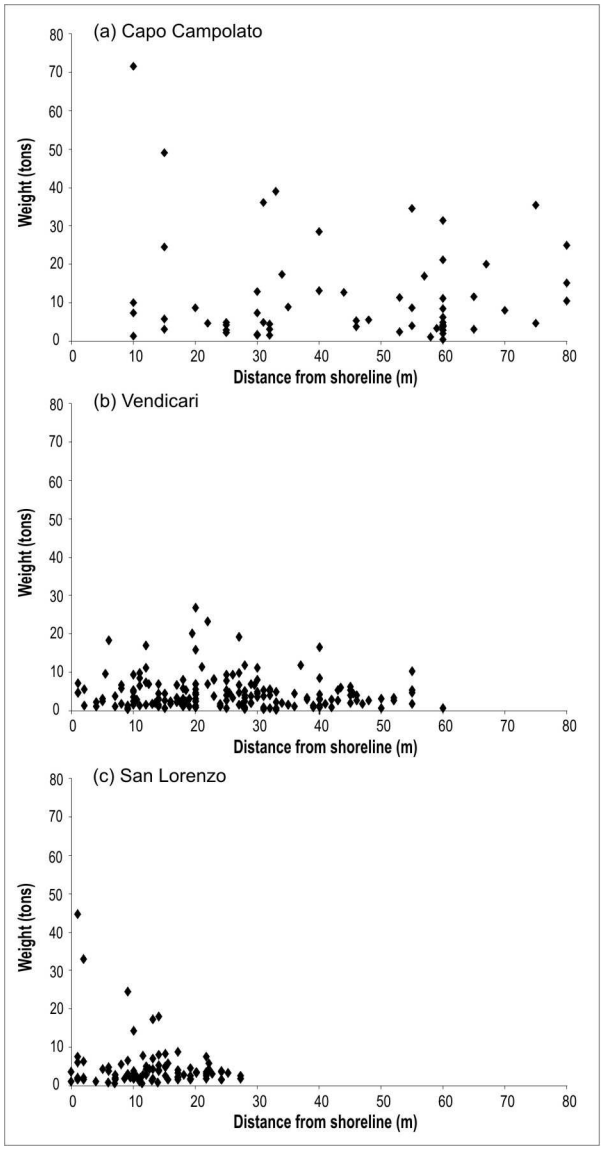

Fig. 6.11: Graphs relating the boulder distribution on the coast with their weight: (a) Capo Campolato; (b) Vendicari and (c) San Lorenzo (from Barbano et al., in press, BGTA).

6.2.2.2 Vendicari site

At Vendicari the rocky coast shows both a gently sloping wave-cut platform, reaching a average slop of about 5° to 10° and maximum elevations of 5 m a.p.s.l, and a steep cliff about 10 m a.p.s.l..

In this site the strongest storms of the Ionian Sea, which occurred in February 1996, January 2005 and October 2004, produced waves that, according to the

attenuation curves, reached about 30-40 m of distance from the shoreline (Fig. 6.9). This data is also supported by direct field observations of boulders moved until 32 m by the January 2009 storm.

In all 175 calcarenitic boulders (Fig. 6.12), up to 27 t and a maximum distance of 60m from the shoreline, have been investigated. Some of them show fresh algal, and other biogenic encrustations (Vermetids and Serpulids) and Lithophaga, sometimes so fresh that suggest a very recent age of the boulder displacement.

Comparing the attenuation curves, obtained for storm waves, with the wave heights required to emplace boulders inland, some megaclasts are beyond the possible transport limit and these could be deposited by tsunamis (Fig 6.9c and Fig 6.9d). Indeed, in the graphs of figure 6.10c and 6.10d the boulder distribution is compatible with the attenuation curves of both the 1908 and the 1693 tsunamis, considering its minimum and medium run up.

Relationships between boulder distribution and their weight shows three fining landward trends indicating the possible occurrence of three different waves during the time (Fig. 6.11b).

Dating on three samples collected on boulders beyond the transport limit of the storm waves was performed. Results indicate that a sample (V27) is old in age whereas two samples, collected from two close blocks, have a very recent age and their deposition would have occurred about two or three centuries ago (Tab. XIII).

Tab. XIII. 14C dating of samples collected from three boulders at Vendicari site.

Boulder	ID sample	Description	δ13C (‰)	Radiocarbon age (BP)	ΔR	Calibrated age	1 σ	2 σ
V27	Poz-16592	Serpulids		1738±30	124±60	AD 697–843 AD 657–939	1.000	1.000
V106	LTL4219A	Serpulids	+4.1±0.5	337±35	124±60	Modern		
V107	LTL4220A	Lithophaga	+4.5±0.4	617±30	124±60	AD 1760–787 AD 1803–910 AD 1915–950 AD 1700–950	0.141 0.660 0.198	1.000

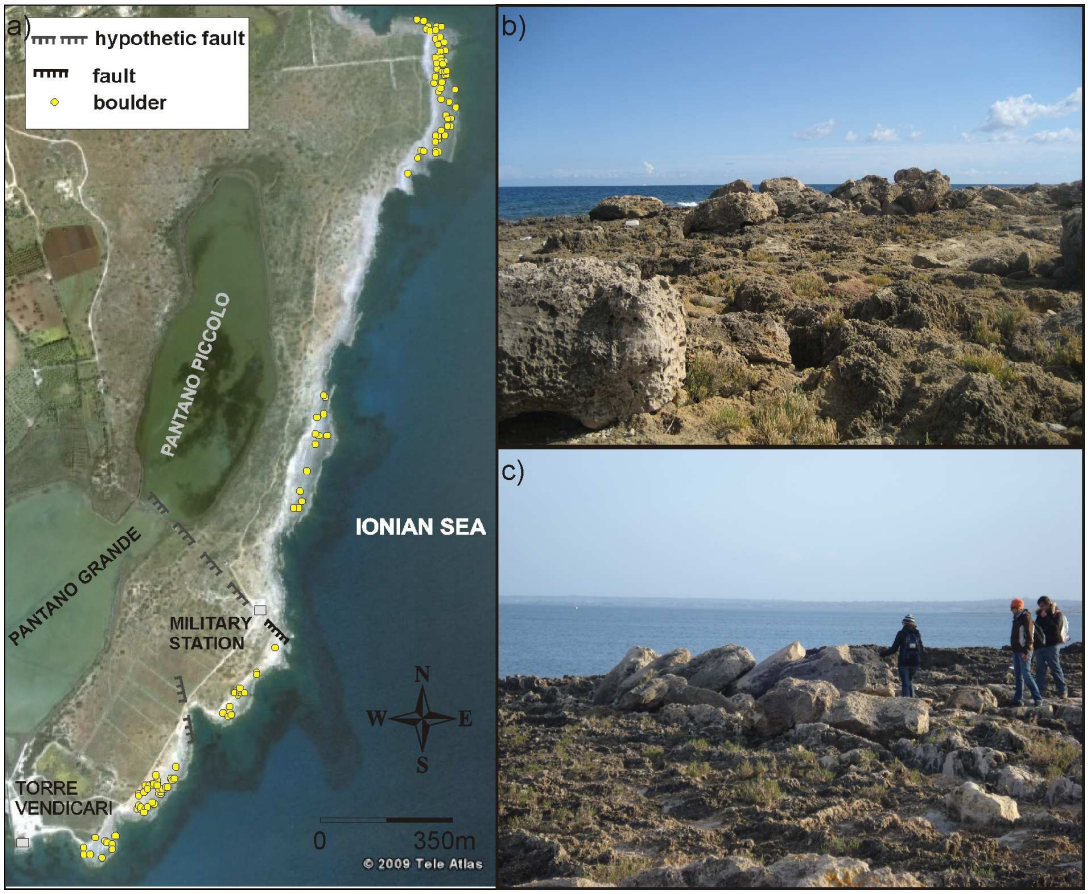

Fig. 6.12: (a) Google Earth map of Vendicari site showing boulder distribution on the coast; (b) and (c) pictures of boulders (from Barbano et al., 2010).

6.2.2.3 S. Lorenzo site

The coast of San Lorenzo is characterized by a gently sloping rocky platform about 400 m long and 60 m wide (Fig. 6.13a), with an average slope of about 8-10°. Here 90 calcarenitic boulders were observed, having an average volume of about 2.5 m^3 and an estimated weight of about 6.2 t., up to 28 m of distance from the shoreline. Most of the mega-blocks do not show fresh biogenic concretions or marine erosive features but they are characterized by alveolar weathering (Fig. 6.13b, 6.13c and 6.13d).

Several small-size boulders were observed removed and new blocks were emplaced on the coast near the shoreline by recent storms.

Graphs of figure 6.9e and 6.9f show that all the megaclasts are placed within the flooding limit of the strongest storm waves. So these kinds of wave could be responsible of their deposition inland. This is confirmed by the graph of figure 6.11c showing a unique landward fining trend distribution that should indicate the lack of tsunami effect. However tsunami occurrence can't be excluded as responsible of the block distribution on the coast as showed in figures 6.10e and 6.10f.

.

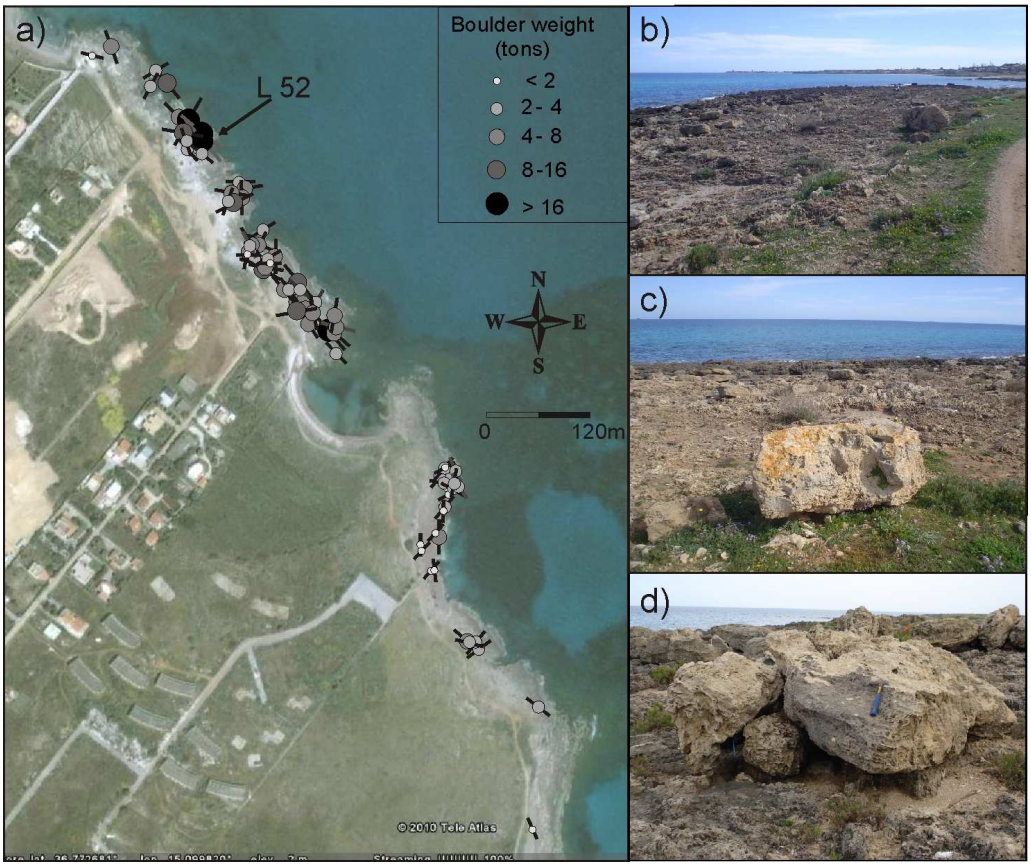

Fig. 6.13: (a) Google Earth map of San Lorenzo site showing the boulder distribution, their weight and the longest axis orientation; (b), (c) and (d) pictures of boulders (from Barbano et al., in press, BGTA).

6.3. Data Analysis

This study allowed to delineate some general criteria to distinguish between storm and tsunami deposits. In particular some features of sandy deposits useful to highlight their tsunamigenic origin have been defined: grain size coarser respect to the local

sedimentary sequence; upward normal grading; sharp erosive basal contact; presence of chaotic and heterogenic material; marine origin of the micro and macrofauna; frequency in the sedimentary sequence different and generally lower than that of storms; ages confirming a sudden deposition that cannot to be related to environmental changes. Moreover, the reconstruction of the wave height attenuation curves of the strongest storms and tsunamis occurred in the study sites was useful to distinguish between boulders deposited by storm from that deposited by tsunami.

6.3.1 Study of sandy deposits

Multi –theme study on sandy deposits allowed to provide evidence for tsunami inundations in south-eastern Sicily. Both historical events with local sources, that are the 1169, 1693 and the 1908, and more ancient events coming from eastern Mediterranean, such as the 365 AD Crete and the Santorini (about 3600 BP) tsunamis, were recorded together with further 7 paleo-events old in age up to about 4500yr.

Further analyses are in progress and new studies should be undertaken to found new evidence of tsunami inundations in eastern Sicily with the main purposes to reconstruct the inundation scenario and to extend back in time the record of tsunami occurrence.

6.3.2 Boulder study

This work highlights that storm waves as that registered in the Ionian Sea during February 1996, October 2004, and January 2005, are capable to transport large blocks onto the coast. However, blocks very far from the shoreline testify the flooding of stronger waves. At Vendicari and Capo Campolato, the presence of some boulders beyond the limit of the landward flooding of the strongest known storm waves indicate that more energetic waves, that attenuate further inland, could be responsible of their deposition. These waves could be stronger unknown storm waves or, more probably, tsunamis that, having a longer period, are characterized by lower attenuation. At San

Lorenzo site all the boulders are compatible with the waves related to known storms occurred in the Ionian Sea.

However, boulder distribution is also influenced by the geographic position of the coast and by its morphology and direction. Capo Campolato site lies at the northern tip of an almost NW-SE trending promontory, so it seems less exposed to the effects of the strongest storms, that come from ESE and SE, but it is better exposed to the tsunamis, related to the eastern Sicily sources, that come from NE. Moreover, the site is very close to the sources of the 1169 and 1693 events. This remark is also supported by the lack of blocks in the first 30 m of the platform. On the contrary, at Vendicari and San Lorenzo sites the coast has an about NNE-SSW direction so it seems to experience more intensely the Ionian storms. This is confirmed by the observation of some boulders removed and emplaced during recent storms. Moreover, for the southernmost coast of Sicily, where Vendicari and San Lorenzo sites are located, tsunami historical data report smaller run-up with respect the ones observed near Capo Campolato. Finally, at San Lorenzo the low slope of the sea bottom could has attenuated the action of waves, both storms and tsunamis, causing the lack of boulders farther than 30 m from the coastline.

Comparing the radiocarbon ages of samples collected on three blocks at Vendicari site (V27, V106 and V107 in Table XIII), with historical tsunami catalogue the deposition of two boulders could be related to the 1693 or 1908 tsunamis. The first is preferred because its probable source is closer to the study area than that of the 1908 tsunami. Emplacement of the third boulder occurred probably after 650-930 A.D. This inundation could be both an unknown event and also one of the historical tsunamis (1169, 1542 and 1693) that affected the Ionian coast of Sicily. In fact, since the radiocarbon dating was made on *serpulids* and on *lithophaga* shells, the estimate age is the time of organism death, but probably not the moment of the boulder final displacement.

7. DISCUSSIONS AND CONCLUSIONS

In this thesis an original, multi-theme, paleoseimological research was performed combining the analysis of historical data of past earthquakes with field studies of seismoinduced effects (brittle and soft sediment deformations and tsunami deposits).

The examination of the historical data allowed to update the datasets of seismogeological effects (landslides, ground deformations, liquefactions and hydrological anomalies) and to elaborate interactive maps of their distribution and maps of susceptibility to their occurrence, for Sicily. Finally, empirical relationships between source parameters, M_{aw}, M_{as} and I_o, and epicentral distance have been obtained.

This study showed up that Sicily is a region highly prone to the seismogeological effect development. In particular, landslides and ground deformations represent the most frequent observed phenomena (38% and 26% of total respectively) triggering for lower values of source parameters than the other effects. Both landslides and ground deformations are frequent in the eastern flank of Mt. Etna and in the northern sector of Sicily where complex structural formations, belonging to the orogenic system (Kabilo Calabride and Apenninic Maghrebian Chains), crop out in persistent instable condition. On the contrary, liquefactions and hydrological anomalies, that are also less frequent (21% and 15% of the total respectively), need more energy to be triggered and their happening is linked to the geological and hydrological site setting. These effects are mainly clustered in the Belice Valley and in the Catania Plain, characterized by young, loose sediments saturated by water.

Databases analysis and successive elaborations (maps and empirical relationships) allowed defining the epicentral areas where a given effect is expected for a future event with specific seismic parameters. Upper bound-curve graphs also highlighted possible misinterpretation of source parameters, obtained from macroseismic data, revealed by the presence of anomalous points. For instance, the magnitude of the 1823 earthquake (M = 5.87) could be underestimated and the new value (M = 6.7) proposed by some Authors seems to be more plausible. Moreover, effects occurred at unexpected long distance could reveal possible site amplifications and/or exceptional site response, such as ground deformations and liquefactions happened during the moderate 1783 (M=4.20) earthquake at Messina that seem to be a high prone are. Similarly, liquefactions and

ground deformations created during the 1693 earthquake at Calatafimi (TP), 210 Km away from the epicentre, could be due to the critical geological and geomorphologic setting of the site.

Field study of deformation structures was performed in three sites, Minissale, Agnone and Vendicari.

At Minissale site the deformational pattern consists of lateral spreading, dikes and boudinage. Analyses revealed that they are ascribable to seismically-induced liquefaction mechanisms due to two different earthquakes. Radiocarbon dating, combined with the upper bound curves, allowed to associate the seismites with the 1169 and the 1693 earthquakes.

The deformational patterns found at Agnone site consist of lateral spreading, dikes, faults, drag folds, recumbent folds and sheet slumps, warped top levels and boudinage. These forms can be ascribed to two distinct liquefaction- driven deformational events due to earthquake shaking. Radiocarbon dating, combined with the upper bound curves support their association with the 1542 and the 1693 earthquakes.

At Vendicari site the investigated structures are both soft sediment deformations (autoclastic breccias, diapyr-like injections and thyxotropic wedges), probably linked to liquefaction mechanisms, and brittle deformations, consisting of fractures generally opened and filled by sediments. Earthquake shaking should be largely responsible for their development and at least four seismic events seem to be occurred since the Pliocene age. Fractures also appear due to a tectonic stress, characterized by a NW-SE-trending σ_1, compatible with the regional stress field. Unfortunately the lack of datable material doesn't permit to constrain the age of the deformational events. However, the last two events happened after Pleistocene age and probably in recent time because they should be responsible of sedimentary dike formation, whose diagenesis and erosion should be extremely rapid, whereas at the site they are not yet eroded although the recent strong karstification. In any case, this seismite association testifies the happening of events with magnitude greater than 5 and intensity greater than IX, that are the thresholds for its triggering in a site. Moreover, on the basis of the upper bound curves, the earthquakes that could be responsible for these deformations occurred at an epicentral distance shorter than 20 km or at a longer distance but with magnitude bigger than the threshold parameters. Considering the closest historical earthquakes the 1169,

1542 and the 1693 should be the best candidates for the last two deformational events triggered at Vendicari.

Deposits such as sandy layers and boulder accumulations, marking the inland flooding of tsunamis, were observed and studied in some sites along the eastern coast of Sicily.

At Augusta three sandy deposits were found on-land and they were associated with paleo-events and with the 365 AD Crete tsunami. Eleven anomalous layers were found off-shore and linked to the 1169, 1693 and 1908 tsunamis and to events originated from Eastern Mediterranean such as the 365 AD Crete and the Santorini (about 3600 BP) ones. Pantano Morghella recorded evidences of the 365 Crete tsunami. The distribution of the sandy deposit also allowed reconstructing a minimum inundation of about 1200 m and a run up of about 3 m for this event. Further investigations on other two levels are in progress to understand if they have a tsunamigenic origin.

At Capo Campolato, Vandicari and San Lorenzo boulder study highlighted that, even if strong storms are capable to deposit large megaclasts inland, blocks that are behind a give distance from the shoreline need a more energetic wave to be emplaced and this wave could be a tsunami or a wave due to an unknown exceptionally strong storm. Investigations revealed the happening of at least two events. According to the radiocarbon dating the first could be associated to a tsunami among the 1169, the 1542 and the 1693, whereas the more recent could be the 1693 or the 1908 one.

This research was undertaken with the aim to test different paleoseimological methodologies and to evaluate their applicability and usefulness. Different approaches were combined and already known practices were also used as innovative method for paleoseismological purposes, such as the application of mesostructural, systematic and thin section microscopy examinations to distinguish between tectonic or seismically induced fractures.

The study in field offered the possibility to enhance the research methods, to contribute to the definition of criteria useful to distinguish between seismically induced geological effects and no seismic ones, to enrich the knowledge and to upgrade the study cases of the effects.

Thanks to this research original data have been provided and, if integrated with further results, they could contribute to the definition and characterization of the

seismogenic sources and of the tsunami scenario in Sicily. For instance the finding and dating of tsunamiites in a given area may provide a unique opportunity to reconstruct the inundation scenario and to obtain realistic average tsunami recurrence interval, the minimum inundation distance and the elapsed time since the last event.

This work also showed that the studied sites were affected by both known historical events and paleo-earthquakes and tsunamis and so they are highly susceptible to the occurrence of the same effects for future events. Therefore, obtained results, combined with other information, can be useful for seismic hazard assessment, risk scenario definition and for engineering and Civil Protection Department activities. This is especially important for eastern Sicily that is a very densely inhabited coastland with areas, such as Augusta and Priolo (southern sector), that host important military and industrial sites.

Appendix A

Historical reports describing seismically induced secondary effects (landslides, ground deformations, liquefactions and hydrological anomalies) triggered in Sicily by earthquakes of Sicily and southern Calabria with M > 4.0.

Landslides and rockfalls

4.02.1169 (E-Sicily)

Aci Antica: "Aci non era in quel medesimo luogo dove ora è, ma dal monte ove o fu posto in piano dall' incendio o tremuoto di Mongibello ovvero cascò da sè medesimo, e divenne piano il che se così fosse bisogna, che il monte dove ora Iaci non per altra cagione fu posta in egual suolo, che per quella del tremuoto o fuoco etneo." (Biblioteca Zelantea di Acireale, 1835b).

Lentini: "subito Lentini fu chiusa fra due monti" (Marangone, 1866).

Mongibello: "quella parte altissima del Mongibello si abbassò crollò parte dell'Etna, Mongibello" (Aprile, 1725). "Il Monte Etna detto oggi Mongibello allora si abbassò un pezzo nella cima." (Biblioteca Zelantea di Acireale, 1835b).

10.12.1542 (SE-Sicily)

Lentini: "Nei pressi di Lentini, sul colle "Yrapolis" (Hieropolis), localizzabile nell'area archeologica dell'antica Leontinoi, si aprì una spaccatura nel terreno lunga circa 1,5 km"; "In alcuni paesi, in particolare a Sortino e a Lentini, i danni furono aggravati da frane e scoscendimenti e cedimento dei terreni di fondazione" (CFTI97, Boschi et al., 1997; Fazello, 1628; Bonito, 1691).

Licodia: "Tutta parimente la Rocca di Bizini (Vizzini), e la parte pi eminente ancora di quella di Licodia cascò." (Bonito, 1691).

Scicli: "A Scicli, lungo la cava di Santa Maria la Nova, franarono molti massi rocciosi staccatisi dai bordi del dirupo." (CFTI, 2000, Boschi et al., 2000).

Sortino: "la rocca di Sortino all' improvviso rovinando ammazzò miseramente Beatrice signora di quel Castello.. furono trovati i loro cadaveri ..sotto un monte di sassi" (Bonito, 1691). "In alcuni paesi, i particolare a Sortino e a Lentini, i danni furono aggravati da frane

e scoscendimenti e cedimento dei terreni di fondazione." (CFTI00, Boschi et al, 2000).

Vizzini: "Tutta parimente la Rocca di Bizini (Vizzini), e la parte pi eminente ancora di quella di Licodia cascò" (Bonito, 1691).

25.08.1613 (Naso)

Naso: "videro i monti fendersi da sommo a imo, spaccarsi immensi e rugginosi macigni". "Apertura di una fenditura larga oltre 5cm e molto profonda, dalla quale uscì denso vapore bituminoso". "Nei dintorni dell'abitato frane e spaccature del suolo" (Incudine, 1882).

9/11.01.1693 (E-Sicily)

Southeastern Sicily: "Frane e smottamenti furono segnalati a Paternò, Sortino, nel territorio di Noto, nel territorio fra Ferla e Cassaro. Nuovi invasi d' acqua, originati dall'ostruzione di fiumi e torrenti a causa di frane e smottamenti, vennero segnalati lungo il corso del fiume Irminio (Modica- Ragusa) e lungo la via da Noto a Siracusa." (Boschi et al., 2004).

Augusta Libitina (Augusta): "collisione di pietre che crollavano" (Bottone, 1718).

Cassaro: "s' accozzarono rupi ad impedire il corso dei fiumi come vedemmo sotto la terra del Cassaro" (Aprile, 1725; Bottone, 1718). "Poco distante dalla terra del Cassaro, da due punte, nelle estremità di due Monti, in mezzo d quali per una lunga Valle correva un fiume, si spiccarono due grandissime rupi, che precipitando dall' erto, andarono egualmente a portare nella bocca della Cava, della Valle fino a pareggiare l' altezza delle precipitate rupi, per dove sgorgando, lasciarono un Lago di giro tre miglia, e di profondità confiderabile" (Boccone, 1697). "Non lungi della contea di Cassaro, due gran massi furono staccati dalla cima di due montagne che formavano una lunga valle, in cui scorrea un fiume venendosi ad incontrare nella valle, l'hanno chiusa, ed hanno fermato il corso del fiume che ..ha empito la valle ..formando un lago di tre miglia di circuito" (Bonaiuti, 1793).

Ferla-Cassaro: "tra Ferla e Cassero due monti di ragguardevole grandezza, che un torrente separava nel mezzo, dopo la scossa, per il colpo, furono distrutti e, dal momento che furono completamente spianati e le onde traboccarono, si formò subito una palude profonda e navigabile di circa 256 passi". "Tra Ferla e Cassaro due colline separate da un affluente

dell' Anapo franarono ostruendo il corso dacqua e originando così una palude profonda e navigabile" (Bottone, 1718).

Ibla: "noto che vicino a Ibla due monti, aspri per le stesse foreste, con tanta forza precipitarono, che le loro cime pendevano dal basso e, rivolti gli alberi in senso contrario dalla prima scossa, accadde che ci che sprofondava verso il basso oltrepassò le cime, e ci che era posto in alto, precipitò verso il basso, e ci avvenne per gli alberi come per gli edifici". (Bottone, 1718).

Lentini: "Qui con violento impeto, e grande forza si spaccarono le rupi, per una grandezza che contiene un uomo intero così la patria di Leontini fece una violenta fine". (Bottone, 1718).

Militello: "Sul pendio di un eccelso monte e la sua parte inferiore, sebbene edificata sopra una roccia bianca e resistente precipitarono e dall'interno della terra riecheggi un boato" (Bottone, 1718).

Modica- Ragusa: "Nuovi invasi d'acqua, originati dall'ostruzione di fiumi e torrenti a causa di frane e smottamenti...lungo il corso del fiume Irminio (tra Modica e Ragusa) e lungo la via da Noto a Siracusa". "Vicino al fiume di Ragusa (fiume Irminio), dove una grande quantità di terra crollò dopo aver abbattuto spessi alberi per il pezzo che scendeva a valle, e qui si formò un lago di tale ampiezza, che era accessibile alle navi" (Bottone, 1718).

Mongibello: "La sommità del monte Etna sia abbassata" (Boccone, 1697).

Noto: "Dalla superficie di alcuni monti ..che circondano la città di Noto.. fatto saltar dal terreno massiccio grossi massi; scinduta di noto da una improvvisa apertura del terreno furono assorbiti tutti" (Boccone, 1697).

Noto Antica: "Furono squarciati non solo gli edifici, ma anche gli stessi sassi e rupi, che si videro dispersi ovunque dai monti e precipitare verso il basso". "Furono viste una roccia inusitata grandezza e una grande quantità di alberi spinte avanti e rivolte qua e là con gli alberi inclinati, come in un giardino pensile". "..nella alture circostanti la città (Noto antica) si aprirono spaccature dalle quali si distaccarono enormi massi" (Bottone, 1718).

Noto- Scala di Militello: "Distacco di enormi massi con aperture di squarciature nei rilievi circostanti la città, una grande fenditura si aprì fra Scala di Militello e Noto" (Romeo and

Delfino, 1997).

Noto- Siracusa: "Nuovi invasi d'acqua, originati dall'ostruzione di fiumi e torrenti a causa di frane e smottamenti...lungo il corso del fiume Irminio (tra Modica e Ragusa) e lungo la via da Noto a Siracusa". "In quella via che da noto porta a Siracusa si formò un lago poichè fuoriuscì una vena d'acqua e fu deviato il corso dei fiumi che sgorgano…. la parte intatta di un campo fu spostata altrove di circa cinquanta passi (Bottone, 1718).

Paternò: "Vediamo la stessa terra abbassarsi, come se fosse sradicata dal cardine, i monti posti davanti alla città di Paternò, che in ogni tempo impedirono la vista del mare di Catania, ora, dal momento che sprofondarono nella parte orientale, permisero la vista del mare dalla zona della città vecchia; i rilievi nei pressi dell'abitato dalla parte orientale, franarono permettendo la vista del mare dalla zona più antica della città" (Bottone, 1718).

Ragusa: "A causa frana e smottamenti, si formarono nuovi specchi d' acqua originati dall' ostruzione di fiumi e torrenti". "Lungo il corso del fiume Irminio si formarono degli stagni". "Vicino al fiume di Ragusa (fiume Irminio), dove una grande quantità di terra crollò dopo aver abbattuto spessi alberi per il pezzo che scendeva a valle, e qui si formò un lago di tale ampiezza, che era accessibile alle navi"…. "rese uguali al suolo Ragusa, Scicli, Ibla, Chiaromonte e i rimanenti luoghi fondati su resistentissimi sassi e colline rocciose" (Bottone, 1718).

Sortino: "Gran pezzi di rocce furon per tutto staccati e precipitati dall' alto della montagna; nella contrada di Sortino... un gran numero ne perì nelle case che queste rocce abbatterono nella loro caduta...S' aprirono grandi fenditure .." (Bonaiuti, 1793). " Un campo o pezzo di terra avvallò pari pari, otto palmi d' altezza sotto il livello del terreno adiacente..". "Dalla montagna sopra Sciortino per la grande scossa si staccò un sasso"… "si cede affondata la terra all' ultima parte finisce con una voragine circolare… dalle montagne si distaccarono rupi smisurate nella terra di Sortino" (Boccone, 1697).

Val di Noto: "Questa straordinaria trasformazione di monti avvenne non in un luogo o in un altro, ma in molti luoghi della stessa Val di Noto" (Bottone, 1718).

10.05.1783 (Naso)

Naso: "Una forte replica provocò il distacco di alcuni massi nei rilievi circostanti la zona

colpita il 21 maggio". "Videro fendersi enormi macigni e scagliarsi per aria e rotolare nei fondi delle valli con orribil fragore; la terra, instabile, franante travolta trarre inauditi fragori dai suoi abissi" (Incudine, 1882).

San Marco d'Alunzio: "Nella campagna si spaccò più volte il suolo; si staccarono massi dalle montagne" (Mongitore, 1743).

5.02.1783 (S-Calabria)

Messina: "Si abbassò in più di un luogo il terreno, si ruppero le Montagne in varie parti" (Relazione istorico-fisica 1783). "Le medesime fenditure si vedono ancora nelle vicine colline presso alle loro cime..". "Regarding the great Messina earthquakes (1783) a great number of crater-like sink holes appeared in the wet depressions of the Mesima plain … the bank of the Jeropotamo collapsed and a tremendous crack opened from the Sirocco, i.e. the south, to the Mistral, i.e. the north, and the downside has subsided with the rest of the Mesima plain". (Relazione istorico-fisica, 1783; Gallo, 1784; Torcia 1784).

Naso: "Una frana si staccò a poca distanza dall'abitato" (Corrao, 1784).

Rometta: "Una frana si staccò dal monte di fronte al paese e il terreno raggiunse il fiume sottostante" (Romeo and Delfino, 1997; Corrao, 1784).

26.04.1783 (Milazzo)

Messina: "le medesime fenditure si vedono ancora nelle vicine colline presso alle loro cime con buona parte di terreno smottato di una falda" (Gallo, 1784).

08.09.1818 and 24.2.181(Madonie)

Collesano: "La frana che si aprì nel territorio di Gollisano ebbe origine dall'urto del terremoto che premette la terra argilloso-sabbiosa, questa staccatosi dalle rocche, e dai punti che prima appoggiavasi dovette lasciare un gran vano"... "Più rocche precipitarono uno o due giorni dopo quel terremoto dai monti d'Ismello e Gollisano e la terra in un lungo giro si aprì il giorno appresso nel territorio di Gollisano sotto le Madonne". "Questa apertura, ellittica, comprende nel suo circuito…" (Scinà, 1819; Mazzarella, 1988).

Geraci Siculo: "Un gran masso diroccò, e più atri si fessero e si sarganarono nell'orlo della

montagna di Geraci, che riguarda Scirocco e Mezzogiorno". "Più rocche precipitarono uno due giorni dopo quel tremuoto" (Scinà, 1819; Mazzarella, 1988).

Isnello: "Più rocche precipitarono uno o due giorni dopo quel terremoto dai monti d'Ismello e Gollisano e la terra in un lungo giro si aprì il giorno appresso nel territorio di Gollisano sotto le Madonne". "Questa apertura, ellittica, comprende nel suo circuito .." (Scinà, 1819).

5.03.1823 (N-Sicilia)

Caltanissetta: "In una collina vulcanica distante due miglia a oriente dalla città si aprirono diverse fessure." (CFTI, 2000, Boschi et al., 2000).

Collesano: "..nel suolo della campagna presso il paese, nell' ex feudo di Sant'Anna, si verificò una grossa frana" (Ferrara, 1823).

Gordano: "Dalla vicina montagna Disarma, si staccarono enormi massi" (Ferrara 1823; Archivio di stato di Palermo, 1823).

Naso: "nel suolo si produsse una fenditura trasversale e si temette la caduta dell'altura sulla quale situato il paese" (Ferrara 1823).

Ogliastro: "si verificarono lunghe fessurazioni e frane nel terreno creto-argillosointorno al paese nel feudo chiamato del Bosco. Una di queste (fessure) risultò particolarmente profonda e larga da causare l'abbassamento del livello di alcuni alberi e da lacerare molte radici di viti e ulivi. Le frane costrinsero l'acque del torrente a cambiare corso". (Archivio di Stato di Palermo, 1823).

19.07.1865 (Area Etnea)

Moscarello: "Sicchè concludendo sembra che la commozione del suolo abbia avuto il suo massimo nel Fondo Macchia alla base del Monte Muscarello, il quale pure, da alcune frane avvenute, dimostra di aver risentito una scossa" (Silvestri, 1865).

17.06.1870 (Etna)

Fondo Macchia: "Scoscendimenti del terreno in campagna" (Romeo and Delfino, 1997).

Giarre: "Scoscendimenti del terreno in campagna" (Romeo and Delfino, 1997).

Moscatello : "Scoscendimenti del terreno in campagna" (Romeo and Delfino, 1997).

Riposto: “Scoscendimenti del terreno in campagna” (Romeo and Delfino, 1997).

22.04.1893 (Montalbano Elicona)

San Piero Patti: “sulla riva sinistra del fiume Timeo si produsse una gran frana..” (Riccò, 1893).

8.08.1894 (Catanese)

“In tutta l’area colpita dal terremoto si aprirono spaccature nel terreno e furono osservate frane....Una frana di notevoli dimensioni cadde da monte Rosso” (Boschi et al., 2004).

Mazzasette: “La scossa causò profondi scoscendimenti e ampie spaccature nel suolo.” (Patanè, 1992).

Monterosso :”la scossa causò un esteso movimento franoso, che danneggiò le viti e ingombrò la strada per Fleri” (Giornale di Sicilia, 1894).

Zerbate: “La scossa causò frane ed enormi spaccature nel terreno, che resero quasi intransitabile la strada che collegava la borgata ad Acireale” (La tribuna, 1894).

28.12.1908 (Messina Strait)

Caltanissetta: ”si produssero spaccature alle falde del monte S. Giuliano” (Baratta, 1910).

Fiumara della Guardia: “Scoscendimenti nei sabbioni quaternari” (Baratta, 1910).

Fiumara Pace: “Danni alla Stazione fotoelettrica della R.Marina, scoscendimento nei sabbioni” (Baratta, 1910).

Messina: “il terremoto attiv una frana che danneggiò le condutture dell’acquedotto”. (Baratta, 1910).

S. Agata (ME): “lungo la strada verso Faro Superiore si verificarono molti scoscendimenti superficiali; lungo la fiumara della Guardia furono osservati alcuni notevoli scivolamenti“ (Baratta, 1910).

Pietraperzia: ” nelle campagne circostanti ..si produssero molte fenditure nel suolo.. fu notata una grande frattura a forma darco.. producendo dislivelli nel terreno di circa m 2.” (Baratta, 1910).

15.10.1911 (Etna)

Giarre: "Le contrade danneggiate nella zona franata sono in territorio di Giarre, Sciarra, Fondo Macchia, Baglio, Rondinella, Fano fino al torrente S. Leonardello, che segue il confine comunale." (Romeo and Delfino, 1997).

8.05.1914 (Etna)

Timpa: "della galleria un casello abbandonato perchè minacciato da massi che franano" (Romeo and Delfino, 1997).

Passopomo: "Enormi blocchi lavici caddero nel letto del torrente vicino Passopomo. Sei fratture vennero rilevate nella strada a NE del ponte." (Romeo and Delfino, 1997).

Pisano: "Il ponte seguente trovasi sopra un torrente incassato nella lava, delle pareti delle quali si staccarono massi voluminosi. Dopo il ponte suddetto si osservò sulla rotabile da Fleri a Pisano un tratto di frattura N15W e poco a monte un avvallamento" (Romeo and Delfino, 1997).

13.05.1914 (Randazzo)

Passopomo: "Lungo la strada da Pisano a Passopomo si verificarono un avvallamento di pochi centimetri e il distacco di massi in corrispondenza del ponte sul torrente Pisanello" (Cavasino, 1935; Platania, 1916; Ghersi et al., 1914; Sabatini, 1914).

6.07.1925 (Giarre)

Acireale: "Il suolo si riga di spaccature in vari punti; son travolti e spezzati i macigni. Frana lungo la ferrovia vicino la città" (Timpe) (Romeo and Delfino, 1997).

Fondo Macchia: "...la terra si aperta in orrende fenditure, mostrando in varie parti degli abbassamenti. Il suolo dappertutto rigato di crepature; enormi massi precipitati dall'alto delle colline....la pendice che dal fianco orientale forma barriera al torrente, che .....il suolo mostra qua e là delle crepature trasversali alla direzione della scossa altre ad un piccolo avvallamento. Alla base del M. Muscarello ci sono state alcune frane" (Romeo and Delfino, 1997).

31.10.1967 (Nebrodi)

Ristretta: "La strada fu chiusa al traffico per prevenire il pericolo di caduta massi" (ANSA, 1967).

15.01.1968- 01 (Belice)

Ghibellina: "In seguito alle scosse si verific una frana per crollo alla periferia occidentale del centro abitato ostruendo la strada per Alcamo" (Corriere della sera, 1968a).

Montevago: "Crolli associati allapertura di fenditure ed allabbassamento del suolo, si verficarono sul bordo settentrionale del piano dove sorgeva Montevago" (Bosi et al., 1973).

Santa Margherita del Belice: "Crolli associati allapertura di fenditure e allabbassamento del suolo, fenomeni questi collegati a particolarit morfologiche locali, si verificarono nei pressi di Santa Margherita di Belice" (Bosi et al., 1973).

15.01.1968- 02 (Belice)

Ghibellina: "In seguito alle scosse si verificò una frana per crollo alla periferia occidentale del centro abitato ostruendo la strada per Alcamo" (Corriere della sera, 1968a).

Marinero: "in seguito alle scosse si mosse un fronte franoso che minacciava labitato" (L'Ora, 1968a).

Montevago: "crolli associati all'apertura di fenditure ed allabbassamento del suolo, si verficarono sul bordo settentrionale del piano dove sorgeva Montevago" (Bosi et al., 1973).

Sambuca di Sicilia: "due strade intercomunali vennero bloccate da frane nei giorni successivi alla scossa principale" (La Stampa, 1968a).

Santa Margherita del Belice: "Crolli associati all' apertura di fenditure e all' abbassamento del suolo, fenomeni questi collegati a particolarit morfologiche locali, si verificarono nei pressi di Santa Margherita di Belice" (Bosi et al., 1973).

15.04.1978 (Patti Gulf)

Alcara li Fusi: "Il terremoto riattiv antiche frane ad Alcara li Fusi, dove alcuni massi caddero sulla strada provinciale incontrada Baratta e alle Rocche del Castro" (Giornale di Sicilia, 1978b; Giornale di Sicilia, 1978a; Barbano et al., 1979).

Gioiosa marea: "a capo Calavà, 4km ca. a nord-est di Gioiosa Marea, la scossa causò la caduta di alcuni massi, sulla strada statale 113" (Giornale di Sicilia, 1978b).

Longi: "La scossa causò l'apertura di numerose fessure nelle strade" (Giornale di Sicilia, 1978a).

Militelllo Rosmarino: "Alcuni grossi massi si staccarono anche dalla Roccia del Drago e caddero nel greto del fiume Rosmarino" (Giornale di Sicilia, 1978a).

13.12.1990 (SE-Sicily)

Brucoli: "furono osservati piccoli movimenti franosi su terreni terrazzati nei pressi di questa località e sporadiche cadute di massi" (De Rubeis et al., 1993).

Ispica: "Nella zona archeologica, una parte di roccia dell'antica Spaccafono cadde sul fondovalle" (La Sicilia, 1990a).

Palagonia: "Il terremoto caus la parziale riattivazione di una frana preesistente" (De Rubeis et al, 1993).

26.06.1993 (Pollina)

Pollina: seismogeological effects such as changes in spring flows and rockfalls, also occurred in this area" (Azzaro and Barbano, 1995).

6.09.2002 (Palermo)

Cerda: "landslide in the Argille Scagliose Fm." (Azzaro et al., 2004).

Ground Deformations

25.08.1613 (Naso)

Naso: "La Terra di Naso rimase quasi disfatta dal Terremoto, ove accadde, che saperse la terra, e uscì fuori una pessima esalazione di zolfo. Nel piano dell'ospedale comparve una gran fessura, larga due palmi, profonda non si sa dir quanto" (Mongitore, 1743). "Apertura di una fenditura larga oltre 5cm. e molto profonda, dalla quale uscì denso vapore bituminoso". "Nei dintorni dell'abitato frane e spaccature del suolo" (Incudine, 1882).

9/11.01.1693 (E-Sicily)

Augusta: "Fenditure con fuoriuscita di fiamme e gas" (Romeo and Delfino, 1997).

Calatafimi: "Fenditura dalla quale fuoriuscirono esalazioni sulfuree". "Nella terra di Calatafimi seguì una apertura di miglia di lunghezza e due o tre palmi di larghezza ma dopo la scossa si restrinse" (Boccone, 1697).

Caltanissetta: "Una spaccatura fu vista nello stesso tempo in Caltanissetta accanto al collegio dei Gesuiti, la lunghezza della quale era di duemila passi la larghezza di due palmi e la profondità talmente grande, che appariva un baratro" (Bottone, 1718).

Catania: "Spaccature anche a Catania". "A Catania si vedono strade aperte in trincea nella lava". (Bottone, 1718). "La terra si aprì in molti luoghi con fenditure lunghissime alcune della larghezza della mano, altre di mezzo palmo, ed altre come gran voragini" (Romeo and Delfino, 1997).

Lentini: "Sulla strada da Lentini a Catania, appena verificata la scossa, un'enorme fenditura inghiottì un mulattiere e i suoi muli richiudendosi su di loro. ...la terra si aprì in molti luoghi con fenditure lunghissime alcune della larghezza della mano, altre di mezzo palmo, ed altre come gran voragini. Da queste aperture usc una gran quantit d'acqua, che vi fu molto terreno allagato. Qui con violento impeto, e grande forza si spaccarono le rupi, per una grandezza che contiene un uomo interocos la patria di Leontini fece una violenta fine" (Bottone, 1718).

Melilli: "Dopo aperto in più luoghi il terreno" (Boccone, 1697).

Mineo: "Spaccature del terreno che si aprirono e si richiusero. Si aprirono fenditure che si richiusero immediatamente" (Del Bono, 1745). "Nella terra di Mineo (collegio padri gesuiti) crepatura di terreno in strada" (Boccone, 1697).

Noto: "Altro pezzo di campo avvallò dal livello del terreno otto palmi..e ci si osserva nel Val di Noto" (Boccone, 1697).

Noto Antica: "Alle falde della Città di Noto in un Vallone fi fece una apertura di terreno mezzo miglio di lunghezza, e tanto larga, che non poteva essere falcata da veruno, anche per essere la voragine profonda". Nella contrada dell'Isola per causa di una crepatura repentina, fatta nel tempo del terremoto, restarono ancora inghiottiti alcuni buoi, con il loro pastore" (Boccone, 1697). "Nel territorio compreso tra Noto e la Scala di Militello si aprì

una grande fenditura in seguito alla forte replica del 28 aprile 1693" (Del Bono, 1745). "Nella città di Noto c'è una strada lunga mezzo miglio, tutta lastricata che al presente piantata nel terreno in una situazione intieramente piegata di fianco, come un muro inclinato; e in unaltra strada davanti all' Assento del Durbo si vede un'apertura bastantemente grande per inghiottire un uomo a cavallo" (Bonaiuti, 1793). "..un pezzo di campo di 4 miglia di circuito si sprofondò di 12 palmi. Alle falde di Noto si determinò una profonda voragine; nella alture circostanti la città (Noto antica) si aprirono spaccature dalle quali si distaccarono enormi massi comparvero nuove sorgenti con getti di acqua calda e sulfurea" (Bottone, 1718).

Noto e Scala di Militello: "Nel territorio tra Noto e Scala di Militello si aprì una grande fenditura in seguito alla forte replica del 28 aprile 1693" (Del Bono, 1745). "Tra Noto e Scala di Militello mezza salmata di terreno sprofondò lasciando una voragine" (Boccone, 1697).

Paternò: "Vedono questi monti fendersi e per lo stesso urto la terra spezzarsi e fendersi nei campi in lunghe spaccature e profondi baratri, come dimostra l'ampia piana di Lentini" (Bottone, 1718).

Siracusa: "Si aprirono spaccature nel terreno immediatamente richiusesi" (Del Bono, 1745). "In Siracusa la Piazza d'arme non solamente si aprì, e si chiuse nel tempo di questo horribile Terremoto, ma ancora da tre voragini venne fuori acqua salata di mare" (Boccone, 1697). "Si aprirono fenditure da cui sgorgò acqua salmastra" (Romeo and Delfino, 1997). "Si aprirono spaccature nel terreno immediatamente richiusesi" (Del Bono, 1745).

Sortino: "Nel territorio di Sortino in una tenuta di Terrelunga un mezzo miglio, e assai meno larga fi vede interpellaneamente a poca distanza, affondata la Terra, e abbassata dalla parte dello stretto a lunghissime trince, dove due, dove tre, e dove pi palmi, e all'ultima parte finisce con una Voragine circolare assai profonda" (Boccone, 1694). "Nel territorio di Sortini, in un pezzo di terreno lungo mezzo miglio, ma strettissimo, il suolo affondato di distanza in distanza alla profondità di due o tre palmi, e finisce con una voragine circolare fondissima; S' aprirono grandi fenditure .." (Bonaiuti, 1793).

Val di Noto: "Altro pezzo di campo avvallò dal livello del terreno otto palmi e ci si osserva nel Val di Noto" (Boccone, 1697).

Vizzini-Monterosso: "..apertura di fenditure nel terreno fra Monterosso e Vizzini". "Scomparvero sorgenti e si aprirono fenditure nel terreno tra Vizzini e Monterosso Almo" (Naselli, 1931).

10.05.1783 (Naso)

Naso: "Furono osservate spaccature nel terreno e avvallamenti" (Bottone, 1718).

San Marco d'Alunzio: "Nella campagna si spaccò più volte il suolo; si staccarono massi dalle montagne" (Mongitore, 1743).

5.02.1783 (Calabria meridionale)

Ganzirri: "Aperture del terreno con fuoriuscita d'acqua" (Baratta, 1910).

Messina: "..si abbassò in più di un luogo il terreno" (Relazione istorico-fisica, 1783). "..le medesime fenditure si vedono ancora nelle vicine colline presso alle loro cime" (Gallo, 1784). "Si aperse con lunghe fenditure il suolo, si abbassò in più di un luogo il terrenosi ruppero le Montagne vicine alla Città" (Gallo, 1783). "Anzi nello stesso suolo di Messina sono comparse in tutta la spiaggia del Porto non vulgari aperture. Simili eventi si sono pure osservati nelle Campagne, che le stanno dintorno; anche nel terreno all'interno della citt, nella Cittadella e nella fortezza del Salvatore si aprirono molte fenditure. La Terra parimenti nel smemorato luogo marittimo si veduta abbassare alquanto, talchè vi rimasta la Pescheria immersa tutta nell'onde" (Corrao, 1784).

Torre del Faro: "Ricordo a questo proposito che anche nel periodo sismico del 1783 si erano determinate nei pressi del Pantano delle fenditure, ed altre pure si sono aperte anche nel terremoto del 1894" (Baratta, 1910).

7.02.1783 (Calabria)

Messina: "Abbassamento del suolo nel porto.. nel suolo si aprirono fenditure dalle quali uscirono gas dall'odore di zolfo anche allinterno della Cittadella si aprirono molte fenditure" (Lallement, 1785).

26.04.1783 (Milazzo)

Messina: "Si aprì il terreno nel Teatro marittimo da sotto il palazzo reale fino al palazzo senatorio con due e tre lunghe fenditure una dietro laltra dove più, dove meno larghe, abbassandosi parecchi piedi dalla parte del mare" (Gallo, 1783; Gallo 1784).

20.02.1818 (Etna)

Paraspolo: " Five or six minutes after the earthquake there suddenly sprang forth 14 jets of water, arising up to 6 palms (about 1,5m) creating considerable clamour."…the water emanated was salty …." (Longo, 1818).

5.03.1823 (N-Sicilia)

Caltanissetta: "In una collina vulcanica distante due miglia a oriente dalla citt si aprirono diverse fessure" (CFTI00, Boschi et al., 2000).

Librizzi: "Si produsse una lunga lesione che interess buona parte delle case" (Archivio di stato di Palermo, 1823).

Naso: "..nel suolo si produsse una fenditura trasversale e si temette la caduta dellaltura sulla quale situato il paese" (Ferrara, 1823).

Ogliastro: "Si verificarono lunghe fessurazioni e frane nel terreno creto-argilloso intorno al paese nel feudo chiamato del Bosco. Una di queste (fessure) risult particolarmente profonda e larga da causare labbassamento del livello di alcuni alberi e da lacerare molte radici di viti e ulivi" (Archivio di Stato di Palermo, 1823).

1.11.1848 (Augusta)

Augusta: "Ad Augusta nella parte estrema del molo sotto il convento di S. Domenico, dalla parte di occidente, la terra si fendè in due punti e vomitò delle pietre e dell'acqua, che spruzzando per aria ricadeva su dei piccoli navili vicini" (Ferruggia Russo, 1852).

19.07.1865 (Area Etnea)

Scarronazzi: "Si verificarono fessurazioni e abbassamenti del suolo; venne notato un innalzamento termico anomalo del terreno di circa 6 gradi, che fu attribuito a esalazioni di

gas dal sottosuolo." (Grassi, 1865; Biblioteca Zelantea di Acireale, 1865).

22.04.1893 (M. Elicona)

San Piero Patti: "si produsse una gran frattura lunga 200 m" (Riccò, 1893).

16.11.1894 (S-Calabria)

Barcellona: "Fenditura di 50m si apr nel terreno" (Riccò, 1907).

Ganzirri: "Si produssero nel suolo diverse fratture convergenti esalazioni di idrogeno solforato.. fuoriuscita di melma fumante maleodorante..; Presso il Faro per un giro di 90 da W a S attorno al lago, si produssero diverse fratture convergenti lunghe fino a 4m e larghe 5 cm; alcune erano parallele al contorno del lago, indicando un vero distacco del terreno; altre in direzione diverse; Nella riva meridionale del lago si produssero nel suolo diverse fratture convergenti in una, colla lunghezza perfino di 4m, colla larghezza di fino 5 cm, talch vi entravano i bastoni da passeggio; delle dette linee di frattura alcune erano parallele al contorno lago, indicando un vero distacco dal terreno o rivaaltre in direzione diversa; nelle loro estremit orientali si prolungavano verso il lago" (Riccò, 1907).

Messina: "nel bacino di carenaggio si verificarono sprofondamenti e lunghe fenditure" (Riccò, 1907).

Torre del Faro: "Ricordo a questo proposito che anche nel periodo sismico del 1783 si erano determinate nei pressi del Pantano delle fenditure, ed altre pure si sono aperte anche nel terremoto del 1894" (Baratta, 1910).

28.12.1908 (Messina Strait)

Caltanissetta: "In seguito al terremoto si produssero spaccature alle falde del monte S.Giuliano in direzione E-W"... "si produssero spaccature alle falde del monte S. Giuliano" (Baratta, 1910).

Ganzirri: "Questo lago era costeggiato da una rotabile che si in parte sprofondata, onde alcuni tratti sono sott'acqua. Le parti ancora emerse sono attraversate da fratture" (Baratta, 1910; Lo Giudice, 1909).

Messina: "Fenditure, avvallamenti e un generale scivolamento verso il mare si verificarono

nelle banchine del porto e nelle zone adiacenti alla Marina; in alcuni punti le fenditure, parallele o quasi alla spiaggia, risultarono profonde 5cm e larghe da 7a 10cmuna grande fenditura si aprì nel terreno al Forte San Salvatore…modeste variazioni della linea di spiaggia si verificarono nella penisola falcata antistante il porto e nella parte meridionale della città". "L'intera penisoletta falcata per compressione e assestamento dei materiali, in seguito al violentissimo fenomeno sismico ed al maremoto, si abbassò verso il centro la depressione raggiunse 40-5cm" (Baratta, 1910). "A completamento delle notizie già date, credo utile riportare queste altre che tolgo dalla relazione dell'Ing. S. Franchi solo ora venuta in luce nel Bollettino del R. Comitato Geologico. Riferisce adunque il Franchi che l'Ufficio delle Ferrovie dello Stato a Messina a trovato un abbassamento costante di m. 0,47 in tutto il piano del ferro dalla stazione deiferry-boats al ponte sullo Zaera, e che la livellazione eseguita dall'Istituto Geografico Militare dimostra essa pure un abbassamento di m. 0,37 in tutta la parte bassa della città". "La lanterna del Forte S. Ranieri infine si sarebbe abbassata di m. 0,51" (Baratta, 1910). "Presso il Lazzaretto la spiaggia appare abbassata in diversi punti di 5cm., e per tale abbassamento o per l'asportazione della sabbia causata dal maremoto, si formata una piccola insenatura di circa 10m. di saetta..". "Le banchine tutte intorno al porto si sono abbassate ed in parte franate. Anche in altri punti vi fu abbassamento della costa". (Platania, 1909; Franchi, 1909).

Pietraperzia: "Fenditure apertasi nei pressi di Pietraperzia. A circa 2 Km. dall'abitato fu notata una grande frattura a forma di arco con orientazione NE-SW, della lunghezza di circa 150m. con profondità di parecchi punti di alcuni metri e larghezza di 1.5 m. producendo dislivelli di terreno di circa 2 m. nelle campagne circostanti... si produssero molte fenditure nel suolo.. fu notata una grande frattura a forma d'arco.. producendo dislivelli nel terreno di circa m 2" (Baratta, 1910).

Raddusa: "Si aprì una fenditura della larghezza di mezzo metro, profonda da 2 a 4 metri e di circa 5 Km di lunghezza, orientata in direzione NW-SE. si aprì una fenditura nel terreno della lunghezza di mezzo metro profonda da 2 a 4 m" (Baratta, 1910).

Torre Faro: "un lembo di spiaggia scivolò in mare per 1o 12 metri" (Platania, 1909). "Nella strada Torre Faro-Granatari si aprì una lunga fenditura longitudinale con un abbassamento di circa 7cm. La strada verso il Pantano Piccolo si avvallò"; "fenditure con

fuoriuscita di acqua e fango con odore di zolfo" (Baratta, 1910).

31.10.1967 (Nebrodi Mts.)

Nicosia: "In contrada Valpretoso si aprì una voragine della lunghezza di circa 20m e della profondità di oltre 2m" (Corriere della Sera, 1967).

15.01.1968- 01(Belice)

Ghibellina: "Fenditure si aprirono nelle altre strade" (Corriere della sera, 1968b).

Montevago: "Crolli associati all'apertura di fenditure ed all'abbassamento del suolo, si verificarono sul bordo settentrionale del piano dove sorgeva Montevago" (Bosi et al., 1973).

Santa Margherita del Belice: "Crolli associati all'apertura di fenditure e all'abbassamento del suolo, fenomeni questi collegati a particolarità morfologiche locali, si verificarono nei pressi di Santa Margherita di Belice" (Bosi et al., 1973).

Sciacca: "In contrada Campo dei Tiri, in occasione della violenta replica del 25 gennaio 1968, si aprirono delle fenditure dalle quali fuoriuscirono vapori sulfurei" (Corriere della sera, 1968d).

15.01.1968- 02 (Belice)

Ghibellina: "Fenditure si aprirono nelle altre strade" (Corriere della sera, 1968b).

Marsala: "In contrada Ventrischi, nei pressi di Marsala, in seguito alla forte replica del 25 gennaio si aprì una voragine profonda 20m dalla quale fuoriuscivano gas" (La stampa 1968a).

Montevago: "Crolli associati all'apertura di fenditure ed all'abbassamento del suolo, si verificarono sul bordo settentrionale del piano dove sorgeva Montevago" (Bosi et al., 1973).

Santa Margherita del Belice: "Crolli associati all'apertura di fenditure e all'abbassamento del suolo, fenomeni questi collegati a particolarità morfologiche locali, si verificarono nei pressi di Santa Margherita di Belice" (Bosi et al., 1973).

Sciacca: "In contrada Campo dei Tiri, in occasione della violenta replica del 25 gennaio

1968, si aprirono delle fenditure dalle quali fuoriuscirono vapori sulfurei" (Corriere della sera, 1968d).

11.03.1978 (S-Calabria)

Ferruzzano: "Il terremoto causò l'apertura di larghe crepe nelle strade" (ANSA, Notiziario italiano, 1978).

15.04.1978 (Patti Gulf)

Longi: "La scossa causò l'apertura di numerose fessure nelle strade" (Giornale di Sicilia, 1978a).

Naso: "La scossa causò l'apertura di notevoli fenditure nel terreno" (Barbano et al., 1979).

Oliveri: "La scossa causò l'apertura di notevoli fenditure.. " (Barbano et al., 1979).

13.12.1990 (Augusta)

Augusta: "Fessure nell'asfalto del piazzale Fontana.." (De Rubeis et al 1993; Appunti sugli effetti, 1991).

Liquefactions

4.02.1169 (E-Sicily)

Catania: "..s'aperse di pi la terra in molti luoghi di quel paese e mandò fuori nuovi fonti d'acqua e molti dei fonti antichi si copersero di terra e non fu pi veduta acqua in quel luogo. ...sentì quasi lo stesso danno il contorno fra Leontino, Catania e Siracusa scaturendo per le aperture della terra nuove fontane d'acqua...." (Samperi, 1644).

Lentini: "..sentì quasi lo stesso danno il contorno fra Leontino, Catania e Siracusa scaturendo per le aperture della terra nuove fontane d'acqua" (Samperi, 1644).

Siracusa: "sentì quasi lo stesso danno il contorno fra Leontino, Catania e Siracusa scaturendo per le aperture della terra nuove fontane d'acqua" (Samperi, 1644).

10.12.1542 (SE-Sicily)

Augusta: "Il terremoto ha raso al suolo grandi e poderosi edifici, trasformandoli in laghi d'acqua" (BTJN, 16th cent.).

Siracusa: ".. trasformazione di edifici in laghi d'acqua, probabile effetto di liquefazione" (BTJN, 16th cent.).

25.08.1613 (Naso)

Naso: "Apertura di una fenditura larga oltre 5cm e molto profonda, dalla quale usc denso vapore bituminoso. Nei dintorni dell'abitato frane e spaccature del suolo (Incudine, 1882); La Terra di Naso rimase quasi disfatta dal Terremoto, ove accadde, che s'aperse la terra, e uscì fuori una pessima esalazione di zolfo" (Mongitore, 1743).

3.10.1624 (Mineo)

Palagonia: "Nei pressi dell'abitato, a causa della scossa, sgorgò una sorgente di acqua calda e sulfurea" (Mongitore, 1743).

11.01.1693 (SE-Sicily)

Augusta: "..nel territorio limitrofo si aprirono profonde spaccature che eruttavano materiali bituminosi e vicino al tempio sacro dei divi Cosma e Damiano si formò una voragine da cui emersero fiamme di zolfo e il maleodorante fumo di queste" (Bottone, 1718).

Calatafimi: "Fenditura dalla quale fuoriuscirono esalazioni sulfuree. nella terra di Calatafimi seguì una apertura di miglia di lunghezza e due o tre palmi di larghezza ma dopo la scossa si restrinse "(Boccone, 1697).

Catania: "Quell'immane scossa di Catania lacerò con molte fenditure anche quelli che si estendono in lunghezza intorno alle mura; Grande fenditura che si aprì presso le mura di Catania, nella pianura a Sud della città dalla quale uscì un getto d'acqua calda.. Da queste aperture uscì una gran quantità d'acqua, che vi fu molto terreno allagato....sulla strada da Lentini a Catania, appena verificata la scossa, un'enorme fenditura inghiottì un mulattiere e i suoi muli richiudendosi su di loro" (Bottone, 1718; Anonimous, 1693).

Catania Plain: "..una grande spaccatura nel terreno dalla quale fuoriusc un getto di acqua

calda si formò in contrada botte d'aceto In particolare, in quel rione a cui diedero il nome i Siculi (Botte daceto), la terra si aprì in modo spropositato, della quale fenditura la larghezza misurava otto palmi, la lunghezza 25 passi e la profondità fu tale che alcuni contadini vi gettarono dei sassi, ma udirono un cupo strepito soltanto dopo lungo tempo. Da questa fenditura fuoriuscì una polla di acqua calda si osservò che ci era avvenuto in molti luoghi della pianura. E non lontano da qui si aprì una sola profonda voragine che inghiottì i mulattieri insieme alle mule" (Bottone, 1718).

Lentini: "..sgorgarono molte sorgenti in molti luoghi inconsueti e scaturirono getti di acqua sulfuree ribollenti....squarciature del suolo da cui vengono proiettate fuori terra e acqua che costruiscono al suolo piccoli monticelli. Nella via regia che, da Lentini conduce a Catania, una volta avvenuta la scossa, una grande voragine, apertasi al suolo, inghiottì nelle profonde fauci alcuni mulattieri e anche le mule" (Bottone, 1718).

Mascali: "...la terra si aprì emettendo liquidi bituminosi e zolfo, comparvero sorgenti d'acqua. Una grande fenditura si trasformò in una pozza in seguito alla fuoriuscita d'acqua frammista a zolfo e sabbia. Ai suoi confini la terra fu vista aprirsi rigurgitando bitume e zolfo, e in alcuni luoghi l'acqua sgorgare copiosamente. E degno di ammirazione ci che accadde nel luogo detto Lazzaretto:dopo il terremoto apparve una grande fenditura, che crebbe fino a diventare una pozza, dal momento che emetteva di continuo abbondante acqua mista a zolfo e sabbia. Nelle vicinanze di questa si osservarono alcune sorgenti dello stesso materiale e di non dissimile odore" (Bottone, 1718).

Melilli: "Nella Contrada di S. Cosimano vicino la terra di Mililli, dopo aperto in pi luoghi il terreno, si accesero le miniere di zolfo nell'atto del Terremoto" (Boccone, 1697).

Messina: "...fenditura apertasi sulla spiaggia di Messina dalla quale esalarono gas e fuoriuscirono fluidi; dopo un'ora la terra si aperse a Messina per tutta quanta la lunghezza del Teatro Grande, la profondit della quale apertura ignota, la larghezza mezzo palmo; da questa ribollendo fuoriusciva una esalazione; poi traboccando del materiale fluido invase ogni zona; si aprì una grande fenditura dalla quale esalavano gas e fuoriuscivano materiali fluidi" (Bottone, 1718).

Naso: "Descrizioni di liquefazione" (Romeo and Delfino, 1997).

Noto Antica: "...la terra si aprì in molti luoghi con lunghissime fenditure,dalle quali sgorgò

acqua con odore sulfureo..” (Romeo and Delfino, 1997).

Piazza Armerina: “..fu notata la fuoriuscita dal terreno di acqua mista a zolfo, cenere e bitume” (Del Bono, 1745).

Siracusa: “In vicinanza di Siracusa furono osservate molte polle d’acqua sorgente nel tempo del terremoto, che spillavano in alto vicino a quattro braccia, e ci da ampio forame, portando fuori arena ed acqua” (Boccone, 1697). Nel colle del divo Teodoro apparve una spaccatura di non misurabile profondità, e per tutta la sua superficie apparvero delle spaccature, dalle quali fuoriusciva una esalazione di zolfo, fenomeno questo che si osservò fuori le mura di Siracusa” (Bottone, 1718).

28.03.1783 (NE-Sicily)

Fiumedinisi: “the water gushing from the hill springs turned milky, agitated and strong-tasting “ (Gallo, 1784).

5.02.1783 (Calabria)

Ganzirri: “Aperture del terreno con fuoriuscita d'acqua” (Romeo and Delfino, 1997).

Messina: “Si aperse con lunghe fenditure il suolo, si abbassò in pi di un luogo il terreno” (Gallo, 1783). Anzi nello stesso suolo di Messina sono comparse in tutta la spiaggia del Porto non vulgari aperture anche nel terreno all’interno della città, nella Cittadella e nella fortezza del Salvatore si aprirono molte fenditure. La Terra parimenti nel smemorato luogo marittimo si veduta abbassare alquanto, talchè vi rimasta la Pescheria immersa tutta nell’onde” (Corrao, 1784).

Torre del Faro: “Ricordo a questo proposito che anche nel periodo sismico del 1783 si erano determinate nei pressi del Pantano delle fenditure, ed altre pure si sono aperte anche nel terremoto del 1894” (Baratta, 1910).

7.02.1783 (Calabria)

Messina: “Abbassamento del suolo nel porto.. nel suolo si aprirono fenditure dalle quali uscirono gas dall’odore di zolfo anche all’interno della Cittadella si aprirono molte fenditure” (Lallement, 1785).

26.04.1783 (Milazzo)

Messina: "Una fenditura lunga avere nella laterale superficie dell'una e l'altra parte rivoltata la terra, che parea espulsa del suo seno ed ammontata intorno" (Gallo, 1784).

20.02.1818 (**Catanese**)

Paraspolo: "Five or six minutes after the earthquake there suddenly sprang forth 14 jets of water, arising up to 6 palms (about 1,5m) creating considerable clamour."…the water emanated was salty" …."Paraspolo nel fondo del duca di Misterbianco detto Paraspolo non molto lungi dal Simeto era pure notabile una fenditura nel terreno non lunga pi di 6 palmi, e larga quattro dita traverse, che giungeva fino al cennato livello del mare" (Logo, 1818).

Paternò: "Aumento delle scaturigini di acque salse, presso di queste sgorgò acqua salsa e limacciosa e di odore di zolfo. Essa formò un rialto di terra conico alto 2 palmi" (Romeo and Delfino, 1997).

Ramondetta: Lquefactions occurrence (Longo, 1818).

11.01.1848 (Augusta)

Augusta: "Ad Augusta nella parte estrema del molo sotto il convento di S. Domenico, dalla parte di occidente, la terra si fendè in due punti e vomitò delle pietre e dell'acqua, che spruzzando per aria ricadeva su dei piccoli navili vicini" (Ferruggia Russo, 1852).

19.07.1865 (Area Etnea)

Scarronazzi: si verificarono fessurazioni e abbassamenti del suolo; venne notato un innalzamento termico anomalo del terreno di circa 6 gradi, che fu attribuito a esalazioni di gas dal sottosuolo (Grassi, 1865; Biblioteca Zelantea di Acireale, 1865).

16.11.1894 (S-Calabria)

Ganzirri: "Diverse fenditure si formarono nel terreno. Una serie di effetti furono infine riscontrati nel lago di Ganzirri (o Pantano Grande), dove dalle fenditure prodottesi in prossimità del lago stesso, e sul quale terminano, fuoriuscirono idrogeno solforato, fanghi

maleodoranti e infine vapore acqueo". "Apertura del terreno con fuoriuscita di fango e/o sabbia e/o ghiaia. Si dice che in prossimità delle fratture ed in prossimità delle acque del lago si aprì un foro da cui emanava vapore acqueo. La piccola banchina di pietra a SW e la piccola palizzata a sud sono state spinte verso il lago, e la terra attorno e contro di esse si abbassata fin di 0,4m; presso quel luogo si dice che il lago sia aumentato di profondità" (Riccò, 1907).

Torre del Faro: "Ricordo a questo proposito che anche nel periodo sismico del 1783 si erano determinate nei pressi del Pantano delle fenditure, ed altre pure si sono aperte anche nel terremoto del 1894" (Baratta, 1910).

2.11.1898 (Caltagirone)

C. Racineri: liquefactions (CEDIT catalogue).

28.12.1908 (Messina Strait)

Ganzirri: "Ricordo a questo proposito che anche nel periodo sismico del 1783 si erano determinate nei pressi del Pantano delle fenditure, ed altre pure si sono aperte anche nel terremoto del 1894". (Baratta, 1910). "Aperture nel terreno, formazione dei vulcanelli di fango" (Romeo and Delfino, 1997; Lo Giudice, 1909).

Messina: "Fenditure, avvallamenti e un generale scivolamento verso il mare si verificarono nelle banchine del porto e nelle zone adiacenti alla Marina; L'intera penisoletta falcata per compressione e assestamento dei materiali, in seguito al violentissimo fenomeno sismico ed al maremoto, si abbassò verso il centro la depressione raggiunse 40-5cm". "La lanterna del Forte S. Ranieri infine si sarebbe abbassata di m. 0,51. (Baratta, 1910); Presso il Lazzaretto la spiaggia appare abbassata in diversi punti di 5cm., e per tale abbassamento o per l'asportazione della sabbia causata dal maremoto, si formata una piccola insenatura di circa 10m. di saetta; Le banchine tutte intorno al porto si sono abbassate ed in parte franate…". "Anche in altri punti vi fu abbassamento della costa" (Platania, 1909; Sauret and Bosquè, 1984).

Torre del Faro: "Presso il faro antico vi un abbassamento progressivo attuale del suolo, indicato dallo scalzamento operato dal mare alla base della torre del faro ed ai muri di cinta.

Nella strada che da Faro Inferiore conduce a Granatari si trova, specie verso il Pantano, una fenditura longitudinale ed altre pi o meno estese con abbassamento di circa 7cm.i muri pendono tutti verso l'interno, cioè verso S-W... La strada presso il Pantano si sprofondata oppure pi o meno affondata qua e là si sono prodotte fenditure da cui sprizzata una melma con spiccato odore di idrogeno solforoso". "Ricordo a questo proposito che anche nel periodo sismico del 1783 si erano determinate nei pressi del Pantano delle fenditure, ed altre pure si sono aperte anche nel terremoto del 1894" (Platania, 1909; Baratta, 1910).

15.01.1968-01 (Belice)

Contessa Entellina: "In seguito ai terremoti si osservarono fenomeni di liquificazione a Contessa Entellina" (L'Ora, 1968a; Bosi et al., 1973).

15.01.1968-02 (Belice)

Camporeale: "In seguito ai terremoti si osservarono fenomeni di liquificazione e l'apertura di fenditure nei pressi di Camporeale. Dai vulcanetti di fango fuoriuscirono anche sostanze gassose accumulatesi in occasione di vecchi movimenti franosi" (Giornale di Sicilia, 1968a; Giornale di Sicilia, 1968b; La Stampa, 1968c; Bosi et al., 1973; Corriere della Sera, 1968b; Corriere della sera, 1968c).

Contessa Entellina: "In seguito ai terremoti si osservarono fenomeni di liquificazione a Contessa Entellina" (L'Ora, 1968a; Bosi et al., 1973).

Bisaquino: "In seguito ai terremoti si osservarono fenomeni di liquificazione a Bisaquino" (Bosi et al., 1973).

Marsala: "In contrada Ventrischi, nei pressi di Marsala, in seguito alla forte replica del 25 gennaio si aprì una voragine profonda 20m dalla quale fuoriuscivano gas" (La stampa 1968b).

Portanna: "In seguito ai terremoti si osservarono fenomeni di liquificazine in località Timpone Perollo posta a qualche chilometro a sud-est dell'abitato di Partanna" (Bosi et al., 1973).

Sciacca: "In contrada Campo dei Tiri, in occasione della violenta replica del 25 gennaio 1968, si aprirono delle fenditure dalle quali fuoriuscirono vapori sulfurei" (Corriere della

sera, 1968d).

13.12.1990 (Augusta)

Augusta: "In seguito al terremoto furono osservate fessure nell'asfalto nel piazzale Fontana.. secondo una prevalente direzione N-S; nello stesso luogo fu osservata la risalita di fluidi probabilmente dovuta a processi di liquefazione dei materiali utilizzati per la bonifica delle antiche saline, mentre, all'interno dello stadio, si verificò l'affioramento di larghe chiazze di pirite attraverso la formazione di minuscoli vulcanetti" (De Rubeis et al., 1993).

Hydrological anomalies

6.07.1125 (Siracusa)

Siracusa: "Nell' acqua della sorgente Aretusa ci furono infiltrazioni di acqua salata" (Di Poitou, 1882).

4.02.1169 (E-Sicily)

Catania Plain: "Esondazioni nei pressi della foce del fiume Simeto" (Sciuto, 1931; Amico, 1733).

Siracusa: "Variazioni nella portata d'acqua, sapore e nel colore della fonte Aretusa di Siracusa. La fonte Aretusa divenne salmastra per la commistione con l'acqua del mare" (Falcando, XII cent.).

25.08.1613 (Naso)

Naso: "Le acque videro.. le fontane dare acque torbide e limacciose" (Incudine, 1882).

3.10.1624 (Mineo)

Palagonia: "Nei pressi dell'abitato a causa della scossa sgorgò una sorgente di acqua calda e sulfurea" (Mongitore, 1743).

9/11.1.1693 (E-Sicily)

Nuovi invasi d'acqua, originati dall'ostruzione di fiumi e torrenti a causa di frane e smottamenti, vennero segnalati lungo il corso del fiume Irminio (Modica- Ragusa e lungo la via da Noto a Siracusa)" (CFTI97, Boschi et al, 1997).

Catania Plain: "..si dice, che da una di queste aperture lunghissime e distante da mare 4 miglia, e più avesse salito l'acqua falda appunto, come la stessa del mare" (Boccone, 1697).

Cassaro: "S'accozzarono rupi ad impedire il corso dei fiumi come vedemmo sotto la terra del Cassaro" (Aprile, 1725; Bottone, 1718). "Poco distante dalla terra del Cassaro, da due punte, nelle estremità di due Monti, in mezzo dè quali per una lunga Valle correva un fiume, si spiccarono due grandissime rupi, che precipitando dall'erto, andarono egualmente a portare nella bocca della Cava, della Valle fino a pareggiare l'altezza delle precipitate rupi, per dove sgorgando, lasciarono un Lago di giro tre miglia, e di profondità confiderabile (Boccone, 1695). Non lungi della contea di Cassaro, due gran massi furono staccati dalla cima di due montagne che formavano una lunga valle, in cui scorrea un fiume venendosi ad incontrare nella valle, l'hanno chiusa, ed hanno fermato il corso del fiume che ..ha empito la valle ..formando un lago di tre miglia di circuito" (Bonaiuti, 1793).

Ferla-Cassaro: "Tra Ferla e Cassaro due colline separate da un affluente dell'Anapo franarono ostruendo il corso d'acqua e originando così una palude profonda e navigabile" (Bottone, 1718).

Ispica: "Il lago esistente nei pressi della cava grande nel territorio di Spaccarono (l'attuale Ispica) si disseccò il giorno del terremoto e rimase asciutto fino al febbraio del 1700" (CFTI97, Boschi et al., 1997).

Lentini: "…scaturivano sorgenti di zolfo e di acque calde ribollenti e bituminose in luoghi inconsueti sorgevano nuove fonti, la terra si apriva si vedevano i fiumi deviare il loro corso sgorgando in pi rivi." (Bottone, 1718).

Mascali: "..comparvero alcune sorgenti d'acqua; sul litorale le fonti subirono variazioni di portata e le acque aumentarono di temperatura" (Bottone, 1718).

Modica- Ragusa: "..nuovi invasi d'acqua, originati dall'ostruzione di fiumi e torrenti a causa di frane e smottamenti...lungo il corso del fiume Irminio (tra Modica e Ragusa) e lungo la via da Noto a Siracusa" (Bottone, 1718).

Noto antica: “Nella alture circostanti la città (Noto antica) si aprirono spaccature dalle quali si distaccarono enormi massi comparvero nuove sorgenti con getti di acqua calda e sulfurea” (Bottone, 1718).

Noto- Siracusa: “Lungo la via da Noto a Siracusa si formò un lago causa dello sgorgare di una nuova vena d’acqua, fuoriuscì una vena d’acqua e fu deviato il corso dei fiumi che sgorgano” (Bottone, 1718).

Ragusa: “Dal momento che si aprì la terra e vennero meno gli alvei delle acque, emersero nuovi stagni vicino al fiume di Ragusa; Vicino al fiume di Ragusa (fiume Irminio), dove una grande quantità di terra crollò dopo aver abbattuto spessi alberi per il pezzo che scendeva a valle, e qui si formò un lago di tale ampiezza, che era accessibile alle navi” (Bottone, 1718).

Siracusa: “..la Piazza d’arme non solamente si aprì, e si chiuse nel tempo di questo horribile Terremoto, ma ancora da tre voragini venne fuori acqua salata di mare; In Siracusa in molti pozzi che avevano l’acqua salsa divenne dolce senza che fin’oggi avesse mutato di qualità; Il fonte Aretusa per alcune settimane mandò le sue acque tanto salmastre che li cittadini non se ne poterono fruire, e ora, che sono addolcite, restando alquanto salate, per assai pi abbondanti” (Boccone, 1697). “Fu notato il raddoppio della portata della famosa fonte Aretusa, che per alcuni mesi dopo il sisma fu notevolmente pi salina del solito” (Del Bono, 1745). “..raddoppio della portata della famosa fonte Aretusa che per alcuni fu pi salina del solito” (Del Bono, 1745). “Lungo la via per Siracusa, si formò un lago a causa dello sgorgare di una nuova vena dacquaa e alla deviazione del corso di un fiume non identificato” (Bottone, 1718).

Sortino: “..fu notata la colorazione rossastra di sorgenti” (Bonaiuti, 1793).

Spaccaforno: “Il lago esistente nei pressi della Cava Grande si dissecc il giorno del terremoto e rimase asciutto fino al febbraio del 1700, quando ricomparvero le acque” (Franzò, 1931).

Termini Imprese: “Le acque correnti scomparvero e quelle delle terme accrebbero di un terzo le portata” (Bonaiuti 1793; Gallo 1823).

Vizzini: “scomparvero sorgenti e si aprirono fenditure nel terreno tra Vizzini e Monterosso Almo” (Naselli, 1931).

Vizzini e Monterosso Almo: “Scomparvero sorgenti e si aprirono fenditure nel terreno tra Vizzini e Monterosso Almo” (Naselli, 1931).

22.04.1717 (Castroreale)

Castroreale: “Sul litoraletre miglia dalla città, in una zona gi ricca di acque termali, si formarono nuove sorgenti di acqua calda furono osservate esalazioni gassose dal terreno” (Bottone, 1718).

10.05.173 (Naso)

Naso: “..sparirono antiche sorgenti e se ne formarono di nuove, in altre sorgenti le acque si intorbidirono” (Incudine, 1882; Rezzadore, 1914).

5.03.1823 (N-Sicilia)

Termini Imerese: “le acque termali e quelle dei pozzi vicini crebbero di portata, divennero fangose a causa del movimento subito. Il livello delle acque termali crebbe di quattro volte e anche la temperatura aumentò di quattro gradi Reaumur” (Ferrara, 1823; Archivio di Stato, 1823).

Ogliastro: “Le frane costrinsero l’acque del torrente a cambiare corso” (Archivio di Stato di Palermo, 1823).

16.11.1894 (S-Calabria)

Barcellona P.G.: “In molti pozzi diminuì l’acqua” (Riccò, 1907).

31.10.1967 (Nebrodi)

Nicosia: “..improvviso aumento della capacità delle sorgenti di acqua potabile” (ANSA, 1967).

15.01.1968- 01 (Belice)

Ghibellina: “..gli abitanti segnalarono la mutazione delle qualità organolettiche di alcune sorgenti di acque potabili che in seguito ai terremoti, assunsero odore e sapore sulfurei;

nuove sorgenti di acque sulfuree scaturirono, dopo le scosse più intense" (Bosi et al., 1973).

15.01.1968- 02 (Belice)

Ghibellina: "..gli abitanti segnalarono la mutazione delle qualità organolettiche di alcune sorgenti di acque potabili che in seguito ai terremoti, assunsero odore e sapore sulfurei; nuove sorgenti di acque sulfuree scaturirono, dopo le scosse più intense" (Bosi et al., 1973).
Terme Segesta: "…in seguito ai terremoti nelle vicinanze delle Terme Segestane comparvero nuove sorgenti calde, alcune delle quali ebbero durata effimera; due sorgenti preesistenti aumentarono la loro portata" (Bosi et al., 1973).

13.12.1990 (SE-Sicily)

Brucoli: "..nella zona del canale di Brucoli fu osservata l'apertura di una sorgente di acqua sulfurea da decenni inattiva" (Appunti sugli effetti, 1990).

26.06.1993 (Pollina)

Pollina: seismogeological effects such as changes in spring flows and rockfalls, also occurred in this area" (Azzaro and Barbano, 1995).

6.09.2002 (Palermo)

Termini Imerese: change in the well water level and springs that had dried up in the last decades were observed to flow again, increasing in the water temperature from 41.3 to 43.6° C (Grassa et al., 2006).

Earthquake parametres											Recorded effect: landslides						
N	Year	Month	Day	Epicentral area	Rt	Lat	Long	Io	Maw	Mas	Site	Lat (s)	Long (s)	Is(MCS)	Re (km)	Observed effect	Historical source
1	1169	2	4	E-Sicily	CFTI	37,32	15,03	10	6,60	6,60	Aci antica	37,612	15,165	10	33,53	A	Biblioteca Zelantea di Acireale (1835b)
2	1169	2	4	E-Sicily	CFTI	37,32	15,03	10	6,60	6,60	Lentini	37,284	14,998	10	5,38	A	Marangone (1866)
3	1169	2	4	E-Sicily	CFTI	37,32	15,03	10	6,60	6,60	Mongibello	37,754	14,995	n.p.	45,70	A2	Aprile (1725); Biblioteca Zelantea di Acireale (1835b)
4	1542	12	10	SE-Sicily	CFTI	37,22	14,95	10	6,62	6,62	Lentini	37,284	14,998	9; 10	6,91	A	Bonito (1691); Fazello (1628)
5	1542	12	10	SE-Sicily	CFTI	37,22	14,95	10	6,62	6,62	Licodia	37,160	14,705	7; 8	24,37	A	Bonito (1691)
6	1542	12	10	SE-Sicily	CFTI	37,22	14,95	10	6,62	6,62	Scicli	36,791	14,701	n.p.	52,26	A2	CFTI (2000)
7	1542	12	10	SE-Sicily	CFTI	37,22	14,95	10	6,62	6,62	Sortino	37,156	15,027	9	9,92	A2	Bonito (1691)
8	1542	12	10	SE-Sicily	CFTI	37,22	14,95	10	6,62	6,62	Vizzini	37,161	14,751	8; 9	19,55	A	Bonito (1691)
9	1613	8	25	Naso	CFTI	38,12	14,78	8	5,57	5,40	Naso	38,120	14,790	9	1,50	A	Incudine (1882)
10	1693	1	11	E-Sicily	CFTI	37,13	15,02	11	7,41	7,41	Augusta	37,221	15,221	10	21,07	A2	Bottone (1718)
11	1693	1	11	E-Sicily	CFTI	37,13	15,02	11	7,41	7,41	Cassaro	37,106	14,948	10; 11	9,19	A2; A-D; A-D1	Aprile (1725); Boccone (1697); Bonaiuti (1793); Bottone (1718)
12	1693	1	11	E-Sicily	CFTI	37,13	15,02	11	7,41	7,41	Ferla -Cassaro	37,111	14,944	10; 11	7,10	A-D1	Bottone (1718)
13	1693	1	11	E-Sicily	CFTI	37,13	15,02	11	7,41	7,41	Ibla	36,926	14,743	n.p.	33,92	A	Bottone (1718)
14	1693	1	11	E-Sicily	CFTI	37,13	15,02	11	7,41	7,41	Lentini	37,284	14,998	10; 11	17,33	A	Bottone (1718)
15	1693	1	11	E-Sicily	CFTI	37,13	15,02	11	7,41	7,41	Militello	37,275	14,794	7	24,66	A2	Bottone (1718)
16	1693	1	11	E-Sicily	CFTI	37,13	15,02	11	7,41	7,41	Modica- Ragusa	36,879	14,743	10	36,96	A1; A-D1	Bottone (1718)
17	1693	1	11	E-Sicily	CFTI	37,13	15,02	11	7,41	7,41	Mongibello	37,754	14,995	n.p.	70,68	A	Boccone (1697)
18	1693	1	11	E-Sicily	CFTI	37,13	15,02	11	7,41	7,41	Noto	36,890	15,070	n.p.	29,84	A	Boccone (1697); Bottone(1718)
19	1693	1	11	E-Sicily	CFTI	37,13	15,02	11	7,41	7,41	Noto Antica	36,940	15,023	10; 11	21,06	A1;A2	Bottone (1718)
20	1693	1	11	E-Sicily	CFTI	37,13	15,02	11	7,41	7,41	Noto- Scala di Militello	36,899	15,067	n.p.	26,67	A1	(Romeo and Delfino, 1997)
21	1693	1	11	E-Sicily	CFTI	37,13	15,02	11	7,41	7,41	Noto-Siracusa	37,003	15,029	9	14,02	A; A-D1	Bottone (1718)
22	1693	1	11	E-Sicily	CFTI	37,13	15,02	11	7,41	7,41	Paternò	37,566	14,902	8; 9	49,70	A	Bottone (1718)
23	1693	1	11	E-Sicily	CFTI	37,13	15,02	11	7,41	7,41	Ragusa	36,926	14,727	10	36,53	A-D1	Bottone (1718)
24	1693	1	11	E-Sicily	CFTI	37,13	15,02	11	7,41	7,41	Sortino	37,156	15,027	11	2,96	A2	Boccone (1697); Bonaiuti (1793);Compendio delle Trasn azioni Filosofiche (1793)
25	1693	1	11	E-Sicily	CFTI	37,13	15,02	11	7,41	7,41	Val di Noto	37,070	15,000	n.p.	6,90	A	Bottone (1718)
26	1739	5	10	Naso	CFTI	38,10	14,75	8	5,54	5,35	Naso	38,120	14,790	8; 9	3,70	A2	Incudine (1882)
27	1739	5	10	Naso	CFTI	38,10	14,75	8	5,54	5,35	San Marco d'Alunzio	38,070	14,690	8	6,33	A2	Mongitore (1743)
28	1783	2	5	Calabria	CFTI	38,30	15,97	11	6,91	6,91	Messina	38,187	15,549	8	40,51	~~A~~	Relazione istorico-fisica (1783); Gallo (1783); Gallo (1784); Torcia (1784)
29	1783	2	5	Calabria	CFTI	38,30	15,97	11	6,91	6,91	Naso	38,122	14,788	8; 9	106,65	~~k~~	Romeo and Delfino (1997)

30	1783	2	5	Calabria	CFTI	38,30	15,97	11	6,91	6,91	Rometta	38,170	15,410	8	52,60	~~A~~	Corrao (1784)
31	1783	4	26	Milazzo	CFTI	38,20	15,40	5,0	4,20	-	Messina	38,187	15,549	N.R.	13,71	A	Corrao (1784)
32	1819	2	24	Madonie	CFTI	37,93	14,05	7,5	5,40	5,40	Collesano	37,919	13,933	7; 8	16,06	A; A1	Scinà (1819); Mazzarella (1988)
33	1819	2	24	Madonie	CFTI	37,93	14,05	7,5	5,40	5,40	Geraci Siculo	37,860	14,153	7; 8	6,90	A2	Scinà (1819); Mazzarella (1988)
34	1819	2	24	Madonie	CFTI	37,93	14,05	7,5	5,40	5,40	Isnello	37,994	14,006	7; 8	4,16	A	Scinà (1819)
35	1823	3	5	N Sicily	CFTI	38,00	14,10	8,5	5,87	5,84	Caltanissetta	37,490	14,063	5	56,56	A	(CFT04)
36	1823	3	5	N Sicily	CFTI	38,00	14,10	8,5	5,87	5,84	Collesano	37,921	13,938	7; 8	16,77	A	Ferrara (1823)
37	1823	3	5	N Sicily	CFTI	38,00	14,10	8,5	5,87	5,84	Gordano	37,902	13,429	7; 8	30,85	A2	Ferrara (1823); Archivio di stato di Palermo (1823)
38	1823	3	5	N Sicily	CFTI	38,00	14,10	8,5	5,87	5,84	Naso	38,122	14,788	8; 9	62,07	A	Ferrara (1823)
39	1823	3	5	N Sicily	CFTI	38,00	14,10	8,5	5,87	5,84	Ogliastro	37,964	13,456	n.p.	90,14	A; A-D	Archivio di Stato di Palermo (1823)
40	1865	7	19	Etnean area	CFTI	37,70	15,15	90	5,03	4,59	Moscarello	37,715	15,14	8	1,62	A	Silvestri 1865
41	1879	6	17	Etnean area	CFTI	37,68	15,15	9	5,06	4,64	Fondo Macchia	37,717	15,167	5	4,29	A1	Romeo and Delfino (1997)
42	1879	6	17	Etnean area	CFTI	37,68	15,15	9	5,06	4,64	Giarre	37,726	15,183	5	4,95	A1	Romeo and Delfino (1997)
43	1879	6	17	Etnean area	CFTI	37,68	15,15	9	5,06	4,64	Moscarello	37,714	15,139	n.p.	3,73	A1	Romeo and Delfino (1997)
44	1879	6	17	Etnean area	CFTI	37,68	15,15	9	5,06	4,64	Riposto	37,731	15,203	4; 5	6,51	A1	Romeo and Delfino (1997)
45	1893	4	22	M. Elicona	DOM	38,02	15,02	7,0	5,03	4,60	S. Piero Patti	38,051	14,967	6; 7	5,25	A	(Riccò, 1893)
46	1894	8	8	Etnean area	CFTI	37,65	15,12	9,5	5,30	5,30	Mazzasette	37,650	15,124	9; 10	0,32	A	Patanè (1992)
47	1894	8	8	Etnean area	CFTI	37,65	15,12	9,5	5,30	5,30	Monterosso	37,651	15,097	8	2,71	A	Giornale di Sicilia (1894)
48	1894	8	8	Etnean area	CFTI	37,65	15,12	9,5	5,30	5,30	Zerbate	37,638	15,121	9	1,30	A	La Tribuna (1894)
49	1908	12	28	S-Calabria	CFTI	38,15	15,68	11	7,24	7,24	Caltanissetta	37,489	14,063	n.p.	161,78	A	Baratta (1910)
50	1908	12	28	S-Calabria	CFTI	38,15	15,68	11	7,24	7,24	Fiumara della Guardia	38,255	15,603	8; 9	12,50	A1	Baratta (1910)
51	1908	12	28	S-Calabria	CFTI	38,15	15,68	11	7,24	7,24	Fiumara Pace	38,255	15,603	10; 11	12,00	A1	Baratta (1910)
52	1908	12	28	S-Calabria	CFTI	38,15	15,68	11	7,24	7,24	Messina	38,187	15,549	10; 11	11,59	A	Baratta (1910)
53	1908	12	28	S-Calabria	CFTI	38,15	15,68	11	7,24	7,24	S.Agata	38,255	15,603	10; 11	12,88	A1	Baratta (1910)
54	1908	12	28	S-Calabria	CFTI	38,15	15,68	11	7,24	7,24	Pietraperzia	37,421	14,138	6; 7	157,46	A	Baratta (1910)
55	1911	10	15	Etnean area	CFTI	37,70	15,15	10	5,28	4,96	Giarre	37,726	15,183	5	3,77	A	Romeo and Delfino (1997)
56	1914	5	8	Etnean area	CFTI	37,67	15,13	9	5,30	5,00	La Timpa	37,604	15,171	N.R.	8,32	A2	Romeo and Delfino (1997)
57	1914	5	8	Etnean area	CFTI	37,67	15,13	9	5,30	5,00	Passopomo	37,691	15,108	10	2,91	A2	Romeo and Delfino (1997)

58	1914	5	8	Etnean area	CFTI	37,67	15,13	9	5,30	5,00	Pisano	37,664	15,109	7; 8	2,13	A2	Romeo and Delfino (1997)
59	1914	5	13	Randazzo	POS85	37,88	14,95	6	4,83	4,30	Passopomo	37,675	15,119	N.R.	8,3	A2	Cavasino (1935), Platania (1916), Ghersi et al. (1914), Sabatini (1914).
60	1925	7	6	Giarre	POS85	37,68	15,10	5,5	4,26	3,45	Acireale	37,612	15,165	N.R.	9,56	A2	Romeo and Delfino (1997)
61	1925	7	6	Giarre	POS85	37,68	15,10	5,5	4,26	3,45	Fondo Macchia	37,717	15,167	N.R.	7,18	A; A2; A-D	Romeo and Delfino (1997)
62	1967	10	31	Nebrodi	CFTI	37,87	14,42	8,0	5,5	5,29	Mistretta	37,930	14,363	8	8,38	A2	ANSA (1967)
63	1968	1	15	Belice	CFTI	37,77	13,00	8	5,6	5,4	Ghibellina	37,79	12,976	10	4,22	A2	Corriere della sera, 1968.01.16, a. 93, n.13
64	1968	1	15	Belice	CFTI	37,77	13,00	8	5,6	5,4	Montevago	37,703	12,983	10	7,53	A2	Bosi et al. (1973)
65	1968	1	15	Belice	CFTI	37,77	13,00	8	5,6	5,4	S. Margherita	37,692	13,023	9	9,06	A2	Bosi et al. (1973)
66	1968	1	15	Belice	CFTI	37,77	12,98	10	6,4	5,9	Ghibellina	37,79	12,976	10	4,22	A2	Corriere della sera, 196801.16, a.
67	1968	1	15	Belice	CFTI	37,77	12,98	10	6,4	5,9	Marinero	37,951	13,415	7	42,74	A	L'Ora,1968. 01. 19/20, a.69,n.16
68	1968	1	15	Belice	CFTI	37,77	12,98	10	6,4	5,9	Montevago	37,703	12,983	10	7,53	A2	Bosi et al. (1973)
69	1968	1	15	Belice	CFTI	37,77	12,98	10	6,4	5,9	Sambuca di Sicilia	37,648	13,111	7; 8	16,4	A	La Stampa, 1968.01.18
70	1968	1	15	Belice	CFTI	37,77	12,98	10	6,4	5,9	Santa Margherita	37,692	13,023	9	9,06	A2	Bosi et al. (1973)
71	1978	4	15	Patti Gulf	CFTI	38,15	14,98	9	6,06	6,06	Alcara Li Fusi	38,022	14,700	7	28,21	A; A2	Giornale di Sicilia (1978)a;Giornale di Sicilia (1978)b; Barbano et al. (1979)
72	1978	4	15	Patti Gulf	CFTI	38,15	14,98	9	6,06	6,06	Gioiosa Marea	38,174	14,896	7; 8	8,22	A2	Giornale di Sicilia (1978)b
73	1978	4	15	Patti Gulf	CFTI	38,15	14,98	9	6,06	6,06	Longi	38,028	14,753	7	24,17	A-B	Giornale di Sicilia (1978)a
74	1978	4	15	Patti Gulf	CFTI	38,15	14,98	9	6,06	6,06	Militello Rosmarino	38,045	14,676	7	29,88	A2	Giornale di Sicilia (1978)a
75	1990	12	13	SE-Sicily	CFTI	37,27	15,12	7	5,68	5,26	Brucoli	37,283	15,187	5; 6	5,81	A1; A2	De Rubeis et al. (1993)
76	1990	12	13	SE-Sicily	CFTI	37,27	15,12	7	5,68	5,26	Ispica	36,786	14,910	6	58,34	A2	La Sicilia (1990)
77	1990	12	13	SE-Sicily	CFTI	37,27	15,12	7	5,68	5,26	Palagonia	37,326	14,746	6	34,09	A	De Rubeis et al. (1993)
78	1993	6	26	Pollina	CFTI	37,99	14,14	7	4,70	-	Pollina	37,99	14,14	7	1,00	A2	Azzaro and Barbano (1995)
79	2002	6	9	S-Tyrrhenian Sea	Azz**	38,08	13,42	6	5,6	5	Cerda	37,918	13,799	5	39,71	A	Azzaro et al. (2004)

Earthquake parametres											Recorded effect: ground deformations						
N	Year	Month	Day	Epicentral area	Rt	Lat	Long	Io	Maw	Mas	Site	Lat (s)	Long (s)	Re (km)	Is (MCS)	Observed effect	Historical source
1	1613	8	25	Naso	CFTI	38,120	14,780	8,0	5,57	5,40	Naso	38,120	14,790	1,50	9	B1	Mongitore (1743); Incudine (1882)
2	1693	1	11	E-Sicily	CFTI	37,130	15,020	11,0	7,41	7,41	Augusta	37,221	15,221	21,07	10	B1-C	Romeo and Delfino (1997)
3	1693	1	11	E-Sicily	CFTI	37,130	15,020	11,0	7,41	7,41	Calatafimi	37,922	12,855	210,01	N.R.	B1	Boccone (1697)
4	1693	1	11	E-Sicily	CFTI	37,130	15,020	11,0	7,41	7,41	Caltanissetta	37,490	14,063	88,86	n.p.	B1	Bottone (1718)
5	1693	1	11	E-Sicily	CFTI	37,130	15,020	11,0	7,41	7,41	Catania	37.502	15.087	40,00	10; 11	B1*	Bottone (1718); Romeo and Delfino (1997)
6	1693	1	11	E-Sicily	CFTI	37,130	15,020	11,0	7,41	7,41	Lentini	37.284	14.998	0,73	10; 11	B1; B2-C	Bottone (1718)
7	1693	1	11	E-Sicily	CFTI	37,130	15,020	11,0	7,41	7,41	Melilli	37,180	15,120	11,89	11	B1	Boccone (1697)
8	1693	1	11	E-Sicily	CFTI	37,130	15,020	11,0	7,41	7,41	Mineo	37,266	14,690	32,83	10; 11	B1	Boccone (1697); Del Bono (1745)*
9	1693	1	11	E-Sicily	CFTI	37,130	15,020	11,0	7,41	7,41	Noto	36,890	15,070	29,84	n.p.	B1; B3	Boccone (1697)
10	1693	1	11	E-Sicily	CFTI	37,130	15,020	11,0	7,41	7,41	Noto Antica	36,940	15,023	21,06	10; 11	B1*	Boccone (1697); Bottone (1718); Del Bono (1745)*; Bonaiuti (1739)
11	1693	1	11	E-Sicily	CFTI	37,130	15,020	11,0	7,41	7,41	Noto- Scala di Militello	36,899	15,067	26,67	n.p.	B; B1; B3	Boccone (1697); Del Bono (1745)
12	1693	1	11	E-Sicily	CFTI	37,130	15,020	11,0	7,41	7,41	Paternò	37,566	14,902	49,70	8; 9	B3*	Bottone (1718)
13	1693	1	11	E-Sicily	CFTI	37,130	15,020	11,0	7,41	7,41	Siracusa	37.082	15.285	24,43	9	B1	Boccone (1697); Del Bono (1745); Romeo and Delfino (1997)
14	1693	1	11	E-Sicily	CFTI	37,130	15,020	11,0	7,41	7,41	Sortino	37,156	15,027	2,96	11	B1; B2; B3	Boccone (1697); Bonaiuti (1793)
15	1693	1	11	E-Sicily	CFTI	37,130	15,020	11,0	7,41	7,41	Val di Noto	37.070	15.000	6,90	n.p.	B2	Boccone (1697)
16	1693	1	11	E-Sicily	CFTI	37,130	15,020	11,0	7,41	7,41	Vizzini-Monterosso Almo	37,120	14,755	23,76	10; 11	B1	Naselli (1931)
17	1739	5	10	Naso	CFTI	38,100	14,750	8,0	5,54	5,35	Naso	38,122	14,788	1,30	8; 9	B1	Bottone (1718)
18	1739	5	10	Naso	CFTI	38,100	14,750	8,0	5,54	5,35	S. Marco d'Alunzio	38,070	14,690	6,33	8	B1	Mongitore (1743)
19	1783	2	5	Calabria	CFTI	38,300	15,970	11,0	6,91	6,91	Ganzirri	38.258	15.611	31.66	n.p.	B1	Baratta (1910)
20	1783	2	5	Calabria	CFTI	38,300	15,970	11,0	6,91	6,91	Messina	38,187	15,549	40,51	8	B1; B2; B3	Relazione istorico-fisica (1783); Corrao (1784); Gallo (1784-83?)
21	1783	2	5	Calabria	CFTI	38,300	15,970	11,0	6,91	6,91	Torre Faro	38,266	15,646	29,12	n.p.	B1; B1-C	Baratta (1910)
23	1783	2	7	Calabria	CFTI	38,580	16,200	10,5	6,59	6,59	Messina	38,187	15,549	70,25	8	B1; B2; B1-C	Lallement (1785)
24	1783	4	26	Milazzo	CFTI	38,200	15,400	5,0	4,20		Messina	38,187	15,549	13,71	N.R.	B1	Corrao (1784)
22	1818	2	20	Catania	CFTI	37,60	15,13	9	6,00	6,00	Paraspolo	37.400	15.080	22,68	n.p.	B1	Longo (1818)
25	1823	3	5	N-Sicily	CFTI	38,000	14,100	8,5	5,87	5,84	Caltanissetta	37,49	14,057	56,93	5	B1	(CFT04)
26	1823	3	5	N-Sicily	CFTI	38,000	14,100	8,5	5,87	5,84	Librizzi	38,096	14,958	76,35	7	B1	Archivio di stato di Palermo (1823)
27	1823	3	5	N-Sicily	CFTI	38,000	14,100	8,5	5,87	5,84	Naso	38,122	14,788	62,12	8; 9	B1	Ferrara (1823)

28	1823	3	5	N-Sicily	CFTI	38,000	14,100	8,5	5,87	5,84	Ogliastro	37,964	13,456	90,14	n.p.	B3	Archivio di Stato di Palermo (1823)
29	1848	1	11	Augusta	DOM	37,370	15,150	8,0	5,48	5,26	Augusta	37,231	15,221	0,68	8; 9	B1*	Ferruggia Russo (1852)*
30	1865	7	19	Etnean area	CFTI	37,700	15,150	9,0	5,03	4,59	Scarronazzi	37,684	15,158	9,75	8; 9	B1-C	Grassi (1865); Biblioteca Zelantea di Acireale (1865)
31	1893	4	22	M. Elicona	DOM	38,020	15,015	7,0	5,03	4,60	S. Piero Patti	38,051	14,967	5,25	6; 7	B1*	(Riccò, 1893)
32	1894	11	16	S-Calabria	CFTI	38,280	15,870	9,0	6,05	6,05	Barcellona P.G.	38,146	15,215	58,50	7	B1*	Riccò (1907)
33	1894	11	16	S-Calabria	CFTI	38,280	15,870	9,0	6,05	6,05	Ganzirri	38,248	15,603	22,00	n.p.	B1; B2	Riccò (1907)
34	1894	11	16	S-Calabria	CFTI	38,280	15,870	9,0	6,05	6,05	Messina	38,187	15,529	31,41	7	B2; B3	Riccò (1907)
35	1894	11	16	S-Calabria	CFTI	38,280	15,870	9,0	6,05	6,05	Torre Faro	38,266	15,646	19,50	7	B2*	Riccò (1907)
36	1908	12	28	S-Calabria	CFTI	38,150	15,680	11,0	7,24	7,24	Caltanissetta	37,490	14,063	161,78	n.p.	B1	Baratta (1910)
37	1908	12	28	S-Calabria	CFTI	38,150	15,680	11,0	7,24	7,24	Ganzirri	38,248	15,611	13,49	9	B2*	Lo Giudice (1909)*; Baratta (1910)
38	1908	12	28	S-Calabria	CFTI	38,150	15,680	11,0	7,24	7,24	Messina	38,187	15,549	11,59	10; 11	B1; B2	Franchi (1909); Platania (1909); Baratta (1910)
39	1908	12	28	S-Calabria	CFTI	38,150	15,680	11,0	7,24	7,24	Pietraperzia	37,419	14,137	159,32	6; 7	B1; B3	Baratta (1910)
40	1908	12	28	S-Calabria	CFTI	38,150	15,680	11,0	7,24	7,24	Raddusa	37,473	14,534	126,90	6	B1	Baratta (1910)
41	1908	12	28	S-Calabria	CFTI	38,150	15,680	11,0	7,24	7,24	Torre Faro	38,266	15,646	13,27	10	B1*;B2*; B3*	Baratta (1910); Platania (1909)
42	1967	10	31	Nebrodi	CFTI	37,870	14,420	8,0	5,5	5,29	Nicosia	37,748	14,399	13,42	8	B3	Corriere della Sera (1967)
43	1968	1	15	Belice	CFTI	37,770	13,000	8,0	5,6	5,40	Ghibellina	37,79	12,976	4,22	10	B1	Corriere della sera (1968, n.14)
44	1968	1	15	Belice	CFTI	37,770	13,000	8,0	5,6	5,40	Montevago	37,703	12,983	7,53	10	B1; B2	Bosi et al. (1973)
45	1968	1	15	Belice	CFTI	37,770	13,000	8,0	5,6	5,40	Santa Margherita	37,692	13,023	9,06	9	B1; B2	Bosi et al. (1973)
46	1968	1	15	Belice	CFTI	37,770	13,000	8,0	5,6	5,40	Sciacca	37,508	13,083	30,06	7	B1-C	Corriere della sera, 1968, 01.27, a. 93, n. 23
47	1968	1	15	Belice	CFTI	37,770	12,980	10,0	6,4	5,9	Ghibellina	37,79	12,976	4,22	10	B1	1968.01.17, a. 93, n.14
48	1968	1	15	Belice	CFTI	37,770	12,980	10,0	6,4	5,9	Marsala	37,8	12,439	47,38	7	B1-C	La stampa (1968)
49	1968	1	15	Belice	CFTI	37,770	12,980	10,0	6,4	5,9	Montevago	37,703	12,983	7,53	10	B1; B2	Bosi et al. (1973)
50	1968	1	15	Belice	CFTI	37,770	12,980	10,0	6,4	5,9	Santa Margherita	37,692	13,023	9,06	9	B1; B2	Bosi et al. (1973)
51	1968	1	15	Belice	CFTI	37,770	12,980	10,0	6,4	5,9	Sciacca	37,508	13,083	30,06	7	B1-C	Corriere della sera (1968)
52	1978	4	15	Patti Gulf	CFTI	38,150	14,980	9,0	6,06	6,06	Longi	38,026	14,753	25,07	7	B1	Giornale di Sicilia (1978)a
53	1978	4	15	Patti Gulf	CFTI	38,150	14,980	9,0	6,06	6,06	Naso	38,122	14,788	17,61	7; 8	B1	Barbano et al. (1979)
54	1978	4	15	Patti Gulf	CFTI	38,150	14,980	9,0	6,06	6,06	Oliveri	38,124	15,060	7,37	7	B1*	Gazzetta del sud (1978); Barbano et al. (1979)
55	1990	12	13	SE-Sicily	CFTI	37,266	15,120	7,0	5,68	5,26	Augusta	37,609	15,221	9,70	7; 8	B1	Appunti sugli effetti (1991); De Rubeis et al. (1993)

Earthquake parametres											Recorded effect: liquefactions						
N	Year	Month	Day	Epicentral area	Rt	Lat	Long	Io	Maw	Mas	Site	Lat (s)	Long (s)	Re (km)	Is (MCS)	Observed effect	Historical source
1	1169	2	4	E-Sicily	CFTI	37,32	15,03	10	6,60	6,60	Catania	37,380	15,050	7,52	10	B2 -C	Samperi (1644)
2	1169	2	4	E-Sicily	CFTI	37,32	15,03	10	6,60	6,60	Lentini	37,284	14,998	5,38	10	B2 -C	Samperi (1644)
3	1169	2	4	E-Sicily	CFTI	37,32	15,03	10	6,60	6,60	Siracusa	37,082	15,285	34,50	9	B2 -C	Samperi (1644)
4	1542	12	10	SE-Sicily	CFTI	37,22	14,95	10	6,62	6,62	Augusta	37,231	15,221	24,10	7; 8	C*	BTJN (16th cent.)
5	1542	12	10	SE-Sicily	CFTI	37,22	14,95	10	6,62	6,62	Siracusa	37,082	15,285	26,88	8	C	BTJN (16th cent.)
6	1613	8	25	Naso	CFTI	38,12	14,78	8	5,57	5,40	Naso	38,120	14,790	1,50	9	B2-C	Mongitore (1743)
7	1624	10	3	Mineo	CFTI	37,27	14,75	8	5,57	5,40	Palagonia	37,326	14,745	6,30	9	B2 -C *	Mongitore (1743)
8	1693	1	11	E-Sicily	CFTI	37,13	15,02	11	7,41	7,41	Augusta	37,231	15,221	20,53	10	B1 -C *; B2 -C *	Bottone (1718)
9	1693	1	11	E-Sicily	CFTI	37,13	15,02	11	7,41	7,41	Avola	36,908	15,135	26,70	10	C*	Gubernale (1910)
10	1693	1	11	E-Sicily	CFTI	37,13	15,02	11	7,41	7,41	Calatafimi	37,922	12,855	210,01	N.R.	B1-C	Boccone (1697)
11	1693	1	11	E-Sicily	CFTI	37,13	15,02	11	7,41	7,41	Catania	37,502	15,087	40,00	10; 11	B2 -C *C	Anonimous (1693); Bottone (1718)
12	1693	1	11	E-Sicily	CFTI	37,13	15,02	11	7,41	7,41	Catania Plain	37,502	15,087	32,30	10; 11	B2 –C; C	Bottone (1718)
13	1693	1	11	E-Sicily	CFTI	37,13	15,02	11	7,41	7,41	Lentini	37,284	14,998	17,33	10; 11	B2 –C; C	Bottone (1718)
14	1693	1	11	E-Sicily	CFTI	37,13	15,02	11	7,41	7,41	Mascali	37,757	15,159	70,70	10	B2 -C C	Bottone (1718)
15	1693	1	11	E-Sicily	CFTI	37,13	15,02	11	7,41	7,41	Melilli	37,179	15,128	11,60	11	B1 -C *	Boccone (1697)
16	1693	1	11	E-Sicily	CFTI	37,13	15,02	11	7,41	7,41	Messina	38,187	15,529	127,40	8	B1-C *; B2 -C *	Bottone (1718)
17	1693	1	11	E-Sicily	CFTI	37,13	15,02	11	7,41	7,41	Naso	38,120	14,790	112,04	8	C	Romeo and Delfino (1997)
18	1693	1	11	E-Sicily	CFTI	37,13	15,02	11	7,41	7,41	Noto Antica	36,940	15,023	21,06	10; 11	B1-C	Romeo and Delfino (1997)
19	1693	1	11	E-Sicily	CFTI	37,13	15,02	11	7,41	7,41	Piazza Armerina	37,384	14,368	63,90	8	B2 -C *	Del Bono (1745)
20	1693	1	11	E-Sicily	CFTI	37,13	15,02	11	7,41	7,41	Siracusa	37,082	15,285	24,43	9	B1-C *; B2 -C; C	Boccone (1697); Bottone (1718)
21	1780	3	28	NE-Sicily	Azz*	37,86	15,31	8	5,60	5,10	Fiumedinisi	38,020	15,380	18,70	n.p.	B2 -C *	Gallo (1783)*
22	1783	2	5	Calabria	CFTI	38,30	15,97	11	6,91	6,91	Ganzirri	38.258	15.611	31.66	n.p.	B2-C	
23	1783	2	5	Calabria	CFTI	38,30	15,97	11	6,91	6,91	Messina	38,187	15,549	40,51	8	B2 -C	Gallo (1783); Lallement (1875)
24	1783	2	5	Calabria	CFTI	38,30	15,97	11	6,91	6,91	Torre Faro	38,266	15,646	29,86	n.p.	B2 -C	
25	1783	2	7	Calabria	CFTI	38,58	16,2	10,5	6,59	6,59	Messina	38,187	15,549	70,25	8	B2-C	Lallement (1785)
26	1783	4	26	Milazzo	CFTI	38,200	15,400	5,0	4,20		Messina	38,187	15,549	13,71	N.R.	B1-C	Corrao (1784)
27	1818	2	20	Catanese	CFTI	37,60	15,13	9	6,00	6,00	Paraspolo	37,400	15,080	22,68	n.p.	B2 –C; C	Longo (1818)
28	1818	2	20	Catanese	CFTI	37,60	15,13	9	6,00	6,00	Paternò	37,566	14,902	20,47	7; 8	B2 –C; C	Longo (1818)
29	1818	2	20	Catanese	CFTI	37,60	15,13	9	6,00	6,00	Ramondetta	37,350	15,070	28,24	n.p.	C	Longo (1818)
30	1848	1	11	Augusta	DOM	37,37	15,15	8	5,48	5,26	Augusta	37,231	15,221	16,23	8; 9	C*	Ferruggia Russo (1852)*
31	1865	7	19	Etnean area	CFTI	37,70	15,15	9	5,03	4,59	Scarronazzi	37,684	15,158	1,89	8; 9	B1-C	Grassi 1865, Biblioteca Zelantea di Acireale, 1865
32	1894	11	16	S-Calabria	CFTI	38,28	15,87	9	6,05	6,05	Ganzirri	38,248	15,601	21,80	n.p.	B1 -C; B2 -C	Riccò (1907)
33	1894	11	16	S-Calabria	CFTI	38,28	15,87	9	6,05	6,05	Torre Faro	38,266	15,646	19,50	7	B-C	Baratta (1910)

34	1898	11	2	Caltagirone	DOM	37,23	14,51	6	4,83	4,30	C. Racineri	37,210	14,400	10,33	n.p.	C	Corriere di Catania (1898)*
35	1908	12	28	S-Calabria	CFTI	38,15	15,68	11	7,24	7,24	Ganzirri	38,258	15,611	13,59	9	B1 -C *; B2 –C; C*	Lo Giudice (1909)*; Baratta (1910)
36	1908	12	28	S-Calabria	CFTI	38,15	15,68	11	7,24	7,24	Messina	38,187	15,549	12,29	10; 11	C-A; C*	Platania (1909); Baratta (1910); Sauret and Bousquet (1984)*
37	1908	12	28	S-Calabria	CFTI	38,15	15,68	11	7,24	7,24	Torre Faro	38,266	15,646	13,34	10	C-A; B2 -C *	Platania (1909); Baratta (1910)
38	1968	1	15	Belice	CFTI	37,77	13,00	8	5,60	5,4	Contessa Entellina	37,729	13,185	10,24	8	C	L'Ora, 1968. 01. 22/23, a. 69., n.18. ; Bosi et al. (1973)
39	1968	1	15	Belice	CFTI	37,77	12,98	10	6,40	5,9	Camporeale	37,897	13,096	10,25	8	C; C-B1	Giornale di Sicilia, 1968.01.17, a.108, n. 16; Giornale di Sicilia, 1968.01.18, a.108, n.17; La Stampa, 1968. 01. 27; Bosi et al. (1973); Corriere della Sera, 1968.01.17, a. 93, n.14; Corriere della sera, 1968.01.19, a.93, n.16.
40	1968	1	15	Belice	CFTI	37,77	12,98	10	6,40	5,9	Contessa Entellina	37,729	13,185	10,24	8	C	L'Ora, 1968. 01. 22/23, a. 69., n.18. Bosi et al. (1973).
41	1968	1	15	Belice	CFTI	37,77	12,98	10	6,40	5,9	Bisaquino	37,705	13,259	15,04	7	C	Bosi et a. (1973)
42	1968	1	15	Belice	CFTI	37,77	12,98	10	6,40	5,9	Marsala	37,797	12,447	30,69	7	B1-C	La stampa 1968. 01. 26
43	1968	1	15	Belice	CFTI	37,77	12,98	10	6,40	5,9	Portanna	37,723	12,892	6,74	8; 9	C	Bosi et a. (1973)
44	1968	1	15	Belice	CFTI	37,77	12,98	10	6,40	5,9	Sciacca	37,508	13,083	30,06	7	B1-C	Corriere della sare (1968)
45	1990	12	13	SE-Sicily	CFTI	37,27	15,12	7	5,68	5,26	Augusta	37,231	15,225	9,15	7; 8	C	De Rubeis et al. (1993)

Earthquake parametres											Recorded effect: hydrological anomalies						
N	Year	Month	Day	Epicentral area	Rt	Lat	Long	Io	Maw	Mas	Site	Lat (s)	Long (s)	Is (MCS)	Re (km)	Observed effect	Historical source
1	1125	7	6	E-Sicily	CFTI	37,07	15,3	8,5	5,9	5,9	Siracusa	37.082	15.285	8; 9	3,20	D-1.2	Riccardo di Poitou (1882)
2	1169	2	4	E-Sicily	CFTI	37,32	15,03	10	6,6	6,6	Catania Plain	37,402	15,057	10	9,83	D-2.1	Amico (1733); Sciuto(1896)
3	1169	2	4	E-Sicily	CFTI	37,32	15,03	10	6,6	6,6	Siracusa	37082	15285	9	34,50	D-1.1; D-1.2	Falcando (XII cent)
4	1613	8	25	Naso	CFTI	38,12	14,78	8	5,57	5,4	Naso	38,122	14,788	9	1,50	D-1.1	Incudine (1882)
5	1624	10	3	Mineo	CFTI	37,27	14,75	8	5,57	5,4	Palagonia	37,326	14,746	9	6,30	D-C	Mongitore (1743)
6	1693	1	11	E-Sicily	CFTI	37,13	15,02	11	7,41	7,41	Catania Plain	37,502	15,087	10;11	32,30	D-1.2	Boccone (1697-5?)
7	1693	1	11	E-Sicily	CFTI	37,13	15,02	11	7,41	7,41	Cassaro	37,106	14,948	10; 11	9,19	D-4.1	Boccone (1695); Bonaiuti (1793)
8	1693	1	11	E-Sicily	CFTI	37,13	15,02	11	7,41	7,41	Ferla-Cassaro	37,111	14,944	10; 11	7,10	D-4.1	Bottone (1718)
9	1693	1	11	E-Sicily	CFTI	37,13	15,02	11	7,41	7,41	Ispica	36,79	14,905	10	39,69	D-4.2	(CFTI04)
10	1693	1	11	E-Sicily	CFTI	37,13	15,02	11	7,41	7,41	Lentini	37,284	14,998	10; 11	17,33	D-2.1; D-3.1; D-C	Bottone (1718)
11	1693	1	11	E-Sicily	CFTI	37,13	15,02	11	7,41	7,41	Mascali	37,757	15,159	10	70,70	D-1.1; D-2.2; D-3.1	Bottone (1718)
12	1693	1	11	E-Sicily	CFTI	37,13	15,02	11	7,41	7,41	Modica-Ragusa	36,879	14,743	10	36,96	D-4.1	Bottone (1718)
13	1693	1	11	E-Sicily	CFTI	37,13	15,02	11	7,41	7,41	Noto Antica	36,94	15,023	10; 11	21,06	D-C	Bottone (1718)
14	1693	1	11	E-Sicily	CFTI	37,13	15,02	11	7,41	7,41	Noto-Siracusa	37,003	15,029	9	14,02	D-3.1; D-4.1; D-5	Bottone (1718)
15	1693	1	11	E-Sicily	CFTI	37,13	15,02	11	7,41	7,41	Ragusa	36,926	14,727	10	36,53	D-3.2; D-4.1	Bottone (1718)
16	1693	1	11	E-Sicily	CFTI	37,13	15,02	11	7,41	7,41	Siracusa	37082	15285	9	24,43	D-1.1; D-1.2; D-2.2	Boccone (1697); Bottone (1718); Del Bono (1745)
17	1693	1	11	E-Sicily	CFTI	37,13	15,02	11	7,41	7,41	Sortino	37,156	15,027	11	2,96	D-1.1	Bonaiuti (1793)
18	1693	1	11	E-Sicily	CFTI	37,13	15,02	11	7,41	7,41	Spaccaforno	36,977	15,197	10	22,43	D-4.2	Franzò (1931)
19	1693	1	11	E-Sicily	CFTI	37,13	15,02	11	7,41	7,41	Termini Imerese	37,988	13,688	NR	150,40	D-2.2; D-3.3	Bonaiuti (1793); Gallo (1823)
20	1693	1	11	E-Sicily	CFTI	37,13	15,02	11	7,41	7,41	Vizzini	37,162	14,745	10	24,25	D-3.2	Naselli (1931)
21	1693	1	11	E-Sicily	CFTI	37,13	15,02	11	7,41	7,41	Vizzini e Monterosso Almo	37,12	14,755	10; 11	23,76	D-3.2	Naselli (1931)
22	1717	4	22	Castroreale	CFTI	38,1	15,22	6,5	5,4	4,6	Castroreale	38,099	15,211	8; 9	0,09	D-C	Bottone (1718)
23	1739	5	10	Naso	CFTI	38,1	14,75	8	5,54	5,35	Naso	38,12	14,79	8; 9	3,70	D-1.1; D3.1; D-3.2	Incudine (1882); Rezzaodre (1914)

24	1823	3	5	Northern Sicily	CFTI	38,000	14,100	8,5	5,87	5,84	Termini Imerese	37,984	13,698	7	22,00	D-1.1; D-2.2	Ferrara (1823); Archivio di Stato di Palermo (1823)
25	1823	3	5	Northern Sicily	CFTI	38,000	14,100	8,5	5,87	5,84	Ogliastro	37,964	13,456	NR	90,14	D-2.1	Archivio di Stato di Palermo (1823)
26	1894	11	16	Calabria	CFTI	38,28	15,87	9,0	6,05	6,05	Barcellona P.G.	38,146	15,215	7	58,50	D-2.2	Riccò (1907)
27	1967	10	31	Nebrodi	CFTI	37,87	14,42	8	5,7	5,7	Nicosia	37,749	14,394	8	14,03	D-2.2	ANSA (1967)
28	1968	1	15	Belice	CFTI	37,77	13	8	5,6	5,4	Ghibellina	37,79	12,976	10	4,22	D-1.1; D-C	Bosi et al. (1973).
29	1968	1	15	Belice	CFTI	37,77	12,98	10	6,4	5,9	Ghibellina	37,79	12,976	10	4,22	D-1.1; D-C	Bosi et al. (1973).
30	1968	1	15	Belice	CFTI	37,77	12,98	10	6,4	5,9	Terme Segestane	37,973	12,892	NR	15,05	D-2.2; D-C	Bosi et al. (1973).
31	1990	12	13	SE-Sicily	CFTI	37,266	15,12	7	5,68	5,26	Brucoli	37,283	15,187	5; 6	5,81	D-C	appunti sugli effetti (1990)
32	1993	6	26	Pollina	CFTI	37,99	14,14	7	4,70	-	Pollina	37,99	14,14	7	1,00	A2	Azzaro and Barbano (1995)
33	2002	6	9	S-Tyrrhenian Sea	Azz*	38,08	13,42	6	5,6	5	Termini imerese	37,988	13,688	5; 6	26,23	D.1.1; D.3.1	Azzaro et al. (2004)

Appendix C
Upper-bound curve equations.

Landslides.

Maw = 1.264189801 x ln(Re) + 0.7795109954

Number of data points used = 5
Average ln(Re) = 4.11369
Average Maw = 5.98
Residual sum of squares = 0.138967
Regression sum of squares = 5.58403
Coef of determination, R-squared = 0.975718
Residual mean square, sigma-hat-sq'd = 0.0463224

Mas = 1.255540413 x ln(Re) + 0.4531243682

Number of data points used = 4
Average ln(Re) = 3.97787
Average Mas = 5.4475
Residual sum of squares = 0.346301
Regression sum of squares = 7.04597
Coef of determination, R-squared = 0.953154
Residual mean square, sigma-hat-sq'd = 0.17315

Io = 2.303708092 x ln(Re) - 1.480905079

Number of data points used = 4
Average ln(Re) = 4.06124
Average Io = 7.875
Residual sum of squares = 1.8218
Regression sum of squares = 17.3657
Coef of determination, R-squared = 0.905053
Residual mean square, sigma-hat-sq'd = 0.910901

Ground deformations.

Maw = 0.9031080465 x ln(Re) + 2.368246515

Number of data points used = 5
Average ln(Re) = 3.96603
Average Maw = 5.95
Residual sum of squares = 1.09015
Regression sum of squares = 6.62085
Coef of determination, R-squared = 0.858624
Residual mean square, sigma-hat-sq'd = 0.363385

Mas= 0.9926646616 x ln(Re) + 1.919062305

Number of data points used = 5
Average ln(Re) = 3.96603
Average Mas= 5.856
Residual sum of squares = 0.676656
Regression sum of squares = 7.99906

Coef of determination, R-squared = 0.922006
Residual mean square, sigma-hat-sq'd = 0.225552

Io= 1.524761449 x ln(Re) + 2.256722716
Number of data points used = 4
Average ln(Re) = 3.68469
Average Io= 7.875
Residual sum of squares = 3.9277
Regression sum of squares = 15.2598
Coef of determination, R-squared = 0.795299
Residual mean square, sigma-hat-sq'd = 1.96385

Liquefactions.

Maw= 0.9268045066 x ln(Re) + 2.604217077
Number of data points used = 7
Average ln(Re) = 3.37265
Average Maw= 5.73
Residual sum of squares = 0.973235
Regression sum of squares = 5.89196
Coef of determination, R-squared = 0.858236
Residual mean square, sigma-hat-sq'd = 0.194647

Mas= 1.101662372 x ln(Re) + 1.744984894
Number of data points used = 6
Average ln(Re) = 3.48414
Average Mas= 5.58333
Residual sum of squares = 0.424625
Regression sum of squares = 7.81991
Coef of determination, R-squared = 0.948496
Residual mean square, sigma-hat-sq'd = 0.106156

Io= 1.984650459 x ln(Re) + 1.197677215
Number of data points used = 5
Average ln(Re) = 3.57863
Average Io= 8.3
Residual sum of squares = 4.74617
Regression sum of squares = 24.0538
Coef of determination, R-squared = 0.835203
Residual mean square, sigma-hat-sq'd = 1.58206

Hydrological anomalies.

Maw= 0.5144240042 x ln(Re) + 4.470337003
Number of data points used = 3
Average ln(Re) = 3.64096
Average Maw= 6.34333
Residual sum of squares = 0.417191
Regression sum of squares = 1.40468

Coef of determination, R-squared = 0.771009
Residual mean square, sigma-hat-sq'd = 0.417191

Mas= 0.6010137505 x ln(Re) + 4.06795519
Number of data points used = 3
Average ln(Re) = 3.61397
Average Mas= 6.24
Residual sum of squares = 0.341153
Regression sum of squares = 2.02425
Coef of determination, R-squared = 0.855774
Residual mean square, sigma-hat-sq'd = 0.341153

Io= 1.161221598 x ln(Re) + 4.80338163
Number of data points used = 3
Average ln(Re) = 3.61397
Average Io= 9
Residual sum of squares = 0.443425
Regression sum of squares = 7.55657
Coef of determination, R-squared = 0.944572
Residual mean square, sigma-hat-sq'd = 0.443425

References

Abe, K., Abe, K., Tsuji Y., Imamura F., Katao H., Yoshihisa I., Satake K., Bourgeois J., Noguera E., Estrada F., 1993. Field survey of the Nicaragua earthquake and tsunami of September 2, 1992. Bulletin of the Earthquake Research Institute, 68, 23-70

Adams, J., 1992. Paleoseimology: a search for ancient earthquakes. In Puget Sound, Science, 259, 1592-1593.

Adam, J., Reuther, C. D., Grasso, M., Torelli, L., 2000. Active fault kinematics and crustal stresses along the Ionian margin of southeastern Sicily. Tectonophysics, 326, 217–239.

Albarello, D., Ferrari, G., Martinelli, G., Mucciarelli, M., 1991. Well level variation as a possible seismic precursor: a statistical assessment from Italian historical data. Tectonophysics, 193, 385– 395.

Albarello, D., Martinelli, G., 1994. Piezometric levels as possible geodynamic indicators: analysis of data from a regional deep waters monitoring network in northern Italy. Geoph. Res. Lett., 21, 18, 1955–1958.

Alfaro, P., Delgado, J., Estévez, A., Molina, J.M., Moretti, M., Soria, J.M., 2002. Liquefaction and fluidization structures in Messinian storm deposits (Bajo Segura Basin, Betic Cordillera, southern Spain). International Journal of Earth Science (Geol Rundsch), 91, 505-513.

Allen, J.R.L., 1982. Sedimentary Structures: Their Character and Physical Basis. II. Elsevier, New York. 663 pp.

Ambraseys, N. N., 1988. Engineering seismology. Earthquake Engineering and Structural Dynancics, 17, 1–105.

Ambraseys, N.N., 1991. Engineering seismology. Int. Journal Earthquake Engineering and Structural Dynamics, 17, (1), 1-105.

Ambraseys, N., Sarma, S., 1969. Liquefaction of soils induced by earthquakes. Bull. Seismol. Soc. Am., 59, 651–664.

Amick, D., Gelinas, R., Maurath, G., Cannon, H., Moor, D., Billington, E., Kempinen, H., 1990. Paleoliquefaction features along the Atlantic seabord. U.S.N.R.C, Washington DC 20555 NRC FIN D 1682, NUREG/CR-5613 RA.

Amico, V.M., 1733. Siciliane sacrae, libri quarti. Catania.

Amore, C., Costa, B., Di Geronimo, I., Giuffrida, E., Randazzo, G., Zanini, A., 1994. Temporal evolution, sediment and fauna of the Vendicari lagoons (Siracusa). In:

Matteucci, R. et al (Eds.). Studies, on Ecology And Paleoecology of Benthic Communities, Bollettino Società Paleontologica Italiana Speciale 2 (7), 1-15, Mucchi-Modena.

Anonimo, sul tremuoto avvenuto in Palermo il giorno 5 marzo 1823,

Anonimous, 1693. Vera relazione di quello che è successo nell'ultimo terremoto in Sicilia (veritable ralation de ce qui s'est passé dans le dernier tremblement de terre en Sicile), Toulon.

ANSA, notiziario per la stampa, 1967. 11. 05, Servizio Italiano.

ANSA, Notiziario italiano, 1978. 03.12

Appunti sugli effetti del terremoto del 13. 12. 1990, Camera territoriale della Protezione civile.

Aprile, F., 1725. Della cronologia universale della Sicilia. Palermo 1725.

Archivio di stato di Palermo, 1823 ministero e segreteria di stato per gli affari di Sicilia presso sua maestà in Napoli.

Archivio dell'Ufficio Centrale di Ecologia Agraria, 1894. Cartoline Macrosismiche, n. 58, Relazione del direttore dell'Osservatorio Geodinamico de Catania A. Riccò al direttore dell'Ufficio. 1894.

Archivio General De Simancas 1693a. Relazione del governatore del Porto di Messina B. Bazan al Vicerè di Napoli sui danni causati in Sicilia dai terremoti del 9 e 11 gennaio, 1693. Secretarìa de Estado, Negociòn de Sicilia, legajo 3507 (1693-94), Consultas decretos y notas, no. 4.

Archivio General De Simancas 1693b. Secretarìa de Estado, Negociòn de Sicilia, legajo 3507 (1693-94), Consultas decretos y notas, n°11, Relazione dei luoghi che hanno sofferto in Sicilia nei Terremoti dal nove di gennaio fino al cinque di febbraio del 1693 che si sono sentite ventuno scosse, le primi tre grandi e le altre più lievi, Palermo febbraio 1693.

Asteriadis, G., Livieratos, E., 2003. Pre-seismic responses of underground water level and temperature concerning a 4.8 magnitude earthquake in Greece on October 20, 1988. Tectonophysics, Volume 170, Issues 1-2, 10 December 1989, 165-169

Atwater, B.F., Moore, A.L., 1992. A tsunami about 1000 years ago in Puget Sound, Washington. Science, 258, 1614-1617.

Azzaro, R., 1999. Liquefaction induced features for the scenario earthquake in the Catania area. In The Catania Project: Earthquake Damage Scenarios for High Risk

Area in the Mediterranean, edited by E. FACCIOLI and V. PESSINA (CNR - Gruppo Nazionale per la Difesa Terremoti, Roma), 42-45.

Azzaro, R., 2000. Liquefaction-induced for the scenario earthquakes in the Catania area. Into The Catania Project. Earthquake damage scenario for a high risk area in the Mediterranean. E Faccioli and V Pessina Eds., gNR-Gruppo Nazionale per la Difesa dai Terremoti-Roma, 2000, 225 pp.

Azzaro, R., Barbano, M.S., 1995. The Pollina (Northern Sicily-Italy) earthquakes of 26 June 1993: an application of the new European Macroseismic Scale 1992. Natural Hazards, 12, 289-301.

Azzaro, R., Barbano, M.S., 2000. Analysis of seismicity of Southeastern Sicily: a proposed tectonic interpretation. Annali di Geofisica, 43, 171-188.

Azzaro, R., Camassi, R., D'Amico, S.,Mostaccio, A., Scarfì, L., 2003. Il terremoto di Palermo del 6 settembre 2002: effetti macrosismici. Quad. Geofis., 31, 15 pp.

Azzaro, R., Barbano, M.S., Camassi, R., D'Amico, S.,Mostaccio, A., Piangiamore, G., Scarfì, L., 2004. The earthquake of 6 September 2002 and the seismic history of Palermo (Northern Sicily, Italy): implications for the seismic hazard assessment of the city. J. Seismology, 8 (4), 525-543.

Azzaro, R., Bernardini, F., Camassi, R., Castelli, V., 2007. The 1780 seismic sequence in NE Sicily (Italy): shifting an underestimated and mislocated earthquake to a seismically low rate zone. Nat. Hazards, 42 (1), 149-167.

Baratta, M., 1910. La catastrofe sismica calabro messinese (28 dicembre 1908), 2, Roma.

Barbano, M.S., Bottari, A., Carveni, P., Cosentino, M., 1979. Macroseismic study of the gulf of Patti earthquake in the geostructural frame of North-Eastern Sicily. Bollettino della Società Geologica Italiana, 98, 155-174.

Barbano, M.S., Rigano, S., 2001. Earthquake sources and seismic hazard in Southeastern Sicily. Ann. Geophys. 44 (4), 723–737.

Barbano, M.S., Pantosti, D., De Martini, P.M., Smedile, A., Gerardi, F., **Pirrotta, C.**, 2007. Historical, archaeological and geological records of strong earthquakes at Capo Peloro (southern Italy). In: Riassunti estesi delle comunicazioni. XXVI Convegno del Gruppo Nazionale di Geofisica della Terra Solida. Roma. 13-15 Novembre 2007. (p 211- 215). ISBN/ISSN: 88-902101-2-5. TRIESTE: (ITALY).

Barbano, M.S, De Martini, P.M, Pantosti, D, Smedile, A, Del Carlo, P, Gerardi, F., Guarnieri, P., **Pirrotta, C.**, 2009. In search of Tsunami deposits along the eastern

coast of Sicily (Italy): state of the art In: Recent Progress on Earthquake Geology (P. Guarnieri (Ed.), 121-158. ISBN: 978-1-60876-147-0 Nova Science Publishers, Inc.

Barbano, M.S., **Pirrotta, C.**, Gerardi, F., 2010a. Large boulders along the south-eastern Ionian coast of Sicily: storm or tsunami deposits?. Mar. Geol., 275, 140-154.

Barbano, M.S., Gerardi, F., **Pirrotta, C.**, 2010b. Distinguishing between boulders deposited by tsunamis and storm waves along the south-eastern Ionian coast of Sicily (Italy). Accepted for pubblication in BGTA, Bollettino di Geofisica Teorica Applicata.

Basili, A. 1990. Contributi allo studio del terremoto della Sicilia orientale del 13 dicembre 1990, I.N.G. 537, 115-125.

Basili, R., Valensise, G., Vannoli, P., Burrato, P., Fracassi, U., Mariano, S., Tiberti, M.M., Boschi, E., 2008. The Database of Individual Seismogenic Sources (DISS), version 3: summarizing 20 years of research on Italy's earthquake geology, Tectonophysics, 453, 20-43, doi:10.1016/j.tecto.2007.04.014.

Beaudoin, B., Friès, G., Joseph, P., Paternoster, B., 1983. Sills gréseux sédimentaires injectés dans l'Aptien supérieur de Rosans (Drôme), C. R. Acad. Sci., Paris 296, 387–392.

Behncke, B., 2001. Volcanism in the Southern Apennines and Sicily, in Vai, G.B., and Martini I.P., eds., Anatomy of an Orogen: The Apennines and adjacent Mediterranean basins. Amsterdam, Kluwer, 105–120.

Ben-Avraham, Z., Boccaletti, M., Cello, G., Grasso, M., Lentini, F., Torelli, L., Tortorici, L., 1990. Principali domini strutturali originatisi dalla collisione nogenico–quaternaria nel Mediterraneo centrale. Memorie della Società Geologica Italiana, 45, 453–462.

Berardi, R., Margottini, C., Molin, D., Parisi, A., 1991. Soil, liquefaction: Case histories in Italy. Tectonophysics, 193, 141–164.

Bianca, M., Monaco, C., Tortorici, L., Cernobori, L., 1999. Quaternary normal faulting in southeastern Sicily (Italy): a seismic source for the 1693 large earthquake. Geophys. J. Int., 139, 370-394.

Bianchi, F., Carbone, S., Grasso, M., Invernizzi, G., Lentini, F., Longaretti, G., Merlini, S., Mostardini, F., 1987. Sicilia orientale: Profilo geologico Nebrodi-Iblei: Memorie della Società Geologica Italiana, 38, 429–458.

Biblioteca Apostolica Vaticana, Barberini Latini, 2490, Historia et Annales Pisanorum (471-1174), copia sec. XVII.

Biblioteca comunale di Augusta, 17th cent. Manoscritti, Raccolta Blasco, vol. 638, Cronaca dei terremoti del 9 e 11 gennaio 1693 scritta da una monaca del Monastero di S. Caterina di Augusta (ms), Raccolta Blasco, vol. 638.

Biblioteca Zelantea di Acireale 1865 (a), Manoscritti, III.C.7.29 (B.27) F. Sclafani, Compendio Historico di Sicilia.

Biblioteca Zelantea di Acireale (b), Manoscritti, III 3.8, P. Grasso Gambino, Abbozzo di storia di Aci, ms. sec. XIX. (anno 1832- 1835).

Biblioteca Zelantea di Acireale, Manoscritti A. Messa, Relazione sulla disgrazia avvenuta la notte del 18 al 19 Luglio.

Billi, A ., Minelli, L., Orecchio, B., Presti D., 2010. Constraints to the cause of three Historical tsunamis (1908, 1783, and 1693) in the Messina straits region, sicily, southern italy. Seismogeological Research Letters, 8, n 6, 907- 915.

Boccone, P., 1697. Intorno il terremoto della Sicilia seguito l'anno 1693. Museo di Fisica, 31 pp., Venezia Boccone, 1695.

Bonaiuti, V., 1793. Particolarità intorno al tremuoto che ruinò la Sicilia nel 1693, in Compendio delle Transazioni Filosofiche della Società Reale di Londra, parte 1 (Storia Naturale), tomo 1 (Vulcani e Tremuoti), 33-43, Venezia.

Bonilla, M. G., Buchanan, M. J., 1970. Interim report on worldwide historic surface faulting, U.S. Geol. Surv., Open-File Rept.

Bonito, M., 1691. Terra tremante, o vero continuatione dè terremoti dalla Creatione del Mondo sino al temo presente (ristampa anastatica. Sala Bolognese 1980). Napoli 1691.

Boschi, E., Pantosti, D., Valensise, G., 1989. Modello di sorgente per il terremoto di Messina del 1908 ed evoluzione recente dell'area dello Stretto. Proc. 8° Meeting G.N.G.T.S., Rome 1989, 245-258.

Boschi, E., Ferrari, G., Gasperini, P., Guidoboni, E., Smriglio, G., Valensise, G., 1995. Catalogo dei Forti Terremoti in Italia dal 461 a.C. al 1980, ING e SGA Bologna, 973 pp., con database cu CD-ROM.

Boschi, E., Guidoboni, E., Ferrari, G., Valensise, G., Gasperini, P., 1997. Catalogo dei forti terremoti in Italia dal 461 a.C. al 1990, ING-SGA, Ozzano Emilia, 644 pp.

Boschi, E., Guidoboni, E., Ferrari, G., Gasperini, P., Mariotti, D., Valensise, G., 2000. Catalogue of Strong Italian earthquakes from 461 a.c. to 1997, Ann. Geofis., 43 (4), 43-868 and CD-Rom.

Bosi, C., Cavallo, R., Francaviglia, V., 1973. Aspetti geologici e geologico-tecnici del terremoto della valle del Belice del 1968, Memorie della Società Geologica Italiana, 12, fasc. 2, 81-130.

Bottari, A., Carapezza, E., Carapezza, M., Carveni, P., Cefali, F., Lo Giudice, E., Pandolfo, C., 1986. The 1908 Messina Strait earthquake in the regional geostructural framework. J. Geodyn., 5, 275-302.

Bottone, D., 1718. De immani Trinacrie terremotu. Idea historico-physica, in qua non solum telluris concussiones transacte recensetur, sed novissime anni 1717, Messina.

Bouillin, J.P., Bellomo, D., 1990. Les filons sédimentaires jurassiques de Longobucco-Caloveto (Calabre, Italie); application à l'étude des paléostructures d'une marge téthysienne. Geodinamica Acta 4, 111–120.

Bouillin, J.P., Naak, M., 1989. Découvertes de filons sédimentaires caractérisant une tectonique distensive jurassique dans le Djurdjura (Dorsale calcaire maghrébine, Algérie). C. R. Academy of Sciences, Paris 309, 1371–1376.

Bourgeois, J., Petroff, C., Yeh, H., Titov, V., Synolakis, C., Benson,, B., Kuroiwa J., Lander, J., Norabuena, E., 1999. Geologic setting, field survey and modeling of the Chimbote, northern Peru tsunami of 21 February 1996. Pure and Applied Geophysics, 154, 513-540.

Bourgeois, J., Johnson, S.Y., 2001. Geologic evidence of earthquakes at the Snohomish Delta, Washington, in the past 1200 yr. Geological Society of America Bulletin, 113, 482-494.

Bourgeois, J., Pinegina, T.K., Ponomareva, V., Zaretskaia, N., 2006. Holocene tsunamis in the southwestern Bering Sea, Russian Far East, and and their tectonic implications. Geological Society of America Bulletin, 118, 449-463.

Bourgeois, J., MacInnes, B., 2010. Tsunami boulder transport and other dramatic effects of the 15 November 2006 central Kuril Islands tsunami on the island of Matua. Zeitschrift fuer Geomorphologie, 54 (3), 175–195.

Bousquet, J.C., Lanzafame, G., 2004. The tectonics and geodynamics of Mt. Etna: synthesis and interpretation of geological and geophysical data. In: A. Bonaccorso et al., Editors, Mt. Etna: Volcano Laboratory, Geophysical Monograph Series 143, AGU (2004), pp. 29–47.

Brenchley, P.J., 1985. Storm influenced sandstone beds. Modern geology, 9, 369-396.

Briggs, R.O., 1994. Effects of the earthquakes on surface waters in Waddell Valley. In: The Loma Prieta (California) Earthquake of 17 October 1989 – Hydrologic disturbances, USGS Prof. Paper 1551–E, 21–30.

Bryant, E.A., 2001. Tsunami. The Underrated Hazard. Cambridge University Press, Cambridge, UK, 320 pp.

BTJN, 16th cent. Lettera from Yosef Ha-Kohen to Yishaq ha-Kohen. Raccolta epistolare KM 55, (ms), Biblioteca The Jewish National and University Library.

Buchanan-Banks, J. M., 1987. Structural damage and ground failures from the November 16, 1983 Kaoiki earthquake, island of Hawaii. U.S. Geol. Surv. Profess. Pap. 1350, 1187-1220.

Camassi, R., Stucchi, M., 1996. NT4.1, un catalogo parametrico di terremoti di area italiana del Gruppo Nazionale per la Difesa dei Terremoti (GNDT, 1996).

Campis, P., 1694. Disegno historico o siano l'abbozzate historiae della nobile e fidelissima città di Lipari (ms.), a cura di G. Iacolino, Lipari 1991.

Capaccioni, B., Didero, M., Paletta, C., Didero, L., 2005. Saline intrusion and refreshening in a multilayer coastal aquifer in the Catania Plain (Sicily, Southern Italy): dynamics of degradation processes according to the hydrochemical characteristics of groundwaters, J. Hydrol., 307, 1–16.

Capocci, E., 1861. Catalogo dei tremuoti avvenuti nella parte continentale del Regno delle Due Sicilie, posti in raffronto con le eruzioni vulcaniche ed altri fenomeni cosmici, tellurici. Atti dell'Istituto di Incoraggiamento alle Scienze Naturali di Napoli, (9), 335-378.

Capuano, P., De Natale, G., Gasparini, P., Pingue, F., Scarpa, R., 1988. A model for the 1908 Messina Straits (Italy) earthquake by inversion of levelling data. B. Seismol. Soc. Am., 78, 1930-1947.

Caputo, R., 2005. Stress variability and brittle tectonic structures. Earth-Science Reviews, 70, 103–127.

Carbone, S., Grasso, M., Lentini, F., 1982, Considerazioni sull'evoluzione geodinamica della Sicilia Sud-Orientale dal Cretaceo al Quaternario. Memorie della Società Geologica Italiana, 24, 367–386.

Caruso, G. B., 1781. Storia di Sicilia, p. II, libro V, pag. 360, Palermo.

Casero, P., Cita, M.B., Croce, M., De Micheli, A., 1984. Tentativo di interpretazione evolutiva della Scarpata di Malta basata sui dati geologici e geofisici. Memorie della Società Geologica Italiana, 27, 233–254.

Cassinis, R., Franciosi, R., Scarascia, S., 1979. The structure of the Earth's Crust in Italy: A preliminary typology based on seismic data: Bollettino di Geofisica Teorica e Applicata, 21, 105–126.

Catalano, S., De Guidi, G., Lanzafame, G., Monaco, C., Torrisi, S., Tortorici, G., Tortorici, L., 2006. Inversione tettonica positiva tardo-quaternaria nel plateau ibleo (Sicilia SE). Rend. Soc. Geol. It., 2, nuova serie, 118-120, 1 f.

Cavasino, A., 1935. I terremoti d'Italia nel trentacinquennio1899-1933, in Memorie del Regio Ufficio Centrale di Meteorologia e Geofisica , serie III, vol. 4.

Cheel, R.J., Leckie, D.A., 1993. Hummocky cross-stratification. In: Sedimentological Review, 1 (Ed. V.P. Wright), 103–122. Blackwell Scientific Publication, Cambridge.

Chengmin, W, 1985. Ground-water studies for earthquake prediction in China. Pageoph, 122, 215–217.

Chiodini, G., D'Alessandro, W, Parello, F., 1996. Geochemestry of the gases and of the waters discharged by the mud volcanoes of Paternò, Mt. Etna (Italy). Bull. Volcanol., 58, 51-58.

Clague, J. J., Bobrowsky, P. T., 1994. Evidence for a Large Earthquake and Tsunami 100–400 Years ago on Western Vancouver Island, British Columbia. Quaternary Res., 41, 176–184

Corrao, A., 1784. Memoria sopra i tremuoti di Messina accaduti nell'anno 1783, Messina.

Corriere della Sera, 1967.11.06. Milano.

Corriere della sera, 1968a.01.16, a. 93, n.13, Milano.

Corriere della sera, 1968b.01.17, a. 93, n.14, Milano

Corriere della sera, 1968c.01.19, a.93, n.16, Milano.

Corriere della sera, 1968d.01.27, a. 93, n. 23, Milano

Corriere di Catania (1898): Novembre, Catania.

Corriere di Catania, 1911, 10.17, 284.

Corriere di Catania (1898), Novembre, Catania.

Cotecchia, V., Guerricchio, A., Melidoro, G., 1986. The Geomorphogenetic Crisis Triggered by the 1783 Earthquake in Calabria (Southern Italy), Proceedings of the International Symposium on Engineering Geology Problems in Seismic Areas, Bari, Italy, 6, 245–304.

Cox, J.C., Machemehl, J. 1986. Overland bore propagation due to overtopping wave. J. Waterway, Port, Coastal and Ocean Engineering, 112, 161–163.

Cronaca Pisana, 13th cent. in Italia sacra edited by F. Ughelli, 10, Venezia, 1722.

Cruden, D.M., Varnes, D. J., 1996. Landslide types and processes. In: Turner A.K.; Shuster R.L. (eds) Landslides: Investigation and Mitigation. Transp Res Board, Spec Rep 247, 36–75.

D'Addezio, G., Valensise, G., 1991. Metodologie per l'individuazione della struttura sismogenetica responsabile del terremoto del 13 Dicembre 1990. In: Boschi, E., Basili, A., (Eds.), Contributi allo studio del terremoto della Sicilia orientale del 13 Dicembre 1990, Pubblicazione 537. Istituto Nazionale di Geofisica, Rome, 151–162.

D'Addezio, G., Valensise, G., 1993. Metodologie per l'individuazione della struttura sismogenetica responsabile del terremoto del 13 Dicembre 1990. In: Boschi, E., Basili, A., (Eds.), Contributi allo studio del terremoto della Sicilia orientale del 13 Dicembre 1990, Pubblicazione 537. Istituto Nazionale di Geofisica, Rome, 151–162.

Dalrymple, R.W., 1979. Wave-induced liquefaction: a modern example from the Bay of Fundy. Sedimentology, 26, 835–844.

Dawson, S., Smith, D. E., Ruffman, A., Shi, S., 1996. The Diatom Biostratigraphy of Tsunami Sediments: Examples from Recent and Middle Holocene Events. Phys. Chem. Earth, 21(12), 87–92.

Dawson, A.G., Stewart, I., Morton, R.A., Richmond, B.M., Jaffe, B.E., Gelfenbaum, G., 2008. Reply to Comments by Kelletat (2008) comments to Dawson, A.G. and Stewart, I. (2007) tsunami deposits in the geological record (Sedimentary Geology, 200, 166– 183). Sedimentary Geology 211, 92–93.

De Lange, P.J., Moon, V.G., 2007. Tsunami washover deposits, Tawharanui, New Zealand. Sedimentary Geology, 200 (3-4), 232-247

De Martini, P. M., Burrato, P., Pantosti, D., Maramai, A., Graziani, L., Abramson, H., 2003. Identification of tsunami deposits and liquefaction features in the Gargano Area (Italy): Paleoseismological implication. Annals of Geophysics 46 (5), 883–902.

De Martini, P.M., Barbano, M.S., Smedile, A., Gerardi, F., Pantosti, D., Del Carlo, P., **Pirrotta, C.** 2010. A unique 4000 year long geological record of multiple tsunami inundations in the Augusta Bay (eastern Sicily, Italy). Marine Geology 276, 42–57.

De Natale, G., Pingue, F., 1991. A variable slip fault model for the 1908 Messina Straits (Italy) earthquake, by inversion of levelling data. Geophys. J. Int., 104, 73-84.

De Rubeis, V., Gasparini, C., Maramai, A., Anzidei, A., 1993. Il terremoto siciliano del 13 Dicembre 1990, In Contributi allo studio del terremoto della Sicilia orientale del 13 Dicembre 1990, Roma, 9-44.

De Visser, J. P., Ebbing, j. H. J., Gudjonsson L., Hilgen, F. J.. Jorissen, F. J. , Verhallen, P. J. J. M., Zevenboom, D., 1989. The origin of rhythmic bedding in the Pliocene Trubi Formation of Sicily, southern Italy. Palaeogeography, Palaeoclimatology, Palaeoecology, Elsevier Science Publishers B.V., Amsterdam Printed in The Netherlands, 45-66.

Del Ben, A., Guarnieri, P., 2000, Neogene transpression in the Cefal`u Basin (Southern Tyrrhenian): comparison between land and marine data. Mem. Soc. Geol. It. 55, 27–33.

Del Bono, M., 1745. Discorso sull'origine de' tremuoti, in cui si esamina di proposito una nuova Opinione intorno alla Cagione di essi Palermo, 1745.

De Guidi, G., Catalano, S., Monaco, C., Tortorici, L., 2003. Morphological evidence of Holocene coseismic deformation in the Taormina region (NE Sicily). J. Geodyn., 5 (36), 193– 211.

De Lorenzo, A.: Un secondo manipolo di monografie e memorie reggine e calabresi, Siena, 1895.

Demoulin, A., 1996. Clastic dykes in east Belgium: evidence for Upper Pleistocene strong earthquakes west of the Lower Rhine rift segment. J. Geol. Soc. 153, 803–810.

Dercourt, J., Zonenshain, L.P., Ricou, L.E., Kazmin, V.G., Le Pichon, X., Knipper, A.L., Grandjaquet, C., Sborshchikov, I.M., Geyssant, J., Lepvrier, C., Pechersky, D.H., Boulin, J., Savostin, L.A., Sorokhtin, O., Westphal, M., Bazhenov, M.L., Lauer J.P., and Biju-Duval, B., 1986. Geological evolution of the Tethys belt from the Atlantic to the Pamirs since the Lias. Tectonophysics, 123, 241–315.

Dewey, J.F., Helman, M.L., Turco, E., Hutton, D.H.W., Knott, S.D., 1989. Kinematics of the Western Mediterranean. In: Coward, M.P., et al. (Eds.), Alpine tectonics: Geological Society of London Special Publication, 45, 265–283.

Di Poitou, R., 1882. Cronica [-1172] (sec. XII), ed. G. Waitz, in Monumenta Germaniae Historica , SS., tomo 26, 74-84.

Di Stefano, A., Branca, S., 2002. Long term uplift of the Etnean basement (Southern Italy) based on biochronological data from Pleistocene sediments. Terra Nova, 14, 61–68.

DISS Working Group, 2006. Database of Individual Seismogenic Sources (DISS), Version 3.0.2: A compilation of potential sources for earthquakes larger than M 5.5 in Italy and surrounding areas. http://www.ingv.it/DISS/, © INGV 2006

DISS Working Group, 2009. Database of Individual Seismogenic Sources (DISS), Version 3.1.0: A compilation of potential sources for earthquakes larger than M 5.5 in Italy and surrounding areas. http://diss.rm.ingv.it/diss/, © INGV 2009 - Istituto Nazionale di Geofisica e Vulcanologia.

Doglioni, C., Mongelli, F., Pieri, P., 1994. The Puglia uplift SE Italy: An anomaly in the foreland of the Apenninic subduction due to buckling of a thick continental lithosphere. Tectonics, 13, no. 5, 1309–1321.

Dravis, Jeffrey J., 1996. Rapidity of freshwater calcite cementation-implications for carbonate diagenesis and sequence stratigraphy. Sediment. Geol. 107, l-10.

Dunne, W. M., Hancock, P.L., 1994. Paleostress analysis of small-scale brittle structures. In: Hancock, P. I., (Ed.), Continental Deformation, Pergamon. Oxford, 101-120.

ENEL, 1975. Catalogue of Italian Earthquakes (on magnetic tape), Ente Nazionale Energia Elettrica, Roma.

Esposito, E., Porfido, S., Tranfaglia, G., Avino, R., 1998. Effetti idrologici associati con i terremoti dell'Appennino meridionale, Atti 16 Conv. GNGTS, Trieste.

Esposito, E., Pece, R., Porfido, S., Tranfaglia, G., Onorati, G., 1999. Effetti dei terremoti dell'Appennino meridionale sulle acque superficiali. Atti Acc. Naz. Lincei, 154, 91–96.

Esposito, E., Pece, R., Porfido, S., Tranfaglia, G., 2001. Hydrological anomalies connected to earthquakes in southern Apennines (Italy). Natural Hazards and Earth System Sciences 1, 137–144.

Fabbri, A., Rossi, S., Sartori, R., Barone, A., 1982. Evoluzione neogenica dei margini marini dell'Arco Calabro-Peloritano. Implicazioni geodinamiche: Memorie della Società Geologica Italiana, 24, 357–366.

Falcando, sec XII. La istoria o liber de regno sicilie, ed G.B. Siragusa. In Fonti per la storia d'Italia, S.S., vol. 22.

Fazello, T., 1628. Le due deche dell'Historia di Sicilia. Palermo, 1628.

Ferranti, L., Antonioli, F., Mauz, B., Amorosi, A., Dai Pra, G., Mastronuzzi, G., Monaco, C., Orrù, P. Pappalardo, M., Radtke, U., Renda P., Romano, P., Sansò, P., Verrubbi, V., 2006. Markers of the last interglacial sea-level high stand along the coast of Italy: Tectonic implications. Quaternary International, 145–146, 30–54.

Ferranti, F., Monaco, C., Antonioli, F., Maschio, L., Kershaw, S., Verrubbi, V., 2007. The contribution of regional uplift and coseismic slip to the vertical crustal motion in

the Messina Straits, southern Italy: Evidence from raised Late Holocene shorelines. Journal of Geophysical Research 112, B06401, doi:10.1029/2006JB004473.

Ferrara, F., 1823. Memoria sopra i tremuoti della Sicilia in marzo 1823. Palermo, 1823.

Ferrara, V., 1979. Risultati preliminari delle ricerche idrogeologiche e geochimiche eseguite nell'area della provincia di Catania. Atti 1° Sem. inf. Un. Ric. Sottoprogetto "Energia Geotermia", CNR-PF Energetica, Roma, 18-21 dicembre 1979, 549-555.

Ferrara, V., 1999. Presentazione della carta di vulnerabilità all'inquinamento dell'acquifero alluvionale della Piana di Catania (Sicilia NE). Atti del 3° conv. Naz. Sulla Protezione e Gestione delle Acque Sotterranee per il III Millennio. Parma, 13-14-15, ottobre, 1999.

Ferruggia Russo, S., 1852. Memoria sul tremuoto degli 11 gennaro 1848, Siracusa, 61 pp.

Finetti, I., Lentini, F., Carbone, S., Catalano, S. Del Ben, A., 1996. Il sistema Appennino meridionale – Arco Calabro-Sicilia nel Mediteraneo centrale: studio geologico–geofisico. Boll. Soc. Geol. It. 115, 529–559.

Finetti, I., Lentini, F., Carbone, S., Del Ben, A., Di Stefano, A., Guarnieri, P., Pipan, M., Prizzon, A., 2005. Crustal tectonostratigraphy and geodynamics of the southern Apennines from CROP and other integrating geophysical-geological data. In Finetti, I.R., ed., CROP: Deep seismic exploration of the Mediterranean region, special volume: Amsterdam, Elsevier, chapter 12, 225–262.

Franchi, S., 1909. Il terremoto del 28 dicembre 1908 a Messina, in rapporto alla natura del terreno ed alla riedificazione della città. Boll. Comit. Geol. Ital., 4th series, 10, 111-157.

Franzò, F., 1931. Diario del Vicario Foraneo di Spaccaforno F. Franzò con le notizie relative alla rinascita del paese dopo il terremoto dell'11 gennaio 1693. In G. Agnello, Memorie inedite varie sul terremoto siciliano del 1693. Archivio storico per la Sicilia Orientale, s. 11, a.7, 400 pp.

Fuller, M.L., 1912. The New-Madrid earthquake. U. S. Geol. Surv. 494, 1–119.

Galadini, F., Galli, P., Giraudi, C., 1995. Individuazionie di analisi di deformazioni geologiche associate a liquefazioni indotte da terremoti. Convegno Gruppo Nazionale Geologia Applicata, Messina, 1995.

Galadini, F., Galli, P., Cittadini, A., Giaccio, B., 2001. Late Quaternary fault movements in the Mt. Baldo-Lessini Mts. sector of the Southalpine area (northern Italy). Geologie en Mijnbouw (Netherlands Journal of Geosciences), 80, 119-140.

Galli., P., 2000. New empirical relationships between magnitude and distance for liquefaction. Tectonophysics, 324, 169-187.

Galli, P., Velona`, M., 1991. Liquefazione storica di terreni sabbiosi durante i passati terremoti, ISMES Report RAT-CGA-0023, 29 pp.

Galli, P., Meloni, F., 1993. Nuovo catalogo nazionale dei processi di liquefazione avvenuti in occasione dei terremoti storici in Italia. Il Quaternario 6, 271–292.

Galli, P., Ferreli, L., 1995. A methodological approach for historical liquefaction research. In: Serva, L., Slemmons, B., Eds., Perspectives in Paleoseismology, Association of Engineering Geologists Special Publication 6, 36–48.

Galli, P., Meloni, F., Rossi, A., 1999. Historical liquefaction in Italy: Relationship between epicentral distance and seismic parameters. European Geophysical Society XXIIII General Assembly Natural Hazards NH3, The Hague, Netherlands, 19–23 April.

Galli, P., Bosi, V., 2003. Catastrophic 1638 earthquakes in Calabria (southern Italy): New insights from paleoseismological investigation. Journal of Geophysical Research, 108, no. b1.

Galli, P., Galadini, F., Pantosti, D., 2008. Twenty years of paleoseismology in Italy. Earth-Science Reviews, 88, 89-117.

Gallo, A., 1783. Lettera istorico-fisica dé terremoti accaduti in Messina nel mese di febbraio di quest'anno 1783, scritta dal Sig. D.Andrea Gallo, Messina 8 Marzo, in M. Augusti, Dei terremoti di Messina e di Calabria dell'anno 1783. Memorie e riflessioni , 7-18. Bologna 1823.

Gallo, A., 1784. Lettere scritte da Andrea Gallo e indirizzate al signor Cavaliere N.N. delle reali Accademie di Londra, Bordò e Upsal, pelli terremoti del 1783 con un giornale meterologico dè medemi. Messina, 1784.

Gasperini, P., Bernardini, F., Valensise, G., Boschi, E., 1999. Defining seismogenic sources from historical earthquake felt reports. Bull. Seismol. Soc. Am. 89, 94–110.

Gazzetta del Sud, 1978. Aprile 27, a. 27, n. 115, Messina.

Gelfenbaum, G., Jaffe, B., 2003. Erosion and sedimentation from the 17 July 1998 Papua New Guinea tsunami; landslide tsunamis; recent findings and research directions. Pure and Applied Geophysics, 60, p. 1969-1999.

Gerardi, F., Barbano, M.S., De Martini, P.M., Pantosti, D., 2008. Discrimination of tsunami sources (earthquake vs. landslide) on the basis of historical data in eastern

Sicily and southern Calabria. Bullettin of the seismological Society of America, 98 (6), 2795-2805.

Ghersi, A., Platania, G., Sabatini, V., 1914. Relazione della Commissione per la determinazione delle aree sismiche sulle quali debbono vietarsi le nuove costruzioni nella regione colpita dal terremoto dell'8 maggio 1914 in provincia di Catania, Roma, 1914.

Ghisetti, F., Vezzani, L., 1984. Thin-skinned deformations of the western Sicily thrust belt and relationships with crustal shortening: mesostructural data on the Mt. Kumeta–Alcantara fault zone and related structures. Boll. Soc. Geol. Ital. 103, 129–157.

Gianfreda, F., Mastronuzzi, G., Sansò, P., 2001. Impact of historical tsunamis on a sandy coastal barrier: an example from the northern Gargano coast, southern Italy. Natural Hazards and Earth System Sciences, 1, 213–219.

Giardini, D., Velonà, M., 1991. Deep seismicity of the Tyrrhenian Sea: Terra Nova, 3, 57–64.

Giornale di Sicilia 1894, Novembre 24/25, Palermo.

Giornale di Siclia 1911, 10, 16-17, a.51, n.285.

Giornale di Sicilia, 1968a.01.17, a.108, n. 16 Palermo;

Giornale di Sicilia, 1968b.01.18, a.108, n.17. Palermo;

Giornale di Sicilia, 1978a. 04. 17, a. 118, n. 105. Palermo.

Giornale di Sicilia, 1978b. 04. 18, a. 118, n. 106. Palermo.

Giornale di Sicilia, 1894. 08. 9. 10. Palermo.

Giraudi, C., 1987. Segnalazione di scarpate di faglia legate ad antichi eventi sismici ai Piani di Aremogna e delle Cinque Miglia (Roccaraso, Abruzzo). Proc. 6° Meeting G.N.G.T.S., Rome 1987, 111-116.

Giraudi, C., 1989. Datazione di un evento sismico preistorico con metodi geologici e radiometrici. Piani di Aremogna e delle Cinque Miglia. in: E. Guidoboni (ed), I terremoti prima del Mille in Italia e nell'area mediterranea, I.N.G. and S.G.A (publ), Bologna 1989, 53-64.

Goff, J., Dudley, W.C., De Maintenon, M.J., Cain, G., Coney, J.P., 2006. The largest local tsunami in 20th century Hawaii. Marine Geology 226, 65–79.

Goto, K., Okada, K., Imamura, F., 2009. Characteristics and hydrodynamics of boulders transported by storm wave at Kudaka Island, Japan. Marine Geology 262, 14–24.

Grassa, F., Capasso, G., Favara, R., Inguaggiato S., 2006. Chemical and isotopic composition of waters and dissolved gases in some thermal springs of Sicily, Italy. Pageoph. Special Issue "Hiroshi Wakita", 163, 781-807.

Grassi, M., 1865. Relazione storica ed osservazioni sulla eruzione etnea del 1865 e su tremuoti flegrei che la seguirono. Catania, 1865.

Grasso, M., Lentini, F., 1982. Sedimentary and tectonic evolution of the Eastern Hyblean Plateau (South-eastern Sicily) during Late Cretaceous to Quaternary time: Palaeogeography, Palaeoclimatology, Palaeoecology, 39, 261–280.

Grasso, M., De Dominicis, A., Mazzoldi, G., 1990. Structures and tectonic setting of the western margin of the Hyblean-Malta Shelf, central Mediterranean. Annales Tectonicae, 4, 140–154.

Gresta et al., 1997. S. Gresta, R. Cristofolini and G. Di Grazia, Energy release at Mt. Etna volcano during 1988–1992. Acta Vulcanol. 9 1/2 (1997), 109–112.

Guarnieri, P., Carbone, S., Di Stefano, A., 2002. The Sicilian orogenic belt: A critical tapered wedge?: Bollettino della Società Geologica Italiana, 121, 221–230.

Guarnieri, P., Carbone, S., 2003. Assetto geologico e lineamenti morfostrutturali dei bacini plio-quaternari del Tirreno meridionale. Boll. Soc. Geol. It., 122, 10 pp.

Guarnieri, P., 2005. Plio-Quaternary segmentation of the south Tyrrhenian forearc basin. International Journal of Earth Sciences, 95, 107-118.

Guarnieri, P., **Pirrotta C.**, 2007. The response of drainage basins to the development of the late Quaternary Messina Strait (NE-Sicily). Geomorphology, 95, 260-273, ISSN: 0169-555X.

Guarnieri P., **Pirrotta C**., Barbano M.S., De Martini P.M, Pantosti D., Gerardi F., Smedile A., 2009. Paleoseismic investigation of historical liquefactions along the ionian coast of Sicily. Journal of Earthquake Engineering, 13, 68-79, ISSN: 1363-2469.

Gubernale, G., 1910. Brevi cenni sulla città di Avola, Modica.

Guidoboni, E., Mariotti D., 1999. Gli effetti dei terremoti a Palermo.Codice di pratica per la sicurezza e la conservazione del Centro Storico di Palermo. Giuffrè & Carocci Eds.

Gutscher, M.A., Roger, J., Baptista, M.A., Mirando, J.M., Tinti, S., 2006. Source of the 1693 Catania earthquake and tsunami (southern Italy): new evidence from tsunami modelling of a locked subduction fault plane. Geophys. Res. Lett. 33, L08309, doi:10.1029/2005GL025442.

Hancock, P.L., 1985. Brittle microtectonics: principles and practice. Journal of Structural Geology 7, 437-457.

Hansom, J.D., Hall, A.M., 2009. Magnitude and frequency of extra-tropical North Atlantic cyclones: a chronology from cliff-top storm deposits. Quaternary International 195, 42–52.

Hirn, A., Nicolich, R., Gallart, J., Laigle, M., Cernobori, L., 1997. Roots of Etna volcano in faults of great earthquakes. Earth Planet. Sci. Lett. 148, 171–191.

Hodgson, R. A., 1961. Classification of structures on joint surfaces. American Journal of Sciences 259, 439-502.

Hori K., Kuzumoto R., Hirouchi D., Umitsu M., Janjirawuttikul N., Patanakanog B., 2007. Horizontal and vertical variation of 2004 Indian tsunami deposits: An example of two transects along the western coast o Thailand. Marine Geology, 239, 3-4.

IAEA International Atomic Energy Agency, 1991, Safety Series No. 50-SG-S1 - Rev.1;

IAEA International Atomic Energy Agency, 2002. Evaluation of seismic hazards for nuclear power plants, Safety Guide, Vienna.

Igarashi, G., Wakita, H., Sato, T., 1992. Precursory and coseismic anomalies in well water levels observed for the 2 February 1992, Tokyo Bay earthquake, Geoph. Res. Lett., 19, 15, 1583–1586.

Imamura, F., Goto, K., Ohkubo, S., 2008. A numerical model for the transport of a boulder by tsunami. Journal Geophysical Research 113, C01008.

Incudine G. 1882, Naso Illustrata. Napoli, 1882.

Jacques, E., Monaco, C., Tapponier, P., Tortorici, L., Winter, T., 2001. Faulting and earthquake triggering during the 1783 Calabria seismic sequence. Geophys. J. Int. 147, 499-516.

Jaffe, B. E., Gelfenbaum, G., 2002. Using tsunami deposits to improve assessment of tsunami risk, Solutions to Coastal Disasters ‘02, Conference Proceedings, ASCE, 836-847.

Keefer, D. K., 1996. Investigating landslides caused by earthquakes – a historical review Surveys in Earth and Environmental Science Surveys in Geophysics, 23, Number 6, 473-510.

Keller, E.A., N., Pinter., 1996. Active Tectonics. Englewood Cliffs, New Jersey, Prentice Hall Inc. 338 pp.

Kelletat, D., Schellmann, G., 2002. Tsunami on Cyprus: field evidences and 14C dating results. Zeitschrift fuer Geomorphologie, N.F. 46 (1), 19–34.

Kelletat, D., 2008. Comments to Dawson, A.G. Stewart, I. 2007. Tsunami deposits in the geological record (Sedimentary Geology 200, 166–183). Sedimentary Geology 211, 87–91.

Kissin, I. G., Grinevsky, A. O., 1990. Main features of Hydrogeodynamic earthquake precursors, Tectonophysics, 178, 277–286.

Kuo-Chin, H. Chih-Chiu, T., 2005. On estimating the earthquake-induced changes in hydrogeological properties of the Choshuishi Alluvial Fan, Taiwan. Hydrogeology Journal, 467-480.

Kuribayashi, E., Tatsuoka, F., 1975. in Soil and Foundations 15, 81–92. Soil and Foundations 17, 82–85.

L'Ora, 1908. 12. 29, a.9, n.361. Palermo.

L'Ora 1911. 10. 17-18, a.12, n.290, Palermo.

L'Ora, 1968a. 01. 22/23, a. 69., n.18. Palermo.

L'Ora, 1968. 01. 19/20, a. 69,n. 16. Palermo.

La Sicilia, 1990a. 12. 14, a.46, n. 342. Catania.

La Stampa, 1968a.01.18, Torino.

La Stampa, 1968b. 01. 26, Torino.

La Stampa, 1968c. 01. 27, Torino.

La Tribuna, 1894.08.10. Roma.

Lacisio, P., 1858. Lettera di Paolo LAcisio ad Amerbach, Strasburgo 7 marzo 1543, in Die Amerbachkorrespondens , a cura di A. Hartmann, tomo 5, 414.

Lajoie, K.R., 1986. coastal tectonics. In: Active tectonics, studies in geophysics, notional academy press, whashington D.C., 95-124.

Lallement, M., 1785. Relation envoyée par M. Lallement, viceconsult de France a Messine, au ministre, in J.C.R. de Saint-Non, Vojage pittoresque à Naples et en Sicile, 4, parte I, 5-10.

Lanzafame, G., Leopardi, A., Neri, M., 1999. Nota presentata nella seduta del 23 Aprile 1999, dal Corrisp. Wezel F. C., Rend. Fis. Acc. Lincei s. 9, 10, 63–80.

Lavecchia, G., Ferrarini, F., De Nardis, R., Visini, F., Barbano, M.S., 2007. Active Thrusting as a possible seismogenic source in Sicily (southern Italy): some insights from Integrated structural-kinematic and seismological data. Tectonophysics, 445 (3-4), 145-167.

Lentini, F., Catalano, S., Carbone, S., 1996. The External Thrust System in Southern Italy: A target for petroleum exploration. Petroleum Geoscience 2, 333–342.

Lentini, F., Carbone, S., Di Stefano, A., Guarnieri, P., 2002, Stratigraphical and structural constraints in the Lucanian Apennines (southern Italy): Tools for reconstructing the geological evolution: Journal of Geodynamics, v. 34, 141–158.

Lentini, F., Carbone, S., Guarnieri, P., 2006. Collisional and postcollisional tectonics of the Apenninic-Maghrebian Orogen (Southern Italy). In: Dilek, Y., Pavlides, S. (Eds.), Postcollisional tectonics and magmatism in the Mediterranean region and Asia. Geological Society of America Special Papers 409, 57–81.

Lo Giudice, P., 1909. I laghi di Ganzirri e del Faro (Messina) dopo il terremoto del 28 Dicembre 1908, Rivista mensile di Pesca e Idrobiologia, Anno XI, Luglio-Agosto, 7-8.

Lo Giudice, E., Rasà, R., 1990. Indagine macrosismica sul terremoto ibleo del 13/12/1990: prime valutazioni, CNR- Istituto Internazionale di Vulcanologia di Catania.

Longhitano, S., Colella, A., 2007. Geomorphology, Sedimentology and recent evolution of the anthropogenically modified Simeto River delta system (Eastern Sicily, Italy). Sedimentary Geology 194, 195–221.

Longo, A., 1818. Memoria storico-fisica sul tremuoto dé 20 febbraio 1818. Catania 1818

Malinverno, A., Ryan, W.B.F., 1986. Extension in the Tyrhenian Sea and shortening in the Apennines as a result of Arc migration driven by sinking of the lithospheare. Tectonics, 5, 227–245.

Maouche, S., Morhange, C., Meghraoui, M., 2009. Large boulder accumulation on the Algerian coast evidence tsunami events in the western Mediterranean. Marine Geology, 262, 96–104.

Marangone, B., 1866. Annales Pisani, ed. K.Pertz, in Monumenta Germaniae Historica, SS., tomo 19, 236-266. Hannover.

Mastronuzzi, G., Sansò, P., 2000. Boulders transport by catastrophic waves along the Ionian coast of Apulia (Southern Italy). Marine Geology, 170, 93–103.

Mastronuzzi, G., Sansò, P., 2004. Large boulder accumulations by extreme waves along the Adriatic coast of southern Apulia (Italy). Quaternary International, 120, 173–184.

Mastronuzzi, G., Pignatelli, C., Sansò, P., Selleri, G., 2007. Boulder accumulations produced by the 20th February 1743 tsunami along the coast of southeastern Salento (Apulia region, Italy). Marine Geology 242 (1), 191–205.

Mazzanti, P., 2008. Studio integrato subaereo-subacqueo di frane in ambiente costiero: i casi di Scilla (RC) e del Lago di Albano (RM). Giornale di Geologia Applicata, 8, 2, 245-261.

Mazzarella, 1988. l'abate Scinà fra i terremoti.

McCalpin, J.P., Nelson, A.R., 1996. Introduction to paleoseismology. In: McCalpin, J.P. (Ed.), Paleoseismology. Academic Press, Orlando, FL, 1–32.

McGill, S., Siedh, K., 1991. Surficial offset on the Central and Eastern Garlok fault associated with prehistoric earthquakes. J. Geophysics Research, 96, 21597-21621.

Meletti, C., Galadini, F., Valensise, G., Stucchi, M., Basili, R., Barba, S., Vannucci, G., Boschi, E., 2008. A seismic source zone model for the seismic hazard assessment of the Italian territory. Tectonophysics, 450, 85–10.

Michetti, A. M., 1991. Paleosismologia e pericolosità sismica: stato delle conoscenze ed ipotesi di sviluppo. In: rendiconto n° 2 Consiglio Nazionale delle Ricerche, Gruppo Nazionale per la Difesa dai Terremoti.

Michetti, A.M., 1994. Coseismic surface displacements vs. magnitude: relationships from paleoseismological analyses in the central Apennines (Italy). Journal of Geodetic Society of Japan, special issue, 375–380.

Michetti, A.M., Brunamonte, F., Serva, L., 1995. Paleoseismological evidence in the epicentral area of the January 1968 earthquakes, Belice, southwestern Sicily. In: Serva, L., Slemmons, D.B. (Eds.), Perspectives in paleoseismology. Association of Engineering Geologists, spec. publ., 6, 127–139.

Minasi, G., 1783, Relazione veridica intorno al terribile tremoto accaduto in Scilla a 5 febbraio 1783, Messina (Italy).

Mogi, K., 1987. Comparison of precursory phenomena before the 1975 Haicheng (China) earthquake and the 1978 Izu-Oshima-Kinkai (Japan) earthquake: the possible effect of stress history on precursory phenomena, Tectonophysics, 138, 33–43.

Molina, J.M., Alfaro, P., Moretti, M., Soria, J.M., 1998. Soft-sediment deformation structures induced by cyclic stress of storm waves in tempestites (Miocene, Guadalquivir basin, Spain). Terra Nova 10, 145–150.

Molnar, P., Hanks, T., Nur, A., Raleigh, B., Wu, F., Savage, J., Scholz, C., Craig, H., Turner, R., and Bennet, G., 1976. Prediction of the Haicheng earthquake, The Haicheng Earthquake Study Delegation Report.

Monachesi, G., Stucchi, M.,1997. DOM4.1, un data base di osservazioni macrosismiche di terremoti di area italiana al di sopra della soglia del danno, GNDT, Rapporto Interno, Milano-Macerata.

Monaco, C., Tortorici, L., Tansi, C., Cocina, O., 1995. Recent active tectonics in teh Calabrian Arc. Tectoniphysics, 343, 37-55. Monaco, C., Tapponnier, P., Tortorici, L., Gillot, P.Y., 1997. Late Quaternary sliprates on the Acireale-Piedimonte normal faults and tectonic origin of Mt. Etna (Sicily). Earth Planetary Science Letters 147, 125–139.

Monaco, C., Mazzoli, S., Tortorici, L., 1996. Active thrust tectonics in western Sicily (southern Italy): the 1968 Belice earthquake sequence. Terra Nova 8, 372–381.

Monaco, C., Tortrici, L., Nicolich, R., Cerobori, L., Costa, M., 1996. From collisional to rifted basino: an example from the southern Calabrian arc (Italy). Tectonophysics 266, 233-249.

Monaco, C., Tapponnier, P., Tortorici, L., Gillot, P.Y., 1997. Late Quaternary slip rates on the Acireale-Piedimonte normal faults and tectonic origin of Mt. Etna (Sicily). Earth Planet. Sci. Letters, 147, 125-139.

Monaco, C., Tortorici, L., 2000. Active faulting in the Calabrian arc and eastern Sicily. J. Geodyn. 29, 407-424.

Monaco, C., Catalano, S., Cocina, O., De Guidi, G., Ferlito, C., Gresta, S., Musumeci, C., Tortorici, L., 2005. Tectonic control on the eruptive dynamics at Mt. Etna Volcano (Sicily) during the 2001–2003 eruptions: Journal of Volcanology and Geothermal Research, v. 144, 211–233.

Mongitore, A., 1743. Istoria cronologica de' terremoti di Sicilia, in Id., Della Sicilia ricercata nelle cose più memorabili , tomo 2, 345-445, Palermo 1743.

Montenat, C., Barrier, P., Ott d'Estevou, P., 1991. Some aspects of the recent tectonics in the Strait of Messina, Italy. Tectonophysics, 194, 203–215.

Montenat, C., Barrier, P., Ott d′Estevou, P., Hibsch, C., 2008. Seismites: An attempt at critical analysis and classification. Sedimentary Geology, 196, 5-30.

Moretti, M., 2000. Soft-sediment deformation structures interpreted as seismites in middle-late Pleistocene aeolian deposits (Apulian foreland, southern Italy). Sedimentary Geology, 135, 167–179.

Moretti, M., Soria, J.M., Alfaro, P., Walsh, N., 2001. Asymmetrical soft-sediment deformation structures triggered by rapid sedimentation in turbiditic deposits. Facies, 44, 283–294.

Morton, R. A., Gelfenbuam, G., Jaffe, B. E., 2007. Physical criteria for distinguishing sandy tsunami and storm deposits using modern examples. Sediment. Geol., 200 (3-4), 184-207.

Musumeci, C., Patanè, D., Scarfì, L., Gresta, S., 2005. Stress directions and shearwave anisotropy: observations from local earthquakes in southeastern Sicily, Italy. Bull. Seismol. Soc. Am., 95 (4), 1359–1374.

Naselli, C., 1931. Terremoti etnei e storie di popolo, in Lares , an.2, n.3, ottobre 1931, 9, p. 1-8. Firenze, 1931.

Nicoletti, P. G., 2005. Inconsistent patterns of historical seismicity and earthquake-triggered landsliding in southeastern Sicily: an alarm belt?. Geomorphology, 65, 257–278.

Noormets, R., Crook, K.A.W., Felton, E.A., 2004. Sedimentology of rocky shorelines: 3. Hydrodynamics of megaclast emplacement and transport on a shore platform, Oahu, Hawaii. Sedimentary Geology, 172, 41–65.

Nott, J., 2003. Tsunami or storm waves?—Determining the origin of a spectacular field of wave emplaced boulders using numerical storm surge and wave models and hydrodynamic transport equations. J. Coast. Res., 19, 348–356.

Nunziata, C., Costa, G., Natale, M., Panza, G.F., 1999. Seismic characterization of the shore sand at Catania. Journal of Seismology, 3 (3), 253-264.

Obermeier, S. F., 1996. Use of liquefaction-induced features for paleoseismic analysis: an overview of how seismic liquefaction features can be distinguished from other features and how their regional distribution and properties of source sediment can be used to infer the location and strength of Holocene paleo-earthquakes. Engineering Geology 44, 1–76.

Okal, E.A., Synolakis, C.E., 2004. Source discriminants for near-field tsunamis. Geophys. J. Int. 158, 899-912.

Onorati, G., Pece, R., Tranfaglia, G., Zollo, A. 1994. Sismicità e regime delle falde acquifere nell'Appennino meridionale, Atti 13 Conv. Naz. GNGTS, Roma, 895–906.

Owen, G., 1987. Deformation processes in unconsolidated sands. In: Jones ME, Preston RMF (eds) Deformation of sediments and sedimentary rocks. Geol Soc Spec Publ, 29, 11–24

Owen, G., Moretti, M., 2008. Determining the origin of soft-sediment deformation structures: a case study from Upper Carboniferous delta deposits in south-west Wales, UK. Terra Nova, 20, 237–245.

Pantosti, D., Valensise, G., 1990. Faulting mechanism and complexity of the 23 November 1980, Campania-Lucania earthquake, inferred from surface observations – J. Geophys. Res., 95, 15.319-15.341.

Pantosti, D., Yeats, R.S., 1993. Paleoseismology of great earthquakes of the Holocene. Annali di Geofisica, vol XXXVI, N 3-4, 237-257.

Pantosti, D., Schwartz, D.P., Valensise, G., 1993. Paleoseimology along the 1980 Irpinia earthquake fault and implications for earthquake recurrence in the Southern Appennines. J. Geophysics Research, 98, 6561-6577.

Pantosti, D., Barbano, M.S., De Martini, P.M., Smedile, A., 2008. Geological Evidence of Paleotsunamis at Torre degli Inglesi (NE Sicily). Geophys. Res. Lett., 35, L05311.

Pantosti, D., Barbano, M.S., Smedile, A., De Martini, P.M., Gerardi, F., **Pirrotta, C.**, 2008. Geological evidence of paleotsunamis at Torre degli Inglesi (northeastern Sicily). In: Abstract book 2nd International Tsunami Field Symposium. Ostuni-Puglia (Italy) and Lefkada (Ionian Islands- Greece), 21-28 September 2008, 89-92, IGCP Project 495, ISBN/ISSN: 978-88-7522-015-0.

Papadopoulos, G.A., Lefkopulos, G., 1993. Magnitude- distance relations for liquefaction in soil from earthquakes, Bull. Seismol. Soc. Am., 83, 925-938.

Paris, R., Wassmer, P., Sartohadi, J., Lavigne, F., Barthomeuf, B., Desgages, E., Grancher, D., Baumert, P., Vautier, F., Brunstein, D., Gomez, C., 2009. Tsunamis as geomorphic crises: lessons from the December 26, 2004 tsunami in Lhok Nga, West Banda Aceh (Sumatra, Indonesia). Geomorphology 104, 59–72.

Patacca, E., Scandone, P., 1989. Post-Tortonian mountain building in the Apennines: The role of the passive sinking of a relict lithospheric slab, in Boriani, A., et al., eds., The lithosphere in Italy: Atti Convegni Lincei, 80, 157–176.

Patacca, E., Sartori, R., Scandone, P., 1990. Tyrrhenian basin and apenninic arcs: Kinematic relations since late Tortonian times: Bollettino della Società Geologica Italiana, 45, 425–451.

Patanè, A., 1992. Note sui terremoti etnei del 7 e 8 agosto 1894 nel territorio di Acireale, in –Memorie e Rendiconti dell'Accademia di Scienze Lettere e Belle Arti degli Zelanti e dei Dafnici di Acireale-, s. IV, vol. 2, 237-265. Acireale. 1992.

Pece, R., Tranfaglia, G., Avino, R., 1999. Geochemical monitorino integrated in a real time hydrological network. Il Nuovo Cimento, 22 C, 483–490.

Perrin, N.D., Hancox, G.T., 1992. Landslide-dammed lakes in New Zealand preliminary studies on their distribution, causes and effects. In: Bell, D.H., Editor, 1992.

Landslides. Glissements de Terrain. Proceedings of the Sixth International Symposium 10–14 February 1992, Christchurch, Balkema, Rotterdam, 1457–1466.

Pinegina, T. K., Bourgeois, J., 2001. Historical and paleotsunami deposits on Kamchatka, Russia: long-term chronologies and long-distance correlations. Nat. Hazard Earth Sys., 1, 177–185.

Pino, N.A., Giardini, D., Boschi, E., 2000. The December 28, 1908, Messina Straits, southern Italy, earthquake: Waveform modelling of regional seismograms. J. Geophys. Res. 105, NO B11, 25473-25492.

Pirrotta, C., Barbano, M.S., Guarnieri, P., Gerardi, F. 2007: A new dataset and empirical relationships between magnitude/intensity and epicentral distance for liquefaction in central-eastern Sicily. Annals of Geophysics, 50, 763-774.

Pirrotta, C., Barbano, M.S. Analysis of deformation structures in Pliocene and Quaternary deposits of the Hyblean Plateaux (south-eastern Sicily). Submitted to Tectonophysics.

Platania, G., 1909. Il Maremoto dello Stretto di Messina del 28 dicembre 1908, Boll. Soc. Sism. It., 13, 369-458.

Platania, G., 1916. Sul periodo sismico del maggio 1914 nella regione orientale dell'Etna, in Rendiconti e memorie della Regia Accademie di Scienze, Lettere ed Arti degli Zelanti , s.III, vol. 7-8 (1912-1915), 105-122. Acireale.

Pollard, D.D., Aydin, A., 1988. Progress in jointing over the past century. Geological Society of America Bulletin, 100, 1181-1204.

Pondrelli, S., Morelli, A., Ekström, G., 2004. European–Mediterranean regional Centroid Moment Tensor Catalog: solutions for the years 2001 and 2002. Phys. Earth Planet. Inter. 145 (1/4), 127–147.

Postpischl, D., 1985. Catalogo dei terremoti italiani dall'anno 1000 al 1980, Quaderni della Ricerca Scientifica, 114, 2B, Bologna 1985, 239 pp.

Postpischl, D., Agostini S., Forti P., Quinif Y., 1991. Palaeoseismicity from karst sediments : the "Grotta dei Cervi cave case study. Tectonophysics, 193.

Prestininzi, A., Romeo, R., 2000. Earthquake-induced ground failures in Italy, Eng. Geol., 58 (3-4), 387-397.

Privitera, S., 1878. Storia di Siracusa antica e moderna (ristampa anastatica, Sala Bolognese), Napoli, 1878.

Rasà, R., Azzaro, R., Leopardi, O., 1996. Aseismic creep on faults and flank instability at Mount Etna volcano, Sicily. Geological Society, London, Special Publications, 110, 179-192.

Reimer, P.J., Baillie, M.G.L., Bard, E., Bayliss, A., Beck, J.W., Bertrand, C., Blackwell, P.G., Buck, C.E., Burr, G., Cutler, K.B., Damon, P.E., Edwards, R.L., Fairbanks, R.G., Friedrich, M., Guilderson, TP., Hughen, KA., Kromer, B., McCormac, FG., Manning, S., Bronk Ramsey, C., Reimer, RW., Remmele, S., Southon, JR., Stuiver, M., Talamo, S., Taylor, FW., van der Plicht, J ., Weyhenmeyer, C.E., 2004 Radiocarbon 46:1029-1058.

Relazione istorico-fisica dè terremoti accaduti in Messina in quest'anno 1783. Messina, 1783.

Rendiconti e memorie della Regia Accademia di Scienze. Lettere ed arti degli Zelanti, s.III, vol. 7-8 (1912-1915), 105-122.

Rezzadore, 1914. il mondo né suoi fulgori e tremori.

Rhodes, B., Tuttle, M., Horton, B.P., Doner, L., Kelsey, H., Nelson, A., Cisternas, M., 2006. Paleotsunami research: Eos, Transactions, American Geophysical Union, 87, 205- 209.

Riccò, A., 1893. Periodo di attività geodinamica dal 22 aprile alla fine di maggio1893, Boll. Acc. Gioenia Sc. Nat., n.s., 33, 16-17.

Riccò, A., 1907. Il terremoto del 16 novembre 1894 in Calabria ed in Sicilia. Parte I: Relazione sismologia, in Annali dell'Ufficio Meteorologico e Geodinamico Italiano, s. II, vol. 19 (1897), parte I, 7-261. Roma.

Riccò, A., 1911. Terremoto di Fondo Macchia del 15 ottobre 1911, inBollettino delle Sedute dell'Accademia Gioenia di Scienze Naturali in Catania s. II, fasc. 19, p.5-23.

Riccò, A., 1912. Fenomeni geodinamici consecutivi all'eruzione etnea del settembre 1911, in Bollettino della Società sismologia Italiana vol. 16. (1912), p. 9-38.

Rikitake, T., 1974. Focal processes and prediction of earthquakes. Tectonophysics, 23, 217–318.

Rikitake, T., 1975. Earthquake Precursors – Bulletin of the Seismological Society of America, 65, 5, 1133–1162.

Rodrìguez Pascua, M.A., Calvo, J.P., De Vicente, G., Gomez Gras, D., 2000. Seismites in lacustrine sediments of the Prebetic Zone, SE Spain, and their use as indicators of earthquake magnitudes during the late Miocene. Sediment. Geol. 135 (1–4), 117–135.

Romeo, R., Delfino, L. 1997. Catalogo nazionale degli Effetti Deformativi del suolo indotti da forti Terremoti, C.E.D.I.T., Rapporto Tecnico SSN/RT/97/04.

Ruggieri, G., 1959. Geologia della zona costiera di Torre Vendicari (Sicilia sud orientale). Rivista Mineraria Siciliana 55, 12-14.

Russ, D.P., 1982. Style and significance of surface deformation in the vicinity of New Madrid, Missouri. In: Mckeown, F.A., Pakiser, L.C., (Eds.), Investigations of the New Madrid, Missouri, earthquake region, US Geological Surveys, 1236, 95-l14.

Sabatini, V., 1914. Note sul terremoto di Linera dell'8 maggio 1914, in Bollettino del Regio Comitato Geologico d'Italia , vol. 44, fasc. 3, 3-52. Roma, 1914.

Samperi, P., 1644. Cronologia della gloriosa Vergine Madre di Dio Maria protettrice di Messina. Messina, 1644.

Sarconi, M., 1784. Istoria dé fenomeni del tremoto avvenuto nelle Calabrie, e nel Valdemone nell'anno 1783 posta in luce dalla Reale Accademia delle Scienze, e delle Belle Lettere di Napoli. Napoli.

Sartori, R., Colalongo, M.L., Gabbianelli, G., Bonazzi, C., Carbone, S., Curzi, P.V., Evangelisti, D., Grasso, M., Lentini, F., Rossi, S., Selli, L., 1991. Note stratigrafiche e tettoniche sul rise di Messina (Ionio nord-occidentale). Giornale di Geologia, 53, 49-64.

Sato, H., Shimamoto, T., Tsutsumi, A., Kawamoto, E., 1995. Onshore tsunami deposits caused by the 1993 southwest Hokkaido and 1983 Japan-Sea earthquakes: Pure and Applied Geophysics 144, 693-717.

Saucier, R.T., 1989. Evidence for episodic sand-blow activity during the 1811-1812 New Madrid (Missouri) earthquake series. Geology 17, 103-106.

Sauret, B., Bousquet, J.C., 1984. Manifestation d'instabilité du sol dans la zone littorale du séisme de Messine de 1908. Le rôle de la liquéfaction, Mouvements de terrains (Ground movements), Doc. BRGM, 83, Colloquium of Caen, 63–74.

Savaresky, E. F., Rikitake, T., (Eds): Forerunners of strong earthquakes – Tectonophysics, 14, 3/4, 177–343, 1972.

Scandone, P., Patacca, E., Rodoicic, R., Ryan, W.B.F., Cita, M.B., Rawason, M., Cherzar, H., Miller, E., Mckenzie, J., Rossi, S., 1981. Mesozoic and Cenozoic rocks from Malta Escarpment (Central Mediterranean). American Association of Petroleum Geologists Bulletin 65, 1299–1319.

Scarascia, S., Cassinis, R., Lozej, A., and Nebuloni, A., 2000, A seismic and gravimetric model of crustal structures across the Sicily Channel Rift Zone: Bollettino della Società Geologica Italiana, 19, 213–222.

Scheffers, A., Scheffers, S., 2006. Documentation of the impact of hurricane Ivan on the coastline of Bonaire (Netherlands Antilles). Journal of Coastal Research, 22, 1437–1450.

Scholtz, C. H., Sykes, L. R., Aggarwal, Y. P., 1973. Earthquake prediction: A physical basis. Science, 181, 803–810.

Scicchitano, G., Monaco, C., Tortorici, L., 2007. Large boulder deposits by tsunami waves 919 along the Ionian coast of south-eastern Sicily (Italy). Marine Geology 238 (1–4), 920 75–91.

Scinà, D., 1819. Rapporto del viaggio alle Madonne in occasione dè tremuoti colà accaduti nel 1818 e nel 1819. Palermo, 1819.

Sciuto Patti, 1931. Contribuzione allo studio dei terremoti in Sicilia, in Atti dell'Accademia Gioenia di Scienze Naturali in Catania, s. IV, a. 73, vol. 9 (1896), p. 1-34. Terremoti etnei e storie di popolo, in Lares, an. 2, n. 3, ottobre 1931, 9, 1-8. Firenze, 1931.

Seilacher, A., 1984. Sedimentary structures tentatively attributed to seismic events. Mar. Geol. 55, 1–12.

Seymour, R.J., 1977. Estimating wave generation on restricted fetches. J. Waterway Port C. Div., 103, 12924, 251-264.

Shi, S.Z., Dawson, A.G., Smith, D.E., 1995. Coastal Sedimentation Associated with the December 12th, 1992 Tsunami in Flores, Indonesia: Pure and Applied Geophysics, 144, 525-536.

Shiki, T., Yamazaki, T., 1996. Tsunami-induced conglomerates in Miocene upper bathyal deposits, Chita Peninsula, Central Japan. Sediment. Geol. 104, 175-188.

Sieh, K.E., 1981. A review of geological evidence for recurrence times of large earthquakes. In: Earthquake prediction-An international review, Am. Geophys Union, Washington D.C., 181-207.

Sieh, K.E., Jahns, R.H., 1984. Holocene activity of the San andreas at Wallace Creek California, Geol. Soc. Am. Bull., 95, 883-896.

Silvestri, O., 1865. Relazione sopra i terremuoti dell'Etna, in Giornale della Provincia di Catania , n. 57, 1865. Catania, 1865.

Sims, J.D., 1973. Earthquake-induced structures in sediments of Van Norman Lake, San Fernando, California. Science, 182, 161–163.

Sims, J.D., 1975. Determining earthquake recurrence intervals from deformational structures in young lacustrine sediments. Tectonophysics 29, 141-152.

Sirovich, L., Pettenati, F., 1999. Seismotectonic outline of south-eastern Sicily: an evaluation of available options for the earthquake fault rupture scenario. J. Seismol., 3, 213–233.

Sleiko, D., Valensise, G., 2007. Assessing the seismogenic potential and the probability of strong earthquakes in Italy. Internal report: INGV-DPC Seismological projects – Final report of Project S2 – July 2007, 63 pp.

Smedile, A., De Martini, P.M., Pantosti, D., Bellucci, L., Del Carlo, P., Gasperini, L., **Pirrotta, C**., Polonia, A., Boschi, E., Possible tsunamis signatures from an integrated study in the Augusta Bay offshore (Eastern Sicily–Italy). Submitted to Marine Geology.

Smith, R. P., Jackson, S. M., and Hackett, W. R., 1996. Paleoseismology and seismic hazards evaluations in extensional volcanic terrains, J. Geophys. Res. 101(B3), 6277-6292.

Spirito, F., 2006. Eventi meteorologici estremi in Mediterraneo. M.S. theses, University of Bologna, Italy.

Stewart I.S., Cundy, A., Kershaw, S., Firth, C., 1997. Holocene coastal uplift in the Taormina area, northeastern Sicily: implications for the southern prolongation of the Calabrian seismogenic belt. J. Geodynamics, 24, 37-50.

Stucchi, M., Camassi, R., Rovida, A., Locati, M., Ercolani, E., Meletti, C., Migliavacca, P., Bernardini, F., Azzaro, R., 2007. DBMI04 il database delle osservazioni macrosismiche dei terremoti italiani utilizzate per la compilazione del catalogo parametrico CPTI04

Stuiver, M., Reimer, P. J., 2005. Radiocarbon calibration program CALIB REV5.0.2, copyright, available at http://calib.cub.ac.uk/calib/

Sunamura, T., Horikawa, K., 1974. Two dimensional beach transformation due to waves. Proceedings 14th Coastal Engineering Conference. Am. Soc. Civilian Engineers, 920–938.

Talwani, P., Cox, J., 1985. Paleoseismic Evidence for Recurrence of Earthquakes near Charleston, South Carolina. Science, 229, 379-381.

Timoshenko, S., Goodier, J.N., 1951. Theory of Elasticity. McGraw-Hill, New York, 506 pp.

Torcia, M., 1783. Tremuoto avvenuto nella Calabria e a Messina all 5 febbrajo 1783 descritto da Michele Torcia – Archiviario di S. M. Siciliana e Membro della Accademia Regia, Napoli, 1783.

Torcia, M., 1784. Tremuoto accaduto nella Calabria e a Messina alli 5 Febbrajo 1783. Descritto da Michele Torcia.

Tortorici, L., Monaco, C., Tansi, C., Cocina, O., 1995. Recent and active tectonics in the Calabrian arc (Southern Italy). Tectonophysics, 243, 37–55.

Troften, E., 1997. Neotectonics and paleoseismicity in southern Sweden. Ph.D. Thesis, Stockolm University, Akademitryck AB, Edsbruck, 124 pp.

Tucker, M. E., 2001. Sedimentary petrology: an introduction to the origin of sedimentary rocks. 3rd edition, Blackwell Science, Oxford.

Vachard, D., Barrier, P., Montenat, C., Ott d' Estevou, P., 1987. Dykes neptuniens, brèches internes et éboulis cimentés des escarpements de faille du Détroit de Messine au Plio-Quaternaire. Documents et Travaux de l'IGAL, Paris 11, 27–41.

Valensise, G., Pantosti, D., 1992. A 125 Kyr-long geological record of seismic source repeatability: the Messina Straits (southern Italy) and the 1908 earthquake (Ms 71/2). Terra Nova 4, 472–483.

Valensise, G., Pantosti, D. (Eds.), 2001. Database of potential sources for earthquakes larger than M 5.5 in Italy (DISS version 2.0). Ann. Geophys., vol. 44, Suppl. 1. with CD-ROM.

Valera, J.E., Traubenik, M.L., Egan, J.A., Kaneshiro, J.Y., 1994. A practical perspective on liquefaction of gravels, In: Prakash, S., Dakoulas, P. (Eds.), Ground Failures Under Seismic Conditions, American Civil Engineers Geotechnical, Special Publication 44, 241-257.

Van der Meulen, S., 1990. Major lateral sediment displacement in till–sand–peat associations of the Tjonger Valley fill (The NE Netherlands). Holocene cryoturbation?, Geologie Mijnb 69, 341–350.

Vannucci, G., Pondrelli, S., Argnani, A., Morelli, A., Gasperini, P., Boschi, E., 2004. An Atlas of Mediterranean seismicity. Ann. Geophys. 47(1) (Suppl. 1), 247–306.

Varnes, D.J., 1978. Slope movement types and processes. In: Schuster, R.L., Krizek, R.J. (Eds.), Special Report 176: Landslides: Analysis and Control. TRB, National Research Council, Washington, D.C., 11–33.

Vincent, C.L., 1984. Deepwater wind wave growth with fetch and duration. Technical Reports num. CERCMP8413, Coastal Engineering Research Center Vicksburg Ms.

Vittori, E., Labini, S.S., Serva, L., 1991. Palaeoseismology: review of the state-of-the-art. Tectonophysics, 193, 1-3, 9-32.

Ward, S.N., 1994. Constraints on sismotectonics of the central Mediterranean from Very Long Baseline Interferometry. Geophysics Journal International, 117, 441-452.

Wallace, R.E., 1977. Profiles and age of young fault scarps, North-Central Nevada, Bull. Geol. Am., 88, 9, 1267-1281.

Wangen, M., 2001. A quantitative comparison of some mechanisms generating overpressure in sedimentary basins. Tectonophysics. 334, 211–234.

Wells, D. L., Coppersmith, K. J., 1994. New Empirical Relationships among Magnitude, Rupture Length, Rupture Width, Rupture Area, and Surface Displacement Bulletin of the Seismological Society of America, 84, No. 4, 974-1002.

Westaway, R., 1993. Quaternary uplift of southern Italy, J. Geophys., 98, 21 741–21 772

Whitehead, R. L., Harper, R. W., Sisco, H. G. 1985. Hydrologic changes associated with the 28 October 1983, Idaho earthquake, Pageoph, 122, 280–293.

WORKING GROUP CPTI99, 1999. Catalogo Parametrico dei Terremoti Italiani, (ING, GNDT, SGA, SSN, Bologna), pp. 92.

WORKING GROUP CPTI04, 2004. Catalogo Parametrico dei Terremoti Italiani, versione 2004, CPTI04 (INGV, Bologna), (available on line at http://emidius.mi.ingv.it/ CPTI/).

WORKING GROUP MPS, 2004. Redazione della mappa di pericolosità sismica prevista dall'Ordinanza PCM 3274 del 20 marzo 2003. Rapporto Conclusivo per il Dipartimento della Protezione Civile, INGV, Milano-Roma, aprile 2004, 65 pp. + 5 appendici. http://zonesismiche.mi.ingv.it/.

Wortel, M.J.R., Spackman, W., 1993. The dynamic evolution of the Apenninic-Calabrian, Hellenic and Carpathian arcs: a unifying approach. Terra Nova Abstr. 5, 97 pp.

Youd, T. L., 1977. Discussion of 'Brief review of liquefaction during earthquakes in Japan, by Kuribayashi, E. and Tatsuoka, F., 1975, in Soil and Foundations 15, 81–92. Soil and Foundations 17, 82–85.

Young Yin, L., Joshua, A., White, Heng Xiao, Ronaldo I. Borja, 2009. Liquefaction potential of coastal slopes induced by solitary waves. Acta Geotechnica, 4, 17–34.

Acknowledgments

I wish to thank my Tutor Prof.ssa M.S. Barbano for support during the PhD Course and the useful suggestions and supervisions that contributed to improve this thesis and the scientific papers.

I‘m grateful to F. Gerardi, P. Guarnieri and A. Smedile for the collaboration, the contribution in the research and the stimulating discussions.

I also thank the colleagues P.M. De Martini, D. Pantosti, R. Punturo and S. Pinzi and the Prof.ssa J. Bourgeois for the collaborations and discussions.

Special thanks are for Fabio, my parents and friends for the precious support and encouragement.